INFORMATION TO USERS

This manuscript has been reproduced from the microfilm master. UMI films the text directly from the original or copy submitted. Thus, some thesis and dissertation copies are in typewriter face, while others may be from any type of computer printer.

The quality of this reproduction is dependent upon the quality of the copy submitted. Broken or indistinct print, colored or poor quality illustrations and photographs, print bleedthrough, substandard margins, and improper alignment can adversely affect reproduction.

In the unlikely event that the author did not send UMI a complete manuscript and there are missing pages, these will be noted. Also, if unauthorized copyright material had to be removed, a note will indicate the deletion.

Oversize materials (e.g., maps, drawings, charts) are reproduced by sectioning the original, beginning at the upper left-hand corner and continuing from left to right in equal sections with small overlaps.

Photographs included in the original manuscript have been reproduced xerographically in this copy. Higher quality 6" x 9" black and white photographic prints are available for any photographs or illustrations appearing in this copy for an additional charge. Contact UMI directly to order.

ProQuest Information and Learning
300 North Zeeb Road, Ann Arbor, MI 48106-1346 USA
800-521-0600



Downloaded from SHAREOK. Persistent Handle URL: https://hdl.handle.net/11244/312

UNIVERSITY OF OKLAHOMA
GRADUATE COLLEGE

COUPLED MODELING OF THE AIR QUALITY IMPACTS OF CHEMICAL DEPAINTING AGENTS RELEASED FROM AN INDUSTRIAL WASTEWATER TREATMENT FACILITY

A Dissertation
SUBMITTED TO THE GRADUATE FACULTY
in partial fulfillment of the requirements for the degree of
DOCTOR OF PHILOSOPHY

By

FREDDIE E. HALL, JR.
Norman, Oklahoma
2001

UMI Number: 3009208

UMI®

UMI Microform 3009208
Copyright 2001 by Bell & Howell Information and Learning Company.
All rights reserved. This microform edition is protected against
unauthorized copying under Title 17, United States Code.

Bell & Howell Information and Learning Company
300 North Zeeb Road
P.O. Box 1346
Ann Arbor, MI 48106-1346

© Copyright by FREDDIE E. HALL, JR. 2001
All Rights Reserved.

COUPLED MODELING OF THE AIR QUALITY IMPACTS OF CHEMICAL DEPAINTING AGENTS RELEASED FROM AN INDUSTRIAL WASTEWATER TREATMENT FACILITY

A Dissertation APPROVED FOR THE SCHOOL
CIVIL ENGINEERING AND ENVIONMENTAL SCIENCE

BY

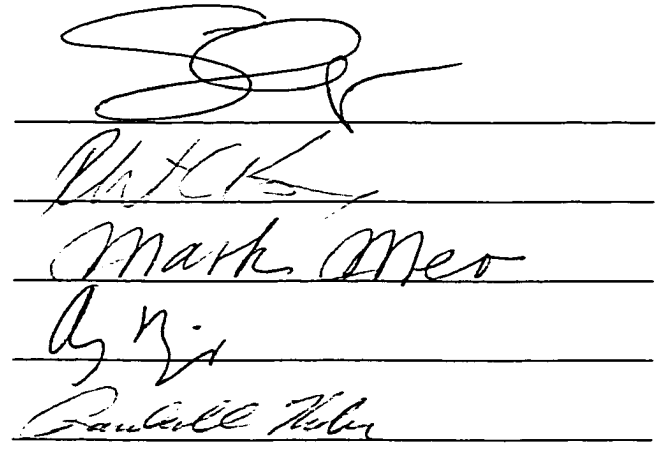

TABLE OF CONTENTS

	Page
CHAPTER 1: Introduction	1
Hypothesis	1
Testing of Hypothesis	2
Proposed Plan of Work	3
Uniqueness of This Research	8
Contents of Dissertation	11
Selected Reference	11
CHAPTER 2: Selection and Application of an Emission Source Model	12
Evaluation of Available General Fate Models	13
Detailed Description of WATER8 Air Emission Model	16
Governing Air Emission Model Equations	20
Application of the WATER8 Model to the Tinker AFB IWTF	23
WATER8 Modeling Results	30
Summary	36
Selected References	38
CHAPTER 3: Selection and Application of an Air Quality Dispersion Model	40
Evaluation of Available Air Quality Dispersion Models	41
Use of the Industrial Source Complex [ISC-ST3] Dispersion Model	49
Governing Air Dispersion Model Equations	50
Application of the ISC-ST3 Model to the Tinker AFB IWTF	60
ISC-ST3 Dispersion Modeling Results	63
Summary	68
Selected References	69
CHAPTER 4: Coupled Model Validation	75
Field Sample Collection Method	76
Tinker AFB Application of the Field Data Collection System	77
Statistical Evaluation: z-Tests and Confidence Intervals	79
Statistical Evaluation: Student's t-Test and Probabilities	84
Comparison of Coupled Model Predictions to Field Sample Data	88
Graphical Presentation of the Data [Statistical Evaluation]	92

Coupled Model Calibration 97
Sensitivity Analysis 105
Selected References 112

CHAPTER 5: Comparison of Coupled Model Predictions to OP-FTIR Data 115
Literature Review 115
Tinker AFB Application of the Open Path Monitoring System . 129
Comparison of Model Predictions to Open Path Monitoring Data 129
Summary 134
Selected References 139

CHAPTER 6: Risk Assessment 142
Literature Review 143
Risk Assessment 146
Methylene Chloride 147
Risk Assessment Computations for the Methylene Chloride Exposures. 148
Phenol 153
Risk Assessment Computations for the Phenol Exposures. . . 162
Selected References 166

CHAPTER 7: Additional Coupled Model Applications 176

CHAPTER 8: Summary and Conclusions 181
Conclusions 182

LIST OF FIGURES

Figure		Page
2.1	IWTF Process Flow Diagram at Tinker AFB	24
2.2	Average Ambient Wind Speed used in WATER8 Model	25
2.3	Primary Stripping Waste Clarifier Influent Phenol Concentration	28
2.4	Histogram [frequency distribution] for Influent Phenol Concentration	28
2.5	Primary Stripping Waste Clarifier Influent Methylene Chloride Concentration	29
2.6	Histogram [frequency distribution] for Influent Methylene Chloride Concentration	29
2.7	Percent of Phenol and Methylene Chloride Released to the Atmosphere from Various Unit Processes at Tinker AFB IWTF.	34
2.8	Mass of Chemicals Released Annually to the Atmosphere from Unit Processes at the Tinker AFB IWTF	35
3.1	Structure of a Typical Air Dispersion Model.	51
3.2	Coordinate System for Gaussian Model	53
3.3	Pasquill-Gifford Rural Horizontal Dispersion Parameter, σ_y [meters]	57
3.4	Pasquill-Gifford Rural Vertical Dispersion Parameter, σ_z [meters]	57
3.5	Receptor Grid Coordinate System for Dispersion Modeling of the Atmospheric Emissions from the Tinker AFB IWTF.	62
3.6	Wind Rose for Entire Ten Years [1984-1993]	64
3.7	Wind Rose for Sampling Period [22 Sep through 8 Nov 1993]	64
3.8	Annual-Average Methylene Chloride Concentration [*ppb*] for 1984 through 1993.	66
3.9	24-hour Maximum Methylene Chloride Concentration [*ppb*] for 1984 through 1993.	72
3.10	Annual-Average Phenol Concentration [*ppb*] for 1984 through 1993	73
3.11	24-hour Maximum Phenol Concentration [*ppb*] for 1984 through 1993	74
4.1	Ambient Air Sample Locations [A1 through A13]	78
4.2	z-values for Methylene Chloride and Phenol	81
4.3	p-value of Students t-test for Methylene Chloride	

and Phenol 86
4.4 Methylene Chloride Sample Data for A1 through A13 Sites . 90
4.5 Phenol Ambient Air Sample Data for A1 through A13 Sites . 92
4.6 Box Plot of Data 93
4.7 Field Data Comparison to Coupled Model Predictions for Methylene Chloride 94
4.8 Field Data Comparison to Coupled Model Predictions for Phenol 96
4.9 Separation Between Wind Speed Categories 98
4.10 Wind Profile Exponents 99
4.11 Field Data Comparison to Coupled Model Predictions for Methylene Chloride following Model Calibration. . . 100
4.12 Field Data Comparison to 1993 Coupled Model Predictions for Methylene Chloride following Model Calibration. . . 102
4.13 Field Data Comparison to Coupled Model Predictions for Phenol following Model Calibration 103
4.14 Field Data Comparison to 1993 Coupled Model Predictions for Phenol following Model Calibration 104
4.15 Methylene Chloride Influent Concentration and Random Numbers. 107
4.16 Methylene Chloride Frequency Distribution and Random Numbers Distribution 107
4.17 Phenol Influent Concentration and Random Numbers . . . 108
4.18 Phenol Frequency Distribution and Random Numbers Distribution 108
4.19 Methylene Chloride Sensitivity Analysis 109
4.20 Phenol Sensitivity Analysis 109
4.21 Z-values for Methylene Chloride and Phenol for the the Randomly Selected Sensitivity Analysis Data . . . 111
4.22 Probability Plot of Random Numbers 113
4.23 Lognormal-Probability Plot of Random Numbers 113
4.24 Probability Plot with Similar Axis [C_i/C_{max}] 114
4.25 Lognormal-Probability Plot with Similar Axis [C_i/C_{max}] . . 114
5.1 Top View of the IWTF Remote Optical Monitoring Paths . . 130
5.2 OPM Path P_1 Concentration Predictions for Methylene Chloride [*ppb*] 132
5.3 OPM Path P_2 Concentration Predictions for Methylene Chloride [*ppb*] 133

5.4 OPM Path P_3 Concentration Predictions for Methylene Chloride [*ppb*] 135

5.5 OPM Path P_1 Concentration Predictions for Phenol [*ppb*] . . 135

5.6 OPM Path P_2 Concentration Predictions for Phenol [*ppb*] . . 136

5.7 OPM Path P_3 Concentration Predictions for Phenol [*ppb*] . . 136

6.1 Equivalent Methylene Chloride Human Dose for Individuals in the General Population, *mg* 154

6.2 Equivalent Methylene Chloride Human Dose for the Individual Worker, *mg* 155

6.3 Maximum Individual Risk for Methylene Chloride in the General Population 156

6.4 Maximum Individual Risk for Methylene Chloride in Workers. 157

6.5 Maximum Number of Excess Cases for Methylene Chloride in the General Population. 158

6.6 Maximum Number of Excess Cases per Year for Methylene Chloride in the General Population 159

6.7 Maximum Number of Excess Cases for Methylene Chloride for Workers 160

6.8 Maximum Number of Excess Cases per Year for Methylene Chloride for Workers 161

6.9 Equivalent Phenol Human Dose for Individuals in the General Population, *mg* 168

6.10 Equivalent Phenol Human Dose for the Individual Worker, *mg* 169

6.11 Maximum Individual Risk for Phenol in the General Population 170

6.12 Maximum Individual Risk for Phenol in Workers 171

6.13 Maximum Number of Excess Cases for Phenol in the General Population 172

6.14 Maximum Number of Excess Cases per Year for Phenol in the General Population. 173

6.15 Maximum Number of Excess Cases for Phenol for Workers . . 174

6.16 Maximum Number of Excess Cases per Year for Phenol for Workers 175

LIST OF TABLES

Table		Page
2.1	Atmospheric Emissions from the Tinker AFB IWTF as Generated by the WATER8 Model.	32
2.2	Emission Factors [grams/cm^2·second] for Methylene Chloride under Average and Maximum Influent Conditions as Developed from the WATER8 Model for the Tinker AFB IWTF	37
2.3	Emission Factors [grams/cm^2·second] for Phenol under Average and Maximum Influent Conditions as Developed from the WATER8 Model for the Tinker AFB IWTF	38
3.1	Descriptive of Atmospheric Stability	56
5.1	Cost Comparison Between Systems	124
6.1	Results from the Coupled Model	143
6.2	Standard Values for Adults	149

CHAPTER 1
INTRODUCTION

During production and maintenance operations at Tinker Air Force Base [AFB] in Oklahoma City, Oklahoma, industrial wastewater streams are generated which contain organic compounds [primarily phenol and methylene chloride]. These streams result from both direct and indirect contact with organic compounds via chemical depainting operations, chemical cleaning processes, and electroplating operations. Organic materials in the combined wastewater are treated at the on-site industrial wastewater treatment facility [IWTF] with unit processes including open surface basins. Some of these treatment processes result in the release of semi-volatile and volatile organic compounds [VOCs] from the wastewater to the ambient air. Because emitted VOCs can create potential health risks for treatment facility workers and the general public in the immediate surrounding areas, Tinker AFB is required to quantify [and report] VOCs released into the atmosphere. Such regulatory reporting can encompass identifying VOC emission sources, estimating emissions from the IWTF, quantifying ambient air concentrations surrounding the facility via dispersion modeling, and evaluating computer-generated numerical concentration estimates with respect to discontinuous field data and an open-path optical remote monitoring system. The focus of this research is on identifying and quantifying phenol and methylene chloride releases and ambient air concentrations surrounding the IWTF located in the northeast quadrant of Tinker AFB.

HYPOTHESIS

Coupling of an appropriate source emission model and an atmospheric dispersion model represents a cost-effective and environmentally-responsible approach for meeting impact prediction and regulatory reporting requirements, as well as problem analysis and pollution prevention needs, associated with emissions of two chemical depainting agents [phenol and methylene chloride] from a liquid industrial wastewater treatment facility.

TESTING OF HYPOTHESIS

Testing of the hypothesis will be accomplished at the IWTP at Tinker AFB located in Oklahoma City in central Oklahoma. Phenol and methylene chloride are used as chemical depainting agents at the base, with the liquid effluent from such uses directed to the on-base IWTF via a wastewater collection system. Hypothesis testing will ultimately be based upon the comparison of three strategies for meeting air quality management requirements: (1) use of the coupled model; (2) use of air quality monitoring data collected via discontinuous air sampling and analysis [referred to herein as *periodic canister monitoring*]; and (3) use of air quality data generated by open-path optical remote monitoring using Fourier Transform InfraRed Spectroscopy [FTIR]. The following activities will be associated with this research and testing of the hypothesis:

(1) Development of the coupled model via review of source emissions models for wastewater treatment unit processes and selection of an appropriate model for phenol and methylene chloride emissions from an IWTF; and via review of atmospheric dispersion models and selection of an appropriate model for local dispersion of phenol and methylene chloride emissions from an IWTF. Coupled modeling will involve using the source emission model to generate emissions data for the dispersion model, and then use of the latter model for calculating ground-level concentrations of the two pollutants in the local environs of the IWTF.

(2) Use of the coupled model in the predictive mode; that is, to develop geographically-based profiles of the ground-level concentrations of phenol and methylene chloride in the nearby environment [at designated specific receptor locations within the local air quality impact region] of the IWTF under differing meteorological conditions, on-base chemical usage practices, and IWTF operating scenarios.

(3) Validation of the predictive accuracy of the coupled model via (a) comparisons and statistical testing of receptor location predictions with air quality data from *periodic canister monitoring*, (b) comparisons and statistical testing of predictions along the open path optical remote monitoring line with measured concentrations

based on FTIR; and (c) comparisons and statistical testing of pertinent field canister monitoring data with open-path monitoring results.

(4) Demonstration of the potential uses, advantages, and limitations of the three air quality management strategies [modeling, canister monitoring, and open-path monitoring] relative to: (a) conduction of site-specific health risk assessments; (b) generation of information for emissions reporting and regulatory compliance determinations for maximum ambient air concentration [MAAC] standards for phenol and methylene chloride; (c) evaluation of on-base process change scenarios and pollution prevention activities regarding the use of phenol and methylene chloride; (d) examination of changes in the design or operation of the IWTF for purposes of minimizing atmospheric emissions of phenol and methylene chloride; and (e) consideration of their applicability for air quality management at U.S. Air Force bases or industrial plants with similar chemical depainting operations.

PROPOSED PLAN OF WORK

The proposed research will be accomplished via completion of four major tasks. The initial task will involve estimating the emissions [emission rates] of phenol and methylene chloride from the individual IWTF process units. Phenol and methylene chloride were chosen because they currently account for over 53 percent [580,000 pounds in 1996] of all targeted hazardous material purchases and releases at Tinker AFB. In addition, phenol and methylene chloride are examples of a semivolatile and volatile organic compound, respectively, which can be used for demonstrating the coupled model strategy.

The second task will focus on quantifying the ambient air concentrations of the two selected chemicals in the environs of the IWTF. Computer simulation software developed by the U.S. Environmental Protection Agency [EPA] will be utilized to estimate treatment process unit emissions [Task 1] and conduct air dispersion modeling [Task 2]. These two models will be used in consonance and thus referred to as the coupled-model approach. Task 3 will focus on validating the predictive accuracy of the coupled model by comparing the estimated computer-generated concentrations with periodic canister monitoring data [Sub-

task 3A] and open-path monitoring [FTIR] data [Sub-task 3B]. As part of the validation task, the field canister data will also be compared to the open-path monitoring data [Sub-task 3C].

The final task will focus on the potential uses of the coupled model methodology. Task 4 will involve the conduction of a health risk assessment of the IWTF local air quality impact region. Health risks associated with phenol and methylene chloride emissions experienced by the general population in the housing community north of the treatment facility, as well as the IWTF personnel, will be quantified. Other comparison of the three strategies, as described above, will be accomplished in the fourth task.

To be more specific, IWTF releases of phenol and methylene chloride will be estimated during Task 1 using a computer simulation model developed by the U.S. EPA. In general, the magnitude of VOC emissions depends on factors such as selected physical and chemical properties of the pollutants, the temperature of the wastewater, and the types and design features of the individual conveyance and process units at the IWTF. The U.S. EPA model that will be employed to estimate phenol and methylene chloride emissions from the IWTF is named WATER8. The WATER8 model utilizes treatment equipment information as the basis for air emission predictions from individual process units. WATER8 also incorporates mass transfer and process unit design information, in addition to selected chemical and physical property data for the targeted chemicals. By inputting process conditions and constraints, WATER8 can be used to determine the waste stream effluent concentrations, the atmospheric release [*i.e.*, air emission rates], and the biodegradation within each individual process units. WATER8 atmospheric outputs [emission rates] will serve as inputs into the air dispersion model to be used in Task 2. The VOC treatability parameters to be used in WATER8 for phenol and methylene chloride have been validated in both pilot-scale testing and at other industrial wastewater treatment facilities, as well as at the Tinker AFB IWTF.

The WATER8 model was selected for use in this research based on several reasons. First, WATER8 and TOXCHEM are the only two emission models for wastewater treatment that adjust Henry's Law constant for target chemicals as a function of wastewater temperature. When

volatilization is the dominant removal mechanism [as with industrial wastewater treatment processes], there is the potential for significant error in the predicted VOC emissions even over a small temperature range. The TOXCHEM model was designed primarily for municipal wastewater treatment while WATER8 was designed specifically for industrial wastewater treatment processes. In addition, WATER8 can be used in conjunction with CHEM8, which is a computer database encompassing 983 chemicals, whereas the TOXCHEM database is limited to 68 chemicals. The larger database for WATER8 would facilitate usage for other VOCs released from industrial waste treatment facilities at U.S. Air Force installations. Finally, WATER8 was chosen because it utilizes a flexible building block approach for simulating common industrial wastewater conveyance / treatment processes.

During Task 2, air dispersion modeling of VOC emissions from the IWTF will be performed using the U.S. EPA Industrial Source Complex Short Term, Version 3 [ISC-ST3] model. The ISC-ST3 model requires inputs related to source type, location, emission strength, selected receptor grid, and hourly average meteorological data consisting of surface conditions and mixing height parameters. The model includes multiple options for calculating the air quality impacts of pollution sources. For example, source emission rates can be held constant throughout the modeling period, or be varied by season, month, day hour-of-day, or other optional time periods. The ISC-ST3 model will be employed to develop geographically based profiles of ground-level, ambient air concentrations in the vicinity [at specific receptor locations within the local air quality impact region] of the IWTF under differing meteorological conditions, on-base chemical usage practices, and IWTF operating scenarios. These ground-level concentration profiles for phenol and methylene chloride will be used, in part, to determine whether Tinker AFB is exceeding any regulatory discharge limits.

The EPA-approved ISC-ST3 model is a widely used dispersion model because it is relevant for analyzing, area, and volume sources in flat or gently rolling terrain with elevations below emission release heights. The model itself is a steady-state Gaussian plume model that includes options for addressing emissions from a wide range of sources at a typical industrial complex. For example, it can be used to model

multiple point source emissions from stacks, stack emissions subject to the effects of aerodynamic downwash due to nearby buildings, and emissions from both isolated and multiple vents.

The short-term ISC model requires hourly meteorological data records to define the conditions for plume rise, transport, and dispersion. It can be used to estimate the concentration or deposition value for each source-receptor combination for each hour of input meteorology, and it calculates user-selected short-term averages, such as one-hour, three-hour, and 24-hour averages. Highest and second-highest concentrations for each averaging time for each receptor can also be determined. Further, the user has the option of selecting averages for the entire period of input meteorology [frequently up to one year]. The regulatory applications of the model are for continuous emissions from industrial source complexes located in rural or urban areas with flat or rolling terrain, and with pollutant transport distances of less then 50 kilometers.

The ISC-ST3 air dispersion model was chosen for this research primarily based on the modeling protocols for the State of Oklahoma permitting process. The general provisions of the protocol require that all modeling to demonstrate compliance with National Ambient Air Quality Standards [NAAQSs] or maximum acceptable ambient concentrations [MAACs] shall be conducted using U.S. EPA steady state models. Several possible model choices were available for the IWTF at Tinker AFB; for example, SCREEN3, COMPLEX1, ISC-ST3, and ISC-LT3. The protocol specifies that any meteorological data from 1984 forward is acceptable. SCREEN3 is primarily a screening model based on a generic range of meteorological data, while COMPLEX1 is a refined model for complex terrain. The IWTF at Tinker AFB is in a simple, essentially flat terrain. Further, the emphasis in this study is on short-term concentrations and their comparisons to relevant 24-hour MAACs; hence, ISC-ST3 was selected over ISC-LT3 [used for long-term concentrations].

In Task 3, the predictive ability of the coupled model will be validated. This validation process will be completed via two sub-tasks. Coupled model output [geographically based profiles of the ground-level concentrations] will be compared to both discontinuous field data [from periodic canister sampling] and concentrations obtained by an open-path

optical remote monitoring system using FTIR. In addition, comparisons and statistical testing of pertinent field canister monitoring data will be made relative to the open-path monitoring results. Canister samples provide a *snapshot* of the air quality at one location, average during the time of collection. The open-path monitoring system yields atmospheric concentrations by differing modulated infrared optical energy to retroreflectors [mirrors] along a physical path that crosses downwind of potential emissions from the IWTF.

Task 4 [demonstration of uses of the coupled modeling strategy] will involve the conduction of a health risk assessment within the IWTF local air quality impact region. The IWTF is located in the northeast quadrant of Tinker AFB, with a small housing addition to the north, an open field and creek system [Soldier Creek] to the south, a four-lane highway on the east [Douglas Boulevard], and a motor-vehicle parking structure to the west. Historically, there has been little concern about chemical exposures in the housing community to the north. Task 4 will quantify the risks to both the population to the north and the wastewater treatment plant workforce. There are two types of risk assessment and dispersions model can play a role in each. These types include chronic [long-term] or acute [short-term] risk assessment. Chronic risk is associated with the concern for pollutants thought to cause effects through an accumulation of exposures over a long period of time. Pollutants that are carcinogenic or suspected to have carcinogenic effects, such as phenol and methylene chloride, are of chronic risk concern; hence, a chronic risk assessment will be accomplished in Task 4.

Risk assessment typically consists of four steps: source assessment, exposure assessment, dose-response assessment, and risk characterization. Dispersion modeling is critical in the exposure assessment phase. Individual lifetime risk at a particular receptor location can be determined from the multiplication of the long-term [for example, five-year average] concentration at that receptor by the unit risk factor. By the use of dispersion modeling, concentrations can be determined at a large number of receptors and multiplied by the appropriate pollutant risk factor. As noted above, the ISC-ST3 model can also be used to determine annual average concentrations; therefore,

it can be used in the health risk assessment study. From this risk assessment, decision-makers can be better informed as to whether the ambient air concentrations of phenol and methylene chloride pose a hazard to the community to the north and the IWTF workforce.

Task 4 will also include a demonstration of how the coupled-model approach [strategy] can be used to demonstrate compliance with emissions reporting and regulatory compliance requirements. For example, the coupled model will be utilized to quantify phenol and methylene chloride concentrations at the boundary of Tinker AFB and to determine compliance relative to their respective MAACs. Other potential uses of this strategy include an evaluation of on-base industrial process change scenarios and pollution prevention activities to minimize the use of chemical depainting agents. In addition, it can be used to evaluate changes in the design or operation of the IWTF for purposes of minimizing atmospheric emissions of phenol and methylene chloride. Perhaps the greatest advantage of this strategy is its anticipated applicability for air quality management purposes at other U.S. Air Force Bases or industrial plants with chemical depainting operations; this issue will also be explored in the final task.

UNIQUENESS OF THIS RESEARCH

There are a number of features of this proposed research effort that are unique. First, no published literature has been identified that addresses air emission modeling, air dispersion modeling, and/or risk assessment of Department of Defense [DOD] wastewater treatment facilities [municipal or industrial]. A related distinctive element is that much of the literature, which has been identified, describes efforts related to modeling air pollutant emissions from municipal wastewater treatment facilities [also called POTWs—publicly owned treatment works] rather than industrial wastewater treatment schemes. The closest identified documentation was related to a health survey conducted by the Agency for Toxic Substances and Disease Registry [ATSDR] for the housing community adjacent to Tinker AFB [1]. Another feature concerns the choice of chemicals. No literature information was identified on emission rates, air dispersion modeling, or risk assessment concerning the two selected chemical depainting agents

[phenol and methylene chloride].

The most unique feature of this research involves the combined use of a source emission model and an air dispersion model within a coupled model for predicting geographically based profiles of ground-level concentrations [phenol and methylene chloride] surrounding the IWTF. No published literature was identified that documents the use of the WATER8 source emission model in conjunction with the ISC-ST3 air dispersion model for predicting ambient air concentrations surrounding an industrial wastewater treatment facility. Further, this research explores the validation of the coupled model via comparisons [with statistical analyses] of model predictions to discontinuous field canister data and open-path monitoring [FTIR] data.

There is limited information related to actually employing the WATER8 model for any purposes related to municipal or industrial wastewater treatment. Most of the identified WATER8 literature is from the initial study [model development] focused on hazardous waste treatment, storage, and disposal facilities. Only minimal information is available on the use of the WATER8 model for predicting emission rates from industrial wastewater treatment processes. Further, there are no documented investigations of chemical depainting agent emissions from industrial wastewater treatment processes using the WATER8 software.

Another feature of this research is the use of an air dispersion model to predict chemical depainting agent [phenol and methylene chloride] concentrations surrounding the IWTF. No published literature was identified on the use of such modeling at DOD industrial [and municipal] wastewater treatment facilities. Further, no documented cases were identified involving modeling of chemical depainting agent concentrations surrounding any private sector IWTF. Existing modeling case studies for other pollutants emitted from wastewater treatment plants are typically focused on the downwind behavior and does not encompass the entire local impact region. In contrast, this research targeted 1200 receptor sites spaced ten meters apart and surrounding the Tinker AFB IWTF. Another distinctive feature involves the use of nine years of meteorological data, whereas much of the published literature is limited to a fraction of a single year [usually several days to

several weeks]. Finally, this research uses the ISC-ST3 air dispersion model to determine compliance with the 24-hour Oklahoma MAAC requirements for phenol and methylene chloride concentrations.

The comparative studies, whereby the coupled model predictions are contrasted with periodic field canister studies and open-path air monitoring data [FTIR], are also distinctive. Information from three canister studies conducted at different times provided more data than a single, short-term sampling routine. The coupled model predictions [and field canister studies] are compared to open-path monitoring data along two Tinker AFB perimeters [three optical paths], whereas most of the literature evaluates a single, downwind path when open-path monitoring is accomplished. The open-path monitoring system at Tinker AFB included multiple retroreflectors that bend the optical path, whereas the literature indicates that most studies are limited to one retroreflector designed to make a single pass along the downwind path [referred to as a monostatic design].

Two chemical depainting agents [phenol and methylene chloride] are analyzed by open-path monitoring in this study; in contrast, much of the published literature involves monitoring primary criteria pollutants or tracer gases [sulfur hexafluoride and carbon tetrafluoride]. Most of the open-path monitoring data reported in published literature is based on limited, short-term tracer gas releases, and comparisons to air dispersion model predictions are not made. Further, open-path monitoring has typically been conducted for other types of industrial sources [industrial complexes, incinerators, petrochemical facilities, landfills, municipal waste sites, Superfund remediation sites, etc.] and has not been directed toward environmental monitoring of IWTF fencelines [facility perimeters].

The final unique feature of this research involves the use of the coupled model to perform a human health risk assessment within the local air quality impact region of the IWTF. The focus is on the housing community population to the north and the IWTF workforce. No published literature was identified on risk assessments for chemical depainting agents released from an industrial wastewater treatment facility.

CONTENTS OF DISSERTATION

This dissertation includes eight chapters. Following this introductory chapter, Chapter 2 is related to the selection of an emission model for use in this research, and to the use of the selected model [WATER8] for determining phenol and methylene chloride emissions from the Tinker AFB IWTF. The third chapter highlights the selection of an air dispersion model and the use of the selected model [ISC-ST3] for predicting short-term and annual average concentrations of phenol and methylene chloride in the immediate environs of the IWTF. Chapter 4 will validate the coupled model predictions with periodic field canister data and will include model calibration and sensitivity analysis. Chapter 5 will compare the coupled model predictions to open-path optical remote sensing monitoring data. Chapter 6 will summarize the chronic health risk assessment conducted for the IWTF workforce and the surrounding community. Chapter 7 will demonstrate other potential uses of this coupled model methodology [*i.e.*, generating information for emissions reporting and regulatory compliance determinations relative to maximum ambient air concentrations, evaluation of on-base process change scenarios and pollution prevention activities, in addition to evaluating changes in the design or operation of the IWTF for purposes of minimizing atmospheric emissions]. Finally, Chapter 8 will summarize the research findings relative to the hypothesis, and the use of the coupled model strategy for various purposes in air quality management.

SELECTED REFERENCE

1. Agency for Toxic Substances and Disease Registry, *Health Statistic Review of the Community Adjacent to Tinker Air Force Base, Oklahoma,* U.S. Department of Health and Human Services, January 1998, Washington, D.C.

CHAPTER 2
SELECTION AND APPLICATION OF AN EMISSION SOURCE MODEL

The Clean Air Act Amendments of 1990 addressed air pollutant emissions from both publicly owned treatment works [POTWs] and industrial wastewater treatment facilities [IWTFs]. These Amendments and related regulations require operators of municipal and industrial treatment facilities to identify in-plant sources and quantify the emissions of VOCs and hazardous air pollutants [HAPs]. Although most IWTFs can be ultimately classified as minor sources, the operators of all such facilities have to identify and quantify atmospheric emission sources. Historically, Tinker AFB IWTF emissions were estimated based on Section 4.3 of the US EPA AP-42 document, with this section including equations for determining evaporative losses from treatment units and collection systems [1]. The AP-42 document contains a flow diagram where each of the collection systems / treatment units are listed along with an appropriate mathematical expression for the specific application. The document includes site specific default parameters, a table of physical and chemical properties of selected chemicals, and example calculations [1]. However, the AP-42 method represents a time-consuming process that must be repeated for each of the individual collection systems / process units and chemicals of interest. In order to simplify the process, computer programs have been developed to provide an efficient means to evaluate the fate of toxic organic chemicals in collection systems and industrial wastewater treatment units, and to quantify atmospheric emissions from such components.

Technical methods for estimating air pollutant emissions include the use of new and innovative models called General Fate Models [GFMs]. GFMs refer to computational models that can be used to develop a mass balance around each specified wastewater unit operation and certain solids handling facilities, as well as the entire treatment facility [2,3,4]. The technical complexity and high cost of direct air monitoring around wastewater treatment facilities prompted the development of GFMs for estimating air pollutant emissions. Most GFMs focus on pathway sources and losses [volatilization, stripping, adsorption, biodegradation, etc.] from the wastewater stream as it moves through the treatment facility.

Using such models, it is possible to estimate emissions from complex treatment configurations while considering split flows, quiescent surfaces, weirs, and drops, as well as aerated, biological, and covered processes or any single operation or process. The outputs from GFMs are typically expressed as the mass of each organic compound emitted into the atmosphere, the portion [mass] that is biodegraded, and the portion in the liquid effluent or related solids removal system [2,3,4].

GFMs are typically designed to be specific for the wastewater treatment facility and particular unit process subject to analysis. Knowledge of facility and process specific data is critical to the calibration and operation of these models. Such necessary data can be divided into three categories: (1) influent wastewater characteristics including wastewater flow rate, temperature, and VOC concentrations, and the ambient temperature and wind speed; (2) physical design characteristics such as unit process dimensions [length, width, and depth], weir characteristics, and other pertinent features [*i.e.*, covered, uncovered, etc.]; and (3) operational data, including the type of biological treatment, air flow rates, return activated sludge, waste activated sludge rates, etc.

GFMs are now widely accepted as a tool for estimating emissions generated from wastewater treatment facilities [2,3,4]. They are particularly advantageous when projecting potential air pollutant emissions under variable existing and future flow conditions and design scenarios. GFMs can also be employed as a planning tool for understanding where emissions are released and the quantities of released compounds, identifying which operational factors are effective in reducing emissions, and the *what if questions* related to emissions when a facility may be expanded and/or changed relative to certain wastewater characteristics [2,3,4].

EVALUATION OF AVAILABLE GENERAL FATE MODELS

Ten computer-based fate and transport models for wastewater treatment were reviewed in relation to their applicability for this research. They include BASTE, CINCI, CORAL, EPA FATE, NOCEPM, PAVE, SIMS, TORONTO, TOXCHEM, and WATER8. BASTE [Bay Area Sewage Toxics Emissions] is a proprietary model developed for a consortium of POTWs

[Bay Area Air Toxics group] in California by the University of Texas at Austin [5]. It is a general fate model that can address split flows, quiescent surfaces, drops, weirs, aerated processes, biological processes, and covered processes. BASTE uses a flexible building block approach for simulating the liquid treatment train. However, like most of the models, BASTE lacks a temperature correction feature for Henry's Law coefficients for specific VOCs. When volatilization is the dominant removal mechanism, this could lead to significant error in the predicted VOC emissions even if the temperature range is small.

CINCI [U.S. EPA Cincinnati model] was developed at the University of Cincinnati for the EPA Risk Reduction Engineering Laboratory [5]. CINCI includes some model components selected from the literature; for example, sorption correlations. CINCI also makes use of group contribution and neural network approaches. CORAL [Collection System Organic Release Algorithm] is a fate model that simulates two-phase, transient VOC transport and gas-liquid partitioning in enclosed wastewater treatment systems, including collection reaches [5]. Thus, CORAL is the only computer-based simulation designed to model VOC stripping in enclosed sewer networks. However, CORAL does not account for sorption and biodegradation in treatment processes. The EPA FATE [Fate and Treatability Estimator] model was developed by ABB Environmental for the EPA Office of Water Regulations and Standards [4,5]; it is designed for municipal wastewater treatment systems. NOCEPM [NCASI Organic Compound Elimination Pathway Model] was developed by the National Council of the Paper Industry for Air and Stream Improvement [NCASI] [5]. NOCEPM is similar to the CINCI model in that it consists of various conceptual model components selected from the available literature. However, it is limited to modeling only activated sludge and aerated lagoon systems in terms of the fate of VOCs typically found in these unit processes in paper and pulp wastewater treatment systems.

PAVE [Programs to Assess Volatile Emissions] refers to a set of computer models for determining volatile emissions from wastewater treatment units and spills of liquid solutions [5]. It was developed by the Chemical Manufacturers Association to simulate only complete-mix activated sludge systems and VOC emissions from chemical spills or either pure components or binary mixtures. PAVE does not account for

sorption of VOCs on various solids. SIMS [Surface Impoundment Modeling System—1990] was developed by Radian Corporation for the U.S. EPA Office of Air Quality Planning and Standards [2,3,4,5]. This broad scale model was used as a means for determining the expected air pollutant emissions from IWTFs on a nation-wide basis; thus, it served as a tool to produce rule-making support data. SIMS was later replaced with the more specific WATER8 model. The TORONTO model can be used for evaluating the fate of organic chemicals in a biological wastewater treatment facility [5]; it was developed by the Institute of Environmental Studies at the University of Toronto.

TOXCHEM is comprised of several conceptual model components selected from the literature to address the fate of contaminants through all stages of municipal wastewater treatment [2,5]. The physical and chemical properties database within TOXCHEM addresses 68 chemicals. Further, TOXCHEM allows for the adjustment of Henry's Law constant for VOCs in its database as the wastewater temperature changes. TOXCHEM is the only proprietary model with unsteady state capability that allows the prediction of an industrial facilities response to a spill condition. This model also addresses the fate of VOCs in aerobic and anaerobic sludge digesters. Treatability parameters for VOCs as included in TOXCHEM have been validated at both the pilot-scale and in specific studies conducted at municipal treatment facilities.

Finally, WATER8 is a fate and transport model developed for aerated and non-aerated wastewater treatment processes and impoundments [2,3,4,5]. It is used in conjunction with CHEM8, which is a database containing information on pertinent physical and chemical properties of 983 compounds. WATER8 was developed by the Research Triangle Institute for the U.S. EPA Office of Air Quality Planning and Standards. Similar to BASTE, it also utilizes a building block approach; however, WATER8 does allow for adjustment of Henry's Law constant for pertinent VOCs as a function of wastewater temperature [5].

The weakness of most GFMs, except for WATER8 and TOXCHEM, is the lack of inclusion of a temperature correction for the Henry's Law constant. As noted earlier, for VOCs in industrial wastewater treatment systems, volatilization is often the dominant removal mechanism; thus, the absence of such correction could result in significant errors

related to quantification of atmospheric emissions. Also, other than PAVEs treatment of binary mixtures, the remaining nine models neglect possible interactions between target chemicals. NOCEPM, PAVE, SIMS, and WATER8 are based on industrial wastewater treatment systems, while the other six are focused on municipal wastewater applications where the dominant treatment process is biological degradation.

No information was found from an extensive literature review, which documented the coupling of the WATER8 model with the ISC-ST3 model for predicting ambient air concentrations surrounding the IWTF. In fact, there is limited information regarding any uses of the WATER8 air emission model. Most of the WATER8 information is from the initial study [model development] concerning hazardous waste treatment, storage, and disposal facilities [2,3,4]. Further, there are no documented investigations of chemical depainting agent emissions from industrial wastewater treatment processes using the WATER8 software.

In summary, the WATER8 source emission model was selected for use in this study because: (1) it had been developed and validated by the U.S. EPA for use in relation to industrial wastewater treatment plants; and (2) it incorporated several desirable features for this research and related uses, including the use of a *building block* approach based on unit treatment processes and the incorporation of a temperature correction for Henry's law constant for the two targeted chemicals. Further, the absence of any detailed studies of phenol and methylene chloride emissions using the WATER8 model suggested a possible unique contribution of this research.

DETAILED DESCRIPTION OF WATER8 AIR EMISSION MODEL

The WATER8 software program was developed by the U.S. EPA in response to federal, state, and local needs for a methodology to estimate emissions from surface impoundments and collection system components located in hazardous waste treatment, storage, and disposal facilities; POTWs; and other industrial wastewater treatment processes [2,3,4]. The user is required to input information related to the total flow rate to the treatment system, equipment features, type of impoundment [basin], impoundment or collection system component surface area, order of treatment units, and industrial chemicals, processes or

categories discharged to the system [2,3]. Based on this input, the program then assigns typical default values to all other input parameters required by the model. WATER8 is also designed to allow the more knowledgeable user to replace most of the computer-assisted default values with actual data when they are available [2,4,6].

By inputting influent concentrations of target chemicals, WATER8 can be used to determine the wastewater effluent concentration, releases to the atmosphere, and the amount of the organic constituent biologically degraded in each individual process unit [2,3,6].

As mentioned above, the default values can be replaced with actual data. This would provide a more realistic estimation of atmospheric emissions. To obtain this higher level of accuracy, WATER8 requires more detailed information [*i.e.*, equipment size, equipment specification, process unit flow rates, detention times, aeration capabilities, etc.] as input. In addition to needing the physical dimensions of each process unit, the method of operation is also required [*i.e.*, mechanically aerated process, diffused air aeration, non-aerated process, biodegradation, no biodegradation, etc.]. The program then utilizes this process information, in addition to physical and chemical property information on the target chemicals, to estimate liquid effluent concentrations and air pollutant emissions.

Several physical and chemical pathways within unit processes were considered in the development of the WATER8 model. The majority of the atmospheric releases are assumed to be driven by volatilization and biodegradation mechanisms. The rate of volatilization is based on the two-film resistance theory, which assumes that the rate-limiting factor for volatilization is the overall resistance to mass transfer at the interface of the liquid surface and the ambient air. The overall resistance is due to individual resistances in the liquid and gas phase films at the interface. Collection and treatment processes at the Tinker AFB IWTF that are driven primarily by the volatilization mechanism include the primary clarifier, diversionary structures, storage [stabilization] tanks, equalization basins, and mixing basins. The biodegradation mechanism is dominant in the aerobic biological digesters [aeration basins]. Emissions from solid contact clarifiers and final [secondary] clarifiers are a function of both volatilization

and biodegradation processes.

As wastewater flows through a treatment unit, organic compounds diffuse through the water to the liquid surface. Such compounds then volatilize into the ambient air above the liquid surface in an attempt to reach equilibrium between the liquid and vapor phases. Since organic vapors above the liquid are in contact with the ambient air, these organic vapors can be further swept into the air by wind blowing across the surface of the treatment unit. Factors affecting atmospheric emissions from clarifiers and other well-mixed, flow-though impoundments [diversionary structures, storage tanks, equalization basins, and mixing basins] include the wastewater characteristics, wind speed, and treatment unit design characteristics. Increases in wastewater temperature, concentrations of organic compounds and their physical properties such as volatility and diffusivity in water, can also serve to increase atmospheric emission rates. Increases in hydraulic detention time in the treatment unit also increase such emissions. Another important physical characteristic in an IWTF is the clarifier waterfall drop height defined as the distance the effluent falls from passing over the weir to the bottom of the perimeter of the clarifier. Greater heights result in more atmospheric emissions because of the cascading effect that increases the surface area of the water exposed to the ambient air and wind influences.

Oil-water separators are often the first unit process in an IWTF. The purpose of these units is to separate and remove oils, scum, and solids contained in the wastewater [7]. Most of the separation occurs as the influent wastewater passes through a quiescent zone in the unit. Oils and scum with a specific gravity less than water flow to the top of the aqueous phase, while heavier solids sink to the bottom. For this reason, VOCs are removed with the skimmed oil leaving the separator. The wastewater stream leaving the separator is thus decreased in organic loading.

Volatilization of organic compounds from the surface of an oil-water separator involves a complex mass transfer phenomenon. For example, most organic compounds tend to partition to the oil phase, which floats to the surface of the separator. The force behind the volatilization then becomes the drive to reach equilibrium between the concentration of

organics in the oil layer and the vapor phase just above this layer. Organic compounds volatilizing into the vapor phase either diffuse or are swept by the wind into the ambient air surrounding the oil-water separator. Therefore, factors affecting atmospheric emissions from oil-water separators include the characteristics of the wastewater and oil layers, ambient wind speed, design characteristics of the separator, the water and air temperatures, and the concentration and physical chemical properties of the organic compounds contained in the wastewater.

Equalization basins are used in many IWTFs to reduce fluctuations in wastewater flow and organic content introduced to downstream treatment processes. Equalization of wastewater flow rates results in more uniform effluent quality from downstream settling units such as clarifiers. Biological treatment units also benefit from the damping of concentration and flow fluctuations. This damping protects biological processes from upset or failure due to shock loading of toxic or treatment-inhibiting compounds. Equalization basins use hydraulic detention time to ensure equalization of the wastewater effluent from the basins. Basins are typically equipped with mixers to promote equalization of the concentration of organic compounds. Further, as wastewater flows through equalization basins, organic compounds can diffuse through the water to the liquid surface. These compounds then volatilize into the ambient air above the liquid surface in an attempt to reach equilibrium between the liquid and vapor phases. Since the organic vapors above the liquid are in contact with the ambient air, they can be further swept into the air by wind blowing across the basin surface.

The component for biodegradation in the WATER8 model requires the treatment units biomass concentration as an input parameter. However, the concentration of biomass in actual treatment systems can be highly variable depending upon the design and method of operation [3,8,9]. Biological wastewater treatment is normally accomplished through the use of aeration basins, whereby aerobic treatment involves the degradation of organic constituents by microorganisms suspended in the reaction tank [*i.e.*, aeration basins]. The biomass of microorganisms requires oxygen to carry out the biodegradation of organic compounds, with the degradation resulting in energy and biomass production. The aerobic

environment [oxygen] in the basin is normally accomplished by the use of diffused or mechanical aeration. This aeration also serves to maintain the biomass in a well-mixed regime, with the goal being to maintain the biomass concentration at a level where the treatment is efficiently optimized and appropriate kinetics are accomplished. The performance of aeration basins is particularly affected by the mass of organic per unit area, temperature and wind patterns, hydraulic detention time, dispersion and mixing characteristics, sunlight energy, characteristics of the solids in the influent, and the quantity of essential microbial nutrients present.

Aeration basins are typically equipped with aerators to introduce oxygen into the wastewater [6,7]. The biomass uses a portion of this oxygen in the process of biodegrading the organic compounds. Further, aeration of wastewater also affects atmospheric emissions. For example, during aeration an increased liquid surface area is exposed to ambient air; and, due to the turbulence caused by the aerators, the liquid and gas phase resistances to mass transfer are reduced. This transfer mechanism significantly increases atmospheric emissions as compared to the emissions from relatively quiescent clarifiers.

GOVERNING AIR EMISSION MODEL EQUATIONS

Predictive emission models have been developed to predict emission rates from hazardous waste treatment sites. The emission rates are calculated by determining the mass transfer coefficient of the chemical or chemical compound of interest [2,3]. Volatilization, which is often the most important mechanism for VOC emissions, occurs when molecules of a dissolved compound escape to an adjacent gas layer [2,3]. The rate of volatilization at a liquid-air interface is a function of the concentration and properties of releasing organics [volatility, vapor pressure, etc.], wastewater properties, and surrounding conditions of the air and wastewater [7]. The mass-transfer between two or more phases within a system is developed primarily from two-film resistance theory of mass transfer and is represented by a mass transfer coefficient [2,3,7]. This theory has two principal assumptions: (1) the rate of mass transfer between the two phases is controlled by the rates of diffusion through the phases on each side of the interface, and (2)

no resistance is offered to the transfer of the diffusing component at the interface itself. The latter implies that the concentration of each component in its respective phases [liquid or gas] at the interface is defined by the equilibrium constant [7]. For aqueous systems, the basic relationship describing the mass transfer of a volatile constituent from the open liquid surface to the air is:

$$E = K_O A C_L \qquad 2.1$$

where E is defined as the air emissions from the liquid surface [g/sec], K_O is the overall mass transfer coefficient [m/sec], A is the liquid surface area [m^2], and C_L is the concentration of the constituent in the liquid phase [g/m^3].

The overall mass transfer coefficient will be in the form of a series of individual mass transfer coefficients and the equilibrium constant. The overall mass transfer coefficient is estimated from a two-phase resistance model that is based on the liquid-phase mass transfer coefficient [K_L], gas-phase mass transfer coefficient [K_G], and Henrys law constant in the form of a partition coefficient [K_E]. The equilibrium constant [K_E] for vapor-liquid equilibrium represents the chemical partitioning between the phases at the steady state. Equilibrium is assumed to exist at the interface of the vapor and the liquid [7].

There are several ways of determining the values for the vapor-liquid equilibrium constant. In some cases, values obtained from the results of vapor-liquid equilibrium experiments can be found in the literature. For other compounds, equilibrium constants can be calculated from Henrys law constants. The following is a discussion of mass transfer fundamentals employed in the air emission model.

The mass transfer coefficients K_L and K_G in liquid and air phases are critical variables in estimating emission rates from liquid surfaces. The liquid-phase mass transfer coefficient has been shown to be a function of the constituent's diffusivity in water, windspeed, and liquid depth. The values of K_L and K_G have been investigated by several researchers [2,3,7]. Two simplified equations have been developed for surface impoundments, based on experimental studies [2]:

$$K_L = 0.00445\ MW^{-0.5}\ [1.025]^{t-20}\ U_{10}^{0.67}\ H_d^{-0.85} \left[\frac{D_w}{D_{ether}}\right]^{0.67} \qquad 2.2$$

where K_L is the liquid-phase mass transfer coefficient [g-mol/cm^2-sec], MW is the molecular weight of the compound [g/g-mol], t is the temperature [°C], U is the surface velocity [cm/sec] at ten meters elevation, H_d is the depth of the impoundment [cm], D_w is the diffusivity of the constituent in water [cm^2/sec], and D_{ether} is the diffusivity of ether in water [cm^2/sec]; and:

$$K_G = 0.0008\, MW^{-1}\, W^{0.78}\, Z^{-0.11}\, N_{Sc}^{-0.67} \qquad 2.3$$

where K_G is the gas-phase mass transfer coefficient [g-mol/cm^2-sec], MW is the molecular weight of the compound [g/g-mol], W is the wind speed [m/hr], Z is the length of the impoundment [m], and N_{Sc} is the gas-phase Schmidt Number [dimensionless]. Most Schmidt Numbers lie between 1.0 to 3.0, the higher values applying to high molecular weight compounds with low diffusivities. For most hydrocarbons and chlorinated hydrocarbons with molecular weights above 200, a suggested value of 0.5 may be used for $N_{Sc}^{-0.67}$. The suggested value was obtained from approximation, and the possible error introduced by this approach should be less than ten percent [7].

The overall mass transfer coefficient, K_O, can be expressed in terms of combining the two identical phase mass transfer coefficients, K_L and K_G, as shown below:

$$\left[\frac{1}{K_O}\right] = \left[\frac{1}{K_L}\right] + \left[\frac{1}{K_E K_G}\right] \qquad 2.4$$

where K_E is the constant establishing the equilibrium between the liquid and gas phases, expressed by

$$K_E = \left[\frac{H_c}{P\,MW}\right] \qquad 2.5$$

where H_c is the Henrys law constant of the compound [atm-m^3/mol], P is the total pressure [atm], and MW is the average molecular weight of the liquid [g/mol].

APPLICATION OF THE WATER8 MODEL TO THE TINKER AFB IWTF

In various production and maintenance operations at Tinker AFB, wastewater streams are generated which contain many organic compounds, including phenol and methylene chloride. These wastewaters are collected and treated via several unit processes in an IWTF. Many of the unit processes are open to the atmosphere and thus allow organic-containing wastewaters to contact ambient air; as a result, VOC emissions to the atmosphere take place. The magnitude of such VOC emissions depends on the physical and chemical properties of the pollutants, the temperature of the wastewater, the design of the individual collection and treatment process units, and the amount of biological degradation that occurs.

The Tinker AFB IWTF has several levels of treatment [*i.e.*, primary, secondary, and tertiary]. Figure 2.1 includes the current process flow diagram. The IWTF receives wastewater from two main sources and treats an average of 835,000 gallons per day [GPD]. The paint stripping process effluent [containing phenol and methylene chloride] accounts for approximately ten percent of the wastewater flow [76,700 GPD] and is discharged into the stripping waste primary clarifier [PC]. This wastewater stream contains high concentrations of a methylene chloride / phenol-based chemical depainting agent [Toxic Release Inventory listed chemicals]. From the PC, the paint stripping process effluent is discharged to the covered D_1-D_2 blending tanks before being blended with the majority of the IWTF influent at the oil-water separator diversionary [OWD] structure. The IWTF receives about 90 percent of the daily wastewater flow from the industrial complex [*i.e.*, Building 3001, etc.] via lift station #2 just upstream of the OWD.

Both streams are blended into the OWD just upstream of the two oil-water separators [OW-North and OW-South]. The oil-water separators were depicted in the WATER8 model as flow-through, oil-film surface impoundments [American Petroleum Institute or API separators] with no biodegradation. The physical design parameters for the separators include a total covered surface area of 525 m^2, liquid depth of 3.30 meters, detention time of 3.08 hours, wastewater temperature of 25°C, wind speed of 4.47 meter per second, and ambient pressure of one

atmosphere. The oil fraction used in the design was 0.20 percent as based on the chemical profile of the wastewater. Figure 2.2 illustrates the average ambient wind speed employed in the WATER8 model. The annual average ambient wind speed was 4.26 meters per second. During the sampling period, the average wind speed was 4.47 meters per second.

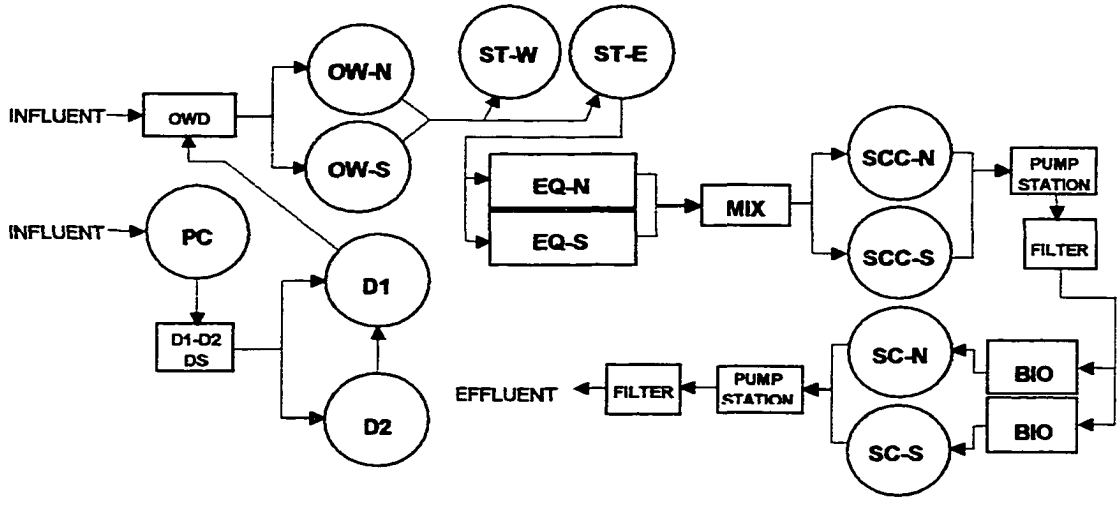

Figure 2.1: IWTF Process Flow Diagram at Tinker AFB

Following OW-N and OW-S, the wastewater passes through two batch-operated 1.1 million-gallon storage [stabilization] tanks [ST-West and ST-East] and into two equalization basins [EQ-North and EQ-South] to equalize the downstream flow. The open flow-through circular storage tanks are modeled in WATER8 as mechanically aerated surface impoundments with no biodegradation. Physical dimensions include a total surface area of 843 m^2 with a liquid depth of 10.7 meters. Operational parameters include a detention time of 35.1 hours, wastewater temperature of 25°C, wind speed of 2.5 meters per second, and two mechanical aerators each. Each aerator has a total power of 30 HP, turbulent surface area of one percent, impeller speed of 6.0 radians per second, impeller diameter of 15.0 centimeters, and an impeller power efficiency of 20 percent. The oxygen rating of each mechanical aerator is 0.60 pounds of O_2 per HP-hour, with an oxygen transfer correction factor of ten percent. Note that the wind speed in all other process unit applications was 4.47 meters per second while the 1.1 million-gallon storage [stabilization] tanks employed 2.5 meters per second. The lower wind speed was used to adjust for fluctuations in the wastewater

level of the tanks. The two tanks are batch operated, whereby one tank is filled while the other tank is emptied. The surface area exposed to wind currents will be impacted by the depth of the wastewater in the tank, thereby indirectly affecting volatile organic compound losses. The wind speed was lowered to adjust for differences in VOC emissions as the surface area exposed to wind currents [water level] changes within each stabilization tank.

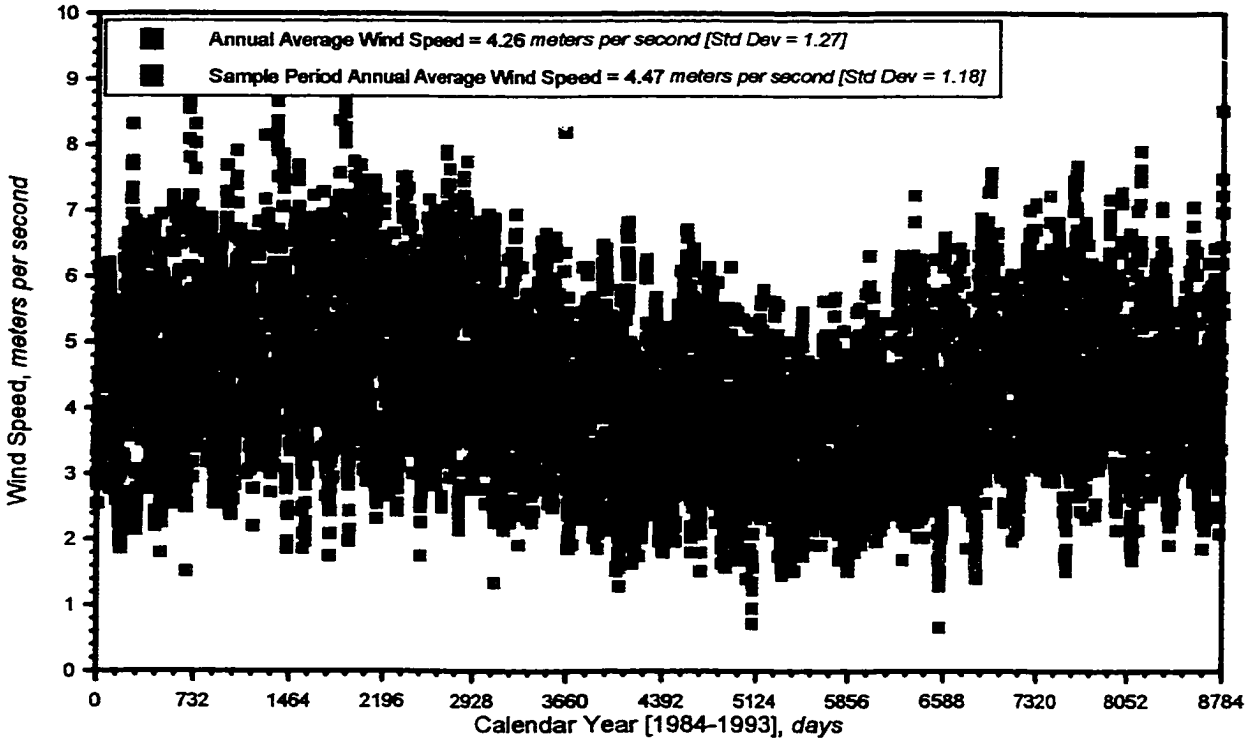

Figure 2.2: Average Ambient Wind Speed used in WATER8 Model

The equalization basins are also modeled in WATER8 as flow-through mechanically aerated surface impoundments with no biodegradation. The physical dimensions of the basins include a total surface area of 929 m^2 with a liquid depth of 3.05 meters. The operational parameters include a detention time of 10.7 hours, temperature of 25°C, and wind speed of 4.47 meters per second. There are two surface aerators per basin, with each delivering 30 HP with an impeller speed of 180 radians per second, impeller diameter of 21.6 centimeters, and a power efficiency of 73 percent. The oxygen rating of each surface aerator is 3.0 pounds of O_2 per HP-hour, with an oxygen transfer correction factor of 83 percent. These oxygen ratings are considerably greater than those for the

aerators in the storage tanks; this is because the equalization basin aerators were designed to volatilize organics while the storage tank aerators were designed to only agitate the liquid contents.

Following the primary treatment portion of the IWTF, the wastewater then enters the metals treatment process, whereby hexavalent chromium is reduced and the metal hydroxides are precipitated. Mixing basins #1 and #2 [MIX] are similar in size and modeled within WATER8 as flow-through mechanically agitated treatment tanks with no biodegradation. The surface area is 16.9 m^2 with a liquid depth of 4.88 meters. Operational parameters include a detention time of 0.626 hours, temperature of 25°C, and a wind speed of 4.47 meters per second. There is one variable-speed agitator each in mixing basins #1 and #2, and each mixer delivers 0.25 HP with an impeller speed of 126 radians per second, impeller diameter of 5.0 centimeters, and a power efficiency of 85 percent. The oxygen rating of each mixer is 3.0 pounds of O_2 per HP-hour with an oxygen transfer correction factor of 83 percent. Mixing basin #3 was also modeled as a flow-through mechanically agitated surface impoundment with no biodegradation. The surface area is 7.52 m^2 with a liquid depth of 3.20 meters. Operational parameters include a detention time of 0.183 hours, temperature of 25°C, and wind speed of 4.47 meters per second. There is one mixer delivering 0.30 HP with an impeller speed of 126 radians per second, impeller diameter of 73.7 centimeters, and a power efficiency of 85 percent. The oxygen rating of the single variable-speed mixer is 3.0 pounds of O_2 per HP-hour with an oxygen transfer correction factor of 83 percent.

From the metals treatment process, the wastewater is directed through a diversionary structure into one of two solid contact clarifiers [SCC-North and SCC-South]. The SCCs are operated with a sludge blanket to filter metal hydroxide flocs and clarify the wastewater. The SCCs were modeled in WATER8 as flow-through surface impoundments. The total surface area is 525 m^2 with a liquid depth of 4.14 meters. Operational parameters include a detention time of 6.64 hours, temperature of 25°C, and wind speed of 4.47 meters per second.

From the SCCs, the wastewater is then passed through multimedia pressure filters and into two aeration basins [*i.e.*, aerobic biological reactors] utilizing a step-aeration feed system. These basins [BIOs]

were modeled in WATER8 as flow-through mechanically aerated surface impoundments with an activated sludge process. The total exposed surface area is 260 m^2 with a liquid depth of 5.49 meters. Operational parameters include a detention time of 5.42 hours, temperature of 25°C, wind speed of 4.47 meters per second, and biomass concentration of 4,000 grams per m^3. There are 48 air spargers delivering 120 HP with an impeller speed of 126 radians per second, impeller diameter of 5.0 centimeters, power efficiency of 85 percent, and a turbulent surface area of 52 percent. The oxygen rating of the spargers is 3.0 pounds of O_2 per HP-hour with an oxygen transfer correction factor of 83 percent. Finally, the wastewater is discharged into two clarifiers for secondary clarification. These secondary clarifiers [SC-North and SC-South] were modeled as flow-through non-aerated surface impoundments with biodegradation. The total surface area is 441 m^2 with a liquid depth of 3.70 meters. Operational parameters include a detention time of 5.10 hours, temperature of 25°C, wind speed of 4.47 meters per second, and biomass concentration of 50 grams per m^3. The wastewater is then passed through additional multimedia garnet pressure filters and discharged to a lift station for transport to the Oklahoma City Public Owned Treatment Works [POTW] for final treatment.

The chemicals of primary interest are phenol and methylene chloride [chemical depainting agents] because they have historically accounted for over 50 percent of all targeted hazardous materials purchased and released at Tinker Air Force Base. Figure 2.3 illustrates the IWTF influent [primary waste clarifier] concentration for phenol for CY96 [calendar year 1996] with an average concentration of 522 milligrams per liter [mg/L]. Figure 2.4 is a histogram or frequency distribution for the influent phenol concentration, which provides a visual impression of the shape of the distribution of the measurements as well as information about the scatter or dispersion of the data. The coupled model annual average phenol calculations [to be described later] were based on the average influent concentration of 522 mg/L. The coupled model 24-hour maximum calculations were based on the maximum phenol concentration occurring one percent of the time. The maximum concentration was determined using probability tables for normally distributed data, thus the concentration occurring one percent of the time was determined to be

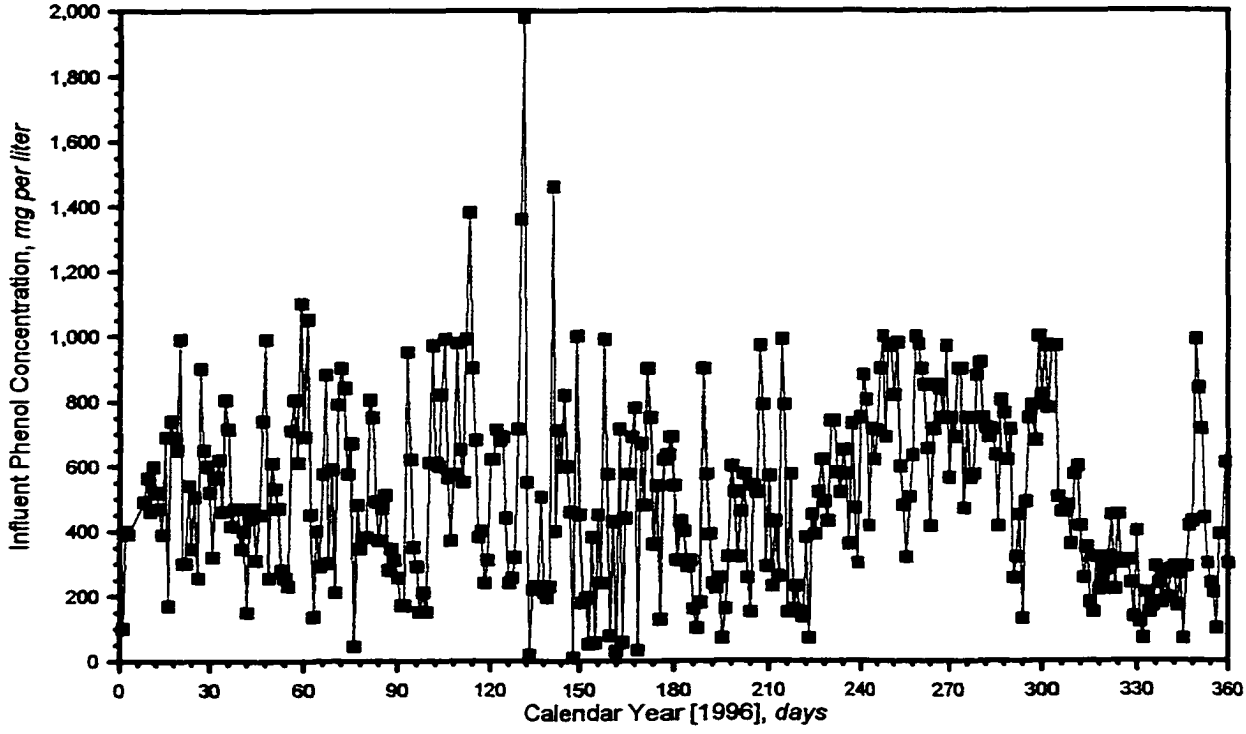

Figure 2.3: Primary Stripping Waste Clarifier Influent Phenol Concentration

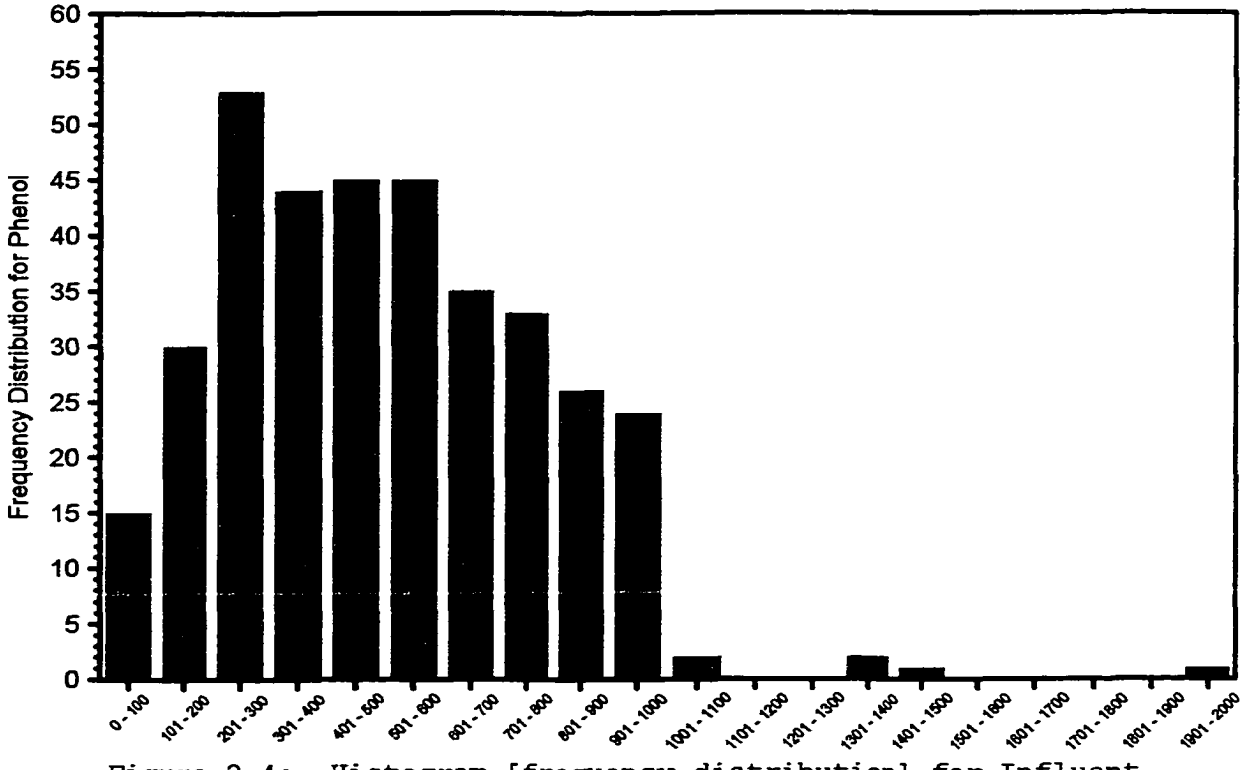

Figure 2.4: Histogram [frequency distribution] for Influent Phenol Concentration [mg per liter]

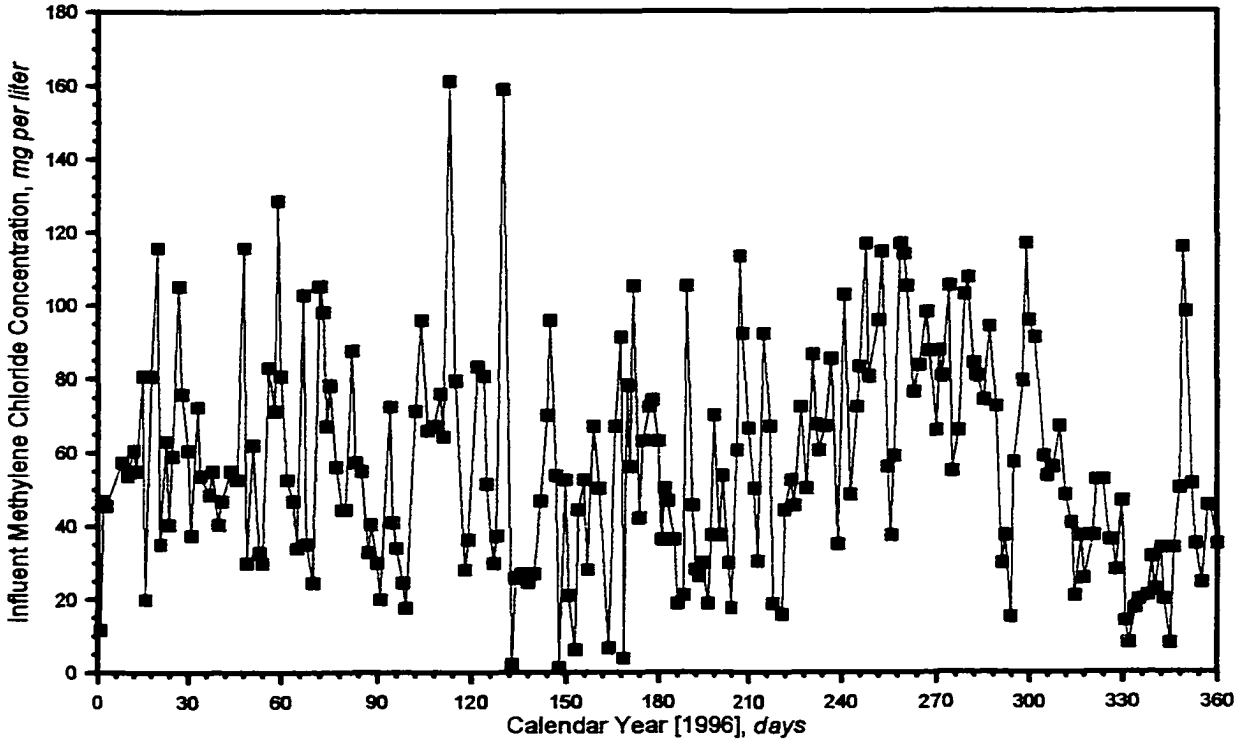

Figure 2.5: Primary Stripping Waste Clarifier Influent Methylene Chloride Concentration

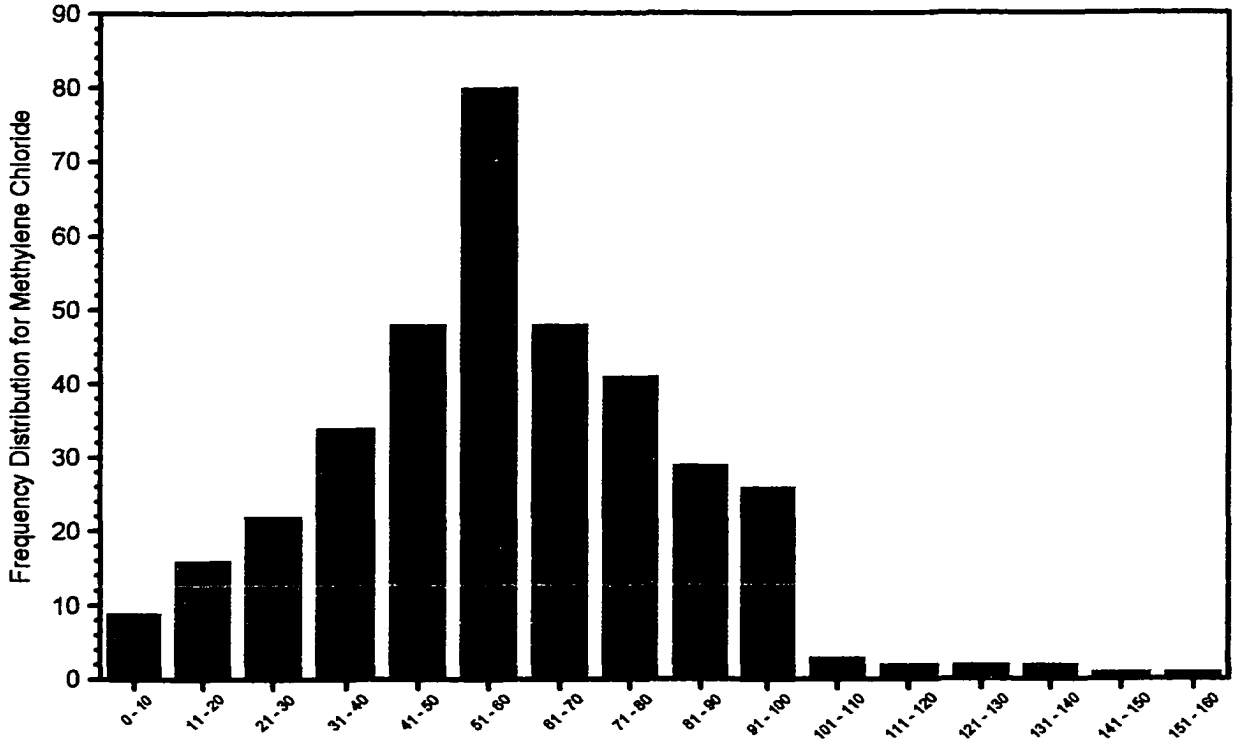

Figure 2.6: Histogram [frequency distribution] for Influent Methylene Chloride Concentration [mg per liter]

1,180 mg/L.

Figure 2.5 illustrates the IWTF influent [primary waste clarifier] concentration for methylene chloride for CY96; the average concentration was 57.1 mg/L. Figure 2.6 is a histogram or frequency analysis for the influent methylene chloride concentration. The coupled model annual average methylene chloride calculations [to be described later] were based on the average influent concentration of 57.1 mg/L. The coupled model 24-hour maximum calculations were based on the maximum methylene chloride concentration occurring one percent of the time. Based on the probability tables for normally distributed data, the maximum methylene chloride concentration occurring one percent of the time was determined to be 127 mg/L.

WATER8 MODELING RESULTS

By reviewing the WATER8 output [*i.e.*, emission rates, emission factors, etc.], intuitive [qualitative] determinations can be made of the location of the major air emission sources at the Tinker AFB IWTF. Table 2.1 contains WATER8 modeling outputs illustrating atmospheric emissions from specific process units at the IWTF. For example, from the primary clarifier, 16 percent of the methylene chloride losses occur from the open clarifier surface, 3.3 percent from the weir waterfall, while less than 0.39 percent is absorbed in the underflow and disposed with the sludge. The total methylene chloride emitted to the atmosphere from the primary clarifier is 19 percent. For the less volatile phenol, 1.8 percent is lost from the open clarifier surface, 0.020 percent is associated with the weir waterfall losses, and approximately 0.41 percent is lost to the underflow. The total atmospheric emissions of phenol from the primary clarifier is 1.8 percent. These results illustrate the influence of volatility on the total emissions to the ambient air relative to the influent concentrations. For methylene chloride, 19 percent is released, while for phenol the number is an order of magnitude less [1.8 percent]; however, phenol has nine times greater concentration [522 versus 57 milligrams per liter] entering the primary clarifier. This difference will be addressed when the actual mass of the atmospheric releases is addressed.

For the D_1-D_2 blending tanks [covered], the atmospheric emission

losses are composed of the tank working losses and tank breathing losses. Methylene chloride working and breathing losses are 3.3 and 1.2 percent, respectively, while similar losses for phenol total 0.0015 and 0.0030 percent. For the oil-water diversionary structure, the total percent volatilized for methylene chloride and phenol are very small at 0.015 and 0.0033, respectively.

The API oil-water separator component in the WATER8 model is composed of three separate zones in the process unit. The percent of the methylene chloride lost from the open surface is 0.22, from the oil layer it is 54, and from the weir waterfall it is 5.3. The percent of methylene chloride lost to the oil phase is 3.4 percent. Methylene chloride emissions to the atmosphere total 56 percent. As expected, the majority of the methylene chloride mass transfer to the atmosphere occurs from the oil layer phase. Phenol losses are considerably less, with open surface losses at 0.013 percent, the oil layer at 0.63 percent, and the weir waterfall at 0.0056 percent. The amount of phenol associated with the oil phase is 5.5 percent. The total combined atmospheric emissions for phenol are 0.65 percent, which is approximately two orders of magnitude less than the methylene chloride losses [56 percent]. It is interesting to note that while the open surface losses, oil layer losses, and weir waterfall losses are almost two orders of magnitude different, the amount of methylene chloride and phenol in the oil phase is about the same [3.4 percent versus 5.6 percent].

For the 1.1 million-gallon storage [stabilization] tanks [uncovered], the total open tank volatilization losses for methylene chloride and phenol are 3.9 and 0.17 percent, respectively. These tanks were modeled differently than the covered D_1-D_2 blending tanks, whose emissions are composed of the tank working and breathing losses. The uncovered storage tanks do not have breathing and working losses because of the open tank design.

For the surface aerated equalization basins, the percent of methylene chloride volatilized to the air is 94 percent, while the corresponding number for phenol is 2.4 percent. The equalization basins are another striking example of the influence of component volatility, with the more volatile constituent [methylene chloride] exhibiting

Table 2.1: Atmospheric Emissions[a] from the Tinker AFB IWTF as Generated by the WATER8 Model

PROCESS UNIT	METHYLENE CHLORIDE	PHENOL
Primary Clarifier		
▪ *fraction lost from open surface*	0.16	0.018
▪ *fraction lost from weir waterfall*	0.033	0.00020
▪ *fraction absorbed in underflow*	0.0039	0.0041
▪ *total fraction lost to the air*	0.19	0.018
D_1-D_2 Blending Tanks		
▪ *tank working losses*	0.033	0.000015
▪ *tank breathing losses*	0.012	0.000030
Oil-Water Diversionary Structure		
▪ *total fraction volatilized*	0.00015	0.000033
API Separator		
▪ *fraction lost from open surface*	0.0022	0.00013
▪ *fraction lost from oil layer*	0.54	0.0063
▪ *fraction lost from weir waterfall*	0.054	0.000056
▪ *total fraction lost to the air*	0.56	0.0065
▪ *fraction absorbed*	0.011	0.038
Circular Storage Tanks		
▪ *open tank volatilization loss*	0.039	0.0017
Equalization Basins		
▪ *total fraction volatilized*	0.94	0.024
Mixing Basin #1		
▪ *total fraction volatilized*	0.15	0.00026
Mixing Basin #2		
▪ *total fraction volatilized*	0.15	0.00026
Mixing Basin #3		
▪ *total fraction volatilized*	0.14	0.00014
Solid Contact Clarifiers		
▪ *fraction lost from open surface*	0.11	0.0037
▪ *fraction lost from weir waterfall*	0.020	0.000013
▪ *total fraction lost to the air*	0.13	0.0037
Bioreactor		
▪ *fraction surface volatilized*	0.80	0.000085
▪ *fraction submerged volatilized*	0.017	0.0000014
▪ *total fraction volatilized*	0.81	0.000086
▪ *fraction biologically removed*	0.17	0.997
Secondary Clarifiers		
▪ *fraction lost from open surface*	0.13	0.0037
▪ *fraction lost from weir waterfall*	0.021	0.000015
▪ *total fraction lost to the air*	0.15	0.0037

a: expressed as a fraction of the influent

considerable more losses to the surrounding environment.

The percent of methylene chloride volatilized in the metals treatment process is 15 percent [mixing basin #1], 15 percent [mixing basin #2], and 14 percent [mixing basin #3]. For phenol, the corresponding numbers are 0.026 percent, 0.026 percent, and 0.014 percent. From the metals treatment process, the wastewater passes through two solid contact clarifiers. For methylene chloride, the SCC losses are from the open clarifier surface [11 percent] and weir waterfall [2.0 percent], with a total emission to the air of 13 percent. The total percent of phenol emitted to the air is 0.37 percent, which is considerably less than the methylene chloride emissions of 13 percent.

The losses in the activated sludge units [bioreactors or BIOs] are the fractions surface volatilized, submerged volatilized, and biologically removed. For methylene chloride, the surface losses are 80 percent, with a total percent volatilized of 81 percent. The amount of methylene chloride biologically removed is 17 percent. The surface losses for phenol are 0.0085 percent, and the total percent volatilized is 0.0086 percent. The percent of phenol which is biologically removed is 99.7 percent, and this high number has been confirmed from other literature [10,11,12]. It is interesting to note that while the biomass biologically degrades both organics, greater degradation is associated with phenol over methylene chloride. This increased degradation of phenol indicates that the biomass was better acclimated to phenol.

Following the bioreactors, the wastewater flows into two secondary clarifiers for final clarification. For methylene chloride, the open surface losses are 13 percent, and the weir waterfall loss is 2.1 percent, thus yielding a total atmospheric emission of 15 percent. For phenol, the losses are 0.37 percent [open surface], 0.0015 percent [weir waterfall], and 0.37 percent [total losses], respectively. Again, the large differences in the releases of the two compounds can be noted.

Figure 2.7 illustrates the percentages of methylene chloride and phenol released to the ambient atmosphere from the unit processes at the Tinker AFB IWTF. The information in Figure 2.7 is from Table 2.1. Careful examination of Figure 2.7 reveals that for methylene chloride releases, the major contributing unit processes include the equalization

basins, aeration basins, and the oil-water separator. The phenol releases, expressed as a percentage, are very low in comparison to the methylene chloride releases. However, consideration needs to be given to the mass of these chemicals entering the unit processes, and the associated atmospheric releases expressed on a mass basis.

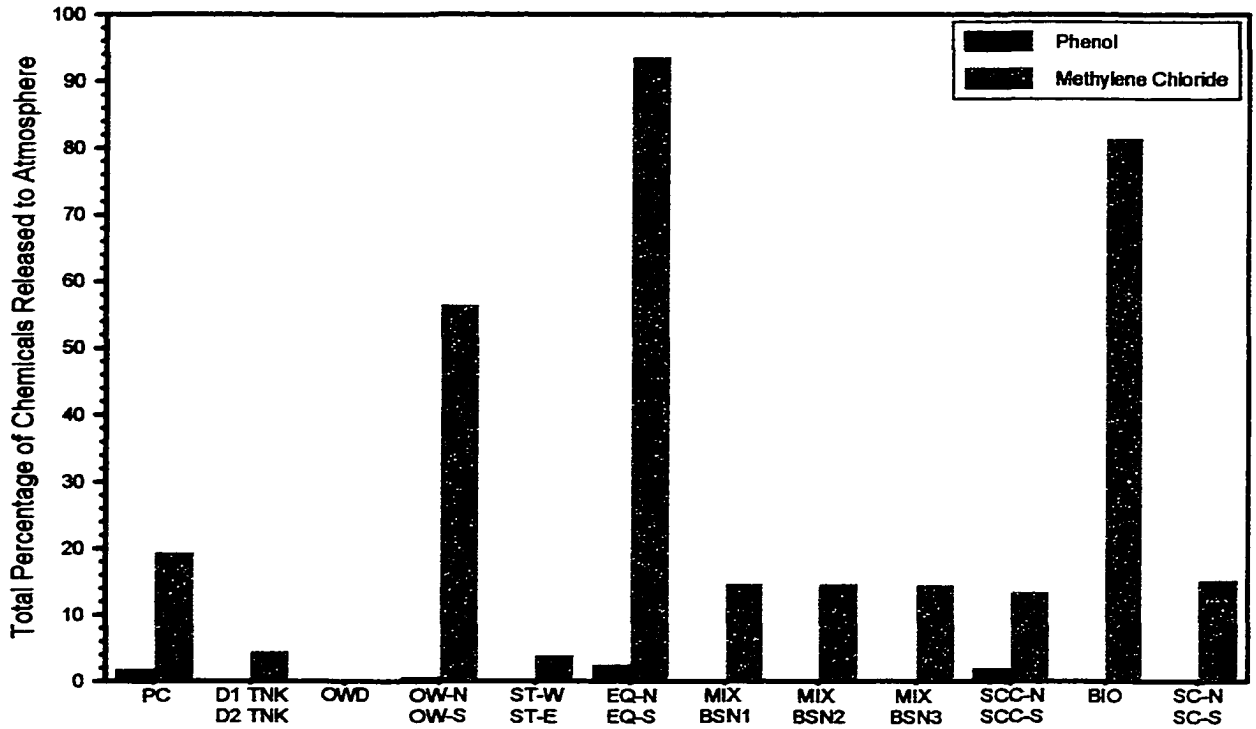

Figure 2.7: Percent of Phenol and Methylene Chloride Released to the Atmosphere from Various Unit Processes at the Tinker AFB IWTF

Accordingly, another benefit of the WATER8 source emission model is the ability to quantify the mass of constituent released to the atmosphere over a given time period. Figure 2.8 illustrates the total mass [million grams] of methylene chloride and phenol released annually to the atmosphere. Approximately 6.14 million grams [6.76 tons] of methylene chloride and 3.41 million grams [3.76 tons] of phenol are released annually to the atmosphere surrounding the IWTF. As expected, the majority [93 percent] of methylene chloride emissions are from three process units: API separator [44.3 percent], equalization basins [30.0 percent], and primary clarifier [19.0 percent]. For phenol, 88 percent of the emissions are attributed to the same three process units: API separator [12.8 percent], equalization basins [46.1 percent], and

primary clarifier [29.6 percent]. Further, it should be noted that the actual mass of constituent entering the downstream unit processes declines as a function of the entering mass to the IWTF, and removals in upstream unit processes.

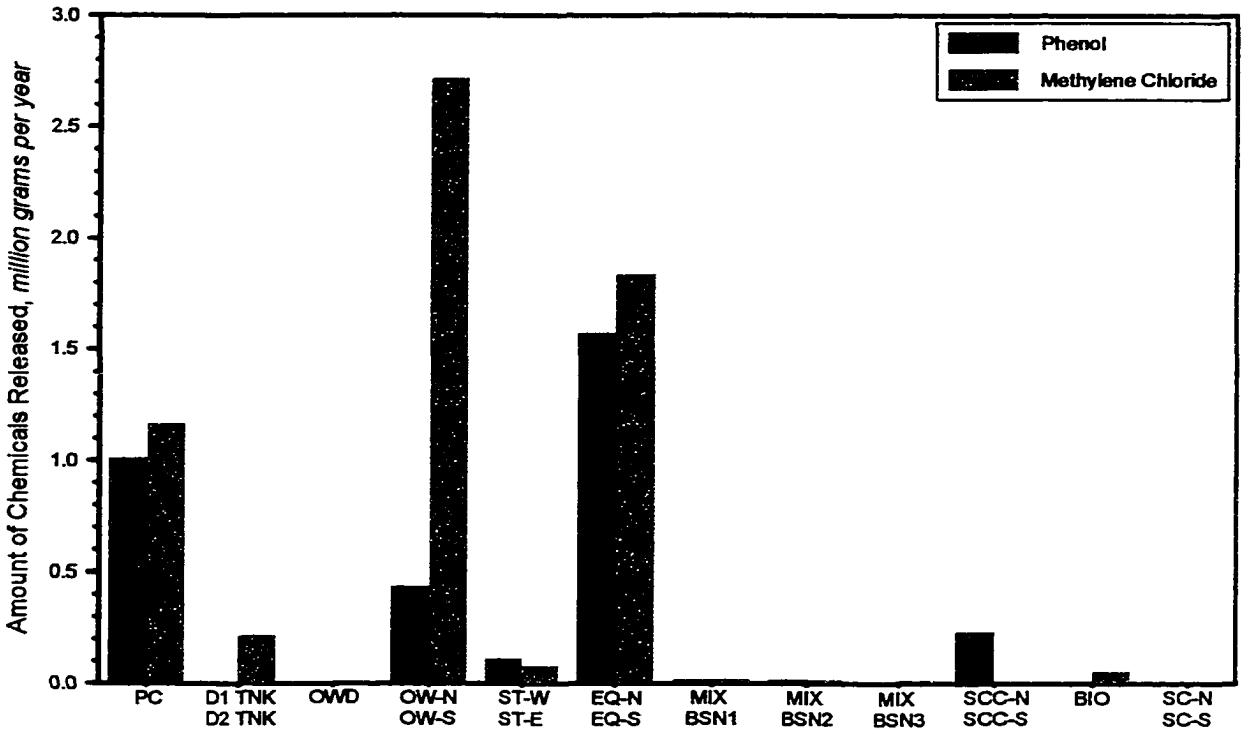

Figure 2.8: Mass of Chemicals Released Annually to the Atmosphere from Various Unit Processes at the Tinker AFB IWTF

From reviewing both Figures 2.7 and 2.8, it can be seen that the majority of the atmospheric emissions of the two target chemicals are from the oil-water separators, equalization basins, and primary clarifier. These processes are located in the primary treatment portion of the IWTF, and are thus characterized by higher concentrations of the target chemicals, longer detention times, and larger surface areas. The primary clarifier is a more important contributor to volatilization than initially thought because of the significantly higher entering component concentrations relative to the downstream basins [API separators and equalization basins]. The initial perspective was that the primary clarifier would emit little to the atmosphere because of the smaller exposed surface area and no surface aeration.

In reviewing the WATER8 output [as illustrated in Figures 2.7 and

2.8] and considering that the prevailing wind direction is from the south at Tinker AFB, the initial hypothesis concerning the atmospheric concentrations is that there should be three concentration peaks for both the methylene chloride and phenol, with only the magnitude and distributions of the concentrations varying. For methylene chloride, the first concentration peak should appear around and to the north of the primary clarifier and should comprise approximately 19 percent of the total concentration area. The next major peak should be to the north and associated with the oil-water separators [44 percent of the concentration area], while the third major peak will occur around and north of the equalization basins and comprise about 30 percent of the concentration area. For phenol 30 percent of the total concentration area should center north of the primary clarifier, 13 percent should be associated with the oil-water separators, and 46 percent should be around and north of the equalization basins. The solid contact clarifiers may also generate a discernible peak for phenol. A detailed discussion of the air dispersion modeling results will be addressed in Chapter 3.

Finally, one of the primary functions of Task 1 was to obtain emission data to serve as input into the selected ISC-ST3 air dispersion model; this dispersion model will be used to quantify the ambient air concentrations for methylene chloride and phenol surrounding the IWTF. Table 2.2 summarizes the emission factor [emission rate] data for methylene chloride for each of the process units under both average and maximum influent conditions. Similar to Table 2.2, Table 2.3 summarizes the emission factor data for phenol for each of the process units under both average and maximum influent conditions. These data will be used as input to the dispersion model to be addressed in Chapter 3.

SUMMARY

Following the review of ten candidate models, the WATER8 source emission model was selected for use in this research. The selection of this EPA-validated model was based on its *building block* approach for modeling the atmospheric emissions of unit processes for industrial wastewater treatment, its incorporation of a temperature correction feature for Henry's Law constant for volatile compounds, and its lack of

previous usage for methylene chloride and phenol emissions. Application of the WATER8 model to the IWTF at Tinker AFB proved to be successful. On the basis of the percentage entering chemicals emitted to the atmosphere, the more volatile methylene chloride exhibited an *order of magnitude* higher emissions from all pertinent unit processes. However, because the mass of phenol entering the IWTF is about nine times greater than for methylene chloride and because phenol is more biodegradable than methylene chloride, the atmospheric emissions on an annual basis total 6.14 million grams [13,540 pounds] for methylene chloride and 3.41 million grams [7,520 pounds] for phenol. The majority of the emissions for both chemicals occur from the primary clarifier, API separators, and equalization basins. Emission factors for both chemicals from each unit process in the IWTF were developed; these factors will be used in subsequent atmospheric dispersion modeling.

Table 2.2: Emission Factors [grams/cm^2·second] for Methylene Chloride under Average and Maximum Influent Conditions as Developed from the WATER8 Model for the Tinker AFB IWTF

PROCESS UNIT	METHYLENE CHLORIDE$_{Average}$	METHYLENE CHLORIDE$_{Maximum}$
Primary Clarifier	0.1679E-07	0.3405E-07
D_1-D_2 Blending Tanks	0.2628E-08	0.5330E-08
Oil-Water Diversionary Structure	0.4386E-09	0.8895E-09
API Separator	0.9770E-08	0.1981E-07
Circular Storage Tanks	0.5993E-09	0.1215E-08
Equalization Basins	0.1255E-08	0.2545E-08
Mixing Basin #1	0.3411E-08	0.6918E-08
Mixing Basin #2	0.2913E-08	0.5908E-08
Mixing Basin #3	0.5520E-09	0.1120E-08
Solid Contact Clarifiers	0.1477E-10	0.2995E-10
Bioreactor	0.1340E-09	0.2718E-09
Secondary Clarifiers	0.2078E-12	0.4214E-12

Table 2.3: Emission Factors [grams/cm^2·second] for Phenol under Average and Maximum Influent Conditions as Developed from the WATER8 Model for the Tinker AFB IWTF

PROCESS UNIT	$PHENOL_{Average}$	$PHENOL_{Maximum}$
Primary Clarifier	0.1451E-07	0.2944E-07
D_1-D_2 Blending Tanks	0.2958E-10	0.6002E-10
Oil-Water Diversionary Structure	0.1368E-08	0.2776E-08
API Separator	0.6270E-08	0.1271E-07
Circular Storage Tanks	0.8267E-07	0.1678E-06
Equalization Basins	0.1074E-07	0.2178E-07
Mixing Basin #1	0.3061E-08	0.6211E-08
Mixing Basin #2	0.3060E-08	0.6209E-08
Mixing Basin #3	0.3613E-08	0.7331E-08
Solid Contact Clarifiers	0.3327E-08	0.6751E-08
Bioreactor	0.1312E-09	0.2662E-09
Secondary Clarifiers	0.8589E-11	0.1743E-10

SELECTED REFERENCES

1. U.S. Environmental Protection Agency, *Wastewater Collection, Treatment, and Storage—Evaporative Loss Sources,* AP-42 Documentation, Section 4.3, Office of Air Quality Planning and Standards, Research Triangle Park, North Carolina, April, 1981.

2. Curto, M.E., and Daly, M.H., *Predicting VOC Emissions from Wastewater Processes using General Fate Models [GFMs],* Internet search, 1998.

3. U.S. Environmental Protection Agency, *Air Emissions Models for Waste and Wastewater,* EPA-453/R-94-080A, Office of Air Quality Planning and Standards, Washington, D.C., 1994.

4. Farino, W., Spawn, P., Jasinski, M., and Murphy, B., *Evaluation and Selection of Models for Estimating Air Emissions from Hazardous Waste Treatment, Storage and Disposal Facilities,* EPA-450/3-84-020, U.S. Environmental Protection Agency, Research Triangle Park, North Carolina, 1984.

5. Melcer, H.K., *Monitoring and Modeling VOCs in Wastewater Facilities,* Environmental Science and Technology, Vol. 28, No. 7, 1994, pp. 328-335.

6. U.S. Environmental Protection Agency, *Hazardous Waste Treatment, Storage, and Disposal Facilities [TSDF] Air Emission Models,* EPA-450/3-87-026, Office of Air Quality Planning and Standards,

Research Triangle Park, North Carolina, December 1987.

7. Metcalf and Eddy, *Wastewater Engineering: Treatment, Disposal, and Reuse*, McGraw-Hill Book Company, New York, New York, 1979.

8. Allen, C.C., and Green, D.A., *Review of VOC Pathway Models*, Draft Report, prepared for U.S. Environmental Protection Agency, Contract No. 68-01-6826, Research Triangle Institute, Research Triangle Par, North Carolina, 1985.

9. Hwang, S.T., *Treatability and Pathways of Priority Pollutants in Biological Wastewater Treatment*, presented at the American Institute of chemical Engineers Symposium, November 1980, Chicago, Illinois.

10. Blackburn, J.W., Troxler, W.L., and Sayler, G.S., *Prediction of the Fates of Organic Chemicals in a Biological Treatment Process—An Overview*, Environmental Progress, Vol. 3, No. 3, August 1984, pp. 163-175.

11. Namkung, N., and Rittmann, R.E., *Estimating Volatile Organic Compound Emissions from Publicly Owned Treatment Works*, Journal of Water Pollution Control Federation, Vol. 59, No. 7, January 1989, pp. 670-678.

12. Patterson, J.W., *Biodegradation of Hazardous Organic Pollutants*, Chemical Engineering Progress, April 1981, pp. 48-55.

CHAPTER 3
SELECTION AND APPLICATION OF AN AIR QUALITY DISPERSION MODEL

Air quality dispersion modeling has become increasingly important in recent years as legislative and permitting requirements have specified scientific analyses of the air quality impacts of existing and proposed projects. An air dispersion model for a point source such as a unit process at an IWTF requires information on the emissions [source coordinates, emission height, dimensions of the source, emission temperatures, and pollutant emission rates], meteorology [wind direction, wind speed, Pasquill stability class, air temperature, and mixing height], and selected receptors [coordinates and height above the ground]. Using this input information, the model simulates the atmospheric chemistry and physics and produces an estimate of the air pollutant concentrations at specific receptors [1].

The extent to which a specific air quality model is suitable for the evaluation of the air quality impacts of a source such as an IWTF depends on several factors; for example, (1) the meteorological and topographical complexities of the area; (2) the level of detail and accuracy specified for the analysis; (3) the technical competence and computer skills of those undertaking such simulation modeling; (4) the financial resources available; and (5) the detail and accuracy of the available input information and related data [emissions inventory, meteorological data, and air quality data]. Obviously, a model that requires comprehensive and precise input data would not be useable when such data are unavailable. Therefore, air quality dispersion modeling typically begins with the selection of an appropriate model. Accordingly, this chapter begins with a description of the process and decision factors used to evaluate and select an appropriate model for the Tinker AFB IWTF. Examples of application of the selected model [Industrial Source Complex—Short Term, Version 3, or ISC-ST3] are also briefly described in the first section. The second section summarizes the fundamental features and input data requirements of the ISC-ST3 model. The parameters associated with applying the ISC-ST3 model to the IWTF relative to modeling scenarios and selected receptor locations are addressed in the third section, with the fourth section containing a

summary of the modeling results. The final section highlights the key findings related to the selection and application of the ISC-ST3 model to the VOC emissions from the Tinker AFB IWTF.

EVALUATION OF AVAILABLE AIR QUALITY DISPERSION MODELS

Air quality dispersion models can be categorized into four generic classes: Gaussian, numerical, statistical or empirical, and physical [1,2,3,4,5]. Within each of these classes, a large number of individual computational algorithms or physical dimensions may exist, each with its own specific applications for air pollution sources. To date, Gaussian models have been the most widely used techniques for estimating the air quality impacts of non-reactive air pollutants. Numerical models may be more appropriate than Gaussian models for urban applications that involve reactive pollutants; however, they typically require considerably more input information and are thus not widely applied [2]. Statistical techniques are frequently employed in situations where incomplete scientific understanding of the physical and chemical processes, or lack of the required input data, make the use of a Gaussian or numerical model impractical. Physical modeling involves the use of a wind tunnel or other fluid modeling facilities and typically requires a high level of technical expertise and monitoring instrumentation [2].

For purposes of this review of dispersion models and the selection of one for application to the VOC emissions from the Tinker AFB IWTF, the following selection criteria were identified. Namely, the selected model should: (1) focus on short-term ground-level concentrations resulting from multiple, closely-spaced emission sources that are at ground level; (2) be adaptable so that long-term ground-level concentrations can also be determined; (3) be useable for both reactive and non-reactive air pollutants, with the emphasis herein being on non-reactive pollutants; (4) be able to generate both short-term and long-term ground-level concentrations at multiple receptor locations nearby the IWTF; (5) be acceptable to the EPA [preferably, it should be an approved EPA model]; and (6) be computerized. A total of nine potential models were identified for further systematic review based on a search of the literature; they included: CALINE, CDM, RAM, CRSTER, EDMS,

AFTOX, WADOCT, ADAM, and ISC. It should be noted that many additional models were identified but eliminated from any further review based on the above-listed six selection criteria.

CALINE3 [the third and latest version of CALINE] is a Gaussian plume model used to estimate the concentrations of non-reactive pollutants from highway traffic. CALINE3 is useful for line sources associated with transportation planning; it was developed in California in 1979. This steady-state model can be used to determine air pollution concentrations at receptor locations downwind of highways located in relatively uncomplicated terrain. The model is applicable for any wind direction, highway orientation, and receptor location [2]. It has adjustments for averaging time and surface roughness, and it has the capability of addressing up to 20 receptors. This model is recommended by the U.S. EPA for highway line sources in urban or rural areas characterized by simple terrain. It can be used for transport distance of less than 50 kilometers, and for one-hour and 24-hour averaging times [2]. However, despite its many desirable features, because of its focus on line sources, CALINE3 was not selected for application to the Tinker AFB IWTF. The emissions sources at the IWTF are more characteristic of point sources than line sources.

The Climatological Dispersion Model [CDM] is a steady-state Gaussian plume model which can be used for determining long-term [seasonal or annual] arithmetic average pollutant concentrations at ground-level receptors in urban areas [2]. CDM is designed specifically for criteria air pollutants where settling and deposition are not significant. Chemical transformations are treated using an exponential decay function with the half-life being required input by the user. This U.S. EPA-approved model is appropriate for point and area sources located in urban environments with flat terrain. Further, it can be applied for transport distances less than 50 kilometers, and for determining long-term averages over one month to one year or longer. The CDM was developed in 1985 and is a useful model for multiple sources [2]. However, and again despite its many desirable features, CDM was rejected relative to application to the IWTF. The primary reason for its rejection was that it focuses on calculating longer-term rather than shorter-term ground level concentrations in the environs of the modeled

sources.

The Gaussian-plume Multiple Source Air Quality Algorithm [RAM model] was developed in 1978 as a steady-state Gaussian plume model for estimating concentrations of relatively stable pollutants, over averaging times from one hour to one year, resulting from point and area sources in a rural or urban setting [2]. The topographic features addressed within the model require level terrain. RAM may be used to model criteria pollutants where settling and deposition are not treated. Chemical transformations are addressed via an exponential decay function with the half-life being required input by the user. This U.S. EPA-approved model can also be used for transport distances of less than 50 kilometers, and for one hour to one-year averaging times [2]. While the RAM model met all the selection criteria, it was rejected for use at the IWTF because a more widely used model meeting all of the selection criteria was identified [ISC-ST3].

The Single Source model [CRSTER] was developed in 1986 and is classified as a steady-state Gaussian dispersion model designed to calculate concentrations from a point source at a single location in either a rural or urban setting [2]. The highest and second highest concentrations can be calculated at each specified receptor for one-hour, three-hour, 24-hour, and annual averaging times. CRSTER does not address settling and deposition; however, chemical transformations are treated using an exponential decay function with the half-life time constant being input by the user. CRSTER is an appropriate model for single point sources in locations where the transport distances of concern are less than 50 kilometers. This U.S. EPA-approved model can be used in flat or rolling simple terrain [no terrain above the stack height]. Finally, because CRSTER is designed for a single point source analysis, it was rejected for use at the Tinker AFB IWTF since the facility itself has several closely-spaced point source release locations as described in Chapter 2.

Because commercial airports and U.S. Air Force Bases often require dispersion modeling of air pollutants emitted from both aircraft landing-and-takeoff cycles, as well as various related operations, including wastewater treatment, an effort was made to explore the availability of any specific models for such operations. Four such

models were identified and reviewed for their applicability to the Tinker AFB IWTF; the models include the previously listed EDMS, AFTOX, WADOCT, and ADAM.

Two types of models are generally used in combination for commercial airports and U.S. Air Force bases; they include one associated with the preparation of an inventory of emissions and the other to calculate ground-level concentrations caused by these emissions as they disperse downwind. Both the U.S. Air Force and Federal Aviation Administration [FAA] initiated the development of models that perform these tasks in the early 1970s. For example, EDMS [Emissions and Dispersion Modeling System] is a complex source emissions and dispersion model for use at civilian airports and Air Force installations. It operates in both a refined and screening mode that accepts pre-processed meteorological information from the National Climatic Center [NCC]. EDMS was developed in 1986 to predict the dispersion of emissions from roadways, parking lots, powerplants, and fuel storage tanks, as well as from accelerating aircraft [6]. This model was rejected for use at the Tinker AFB IWTF because of its lack of focus on emissions from wastewater treatment plants. Further, it is not an U.S. EPA-approved model.

AFTOX [Air Force Toxic Chemical Dispersion Model] is a computer model developed in 1988 for use by the U.S. Air Force in updating its toxic pollutant dispersion prediction capability via the quantification of accidental releases of toxic chemicals into the atmosphere [7]. AFTOX is an interactive Gaussian puff dispersion model for uniform terrain and wind conditions. It can handle continuous or instantaneous releases of liquids or gases from elevated or surface locations, and from point or area sources. The model includes various properties of 129 chemicals in its database. AFTOX is considered to be a screening model designed to provide relatively simple estimations of the air quality impacts of releases from a specific source [7]. Further, because AFTOX is related to discontinuous releases rather than the more continuous emissions associated with unit processes at an industrial wastewater treatment plant, it was rejected for usage at the Tinker AFB IWTF.

The WADOCT [Wind and Diffusion Over Complex Terrain] model was developed as a replacement for the AFTOX model when spill scenarios occur in complex terrain such as at Vandenberg AFB, California [9,10].

Complex terrain is defined as terrain exceeding the height of the stack source being modeled. Although AFTOX allowed for varying surface roughness, it assumed spatially uniform windfield throughout the domain. Accordingly, all meteorological and spill data are manually entered into the WADOCT model. Information on terrain heights and vegetation heights, or surface roughness, is also required. WADOCT is thus recommended for complex terrain where the elevations may vary by several hundred meters [9,10]. However, it was rejected for use at the Tinker AFB IWTF because the surrounding terrain is simple and flat, and it is focused on discontinuous releases to the atmosphere.

The ADAM [Air Force Dispersion Assessment Model] model was developed in 1992 under a contract from the U.S. Air Force to Technology and Management Systems [8]. The current ADAM 2.1 version is a heavy gas, Gaussian puff dispersion model, which can be used to predict the area of hazard resulting from the discontinuous release of a toxic chemical. The model takes into account the chemical reactions that take place when the chemical is released to the atmosphere, the gravitational slumping due to the high density of the cloud [due to aerosol presence, temperature or molecular weight], and the dispersion due to atmospheric turbulence. The far field dispersion is modeled using the Pasquill-Gifford diffusion coefficients. Sixteen different source types are modeled in relation to instantaneous and continuous releases [depending on the severity of the accidental release], pressurized liquid and gas releases, and non-pressurized liquid releases. The chemical database contains information on eight chemicals: ammonia, chlorine, fluorine, hydrogen fluoride, hydrogen sulfide, nitrogen tetraoxide, phosgene, and sulfur dioxide. ADAM was rejected for use at the Tinker AFB IWTF due to the non-inclusion of the two target chemicals [phenol and methylene chloride] in its database, and the fact that it focuses on discontinuous rather than continuous atmospheric emissions.

The Industrial Source Complex [ISC] model is a steady-state Gaussian plume model which can be used to assess pollutant concentrations from a wide variety of sources associated with an industrial complex in an urban or rural setting [2]. The ISC model can account for settling and dry deposition of particulates, building downwash, different types of sources [area, line, and volume], plume rise as a function of downwind

distance, separation of point sources, and limited terrain adjustment. ISC was developed in 1992 and designed to operate in both short-term and long-term modes. Chemical transformations are treated using an exponential decay function with the time constant as required input by the user. This U.S. EPA-approved model is appropriate for industrial complexes in flat or rolling terrain, with transport distances of concern less than 50 kilometers, and for one-hour to annual averaging times. The ISC model is used extensively in the regulatory permitting process. For these collective reasons, and because the ISC-ST3 model met all six selection criteria described earlier, it was chosen for usage at the tinker AFB industrial wastewater treatment facility.

A major reason that the ISC-ST3 model was selected for the Tinker AFB IWTF was that it has been widely used. Several examples of the use of the model can be found in air dispersion modeling literature, and five will be noted herein. First, a rural chemical manufacturing facility in eastern North Carolina used the model in a study regarding model performance in predicting ambient concentration using site specific information from a fully operational facility [11]. The terrain in the surrounding area is predominately flat with elevations changing only a few feet within a few kilometers of the facility. A total of 25 emission sources at the facility were modeled, along with building wake and downwash effects. Stack exhaust parameters [temperature, flow rates, etc.] were based on typical operating parameters and conditions for each source. After performing the dispersion modeling analysis using the ISC-ST3 model, the modeling results on an hourly basis were compared with observed hourly ambient monitoring data. The conclusion of the study was that for short-transport distance evaluations [approximately one kilometer], the model performed well for each meteorological category. The evaluations indicated that the model tends to under-predict for distances close to the source [less than one kilometer] and over-predict for distances further away [six kilometers or more] [11].

The ISC-ST3 model was also used in an odor impact analysis for a biosolids composting facility in Hickory, North Carolina [12]. When it initially opened [July, 1990], the Hickory composting facility caused significant odor impacts on the surrounding community. Shortly afterward

[February, 1991], the facility underwent comprehensive odor mitigation and control improvements that included significant changes in the air handling and odor control systems. As a result, the odors were significantly reduced. However, in response to lingering public concern, an extensive field analysis and odor modeling study was undertaken. Modeling results for existing conditions were compared with results from field analyses. The conclusion of the study was that the model results correlated with quantitative measurements obtained from field sampling. Thus, the ISC-ST3 model appears to generate reasonable results in terms of predicting the frequency of nuisance conditions [12].

A related study was focused on how the Massachusetts Department of Environmental Protection [MDEP] is proposing policy that relates to odor dispersion modeling [13]. The MDEP is requiring new biosolids and municipal solid waste composting facilities to use U.S. EPA-approved air dispersion modeling to predict off-site odor impact levels. As part of the facility permitting process, the MDEP is requiring that applicants demonstrate compliance with a minimum design standard. For example, the applicant must determine the maximum odor threshold levels at the odor source that will not result in an exceedance of the property line and/or most sensitive receptor standard downwind; this determination is to be based on dispersion modeling using the ISC-ST model [13].

Another example relates part of a grant from the U.S. EPA wherein the ISC-ST3 model was used to estimate ambient concentrations of several toxic compounds throughout the Minneapolis / St. Paul, Minnesota metropolitan area [14]. Emissions rates and resultant inventories were calculated for eight VOCs from 69 industrial sources. Metro-wide estimates of air toxic exposures from 38 VOCs were first reported by the Minnesota Pollution Control Agency in a 1992 study entitled *Estimation and Evaluation of Cancer Risks from Air Pollution in the Minneapolis / St. Paul Metropolitan Area* [15]. This study, also known as the *Urban Soup Study*, analyzed sources of air pollutants suspected or known to cause cancer, and also estimated the health risk from exposure to these pollutants. Because an emission inventory for only eight VOCs in the impact region could be readily assembled, air dispersion modeling using ISC-ST3 was conducted for these eight pollutants to provide information

on the expected exposure of individuals in the population [14]. The ISC-ST3 model does not have the capability to simulate chemical transformation in the atmosphere, thus it was assumed that each of the eight modeled pollutants retained its chemical structure. The study was also used to identify three communities in which to conduct personal exposure monitoring. Two communities were selected because dispersion modeling indicated that ambient concentrations are likely to be relatively high, while the other community was selected because ambient concentrations are likely to be relatively low. This example illustrates how air dispersion modeling can be used in conjunction with health risk assessments. A health risk assessment will be conducted for the Tinker AFB IWTF.

The final example is released to the use of the ISC-ST3 model to assess odors from the Central Contra Sanitary District wastewater treatment plant located east of San Francisco Bay in California [16]. This study included performing odor dispersion modeling to predict off-site odor impacts on the surrounding communities. The objective of the modeling study was to balance conservatism and capital expenditures. This was accomplished by conducting the dispersion modeling and formulating a control strategy which builds on the District's current operational strategy. Odor impacts were evaluated based on the frequency of odors exceeding a threshold concentration; therefore, odor sources at the plant were ranked and prioritized based on the modeling results. The odor abatement systems were designed for these site-specific frequencies. In summary, based on this modeling study, the operators of the treatment facility installed odor abatement equipment on the primary treatment processes, thereby minimizing capital expenditures while significantly reducing off-site odors [16].

To summarize this evaluation of the available dispersion models, a distinctive element of this research study is the use of a selected model to predict chemical depainting [methylene chloride and phenol] concentrations surrounding the Tinker AFB IWTF. Much of the literature is directed toward Gaussian models, with only limited reference to numerical, statistical, and physical models, particularly regarding the modeling of emissions from wastewater treatment plants. No published literature was found that discusses the use of air dispersion models at

DOD industrial [and municipal] wastewater treatment facilities. No documented qualitative or quantitative investigations of air dispersions modeling of chemical depainting agent concentrations surrounding a treatment facility using the ISC-ST3 model were identified. Further, most modeling studies focus on downwind behavior and concentrations, not on the entire impact region. As a result, the application of the ISC-ST3 model to the Tinker AFB IWTF appears to be unique regarding the source type and pollutants modeled, and the defined impact region which extends in all directions from the facility.

USE OF THE INDUSTRIAL SOURCE COMPLEX [ISC-ST3] DISPERSION MODEL

There are two basic types of inputs needed to run the ISC-ST3 model. They include the input runstream file and meteorological data file. The runstream setup file contains the selected modeling options, in addition to source location and parameter data, receptor locations, meteorological data file specifications, and selected output options. Since the ISC-ST3 model is designed to support the U.S. EPA regulatory program, the regulatory modeling options represent the default mode of operation. To maintain the flexibility of the model, the regulatory default options were retained for this study of the Tinker AFB IWTF. The user has the option of specifying only simple or only complex terrain calculations, or of using both simple and complex terrain algorithms. Simple terrain calculations were used in this study. The user may also select either rural or urban dispersion parameters, depending on the characteristics of the location of the sources. In this study, urban parameters were used. Further, the user can specify several short-term averages to be calculated in a single run of the ISC-ST3 model, as well as requesting the overall period [up to annual] averages. In this study, 24-hour averages represented the focal point.

The ISC-ST3 model is capable of addressing multiple sources, including point, volume, area, and open-pit source types. Point sources were the primary type addressed herein. Source emission rates can be treated as constant throughout the modeling period, or may be varied by month, season, hour-of-day, or other optional periods. These variable emission rate factors may be specified for a single source or for a group of sources. Constant emission rates for the various unit processes

in the IWTF were used for various scenarios in this study.

The ISC-ST3 model also has considerable flexibility regarding the specification of receptor locations. The user has the capability of specifying multiple receptor networks in a single run, and may mix Cartesian grid receptor networks and polar grid receptor networks in the same run. There is also flexibility in specifying the location of the origin for polar coordinates, other than the default origin at [0,0] in *x-y* coordinates. A total of 1200 receptor sites were used in this study. Finally, the user can input elevated receptor heights in order to model the effects of terrain above the stack base. This option was not necessary for this study.

GOVERNING AIR DISPERSION MODEL EQUATIONS

Dispersion modeling is a technique for calculating concentrations of pollutants resulting from atmospheric emissions. A dispersion model can be used to evaluate gases and particulates, short and long-term concentrations, elevated point sources, ground level point sources, area sources, line sources, urban and rural areas, atmospheric processes, and continuous or discontinuous releases. A single equation can be used to estimate an air pollutant concentration at a single receptor from a single source. However, when plume rise, multiple sources, multiple receptors, varying meteorological condition, building wake effects, and other factors that affect atmospheric dispersion must be considered, a series of equations are needed.

An air dispersion model is a function of several factors including the meteorological and topographical complexities of the area, the level of detail and accuracy needed for the analysis, the technical competence of those undertaking such simulation modeling, the resources available, and the detail and accuracy of the database [*i.e.*, emission inventory, meteorological data, and air quality data] [1,2]. An air dispersion model uses data on the emission source, meteorology, and receptors. It then simulates the atmospheric physics and computes a concentration. Receptors are sites at which concentrations are calculated. Figure 3.1 summarizes the functions from a conventional dispersion model. Refined computer models [*i.e.*, Industrial Source Complex] have the capability of analyzing numerous sources for each hour of a year at a large number of

receptors. The alternative to dispersion modeling is to make actual air quality measurements. Measuring the actual level of pollutants is more accurate than modeling. However, if a potential source has not been constructed, there is no way to measure the effects of its emissions, and modeling must be used to estimate these effects. With modeling, concentration estimates can be made at thousands of locations for the price of a single set of measurements.

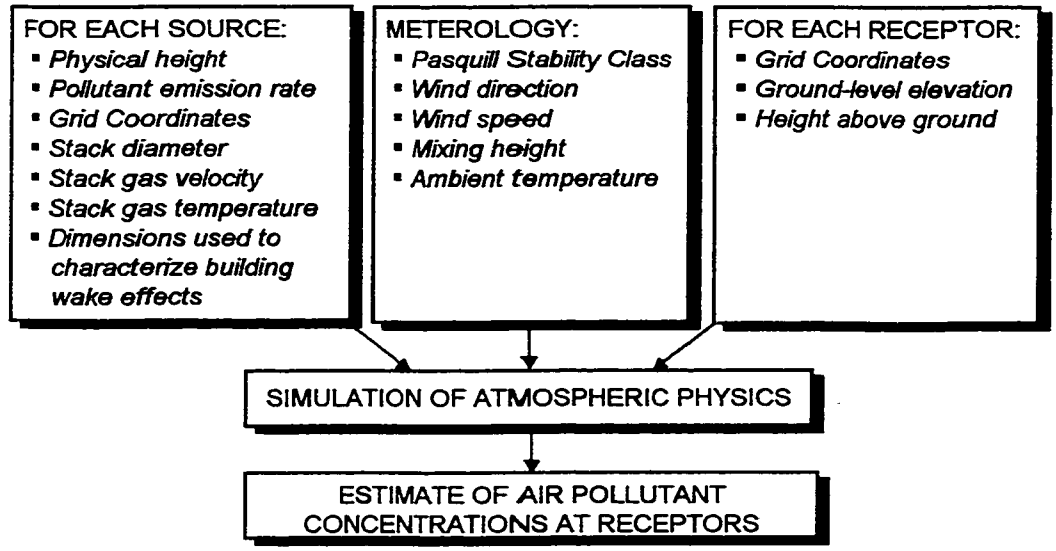

Figure 3.1: Structure of a Typical Air Dispersion Model

In the beginning, dispersion considerations were used as an engineering tool to help design stacks to minimize the nuisance from air pollutants at ground level. Dispersion provided an inexpensive way to determine the optimum stack height or emission configuration from a facility, in addition to optimizing investment in control equipment, analyzing potential or actual toxic gas releases, and studying odors. Modeling can be used to determine the changes in concentrations that will occur with various emission sources. Since about 1973, regulatory uses of dispersion modeling have greatly overshadowed engineering applications.

Dispersion occurs when a continuous stream of pollutants are released into a steady wind in an open atmosphere. The plume will initially rise, then bend over and travel with the mean wind, which will dilute the pollutants and carry them away from the source. This

pollutant plume will disperse in both the horizontal and vertical directions from its centerline. This dispersion is intuitively obvious that matter moves from a region of high concentration to one of lower concentration [molecular diffusion theory]. This spreading of the bent-over plume is due to factors other than simple molecular diffusion. One such factor is the amount of turbulent flow [eddies or swirls] imparted on the plume. Eddies are defined as macroscopic random fluctuations in a turbulent fluid stream and are the result of both thermal [energy from the sun] and mechanical [from shear forces when air blows across a rough surface] influences. The combined effect of many eddies is to broaden and dilute the concentrated pollutant plume by replacing the narrow, concentrated, pollutant plume with pollutant-free air. Another factor for plume spread is the random shifting of the wind. During this random wind shift pattern, the wind may change direction and blow more or less pollutant toward the detector. These random fluctuations in wind direction and flow rate help spread the plume over a larger downwind area.

One of the most used and convenient methods of estimating pollutant concentrations from various release configurations is the Gaussian model. The name is derived from the Gaussian or normal distribution [bell-shaped distribution] from statistics. Gaussian models are the most widely used techniques for estimating the impact of non-reactive pollutants. The Gaussian model assumes that continuously released material is transported in a direction opposite to the wind direction. It also assumes that time-averaged spreading of the pollutants will result in cross-sections of pollutant concentration, horizontally and vertically through the pollutant plume, that have normal distributions.

In order to relate positions of sources to those of receptors, an axis system is required. The usual three-dimensional coordinate system used with the Gaussian model is shown in the following figure [Figure 3.2]. The origin of the system is on the ground directly beneath the point of release of the pollutant. An x-axis [downwind axis] is on the ground oriented directly downwind in the direction of transport caused by the time-averaged wind direction. A y-axis [crosswind axis] is also on the ground, and is perpendicular to the x-axis. The z-axis [perpendicular to both the x and y axes] is vertical and passes through

the point of release. The use of a horizontal plume centerline is reasonably accurate for stable, neutral, and slightly to moderately unstable conditions. The effective stack height and physical stack height are represented as H and h, respectively.

Although Gaussian models are extremely useful as a practical modeling tool, there are assumptions that cause some limitations. These include the Gaussian dispersion of effluent, conservation of mass, steady-state emissions, and steady-state meteorology [1,2,3,4,5]. For

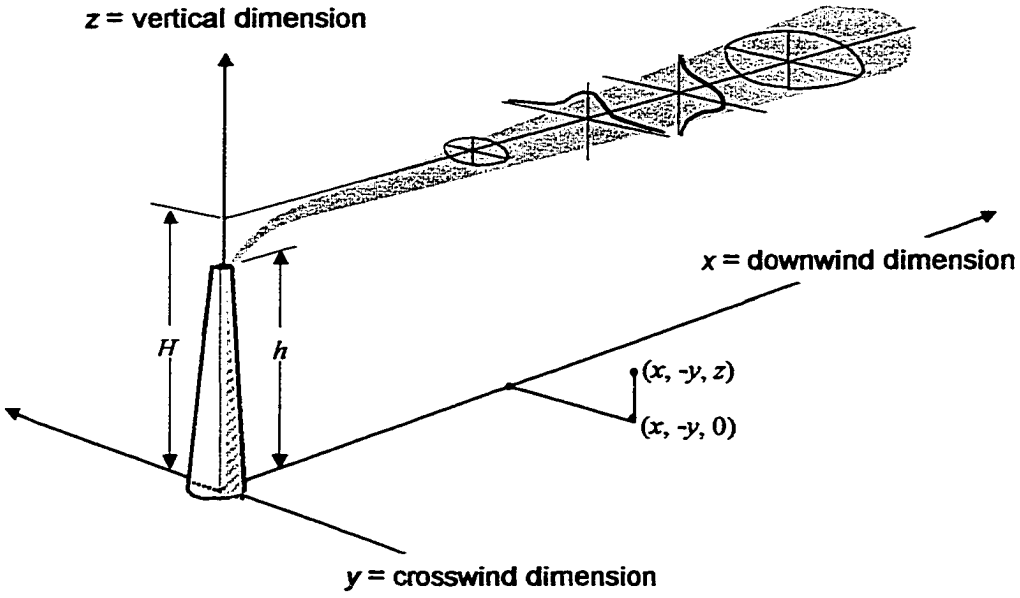

Figure 3.2: Coordinate System for Gaussian Model

Gaussian dispersion, the effluent disperses in the horizontal and in the vertical, resulting in Gaussian [bell-shaped] concentration distributions of the time-averaged plume in these two dimensions. Dispersion from the continuous source in the downwind direction is assumed to be negligible because of the uniform continued replenishment of the plume contents by the source. For conservation of mass, all of the effluent is assumed to remain in the atmosphere. No allowances are made for losses due to chemical conversions, surface deposition, or removal by precipitation. Portions of the plume dispersing toward the ground are assumed to be dispersed back away from the ground by turbulent eddies [eddy reflection]. For the steady-state emissions, the

emission rates are assumed to be constant and continuous. This may not be the case in such facilities as boilers, where loads fluctuate with steam demand, or where emissions are related to upstream workload. For the steady-state meteorology, no variations occur in wind speed, wind direction, or Pasquill stability class during transport from source to receptor. Although this assumption is reasonable within a few kilometers of a source, it may not be reasonable for receptor distances on the order of 50 kilometers or more or during periods of relatively rapid change of meteorology. For example, at a wind speed of two meters per second, it will take nearly seven hours for a plume to travel 50 kilometers, during which time many things can happen [*i.e.*, the sun can set or rise and clouds can form or dissipate with dramatic changes in stability class].

There are a number of variables used in the Gaussian model. The estimated concentrations [χ] for receptor locations are stated in mass per volume. The usual units are grams per cubic meter or micrograms per cubic meter. The emission rate [Q] of a pollutant from a continuous source is considered in terms of mass per time [frequently grams per second]. The effluent is assumed to be diluted upon release by the speed of the wind moving past the point of release. Thus, the time-averaged stack top wind speed [u] is needed. The power-law wind profile normally is used to extrapolate the wind speed measured at a height different from the physical stack height. The effective height of release is the sum of the physical stack height and any plume rise due to momentum or buoyancy. Methods to estimate this from knowledge of the volume flow, stack gas temperature, and wind speed at stack top are documented in the literature [1,2,3,4,5]. The positions of receptor locations, for which concentration estimates are to be made, will be specified by the x, y, and z coordinates. A receptor is defined mathematically to be a point at which one desires to know the concentration. When performing modeling, the receptors usually are uniformly spaced in a grid, using either Cartesian or polar coordinates. Some models allow the specification of z, the height above the local ground elevation either as a value for all receptors or on a receptor-by-receptor basis. A receptor with a specified z value may be referred to as a flagpole receptor.

In order to make estimates of pollutant concentrations at various downwind positions from the source, there must be a way of estimating the magnitude of the spreading parameters at these various distances. This parameter [in the horizontal] is expressed as the standard deviation of the horizontal pollutant distribution and is called σ_y. The vertical spreading is the standard deviation of the vertical distribution referred to as σ_z. The spreading of the pollutant plume will depend upon the characteristics of the atmosphere at the time and the character of the release. The spreading is assumed to increase with time and with distance from the source. In addition, the spreading may be influenced by the surface roughness and the stability of the atmosphere, as well as the characteristics of the release. Pasquill [32, 33] suggests that the horizontal and vertical fluctuation data could be reduced in ways that the horizontal and vertical dispersion parameters [σ_y and σ_z] could be estimated. Pasquill also recommended data on wind fluctuations when measurements are not available. After examining Pasquills suggestions, Gifford [1,2,3,4,5] saw advantages in expressing information that Pasquill had provided directly in Gaussian terms. Gifford restated Pasquills width and height values into values for σ_y and σ_z providing figures as functions of downwind distance from the source and Pasquill stability class. Curves of dispersion estimates for each Pasquill stability class as functions of downwind distance from the source, are show in Figures 3.3 and 3.4. Tabular values using this scheme are given in the literature [2,3]. Because of their origin with Pasquill and the reformulation by Gifford, these are commonly referred to as the Pasquill-Gifford dispersion parameters.

Atmospheric stability is a key parameter which influences both σ_y and σ_z. The atmospheric stability can be estimated by incorporating considerations of both mechanical and buoyant turbulence [2,3]. The mechanical turbulence is considered by the inclusion of the surface wind speed [approximately ten meters above the ground]. The positive generation of buoyant turbulence is included through the isolation [incoming solar radiation]. The negative generation of buoyant turbulence is considered through the nighttime cloud cover. The less the cloud cover the greater the amount of heat that escapes from the surface through infrared radiation. High wind speeds or overcast

cloudiness will produce neutral conditions [*D* class stability]. Unstable conditions are strongly unstable [*A* class stability], moderately unstable [*B* class stability], and slightly unstable [*C* class stability]. Stable conditions are slightly stable [*E* class stability], and moderately stable [*F* class stability]. Table 3.1 provides a descriptive list of stabilities [1,2,3,4,5].

Table 3.1: Descriptive of Atmospheric Stability

CLASSIFICATION	DEFINITION	TYPICAL WEATHER CONDITIONS
A	Strong instability	Sunny with sun ≥ 60° above horizon, light winds
B	Moderate instability	Sunny with sun between 35° to 60° above horizon, light winds
C	Slight instability	Partly sunny with sun 15° to 35° above horizon, light to moderate winds
D	Neutral stability	Cloudy skies day or night, winds at any speed or clear skies with moderate to strong winds
E	Slight stability	Night—mostly cloudy, light winds
F	Moderate stability	Night—partly cloudy or clear, light winds

For Gaussian expressions, a convenient notation is used to label the concentration for the situation being represented. The concentration in mass per volume [usually grams per cubic meter or micrograms per cubic meter] is represented by the Greek letter χ. Within parentheses are the three coordinates for the receptor followed by a semicolon and then the effective height of release. For example, [χ (x, y, z; H)] indicates that the concentration is for the most generalized receptor position [x, y, z] from the effective height [H]. The Gaussian expression shows that concentration is equal to the product of four factors that relate to the emission rate, the x direction, the y direction, and the z direction. The right hand side of the expression [χ (x, y, z; H)] consists of multiplying the four factors together.

The first term is the emission factor [Q] indicating that concentrations are directly proportional to emission rate. The units of emission rate are mass per time, usually grams per second or micrograms per second. If emissions are specified in μg/sec, the calculated concentrations will be in $\mu g/m^3$. The second factor has concentrations inversely proportional to the wind speed due to the downwind stretching

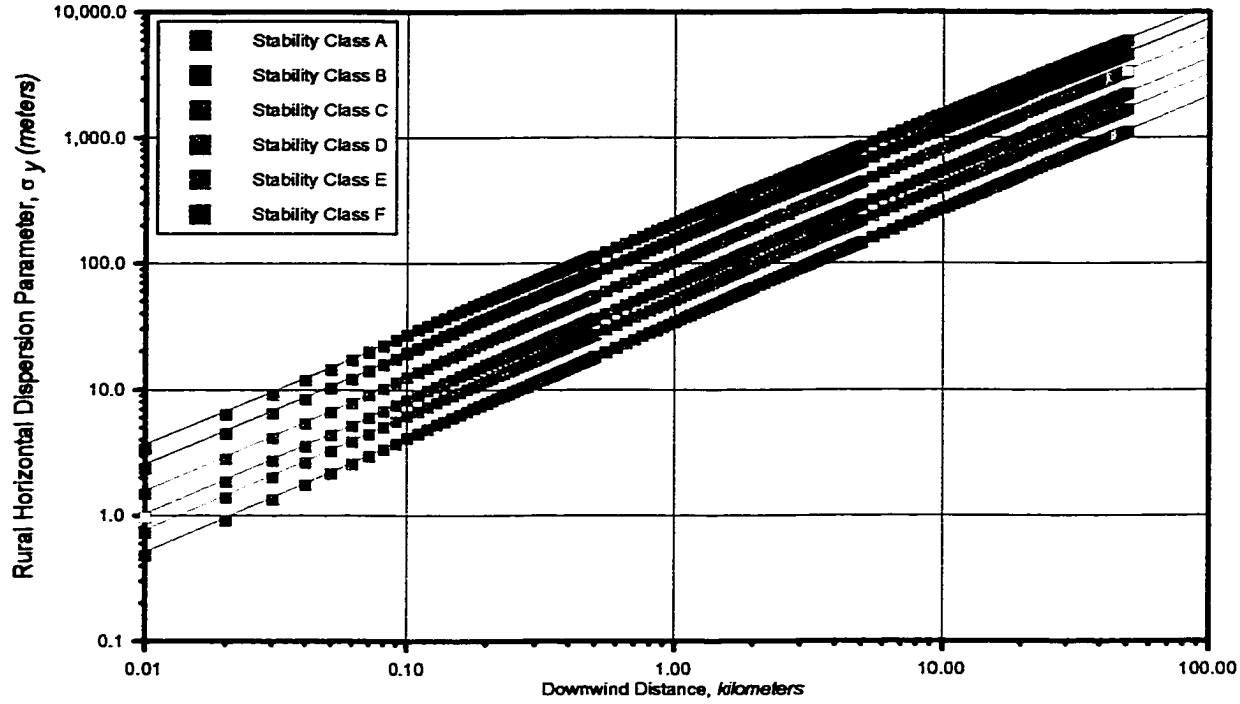

Figure 3.3: Pasquill-Gifford Rural Horizontal Dispersion Parameter, σ_y [meters]

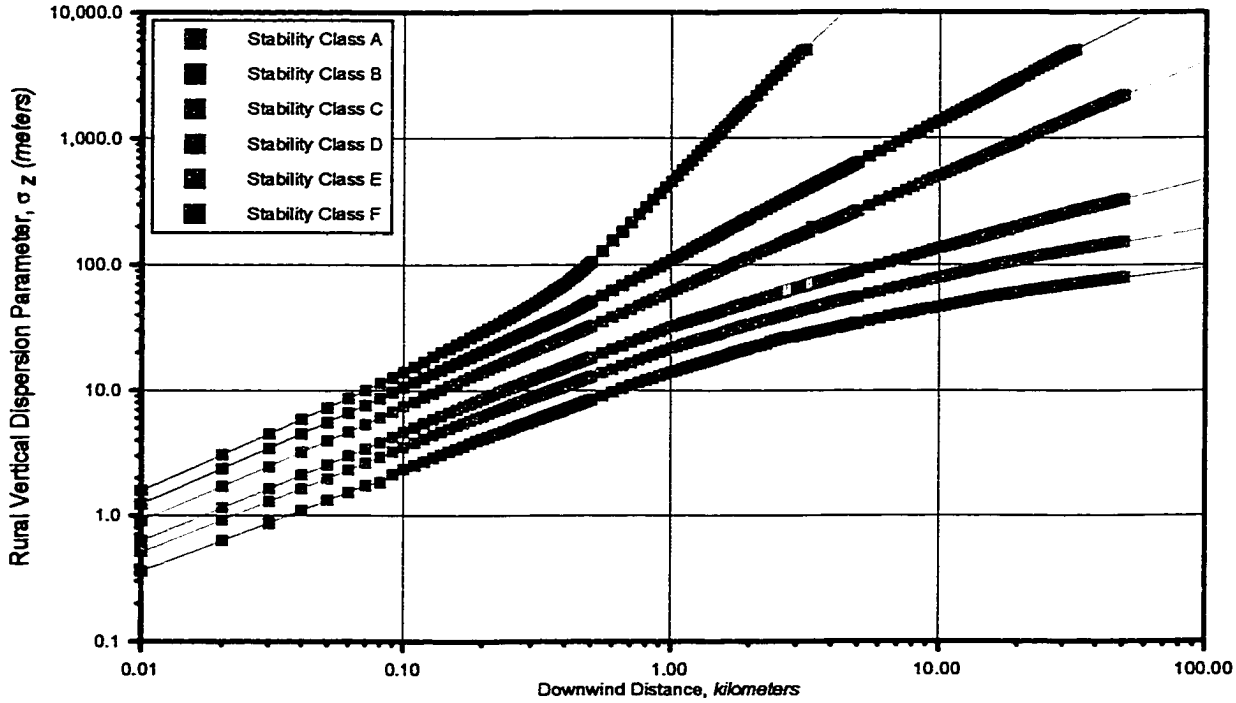

Figure 3.4: Pasquill-Gifford Rural Vertical Dispersion Parameter, σ_z [meters]

by the wind speed [u] expressed in meters per second.

Downwind factor: $\left[1/u\right]$ 3.1

The third factor [describing the spreading in the crosswind direction parallel to the y axis] is a Gaussian distribution function. The concentrations are inversely proportional to the magnitude of the horizontal spreading [σ_y] and the exponential gives the drop off of concentration for receptor positions away from the plume centerline.

Crosswind factor: $$\left[\frac{1}{\sigma_y (2\pi)^{0.5}}\right] \exp\left[\frac{-y^2}{2\sigma_y^2}\right] \qquad 3.2$$

The fourth factor [describing the spreading in the vertical direction parallel to the z axis] is also a Gaussian distribution function. However, this term has two additive exponential terms to account for the effect of eddy reflection at the ground. It is assumed that pollutant material contained within small air parcels or eddies that encounter the ground are eddy-reflected upward in the atmosphere without any loss of material at the boundary. This assumption is appropriate except for large particles that settle out and for gases which are adsorbed on surfaces that are wet or dew covered.

Vertical factor: $$\left[\frac{1}{\sigma_z (2\pi)^{0.5}}\right] \left\{\exp\left[\frac{-(H-z)^2}{2\sigma_z^2}\right] + \exp\left[\frac{-(H+z)^2}{2\sigma_z^2}\right]\right\} \qquad 3.3$$

By rearranging the product of the four factors, the Gaussian expression is simplified to the following:

$$\chi(x, y, z; H) = \left[\frac{Q}{2u\pi\sigma_y\sigma_z}\right] \exp\left[\frac{-y^2}{2\sigma_y^2}\right] \left\{\exp\left[\frac{-(H-z)^2}{2\sigma_z^2}\right] + \exp\left[\frac{-(H+z)^2}{2\sigma_z^2}\right]\right\} \qquad 3.4$$

If the receptor is at ground-level [$z = 0$], the above equation can be simplified to the following:

$$\chi(x, y, 0; H) = \left[\frac{Q}{2u\pi\sigma_y\sigma_z}\right] \exp\left[\frac{-y^2}{2\sigma_y^2}\right] \cdot 2\exp\left[\frac{-H^2}{2\sigma_z^2}\right] \qquad 3.5$$

which when the 2's are canceled, the equation becomes:

$$\chi(x, y, 0; H) = \left[\frac{Q}{u \pi \sigma_y \sigma_z}\right] \cdot \exp\left[\frac{-y^2}{2\sigma_y^2}\right] \cdot \exp\left[\frac{-H^2}{2\sigma_z^2}\right] \qquad 3.6$$

For the concentration at ground-level [z = 0] directly beneath the centerline of the plume [y = 0], the above expressions further simplifies to:

$$\chi(x, 0, 0; H) = \left[\frac{Q}{u \pi \sigma_y \sigma_z}\right] \cdot \exp\left[\frac{-H^2}{2\sigma_z^2}\right] \qquad 3.7$$

As solutions to this equation are determined for increasing downwind distances, the fractional part of the equation decreases with increasing values of σ_y and σ_z while the exponential portion increases from a small value near zero to a value that approaches unity. Thus, there is a point downwind that produces a maximum concentration. There are a number of textbooks that give a graphical summary that indicates the downwind distance that this equation reaches a maximum [x_{max}] in kilometers, and the value of that maximum relative concentration normalized for wind speed, [$\chi\ u/Q]_{max}$ expressed in inverse square meters. Maximum concentrations occur at greater distances for stable conditions. As the plume elevations [effective heights of release] exceed about 70 meters, maximum concentrations are associated with A stability class.

The four terms that influence the air dispersion concentration results as follows:

- The concentrations at the receptor are directly proportional to the emissions.
- Parallel to the x-axis [downwind dimension], the concentrations are inversely proportional to wind speed.
- Parallel to the y-axis [crosswind dimension], the concentrations are inversely proportional to the crosswind spreading [σ_y] of the plume. The greater the downwind distance from the source, the greater the horizontal spreading [σ_y], and the lower the concentration. The exponential involving the ratio of y to σ_y just corrects for how far off the center of the distribution the receptor is in terms of standard deviations. The receptor is y from the center since the

crosswind distribution center is at $y = 0$, that is, directly above the x-axis.

- Parallel to the z-axis [vertical dimension], the concentrations are inversely proportional to the vertical spreading [σ_z] of the plume. The greater the downwind distance from the source, the greater the vertical dispersion and the lower the concentration. The sum of the two exponential terms in the vertical factor represent how far the receptor height [z] is from the plume centerline in the vertical. The first term represents direct distance [$H - z$] of the receptor from the plume centerline. The second term represents the eddy reflected distance of the receptor from the plume centerline, which is the distance from the centerline to the ground [H] plus the distance back up to the receptor [z] after eddy reflection.

APPLICATION OF THE ISC-ST3 MODEL TO THE TINKER AFB IWTF

Task 2 of this research effort involved the use of the coupled model in the predictive mode; that is, to develop geographically-based profiles of the ground-level concentrations of phenol and methylene chloride in the nearby environment [at specific receptor locations within the impact region] of the IWTF under differing meteorological conditions, on-base chemical usage practices, and IWTF operating scenarios. The ISC-ST3 model was used during this task. The model requires inputs related to source types, locations, and emission strengths; selected receptor grid coordinates; and hourly-average meteorological data consisting of surface conditions [wind speed, wind direction, and temperature] and mixing height parameters. The hourly surface and upper air data were combined into a single meteorological file for each year as required by the ISC-ST3 model. The x-y coordinates were determined from the Tinker AFB comprehensive plan. All emission sources at the IWTF were modeled as point sources. The annual emissions predicted for phenol and methylene chloride from each IWTF component under both average and maximum influent conditions, as presented in Chapter 2 [Tables 2.2 and 2.3], were converted into a surface emission rate [with units of grams per m^2·second] using the actual surface area of the process unit. The coupled model annual-average calculations were based on the average influent concentration

into the primary waste stripping clarifier. The coupled model 24-hour maximum calculations were based on a method whereby the maximum chemical concentration occurring one percent of the time was used. The maximum concentration occurring one percent of the time was determined using probability tables for normally distributed data.

For this modeling effort, a nested Cartesian receptor grid covering a 120,000 m^2 area [300 meters by 400 meters] and centered about the IWTF was generated to determine the impact region boundaries. Within this area, a grid system consisting of 1200 receptors spaced ten meters apart in both the west-to-east [x-coordinate] and south-to-north [y-coordinate] directions was used. Figure 3.5 illustrates the resultant receptor grid coordinate system. The notation denotes the different IWTF process units [in blue] as follows: primary clarifier [PC], oil-water separator diversionary structure [OWD], north and south oil-water separators [OW-N, OW-S], blending tanks [D1, D2], west and east storage tanks [ST-W, ST-E], north and south equalization basins [EQ-N, EQ-S], mixing basins [MIX], north and south cold contact clarifiers [SCCN, SCCS], bioreactor [BIO], and north and south secondary clarifiers [SC-N, SC-S]. The process unit Cartesian grid coordinates were also specified. This positioning information was used as input to the ISC-ST3 model and the ground level concentrations calculated for each receptor location.

The phenol and methylene chloride emissions from the IWTF were modeled using each of the ten years of available meteorological data [1984 through 1993]. Ten years of meteorological data were used because of its availability and ease of use. The normal recommended meteorological data set is five years. More current meteorological data than 1993 were not available from the U.S. EPA SCRAM bulletin board so the available historical data were utilized. The ISC-ST3 model was then configured to provide two output concentrations for each year of the data modeled: annual-average ground-level concentrations at each of the 1200 receptors surrounding the IWTF, and the maximum 24-hour average ground-level concentration at each of the receptors.

The two averaging periods; namely, the 24-hour and annual, were selected as the basis for two different types of comparisons. The maximum 24-hour average concentrations were selected as the basis for comparisons between the short-term maximum concentrations and the

corresponding State of Oklahoma's Maximum Allowable Ambient Concentration [MAAC] for phenol or methylene chloride, which is expressed as a 24-hour average concentration. The maximum 24-hour concentrations obtained for each receptor in a modeled year reflect the worst 24-hour period of meteorological conditions, with respect to the dispersion of emissions of phenol and methylene chloride from the IWTF. The annual-average concentration at each receptor provides an estimate of the long-term average concentration at that location for the

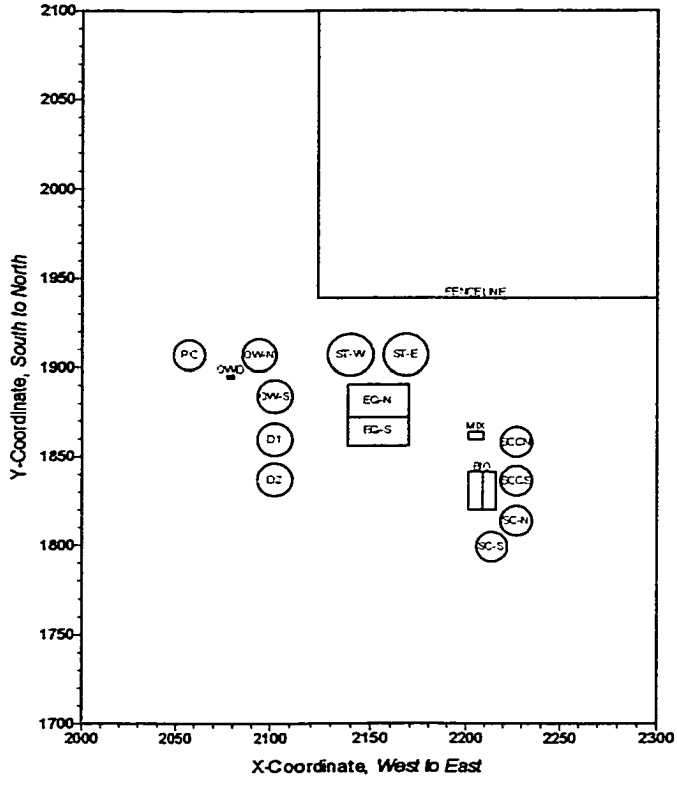

Figure 3.5: Receptor Grid Coordinate System for Dispersion Modeling of the Atmospheric Emissions from the Tinker AFB IWTF

particular VOC modeled; this information can be used for calculations related to long-term human exposure and human health risk assessments.

As mentioned, the pollutant emissions from the IWTF were modeled using ten years of meteorological data [1984 through 1993]. Ten years of meteorological data were used because of its availability and ease of use. An effective way to present graphically the average wind data for a specific location is with a wind rose, as shown in Figures 3.6 and 3.7. The average wind direction is shown as one of sixteen compass

points, each point separated by 22.5 degrees measured from true north. The length of the bar plotted for a given direction indicates the percentage of time that wind came from that direction. Since wind direction is constantly changing, the time percentage for a specific compass point actually includes those times for wind directions 11.25 degrees on either side of the point. The percentage of time for a given velocity range is shown by the thickness of the direction bar. Referring to Figure 3.6, the average wind direction was from the south 19 percent of the time; six percent of the time the southerly wind velocity was 11 to 15 miles per hour. It is important to note that the sample canister data [to which the coupled model will be calibrated] was collected during the fall months, so a second wind rose was included to illustrate the wind direction and velocities for that particular sampling period. Figure 3.7 illustrates the wind rose from 22 September through 8 November 1993 and shows that the average wind direction was from the north 19 percent of the time; nine percent of the time the northerly wind velocity was six to ten miles per hour. It is also important to note that the wind rose indicates that the winds are skewed primarily in a north-south direction, which should translate to wind profiles in an elongated shape running in the north-south direction. Another point illustrated in Figure 3.6 is that the concentration profiles [to be presented in the following section] will be skewed so that the concentration peaks will be centered north of the actual emission sources. The concentration profile peaks will be skewed and centered north of the emission source because the primary wind direction is out of the south to south-southwest. These points will be highlighted in the following discussion and illustrated in the figures presented in the next section.

ISC-ST3 DISPERSION MODELING RESULTS

The initial dispersion modeling emphasis was related to determining the range over which the pollutants would travel under average conditions [modeling constraints]. A nested Cartesian receptor grid covering an area of approximately one-kilometer by one-kilometer and centered about the IWTF was generated for this effort. Within this area, a grid system consisting of 1200 receptors spaced 33.3 meters

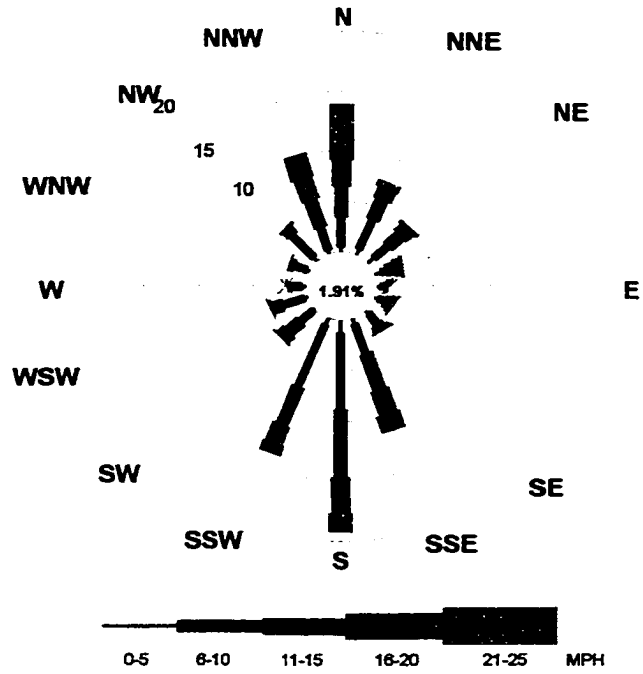

Figure 3.6: Wind Rose for Entire Ten Years [1984-1993]

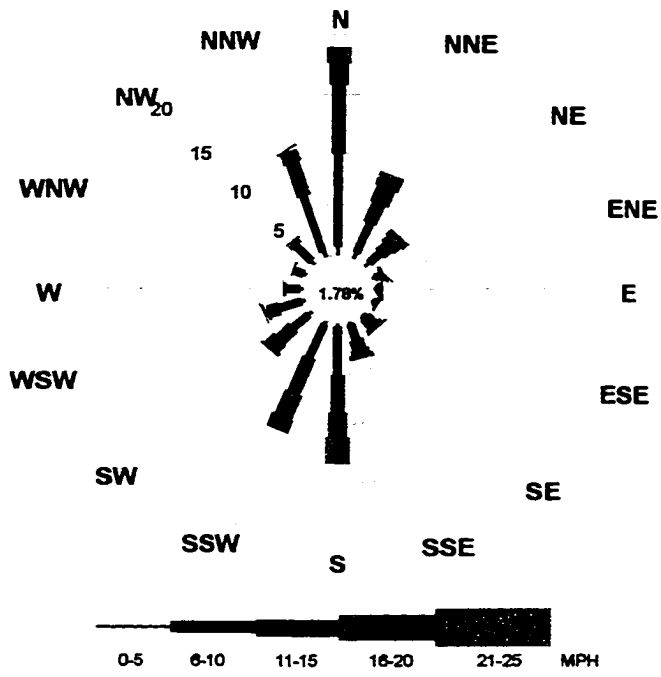

Figure 3.7: Wind Rose for Sampling Period [22 Sep through 8 Nov 1993]

apart was used. Phenol and methylene chloride concentrations outside of the subsequently utilized 300 by 400 meter grid were orders of magnitude below the Oklahoma MAAC limits for both pollutants. The decision was

then made to minimize the region of interest from a one-by-one kilometer grid system to a 300-by-400 meter grid system. The same number of receptors were utilized [1200 receptors], but spaced shorter distances [ten meters] apart, thus allowing greater resolution within the impact region. A related decision was made to elongate the area of interest in the north-south direction because of the predominant southerly wind direction at the Tinker AFB, thereby yielding the 300-by-400 meter rectangle. From historical meteorological data, the Oklahoma wind is predominantly out of the southwest [225°]. The concept was that the greatest likelihoods for exceedances would occur to the north and northeast of the IWTF.

Figure 3.8 illustrates the annual-average methylene chloride concentration for years 1984-1993. The *y*-coordinate extends in the south-to-north direction for 400 meters from the coordinate 1700 to 2100. The *x*-coordinate extends for 300 meters from west-to-east from coordinate 2000 to 2300. Figure 3.8 consists of a two-dimensional contour figure and a three-dimensional surface plot of the same data. The circles [contours in green] indicate concentration gradients at specific locations within the impact region and are similar to a topographical contour map except that elevations have been replaced with methylene chloride concentrations on parts per billion [ppb]. The process units are identified with their individual codes [*i.e.*, primary clarifier—PC, etc.] as detailed in Chapter 2.

As shown in Figure 3.8, there are three prominent peaks positioned north-northeast of the primary clarifier, north-northeast of the oil-water separators, and between the storage tanks and equalization basins. The peak nearest to the primary clarifier rises to a concentration of approximately 58 ppb. This peak is distinct and relatively symmetrical because the primary clarifier is somewhat isolated from the other process units. The second highest peak occurs northeast of the oil-water separators and rises to a concentration of approximately 52 ppb. Like the primary clarifier, the concentration peak is relatively sharp, but is somewhat elongated south to north to include both oil-water separators which contribute to the concentration gradient. The broadest peak is positioned between the storage tanks and equalization basins, and it rises to approximately 48 ppb. This concentration peak is the

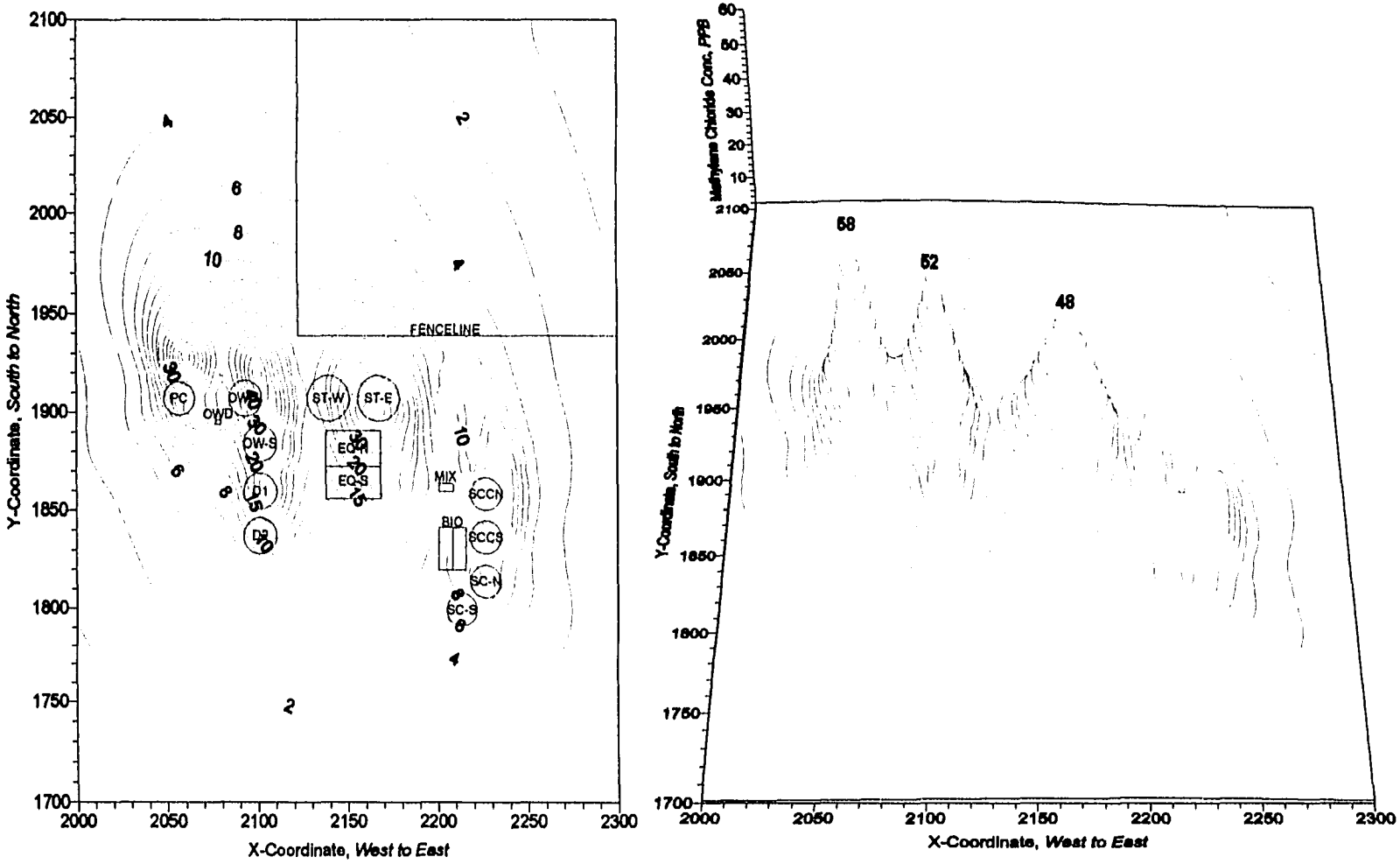

Figure 3.8: Annual-Average Methylene Chloride Concentration [*ppb*] for 1984 through 1993

widest of the three and incorporates all four modeled impoundments [*i.e.*, north-south equalization basins and east-west storage tanks]. It should be noted that this pattern was anticipated from the WATER8 emission model output as discussed in Chapter 2. It is also important to note that the other process units [D_1-D_2 blending tanks, mixing basins, solid contact clarifiers, bioreactors, and secondary clarifiers] contribute very little to the overall ground level concentrations [also predicted from the WATER8 emission model output].

Figure 3.9 illustrates contours of the maximum 24-hour methylene chloride concentration for all ten years of meteorological data. The concentration peaks appear to be flatter and exhibit less resolution as indicated by the peaks being somewhat meshed together. The lower concentration contours are spread out over a larger, less-defined impact region. As suggested by the WATER8 simulation results, there are also three peaks positioned north-northeast of the primary clarifier, north-northeast of the oil-water separators, and between the storage tanks and equalization basins. The peak surrounding the primary clarifier rises to a concentration of approximately 180 ppb. The second highest peak concentration occurs north of the oil-water separators and rises to a concentration of 160 ppb. The broadest peak is again between the storage tanks and equalization basins, also rising to 140 ppb. This concentration peak is the widest of the three and incorporates all four impoundments [*i.e.*, north-south equalization basins and east-west storage tanks]. Finally, it should be noted that the methylene chloride concentrations at the fenceline are between 60 and 70 ppb; these concentrations are well below the Oklahoma 24-hour MAAC of 500 ppb for methylene chloride.

Figure 3.10 illustrates the annual average phenol concentration over the period of meteorological data [1984-1993]. There are four prominent peaks positioned north-northeast of the primary clarifier, north-northeast of the oil-water separators, between the storage tanks and equalization basins, and between the solid contact clarifiers. The peak near the primary clarifier rises to a concentration of approximately 40 ppb; it is relatively sharp in definition primarily because the process is somewhat isolated from the other process units. The peak to the north-northeast of the oil-water separators also rises to a

concentration of approximately 37 ppb. Like the primary clarifier peak, this concentration peak is relatively sharp. However, it is slightly elongated south to north to include both oil-water separators. The broadest peak is positioned between the storage tanks and equalization basins, rising to roughly 45 ppb. This concentration peak is the widest of all four peaks because it incorporates all four impoundments [*i.e.*, north-south equalization basins and east-west storage tanks]. The fourth concentration peak is positioned between the solid contact clarifiers and rise to 26 ppb. A pattern consisting of four peaks was anticipated from the WATER8 emission model output as described in Chapter 2.

Figure 3.11 demonstrates the 24-hour maximum phenol concentrations for the ten years of meteorological data. The 24-hour maximum concentration data, when compared to the annual average data as shown in Figure 3.10, appear to be flatter and have less resolution. Also, note that the lower 24-hour maximum concentration contours are spread over a larger, less-defined impact region. As suggested by the WATER8 simulation results, four prominent peaks were identified. The concentration peak surrounding the primary clarifier rises to approximately 118 ppb, and the oil-water separator peak also rises to a concentration peak of about 105 ppb. The broadest peak is again the one between the storage tanks and equalization basins; it rises to 130 ppb. This concentration peak is the widest of the four since it incorporates the north-south equalization basins and east-west storage tanks. The fourth concentration peak is located between the solid contact clarifiers, and it rises to 60 ppb. Finally, it should be noted that the phenol concentrations at the fenceline are about 40 ppb; this is also below the Oklahoma phenol 24-hour MAAC of 100 ppb for phenol.

SUMMARY

Following the review of nine candidate air quality dispersion models, the U.S. EPA-approved Industrial Source Complex [ISC-ST3] model was selected for use in this research. The selection of the ISC-ST3 model was based on its compliance with six selection criteria as well as its documented usage by others for determining short-term ground level chemical concentrations at multiple receptor locations. Further, the

model is both computerized and user-friendly.

Applications of the ISC-ST3 model to the Tinker AFB IWTF proved to be successful. The model was used in a coupled fashion with the WATER8 model as described in Chapter 2. Concentration peaks [24-hour maximum and annual-average] around the IWTF were identified for both methylene chloride and phenol. Due to the emission quantities from the unit processes at the IWTF, three and four peak locations, respectively, were predicted for methylene chloride and phenol. Peaks for both pollutants were located just to the north-northeast of the primary clarifier, to the north-northeast of the oil-water separators, and between the storage tanks and equalization basins. An additional phenol peak is positioned between the solid contact clarifiers. These patterns of ground level concentrations had been anticipated as a result of the emissions identified through the use of the WATER8 model; these emissions were described in Chapter 2.

The coupled model [WATER8 model coupled with the ISC-ST3] was used to calculate 24-hour maximum concentrations at the Tinker AFB property line for both methylene chloride and phenol. The pertinent Oklahoma 24-hour MAAC for both pollutants was 500 ppb and 100 ppb, respectively. The calculated 24-hour maximum methylene chloride concentration at the Tinker AFB fenceline was between 60 and 70 ppb [approximately 13 percent of the standard]. The highest calculated 24-hour concentration near the IWTF was 180 ppb [approximately 36 percent of the standard]. For phenol, the calculated 24-hour maximum concentration at the Tinker AFB fenceline was 40 ppb [40 percent of the standard]. The highest calculated 24-hour concentration for phenol near the IWTF was 130 ppb which exceeds the MAAC standard. Accordingly, based on these concentration comparisons to their respective MAACs, it can be concluded that phenol may be of greater environmental compliance concern than methylene chloride in the vicinity of the Tinker AFB IWTF.

SELECTED REFERENCES

1. Schulze, R.H., *Fundamental of Dispersion Modeling*, Trinity Consultants, Research Triangle Park, North Carolina, 1996.

2. U.S. Environmental Protection Agency, *Guideline on Air Quality Models [Revised]*, EPA-450/2-78-027R, 40 Code of Federal

Regulations, Chapter 1, Part 51, Appendix W, July 1, 1993 Edition, pp. 962-969, 973, 989, 1002-1012, 1018-1019, and 1060-1064.

3. Zannetti, P., *Air Pollution Modeling: Theories, Computational Methods, and Available Software,* Van Nostrand Reinhold, New York, New York, 1990.

4. Scorer, R.S., *Meteorology of Air Pollution,* Ellis Horwood Publishing, New York, New York, 1990.

5. Stern, A.C., Boubel, R.W., Turner, D.B., and Fox, D.L., *Fundamentals of Air Pollution,* Academic Press, Toronto, Canada, 1984.

6. Federal Aviation Administration, *A Microcomputer Pollution Model for Civilian Airports and Air Force Bases—Model Description,* August 1988, U.S. Department of Transportation, Office of Environment and Energy, Washington, D.C.

7. Defense Technical Information Center, *Users Guide for the Air Force Toxic Chemical Dispersion Model [AFTOX],* Environmental Research Paper No. 992, January, 1988, Ft. Belvoir, Virginia.

8. Defense Technical Information Center, *A Users Manual for ADAM,* December, 1990, Geophysics Laboratory, Air Force Systems Command, Ft. Belvoir, Virginia.

9. Defense Technical Information Center, *WADOCT—An Atmospheric Model for Complex Terrain,* July, 1990, Geophysics Laboratory, Air Force Systems Command, Ft. Belvoir, Virginia.

10. Defense Technical Information Center, *WADOCT—An Atmospheric Model for Complex Terrain,* Environmental Research Paper No. 1062, May, 1990, Ft. Belvoir, Virginia.

11. Taylor, R.K., *Evaluation of ISC-ST3 Dispersion Model Performance using Actual Emissions Data and Ambient Monitoring Data for a Large Chemical Manufacturing Facility located in North Carolina,* Paper presented at the Air and Waste Management Association, 89th Annual Meeting and Exhibition, Nashville, Tennessee, 23-28 June, 1996.

12. Taylor, R.K., *Utilizing ISC-ST to Model Composting Facility Odors,* Paper presented at the Air and Waste Management Association, 90th Annual Meeting and Exhibition, Toronto, Canada, 8-13 June, 1997.

13. Mahin, T.D., *Using Dispersion Modeling of Dilutions to Threshold [D/T] Odor Levels to Meet Regulatory Requirements for Composting Facilities,* Paper presented at the Air and Waste Management Association, 90th Annual Meeting and Exhibition, Toronto, Canada, 8-13 June, 1997.

14. McCourtney, M., and Pratt, G., *Model-Predicted Concentrations of Toxic Air Pollutants in Minneapolis / St. Paul Metropolitan Area,*

Paper presented at the Air and Waste Management Association, 91st Annual Meeting and Exhibition, San Diego, California, 14-18 June, 1998.

15. Minnesota Pollution Control Agency, *Estimation and Evaluation of Cancer Risks from Air Pollution in the Minneapolis / St. Paul Metropolitan Area*, Minneapolis, Minnesota, 1992.

16. Allen, E., Witherspoon, J., and Regan, M., *Using Dispersion Modeling Techniques to Predict Odor Impacts to Surrounding Communities from Wastewater Treatment Plants*, Paper presented at the Air and Waste Management Association, 91st Annual Meeting and Exhibition, San Diego, California, 14-18 June, 1998.

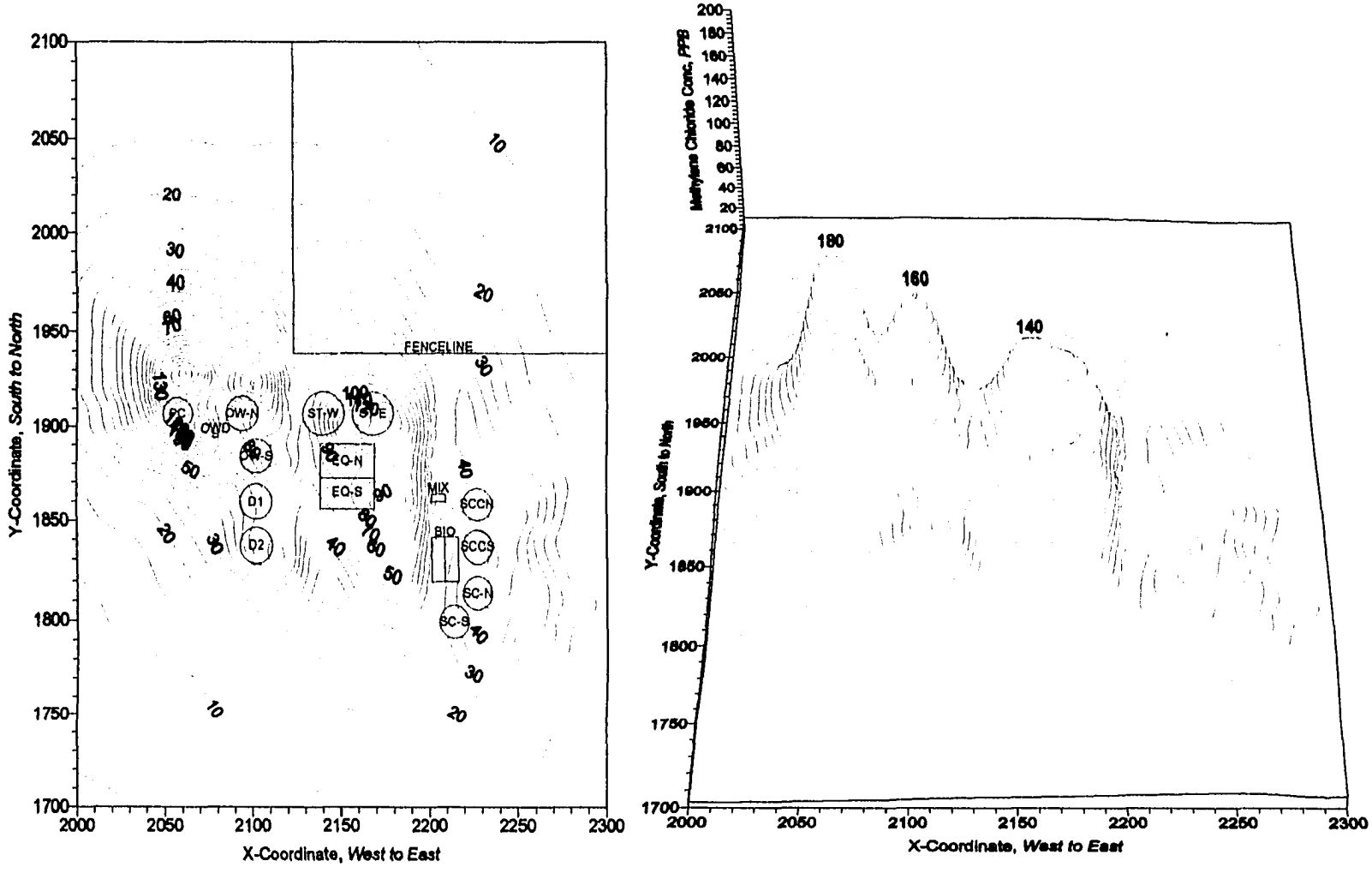

Figure 3.9: 24-hour Maximum Methylene Chloride Concentration [*ppb*] for 1984 through 1993

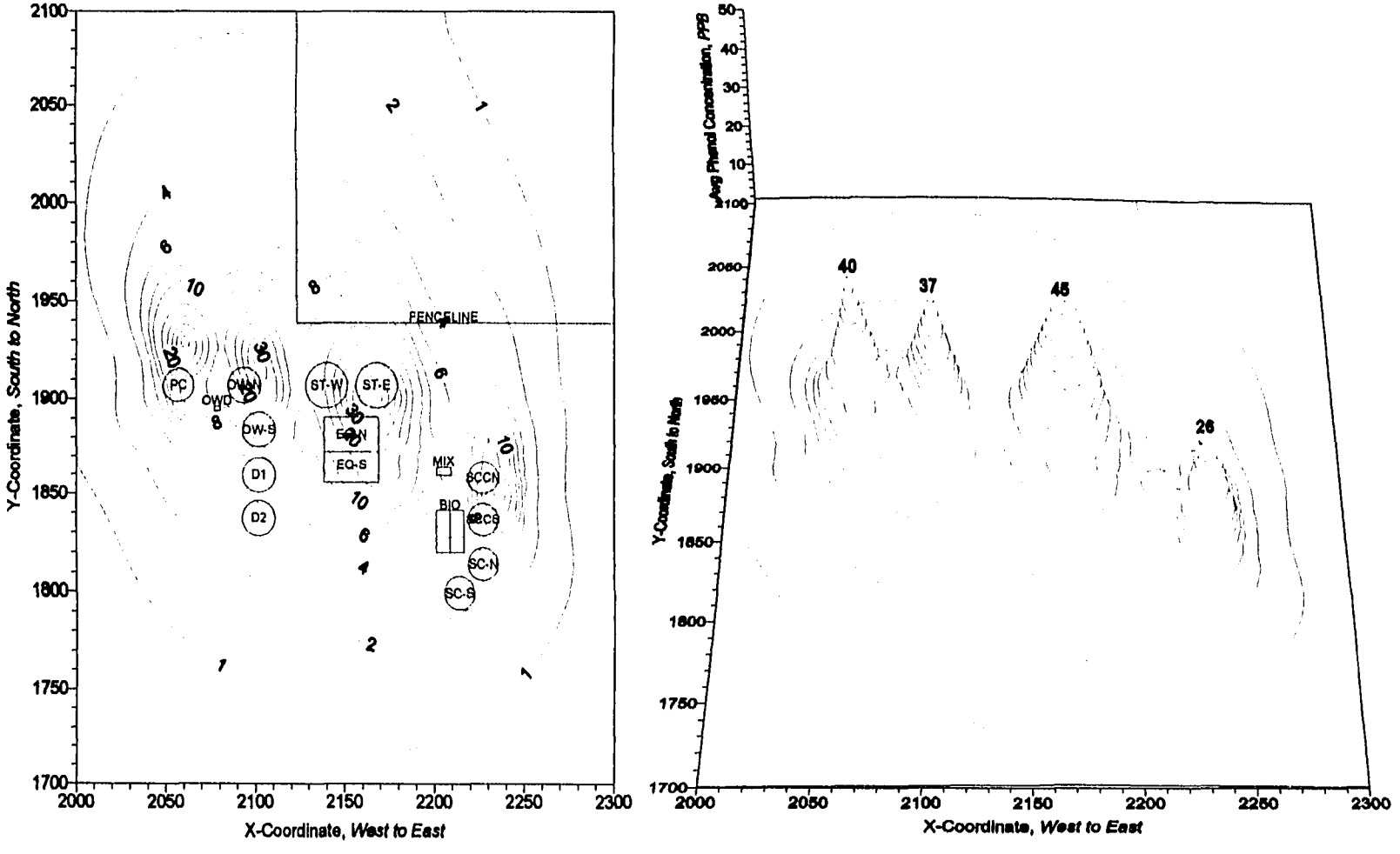

Figure 3.10: Annual-Average Phenol Concentration [*ppb*] for 1984 through 1993

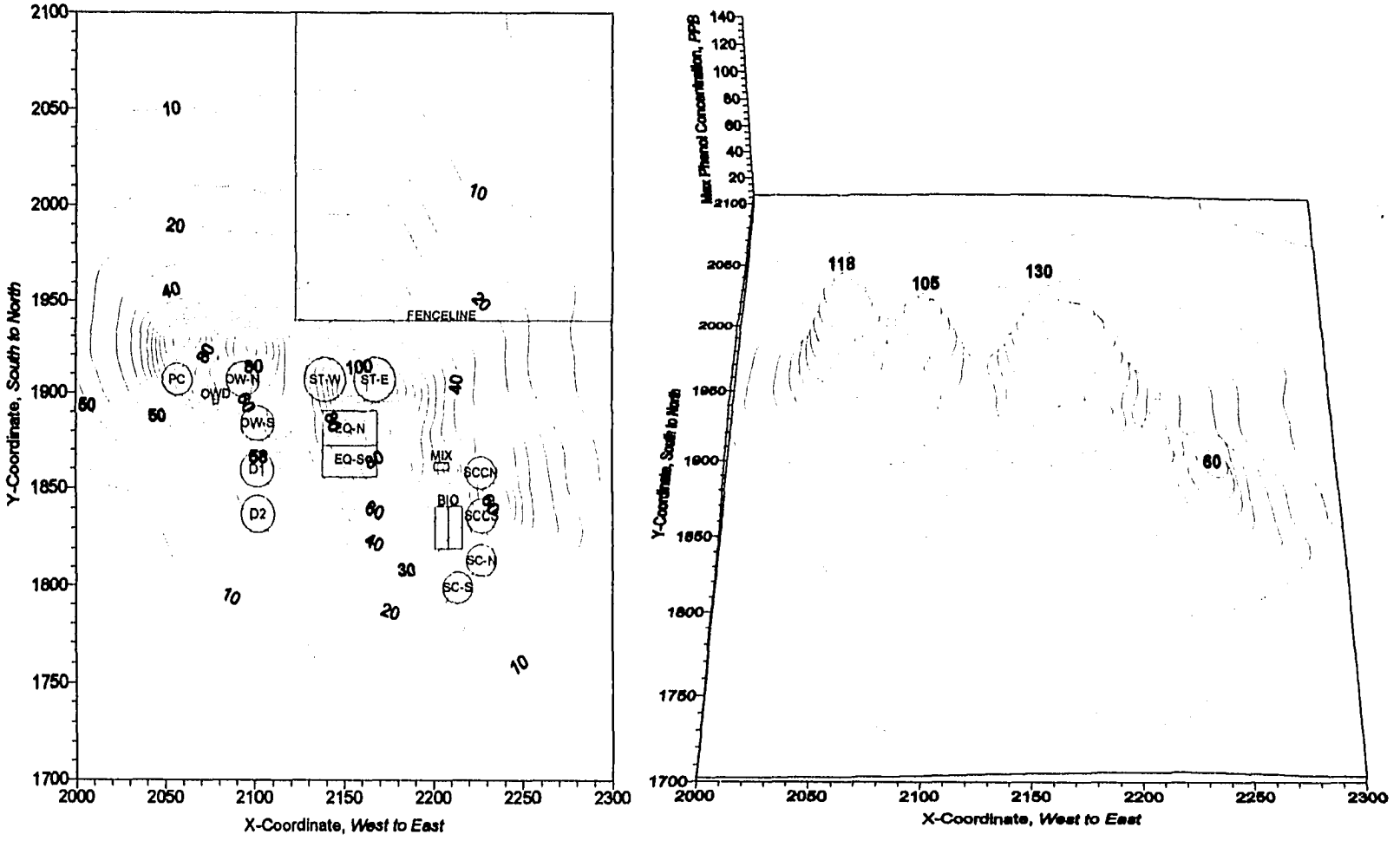

Figure 3.11: 24-hour Maximum Phenol Concentration [*ppb*] for 1984 through 1993

CHAPTER 4
COUPLED MODEL VALIDATION

The predictive accuracy of a developed model should be validated, herein, the predictive accuracy of the coupled model will be validated by comparing the estimated computer-generated concentrations with periodic canister monitoring data [Sub-task 3A] and open-path monitoring [FTIR] data [Sub-task 3B]. This validation process will be completed via two approaches. First, comparisons and statistical testing of pertinent canister monitoring data will be made relative to the predicted computer-generated chemical concentrations [Chapter 4] and open-path monitoring results [Chapter 5]. The coupled model will be calibrated to improve the performance of the predictive capabilities of the model, followed by a sensitivity analysis to determine the responsiveness of the model to input parameters [influent constituent concentrations]. This chapter will validate the coupled model predictions by comparing the model predictions to periodic field canister data.

One of the many distinctive features of this effort is the comparative studies, whereby the coupled model predictions are compared to field data [periodic canister monitoring] and open-path air monitoring data [FTIR] to encompass the entire perimeter of the facility. While much of the literature is limited to the use of a specific model under a strict geographical location or under distinct, limited applications, there is very little comparison of coupled model predictions to field data. When there is mention of comparison information, there is no statistical manipulation of the comparison data and there are a limited number of data points. When there is literature, most of the literature is limited to downwind concentrations over a very short period of time [typically days]. The availability of multiple field data studies [three canister studies] is another feature unique to this effort, whereas the literature is typically limited to a single, short-term sampling routine. An additional distinctive feature is that the model predictions [and field canister studies] are compared surrounding the entire perimeter [360 degrees], whereas most of the literature evaluates a single, downwind plane. Another element unique

to this effort is that there are considerably more field samples collected as compared to any documented literature study. Another distinct feature is the investigation of chemical depainting agents [phenol and methylene chloride], whereas much of the literature is limited to primary criteria pollutants or tracer gases [sulfur hexafluoride and carbon tetrafluoride]. The overall completeness of the comparative evaluations is a distinctive feature of this work, whereby the ISC-ST3 model predictions are compared to both field canister data and OP-FTIR predictions. Most of the FTIR literature is compared to limited, short-term tracer gas releases without comparisons to air dispersion model predictions. Much of the literature pertains to the monitoring of a variety of industrial sources [*i.e.*, industrial complexes, incinerators, petrochemical facilities, landfills, municipal waste sites, etc.] and not directed toward environmental monitoring of industrial wastewater treatment facility fencelines [facility perimeter]. Another unique point is that there is no documented statistical manipulation [*z*-test and *t*-test] of the model predictions or field data to quantify model fit. Probably the most unique feature of this research effort is the calibration of the coupled model to refine the predictive capabilities of the model, followed by a sensitivity analysis to determine the responsiveness of the model to input parameters [influent constituent concentrations].

FIELD SAMPLE COLLECTION METHOD

Sub-task 3A of the project involves comparing the estimated computer-generated methylene chloride and phenol concentrations [using the coupled model] with discontinuous field data. The field work was conducted from 23 September through 8 November 1993 and utilized SUMMA canisters to collect 270 samples from 13 sources distributed around the facility perimeter. Ambient air samples were collected with the guidance of the U.S. EPA Compendium Method TO-14A [1,2], which describes the procedure for sampling and analysis of volatile organic compounds [VOCs] in ambient air. The method is based on collection of whole air samples in SUMMA passivated stainless steel canister. The VOCs are separated by gas chromatography and measured by a mass spectrometer or by multidetector techniques. This method is applicable to specific VOCs

that have been tested and determined to be stable when stored in pressurized and sub-atmospheric pressure canisters. Methylene chloride and phenol have been successfully stored in canisters and measured at the parts per billion by volume level [1]. This method applies under most conditions encountered in sampling of ambient air into canisters.

Samples collected from ambient and process locations for VOC and semi-VOC analysis were collected in SUMMA canisters, whereby the ambient air is drawn through a sampling train comprised of components that regulate the rate and duration of sampling into a pre-evacuated specially prepared passivated canister [in this case, 5.2 milliliters per minute over 24 hours]. After the air sample was collected, the canister valve is closed, an identification tag is attached to the canister, and the appropriate chain-of-custody form is completed. Upon receipt at the laboratory, the canister is attached to the analytical system, separated on a gas chromatograph column, and detected by one or more detectors for identification and quantification.

TINKER AFB APPLICATION OF THE FIELD DATA COLLECTION SYSTEM

For both methylene chloride and phenol, there are three major field data sources [periodic canister data] including a Resource Conservation and Recovery Act [RCRA] facility investigation [3], Oklahoma City Air Logistics Center [OC-ALC] Bioenvironmental sample data, and a 1993 Battelle Study [4]. The RCRA facility investigation was executed to meet the requirements of the U.S. Air force Installation Restoration Program prepared by Engineering-Science Inc., in April 1993. The RCRA investigation focused on releases to the soil and air and quantified the contaminant releases from process units at the industrial and sanitary wastewater treatment plants. As illustrated in Figure 4.1, ambient air samples were collected from thirteen locations [shown in red]. Ambient locations A1 through A11 were chosen to represent the fencelines or boundaries of the treatment plant in all compass directions. Receptors A12 and A13 were located on base property northwest of the industrial wastewater treatment facility to monitor on- and off-base migration. The 24-hour sampling routine at these locations was performed between 08:00 and 12:00 hours on Monday, Wednesday, and Friday [3,4].

In addition to the RCRA facility investigation, methylene chloride

and phenol ambient air samples were collected in an October 1993 Battelle Study [4]. Three methylene chloride and phenol concentrations were measured using a 24-hour SUMMA canister in September through November of 1993. Data from the Battelle Study utilized the same identical locations as with the RCRA facility investigation [A1, A2, and A3]. Along with the RCRA investigation and Battelle Study, there is an additional data source from the Oklahoma City Air Logistics Center Bioenvironmental department. Three samples were collected at locations A1, A2, and A3 for three days [19 May, 6 June, and 16 June 1993].

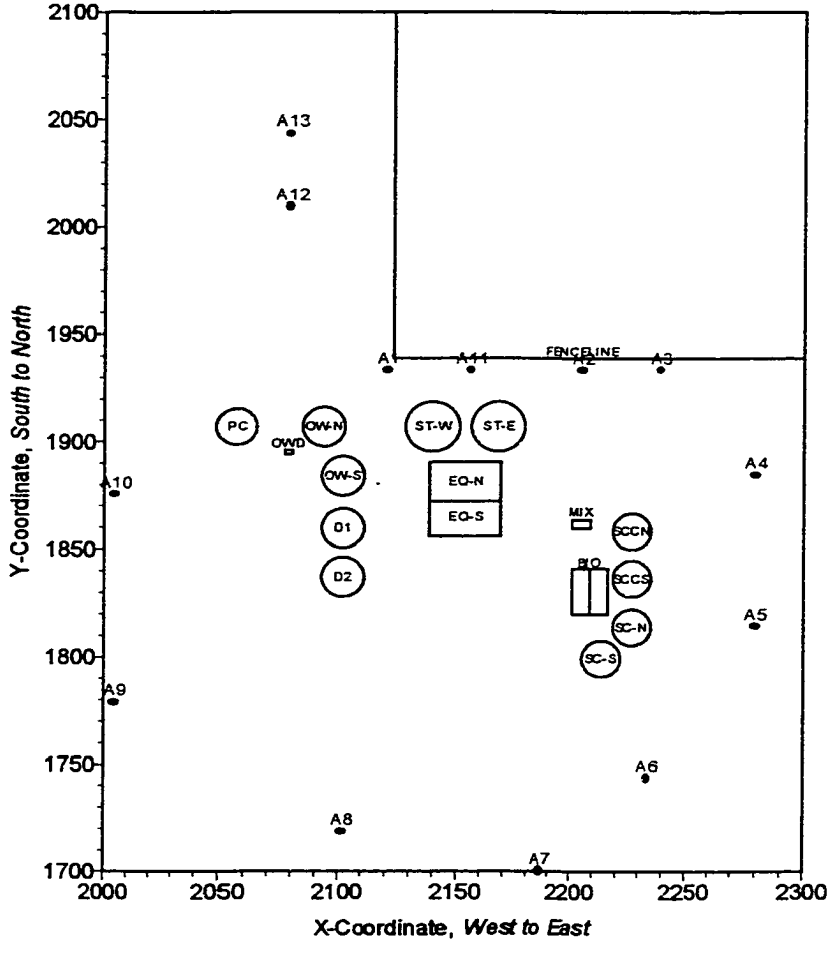

Figure 4.1: Ambient Air Sample Locations [A1 through A13]

The following discussions involve comparing the estimated computer-generated methylene chloride and phenol concentrations [using the coupled model] with periodic field data. To better identify trends between similar sample sites, the sample data were primarily grouped according to their orientation / location [either upwind or downwind]

and secondarily grouped by distance from the major emission sources [less than or greater than 100 meters]. For example, field data points A1, A11, A2, and A3 were grouped together and referred to as downwind and less than 100 meters from the primary emission sources. Field data points A12 and A13 were grouped and called downwind and greater than 100 meters from the primary emission sources. Data points A6, A7, and A8 are upwind and greater than 100 meters from the major sources. Data points A4, A5, A9, and A10 were called crosswind. In the following figures and discussions, the grouping will be made apparent. It is also important to note that the distinction and classification as upwind or downwind were made according to the wind rose illustrated in Figure 3.2, which is an effective way to graphically present average wind data for a specific location. Referring to Figure 3.2, the average wind direction was from the south-southwest to south-southeast the majority of the time, resulting in the above-discussed upwind-downwind notation.

STATISTICAL EVALUATION: *z* TESTS AND CONFIDENCE INTERVALS

In Sub-task 3A of this effort, the predictive accuracy of the coupled model will be validated by comparing the estimated computer-generated concentrations with periodic canister monitoring data. Coupled model output [geographically based profiles of the ground level chemical concentrations] will be compared to discontinuous field data [from periodic canister sampling]. The predictive accuracy of the coupled model will be evaluated using two independent statistical methods: z-test and Student t-test. The statistical investigation will be made after the coupled model was calibrated to field canister data to improve the performance of the predictive capabilities of the model. The objective of this section is to quantitatively determine the coupled model fit to field canister data using the statistical z-test following the model calibration efforts.

The following statistical z-test discussion concerns situations involving the means, proportions, and variances of two different distributions and will quantitatively determine how field data compares to model predictions [5,6,7]. The inferences concern the difference [$\mu_1 - \mu_2$] between the means of two different population distributions. The methodology will involve testing hypotheses about the difference between

the field data and modeling predictions. The initial hypotheses would state that $\mu_1 - \mu_2 = 0$, that is $\mu_1 = \mu_2$. Alternatively, it may be appropriate to estimate $\mu_1 - \mu_2$ by computing a 99.9 percent confidence interval. Such inferences are based on a number of assumptions: x_1, x_2, ..., x_m is a random sample from a population with mean μ_1 and variance σ_1^2; y_1, y_2, ..., y_m is a random sample from a population with mean μ_2 and variance σ_2^2; and, x and y samples are independent of one another, both population distributions are normal, and that the values of both σ_1^2 and σ_2^2 are known [5].

In a hypothesis-testing example, the null hypothesis [H_o] will state that $\mu_1 - \mu_2$ has a specified value. Denoting this null value by Δ_o, the null hypothesis becomes: H_o: $\mu_1 - \mu_2 = \Delta_o$. Often $\Delta_o = 0$, in which case H_o says that $\mu_1 = \mu_2$. Consider the alternative hypothesis H_a: $\mu_1 - \mu_2 > \Delta_o$. A value $\bar{x} - \bar{y}$ that considerably exceeds Δ_o provides evidence against H_o for H_a. Such a value $\bar{x} - \bar{y}$ corresponds to a positive and large value of z. Thus H_o should be rejected in favor of H_a if z is greater than or equal to an appropriately chosen critical value. Because the test statistic z has a standard normal distribution when H_o is true, the upper-tailed rejection region $z \geq z_\alpha$ gives a test with significance level α.

Assuming a significance level of $\alpha = 0.001$, determine the difference between the field mean [μ_1] and mean predicted by the model [μ_2]. The null hypothesis is defined as H_o: $\mu_1 - \mu_2 = 0$. The alternative hypothesis is H_a: $\mu_1 - \mu_2 \neq 0$. If H_a is true, then μ_1 and μ_2 are different and the field data are different than the concentrations predicted by the computer model. When $\Delta_o = 0$, the test statistic value is as given [5]:

$$z = \frac{\bar{x} - \bar{y}}{\left[\left(\sigma_1^2/m\right) + \left(\sigma_2^2/n\right)\right]^{0.5}} \qquad 4.1$$

where z is the distribution, $\bar{x}$ and $\bar{y}$ are the sample means [independent of one another and normally distributed], σ_1^2 and σ_2^2 are the sample variances of each population, and m and n are the number of random samples from each population. The inequality in H_a implies that the test is two-tailed. For $\alpha = 0.001$, $\alpha/2 = 0.0005$ and $z_{\alpha/2} = z_{0.0005} = 3.30$. H_o will be rejected if $z \geq 3.30$ or if $z \leq -3.30$. For example in testing

field data against the model predictions for sample site A1, substitute the field data variables $\bar{x}$, m, σ_1^2, [$\bar{x}=$, $m=$, $\sigma_1^2=$], and the model prediction parameters $\bar{y}$, n, σ_2^2, [$\bar{y}=$, $n=$, $\sigma_2^2=$] into the formula for z yields. The results are illustrated in Figure 4.2.

The field data are in good agreement [with a 99.9 percent level of confidence] with model predictions when the field data fall within the range of -3.30 to 3.30 [6]. For methylene chloride [represented with blue circles in Figure 4.2], the model appears to be in good agreement [99.9 percent level of confidence] with all thirteen field data points. Note that points at A1, A11, and A6 slightly over-predict, while A9 and A10 slightly under-predict, by approaching both confidence limits [± 3.30]. For sample sites downwind and less than 100 meters from the major

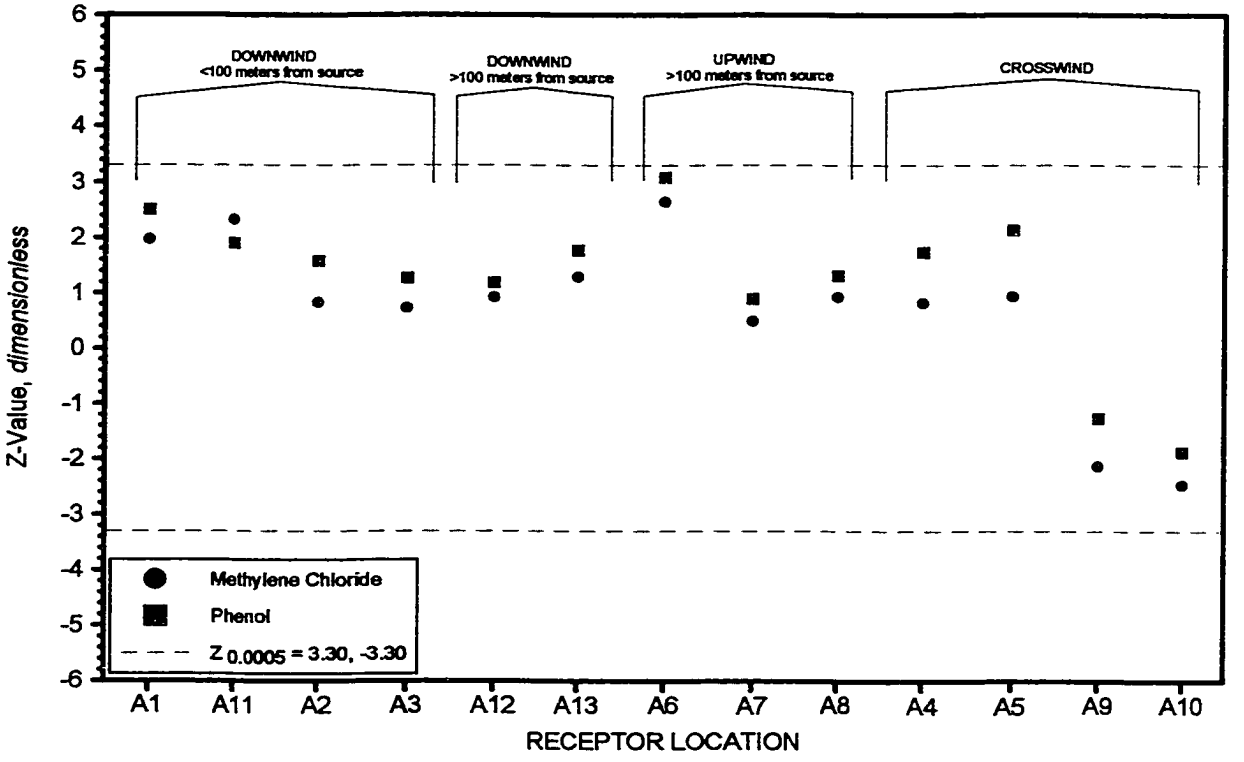

Figure 4.2: Z-values for Methylene Chloride and Phenol

emission sources [A1, A11, A2, A3], there is very good agreement [with a 99.9 percent confidence interval] between the coupled model predictions and field data for A2 and A3, while the model tends to slightly over-predict for points A1 and A11 [closer to the 99.9 percent confidence limit]. For sample sites downwind and greater than 100 meters from the

major emission sources [A12 and A13], there is good agreement [99.9 percent confidence] between the coupled model predictions and field data. For sample sites upwind and greater than 100 meters from the major emission sources [A6, A7, A8], there is relatively good agreement [99.9 percent confidence] between the coupled model predictions and field data for points A7 and A8, while slightly over-predicting for A6. For sample sites crosswind from the major emission sources [A4, A5, A9, A10], there is relatively good agreement [99.9 percent confidence] between the coupled model predictions and field data for all four points [slightly better for A4 and A5]. Qualitatively, the coupled model appears to do a good job of predicting field data. Quantitatively, all thirteen coupled model predictions are within the 99.9 percent confidence interval. In general, the coupled model appears to do a slightly better job of predicting downwind [both less and greater than 100 meters from the major sources] while slightly over-predicting the upwind concentrations and under-predicting the crosswind concentrations. What makes the upwind and crosswind coupled model predictions slightly worse when compared to the other locations can be explained by two thoughts: the range of the field data [indicated by the width of the box and whisker plots] and the location of the receptors outside the major wind pathways. The range of upwind and crosswind concentrations measured in the field are slightly narrower when compared to the downwind receptors, thereby making the model predictions more difficult to correlate with the field canister data. In addition, the major winds are out of the south-southwest and north-northeast with little from the east or west directions, further hampering the coupled models ability to fit the field data.

For phenol [represented by green squares in Figure 4.2], the model appears to be in good agreement [with a 99.9 percent level of confidence] with all field data points. Note that points at A1, A11, A6, and A5 slightly over-predict, while A10 slightly under-predicts, by approaching the confidence limits [$\pm$ 3.30]. For phenol, sample sites downwind and less than 100 meters from the major emission sources [A1, A11, A2, A3], there is very good agreement [with a 99.9 percent confidence interval] between the coupled model predictions and field data for A2 and A3, while the model tends to slightly over-predict with

A1 and A11 [closer to the 99.9 percent confidence limit]. For sample sites downwind and greater than 100 meters from the major emission sources [A12 and A13], there is good agreement [99.9 percent confidence] between the coupled model predictions and field data. For sample sites upwind and greater than 100 meters from the major emission sources [A6, A7, A8], there is relatively good agreement [99.9 percent level of confidence] between the coupled model predictions and field data for all three points, while point A6 slightly over-predicts. For sample sites crosswind from the major emission sources [A4, A5, A9, A10], there is relatively good agreement [99.9 percent confidence] between the coupled model predictions and field data for all four points [slightly better for A4, A9, and A10]. Qualitatively, the coupled model appears to do a good job of predicting field data. Quantitatively, all thirteen coupled model predictions are within the 99.9 percent confidence interval. In general, the coupled model appears to do a slightly better job of predicting downwind [both less and greater than 100 meters from the major sources] while slightly over-predicting the upwind and crosswind [except for A10] concentrations. What makes the upwind and crosswind coupled model predictions slightly worse when compared to the other locations can be explained by two thoughts: the range of the field data [indicated by the width of the box and whisker plots] and the location of the receptors outside the major wind pathways. The range of upwind and crosswind concentrations measured in the field are slightly narrower when compared to the downwind receptors, thereby making the model predictions more difficult to correlate with the field canister data. In addition, the major winds are out of the south-southwest and north-northeast with little from the east or west direction, further hampering the coupled models ability to fit the field data.

The coupled model performs better when predicting methylene chloride [more-volatile] concentrations when compared to the semi-volatile phenol constituent [Figure 4.2]. This can be partially explained by looking at differences in volatility and phase equilibrium [separation between the phases]. When components are approaching equilibrium within the wastewater, the more volatile component will have a tendency to be removed from the wastewater at a faster rate [and extent] than the less volatile component. The vapor pressures for methylene chloride and

phenol are 438 mmHg and 0.348 mmHg, respectively. The equilibrium constants are temperature and pressure sensitive, but are 164.5 and 0.0722, respectively [25°C and one atmosphere]. The value for the Henry's Law constant becomes more critical as the component becomes more volatile. For example, the Henry's Law constant for methylene chloride [0.00296 atm·m^3/mole] is critical to the phase separation, and ultimately to the fit of the coupled model to field data, as compared to the less volatile phenol component [0.00000130 atm·m^3/mole].

STATISTICAL EVALUATION: STUDENT *t*-TEST AND PROBABILITIES

As mentioned in the introduction, the predictive accuracy of the coupled model will be validated by comparing the estimated computer-generated concentrations with periodic canister monitoring data. Coupled model output [geographically based profiles of the ground level chemical concentrations] will be compared to discontinuous field data [from periodic canister sampling]. In this section, the predictive accuracy of the coupled model will be evaluated using the Student *t*-test. After the coupled model was calibrated to field canister data, a statistical investigation was done to improve the performance of the predictive capabilities of the model. The objective of this section is to quantitatively determine the coupled model fit for a single observation [Year 1993] to field canister data using the Students *t*-test.

The following statistical *t*-test discussion concerns situations involving the means, proportions, and variances of a single distribution and its quantitatively relationship to coupled model predictions for a single event year [1993]. Gosset, in 1908, recognized that the use of the variance and standard deviation in calculating *z* values was not trustworthy for small [less than 30] samples and an alternative table was required [5,6,7]. From this, the Students *t*-test was developed.

$$t = \frac{\bar{Y} - \mu}{\sqrt{s^2/n}} \qquad 4.2$$

where t is the distribution [or p-value], $\bar{Y}$ is the model prediction, μ is the population mean, s is the standard deviation, and n is the number of degrees of freedom. Like the chi-squared distribution, t has a

different distribution for each value of the degrees of freedom [5,6,7]. In this case, the degrees of freedom [n] represent the number of sample data points in the field canister data [20 to 25 points for all sample sites]. The t-tables [or p-values] present probabilities and represent the probability that the data point [predicted by the coupled model for 1993] is outside the field canister data distribution. Figure 4.3 illustrates the predictive ability of the coupled model to accurately estimate chemical concentrations using the p-value in the Students t-test. For example in Figure 4.3, a p-value of 0.05 can be interpreted as the mean predicted by the coupled model is in agreement with the mean of the field canister data. Note that all receptor locations are within the 0.05 p-value.

The field data are in good agreement with model predictions with a p-value of 0.05 or greater. For methylene chloride [represented with blue circles in Figure 4.3], the model appears to be in good agreement [with a 0.05 p-value or greater] with the field data for all thirteen receptor points [A1, A11, A2, A3, A12, A13, A6, A7, A8, A4, A5, A9, and A10]. Note that points at A12, A6, A7, A8, and A5, the model under-predicts by approaching the 0.05 p-value limit. For sample sites downwind and less than 100 meters from the major emission sources [A1, A11, A2, A3], there is very good agreement [with a p-value between 0.14 to 0.25] between the coupled model predictions and field data for A2 and A3, while the model tends to slightly struggle with A11 [p-value of 0.14]. For sample sites downwind and greater than 100 meters from the major emission sources [A12 and A13], there is good agreement between the coupled model predictions and field data for A13 while struggling with A12 [p-value of 0.09]. For sample sites upwind and greater than 100 meters from the major emission sources [A6, A7, A8], there is relatively good agreement [p-values of 0.07, 0.09, and 0.10] between the coupled model predictions and field data for all three points. For sample sites crosswind from the major emission sources [A4, A5, A9, A10], there is relatively good agreement [p-values of 0.08 to 0.17] between the coupled model predictions and field data for all four points [slightly better for A4, A9, and A10]. Qualitatively, the coupled model appears to do a good job of predicting field data. Quantitatively, all thirteen coupled model predictions have a p-value greater than 0.05. In

general, the coupled model appears to do a slightly better job of predicting downwind [both less and greater than 100 meters from the major sources] while slightly over-predicting the upwind concentrations [A6, A7, and A8] and under-predicting the crosswind concentrations [A4, A9, and A10]. What makes the upwind and crosswind coupled model predictions slightly worse when compared to the other locations can be explained by two thoughts: the range of the field data [indicated by the width of the box and whisker plots] and the location of the receptors outside the major wind pathways. The range of upwind and crosswind concentrations measured in the field are slightly narrower when compared to the downwind receptors, thereby making the model predictions more difficult to correlate with the field canister data. In addition, the major winds are out of the south-southwest and north-northeast with little from the east or west direction, further hampering the coupled models ability to fit the field data.

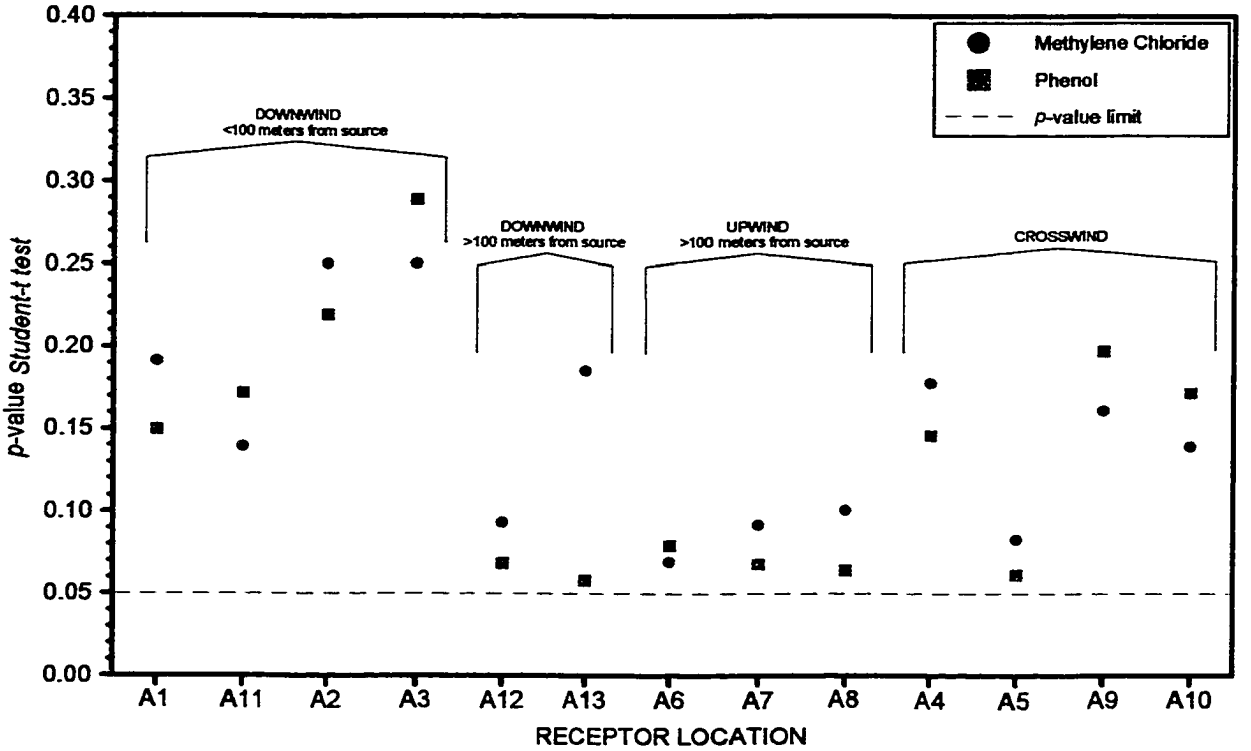

Figure 4.3: p-value of Student t-test for Methylene Chloride and Phenol

For phenol [represented by green squares in Figure 4.3], the model appears to be in good agreement [with a 0.05 p-value or greater] with

the field data for all thirteen receptor points [A1, A11, A2, A3, A12, A13, A6, A7, A8, A4, A5, A9, and A10]. Note that at points A12, A13, A6, A7, A8, and A5, the model slightly over-predicts the field data as illustrated by approaching the 0.05 *p*-value limit. For sample sites downwind and less than 100 meters from the major emission sources [A1, A11, A2, A3], there is very good agreement [with a *p*-value between 0.15 to 0.28] between the coupled model predictions and field data for A2 and A3, while the model tends to slightly struggle with A1 and A11 [*p*-values of 0.15 and 0.17]. For sample sites downwind and greater than 100 meters from the major emission sources [A12 and A13], there less agreement between the coupled model predictions and field data for A12 and A13 [*p*-values of 0.07 and 0.06]. For sample sites upwind and greater than 100 meters from the major emission sources [A6, A7, A8], there is relatively good agreement [*p*-values of 0.08, 0.07, and 0.06] between the coupled model predictions and field data for all three points. For sample sites crosswind from the major emission sources [A4, A5, A9, A10], there is relatively good agreement [*p*-values of 0.06 to 0.20] between the coupled model predictions and field data for all four points [slightly better for A4, A9, and A10]. Qualitatively, the coupled model appears to do a good job of predicting field data. Quantitatively, all thirteen coupled model predictions have a *p*-value greater than 0.05. In general, the coupled model appears to do a slightly better job of predicting downwind [both less and greater than 100 meters from the major sources] while slightly over-predicting the upwind [A6, A7, and A8] and crosswind [A4, A5, and A9] concentrations. What makes the upwind and crosswind coupled model predictions slightly worse when compared to the other locations can be explained by two thoughts: the range of the field data [indicated by the width of the box and whisker plots] and the location of the receptors outside the major wind pathways. The range of upwind and crosswind concentrations measured in the field are slightly narrower when compared to the downwind receptors, thereby making the model predictions more difficult to correlate with the field canister data. In addition, the major winds are out of the south-southwest and north-northeast with little from the east or west direction, further hampering the coupled models ability to fit the field data.

From Figures 4.2 and 4.3, the coupled model does a slightly better job of predicting methylene chloride [more-volatile] concentrations when compared to the semi-volatile phenol constituent. This can be partially explained by looking at differences in volatility and phase equilibrium [separation between the phases]. When components are approaching equilibrium within the wastewater, the more volatile component will have a tendency to be removed from the wastewater at a faster rate [and extent] than the less volatile component. The value for the Henry's Law constant becomes more critical as the component becomes more volatile. For example, the Henry's Law constant for methylene chloride is critical to the phase separation, and ultimately to the fit of the coupled model to field data, as compared to the less volatile phenol component.

COMPARISON OF COUPLED MODEL PREDICTIONS TO FIELD SAMPLE DATA

This section involves comparing the estimated computer-generated methylene chloride and phenol concentrations [using the coupled model] with periodic field data. As previously explained, to identify trends between similar sample sites, the sample data were grouped according to their orientation / location [either upwind or downwind] and distance from the major emission sources [less than or greater than 100 meters]. For example, field data points A1, A11, A2, and A3 were grouped together and referred to as downwind and less than 100 meters from the primary emission sources. Field data points A12 and A13 were grouped and called downwind and greater than 100 meters from the primary emission sources. Data points A6, A7, and A8 are upwind and greater than 100 meters from the major sources. Data points A4, A5, A9, and A10 were called crosswind.

It is important to note the season of the year in which the ambient air field samples were collected. Since the majority of the methylene chloride and phenol samples were gathered in the fall months [22 September through 8 November 1993], the WATER8 and air dispersion models were executed over the same time period using the slightly lower wastewater temperatures [21.2°C] as compared to the standard operating [default] temperature of 25°C. The 21.2°C temperature is the average wastewater temperature and was determined by analyzing the wastewater temperature profile for that time period. As mentioned, the computer

simulations were executed and concentrations predicted at the same ambient air field sample sites [A1 through A13]. The results are shown in Figure 4.4, whereby methylene chloride concentrations in parts per billion [ppb] are shown as a function of the sample sites [A1 through A13]. Ambient air samples were collected with the guidance of the U.S. EPA Method TO-14A [1,2] over the same thirteen locations as illustrated in Figure 4.1 [A1 through A13]. The Resource Conservation and Recovery Act [RCRA] facility investigation [3] are reported for all 13 sample sites [A1 through A13] and are represented by the black circles. The Battelle data exists for A1, A2, and A3, and are represented with the blue diamonds [4]. The OC-ALC Bioenvironmental data are recorded for A1, A2, and A3, and are illustrated with a gray triangle. Note that there is very good agreement [reproducibility] between the three periodic field canister studies [RCRA, Battelle, and OC-ALC Bioenvironmental data] for A1, A2, and A3, illustrating that the field canister data from three independent resources fall within the statistical uncertainty. The coupled model predictions [annual-average] were determined for each of the ten years of meteorological data [1984-93] and are shown as red squares [Figure 4.4]. Qualitatively, there is good agreement between the coupled model predictions and field data. There are trends where the predicted concentrations are greater for the samples closer to the major sources [A1, A11, A2] and lower for the emission sources farther away from the major emission sources [A6, A7, A8]. These trends are similar for all data points, whereby the predicted concentrations are higher for the samples closer to the major sources [A1, A11, A2] and tend to decrease as we move away from the major emission sources [A6, A7, A8]. For sample sites downwind and less than 100 meters from the major emission sources [A1, A11, A2, A3], there is very good agreement between the coupled model predictions and field data for A1 and A2, while the model tends to under-predict for A11 and A3. For sample sites downwind and greater than 100 meters from the major emission sources [A12 and A13], there is relatively good agreement between the coupled model predictions and field data, but the model tends to under-predict for both A12 and A13. For sample sites upwind and greater than 100 meters from the major emission sources [A6, A7, A8], there is relatively good agreement between the coupled model

predictions and field data, but the model tends to under-predict all three points. For sample sites crosswind from the major emission sources [A4, A5, A9, A10], there is relatively good agreement between the coupled model predictions and field data for all four points [slightly better for A9 and A10], but the model continues to under-predict for all four points. Quantitatively, the coupled model predictions will be compared to field data in some of the following discussions. Qualitatively, the coupled model appears to do a good job of predicting field data. In general, the coupled model appears to do a better job of predicting downwind [both less and greater than 100 meters from the major sources], while slightly under-predicting for upwind and crosswind concentrations. At almost all receptor locations [Figure 4.4], the coupled model appears to under-predict the field data.

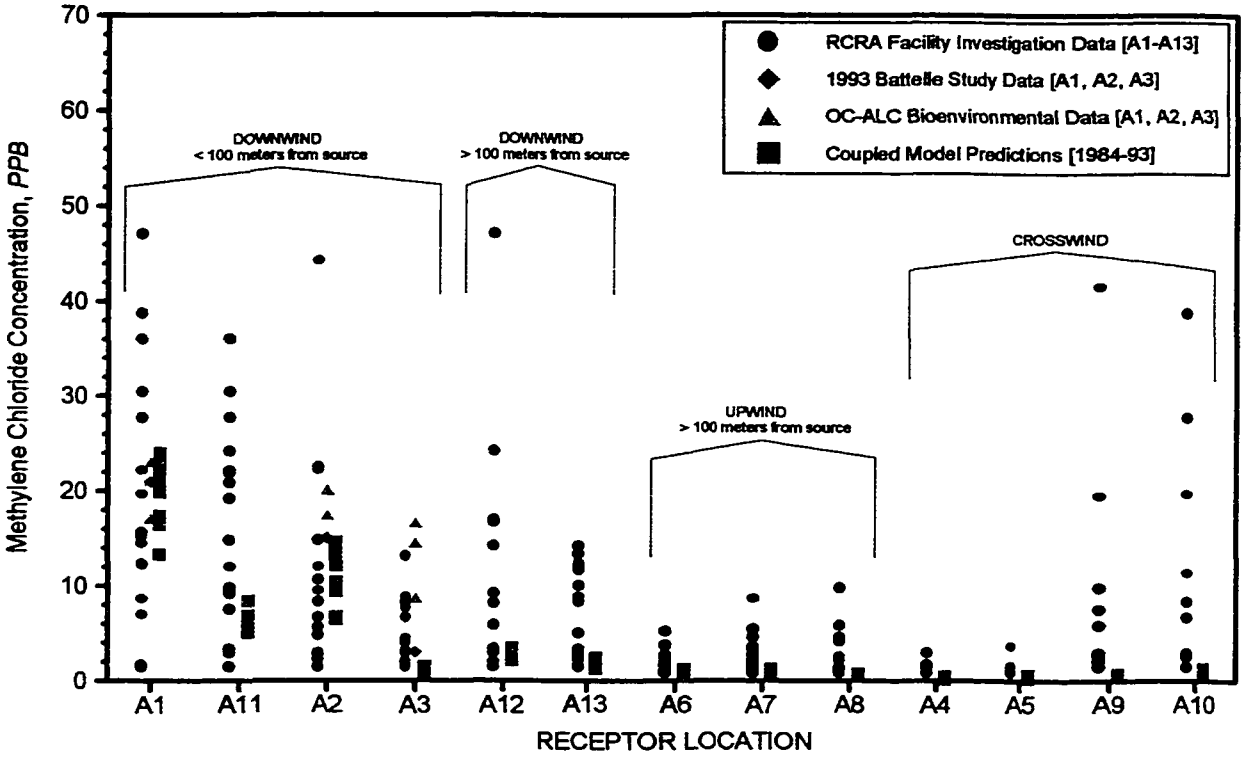

Figure 4.4: Methylene Chloride Sample Data for A1 through A13 Sites

For phenol, there are the same three field data sources including the RCRA facility investigation, OC-ALC Bioenvironmental study, and 1993 Battelle study. As with the methylene chloride studies, ambient air samples were collected with the guidance of the U.S. EPA Method TO-14A

[1,2] over the same thirteen locations. The coupled model was executed under the same constraints [22 September through 8 November and at a wastewater temperature of 21.2°C]. The results are presented in Figure 4.5, whereby phenol concentrations in ppb are shown as a function of the sample sites [A1 through A13]. Again, the sample data are grouped according to their orientation and distance from the major emission sources. The RCRA data are reported for all 13 sample sites [A1 through A13] and are represented by the black circles. The Battelle data exists for A1, A2, and A3, and are represented with the blue diamonds. The OC-ALC Bioenvironmental data are recorded for A1, A2, and A3, and are illustrated with a gray triangle. There is very good agreement [reproducibility] between the periodic field canister data [RCRA, Battelle, and OC-ALC Bioenvironmental data] for A1, A2, and A3. As with the methylene chloride, the reproducibility of the three independent resources are within the statistical uncertainty.

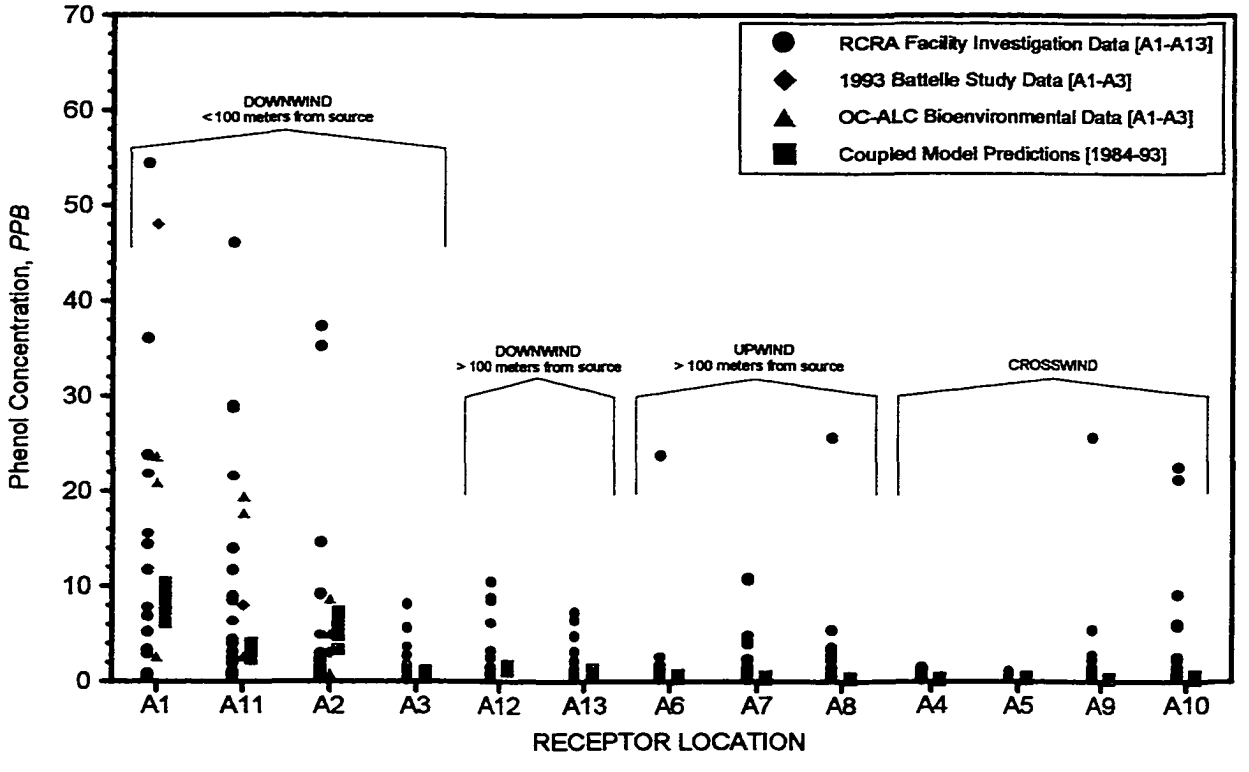

Figure 4.5: Phenol Ambient Air Sample Data for A1 through A13 Sites

The coupled model predictions [annual-average] were determined for each of the ten years of meteorological data [1984-93] and are shown as

red squares. Qualitatively, there is good agreement between the coupled model predictions and field data. Note that the trends are similar for all data points, whereby the predicted concentrations are higher for the samples closer to the major sources [A1, A11, A2] and tend to decrease as we move away from the major emission sources [A6, A7, A8]. For sample sites downwind and less than 100 meters from the major emission sources [A1, A11, A2, A3], there is very good agreement between the coupled model predictions and field data for A1, A2 and A3, while the model tends to slightly under-predict for A11. For sample sites downwind and greater than 100 meters from the major emission sources [A12 and A13], there is very good agreement between the coupled model predictions and field data, but the model tends to slightly under-predict for both A12 and A13. For sample sites upwind and greater than 100 meters from the major emission sources [A6, A7, A8], there is good agreement between the coupled model predictions and field data, but the model tends to slightly under-predict all three points. For sample sites crosswind from the major emission sources [A4, A5, A9, A10], there is very good agreement between the coupled model predictions and field data for all four points, but the model continues to under-predict for all four points. Quantitatively, the coupled model predictions were compared to the field data in the statistical analysis section of this chapter where all thirteen data points were within a 99.9 percent level of confidence.

In general, the coupled model appears to better predict downwind [both less and greater than 100 meters from the major sources], while under-predicting with upwind and crosswind concentrations. It is interesting to note that the coupled model appears to consistently under-predict the field data. In addition, the coupled model appears to do a qualitatively better job of predicting the more-volatile methylene chloride component when compared to the semi-volatile phenol constituent. This difference may be partially explained by the differences in volatility and Henry's law constant.

GRAPHICAL PRESENTATION OF THE DATA [STATISTICAL EVALUATION]

This segment of the effort is where computer-generated predictions are compared to field-collected sample canister data [Sub-task 3A]. This

effort is a continuation of the previous discussion where the coupled model predictions and periodic canister sample data will be statistically evaluated. Statistics is employed because the scientific methodology can be used to objectively evaluate a hypothesis based on experimental results [numerical data]. The following discussion explains the statistical manipulation and graphical presentation of the data involving the first quartile [q_1], median [q_2], third quartile [q_3], and the inter-quartile range [IQR] called box and whisker plots. A box is drawn from the first to third quartile and theoretically includes 50 percent of the data points. The box is used to present a visual impression of the spread or clustering of the middle 50 percent of the data. The median is located in this box and helps consider the symmetry of the middle 50 percent of the data. The inter-quartile range is the difference between the first and third quartile. The whiskers shown above and below the box technically represent the largest and smallest observed scores that are less than 1.5 box lengths from the end of the box. In a simple plot, the range and variability of the data are shown immediately, as are the major location points [the median and the first and third quartiles]. The whiskers of the box plot are the line segments that run from the extremes of the box to the nearest values. The notation is highlighted in Figure 4.6. It is important to note for the following discussions, qualitatively comparisons will be made until the model is calibrated, at which point, quantitative comparisons will be discussed.

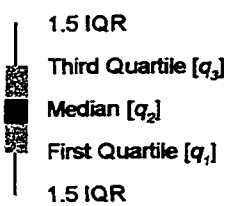

Figure 4.6: Box Plot of Data

Figure 4.7 illustrates the methylene chloride ambient air sample data [from Figure 4.4] after statistical manipulation of the data. The black points represent the field data while the red represents the coupled model predictions. Note that the trends are similar for all data points, whereby the predicted concentrations are higher for the

samples closer to the major sources [A1, A11, A2] and tend to decrease as we move away from the major emission sources [A6, A7, A8]. For sample sites downwind and less than 100 meters from the major emission sources [A1, A11, A2, A3], there is very good agreement between the coupled model predictions and field data for A1 and A2, while the model tends to under-predict for A11 and A3. For sample sites downwind and greater than 100 meters from the major emission sources [A12 and A13], there is relatively good agreement between the coupled model predictions

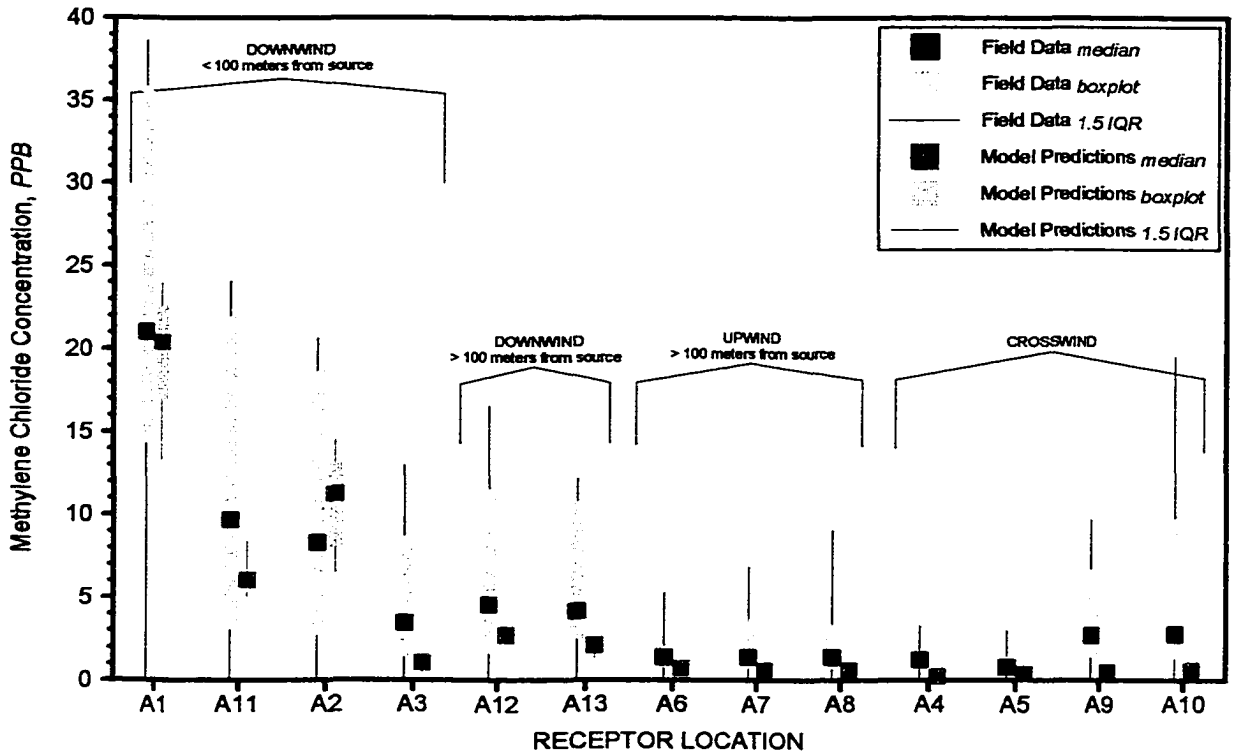

Figure 4.7: Field Data Comparison to Coupled Model Predictions for Methylene Chloride

and field data, but the model tends to slightly under-predict for both A12 and A13. For sample sites upwind and greater than 100 meters from the major emission sources [A6, A7, A8], there is relatively good agreement between the coupled model predictions and field data, but the model tends to under-predict all three points. For sample sites crosswind from the major emission sources [A4, A5, A9, A10], there is relatively good agreement between the coupled model predictions and field data for all four points [slightly worse for A9 and A10], but the

model continues to under-predict for all four points. In general, the coupled model appears to do a better job of predicting downwind [both less and greater than 100 meters from the major sources], while slightly under-predicting for the upwind and crosswind concentrations. It is interesting to note that the coupled model appears to under-predict all of the field data [except for A2]. What makes the upwind and crosswind coupled model predictions slightly worse when compared to the other locations can be explained by two thoughts: the range of the field data [indicated by the width of the box and whisker plots] and the location of the receptors outside the major wind pathways. The range of upwind and crosswind concentrations measured in the field are slightly narrower when compared to the downwind receptors, thereby making the model predictions more difficult to correlate with the field canister data. In addition, the major winds are out of the south-southwest and north-northeast with little from the east or west direction, further hampering the coupled models ability to fit the field data.

Figure 4.8 illustrates the phenol ambient air sample data [from Figure 4.5] after statistical manipulation of the data. As with the methylene chloride, the black symbols represent the field canister data while the red squares represent the annual-average model predictions for each of the ten years of meteorological data [1984-93]. Qualitatively, there is good agreement between the coupled model predictions and field data. For sample sites downwind and less than 100 meters from the major emission sources [A1, A11, A2, A3], there is good agreement between the coupled model predictions and field data for A1, A11, and A3, while the model tends to over-predict for A2. For sample sites downwind and greater than 100 meters from the major emission sources [A12 and A13], there is very good agreement between the coupled model predictions and field data, but the model tends to slightly over-predict for both A12 and A13. For sample sites upwind and greater than 100 meters from the major emission sources [A6, A7, A8], there is good agreement between the coupled model predictions and field data, but the model tends to slightly under-predict all three points. For sample sites crosswind from the major emission sources [A4, A5, A9, A10], there is very good agreement between the coupled model predictions and field data for all four points [slightly better for A4 and A5], but the model continues to

under-predict for all four points. The coupled model appears to do a good job of predicting field data. In general, the coupled model appears to do a slightly better job of predicting downwind [both less and greater than 100 meters from the major sources] while slightly under-predicting the upwind and crosswind concentrations. What makes the upwind and crosswind coupled model predictions slightly worse when compared to the other locations can be explained by two thoughts: the range of the field data [indicated by the width of the box and whisker

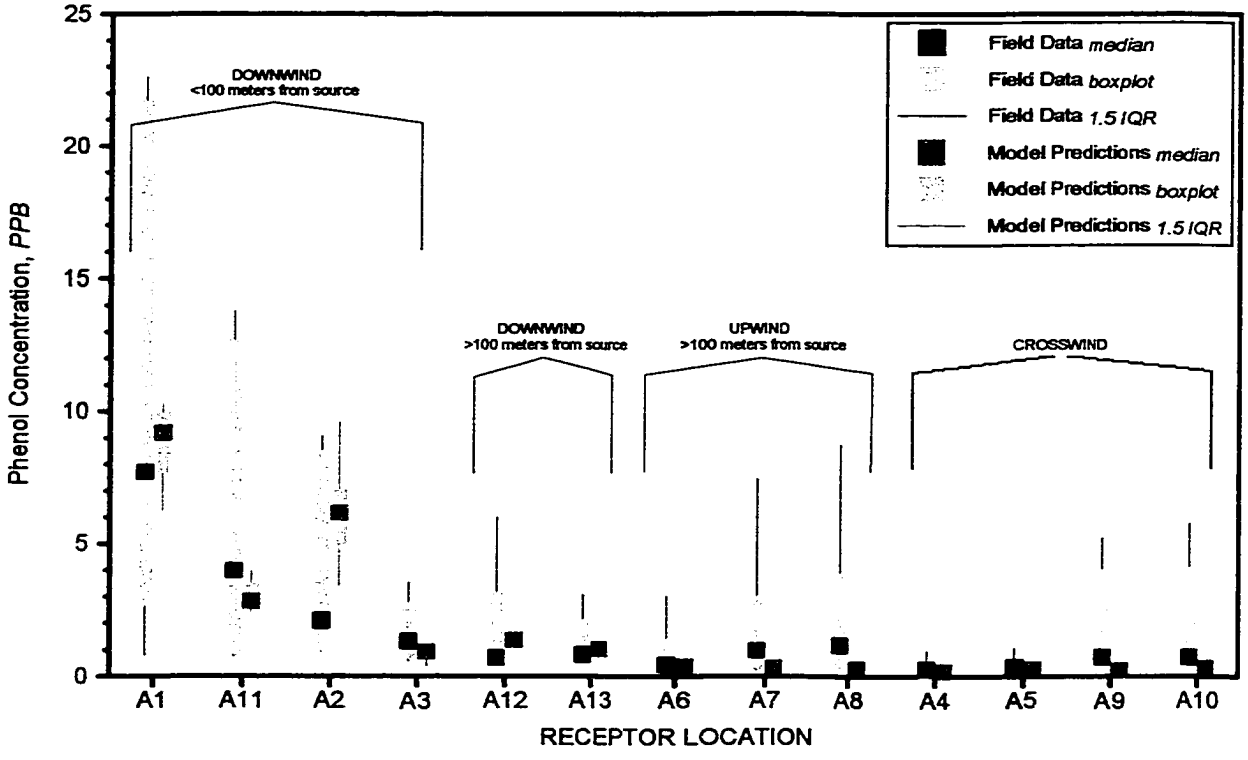

Figure 4.8: Field Data Comparison to Coupled Model Predictions for Phenol

plots] and the location of the receptors outside the major wind pathways. The range of upwind and crosswind concentrations measured in the field are slightly narrower when compared to the downwind receptors, thereby making the model predictions more difficult to correlate with the field canister data. In addition, the major winds are out of the south-southwest and north-northeast with little from the east or west direction, further hampering the coupled models ability to fit the field data. It is interesting to note that the coupled model appears to

slightly under-predict all of the field data [except A2]. Also, note that the coupled model does a qualitatively better job of predicting the more-volatile methylene chloride when compared to the less-volatile phenol.

Note that this investigation was prior to model calibration. This portion of the investigation was done prior to the model calibration tasking in order to determine the ability of the coupled model methodology to correlate with field canister data using the models default settings. The coupled model default settings will be modified in the following section to improve the models predictive performance.

COUPLED MODEL CALIBRATION

Probably the most unique feature of this research effort is the calibration of the coupled model to improve the performance by refining the predictive capability of the model. The purpose is to determine which factors are most sensitive and to understand how the variation in input parameters will impact the predictive capability of the coupled model methodology. Sensitivity analysis is a means of identifying and evaluating the critical model parameters. During the execution of the coupled model, several input variables were modified from what was tabulated in the manuals to improve the model fit.

There are a number of model parameters [*i.e.*, atmospheric stability categories, wind speed profile exponents, vertical potential temperature gradients, etc.] that control the dispersion of the plume in both the downwind and vertical directions [8,9]. The industrial source complex [ISC] dispersion model presents values for each of these parameters that are set as part of a default option. These default values can be overridden and replaced by the more knowledgeable user. As part of the model calibration step, these model parameters were changed to improve the predictive capability of the model.

Some of the parameters that may be input to the models are allowed to vary by wind speed category. The model uses six wind speed categories, and these are defined by the upper bound wind speed for the first five categories [the sixth category is assumed to have no upper bound] and are illustrated in Figure 4.9. The default values for the wind speed categories are as follows: 1.54, 3.09, 5.14, 8.23, and 10.8

meters per second [8]. These default values were changed to the following: 1.0, 2.5, 4.0, 6.0, and 8.5. This essentially redefines the breaks between wind speed categories and acts to depress the turbulent mixing of the surface winds yielding an increase in the ground-level chemical concentrations. Note that while many combinations [five by five matrix] were checked, this combination appeared to offer the greatest improvement through all thirteen sample sites [A1 through A13].

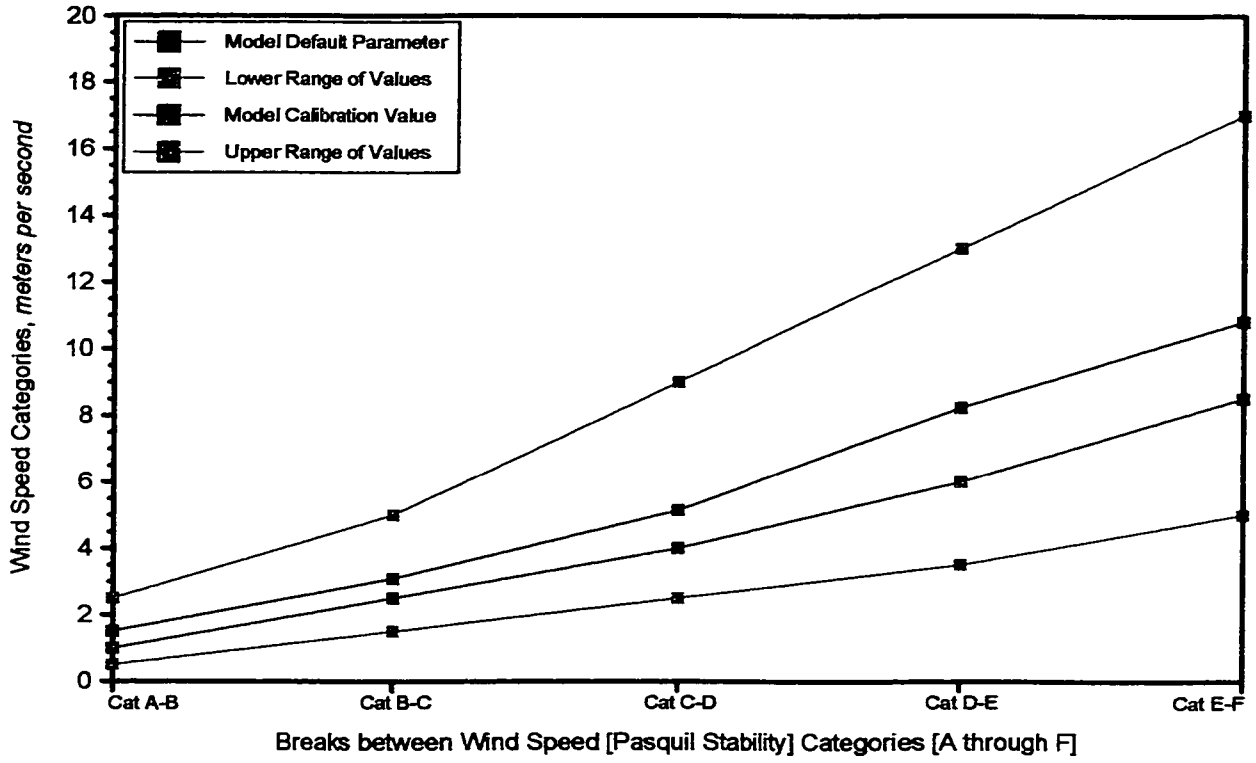

Figure 4.9: Separation between Wind Speed Categories

Another parameter that was modified during the model calibration procedure was the wind profile exponents. The wind profile exponents are a function of the surface terrain [flat, smooth, rough, etc.] and surrounding topographical contours [rural or urban]. While the model uses default wind profile exponents in the regulatory default option, non-regulatory default applications allows the user to specify wind profile exponents depending on the site-specific applications [8]. The wind profile exponents for each of the six wind speed categories [Pasquill Stability Category] are illustrated in Figure 4.10. Note the crossing of the urban and rural wind profile exponents at the breaks

between wind speed Categories E and F. This is the result of the differences between the urban and rural environments on the wind profiles at higher wind speeds. In the rural environment, there are few obstructions to the wind patterns, yielding greater uninterrupted wind profiles. In urban environments, there are many obstructions due to man-made structures, which lower the wind profiles. These man-made structures obstruct and divert the wind flow patterns and the model compensates for this impact by lowering the wind profile exponent [at higher wind speeds].

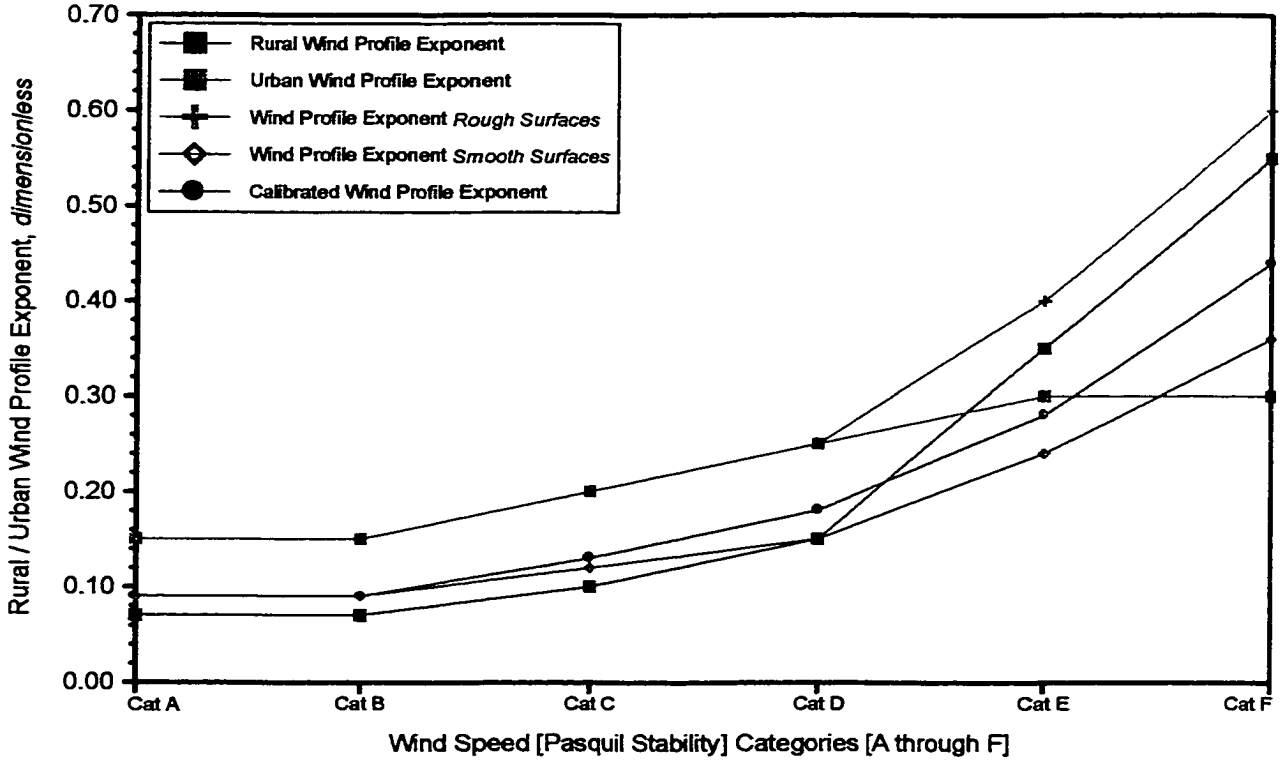

Figure 4.10: Wind Profile Exponents

The vertical potential temperature gradient was another variable that could be modified. The temperature gradient tabulated in the literature was the values utilized in this application [8,9]. The recommended profile was used because it appears in the literature in several different publications. The temperature gradient utilized was 0.0, 0.0, 0.0, 0.020, and 0.035 for each of the Pasquill Stability categories [A through F], respectively [8,9].

Figure 4.11 illustrates the methylene chloride ambient air sample

data [from Figure 4.4] after statistical manipulation of the data and model calibration efforts. As before, the black points represent the field data while the red represents the coupled model predictions following calibration. For methylene chloride, the model appears to be in good agreement [99.9 percent level of confidence] with the field data for points A1, A11, A2, A3, A12, A13, A7, A8, A4, A5, A9, and A10. Note that coupled model slightly over-predicts points A1 and A11, and under-predicts A9 and A10. For data point A6, the coupled model predictions

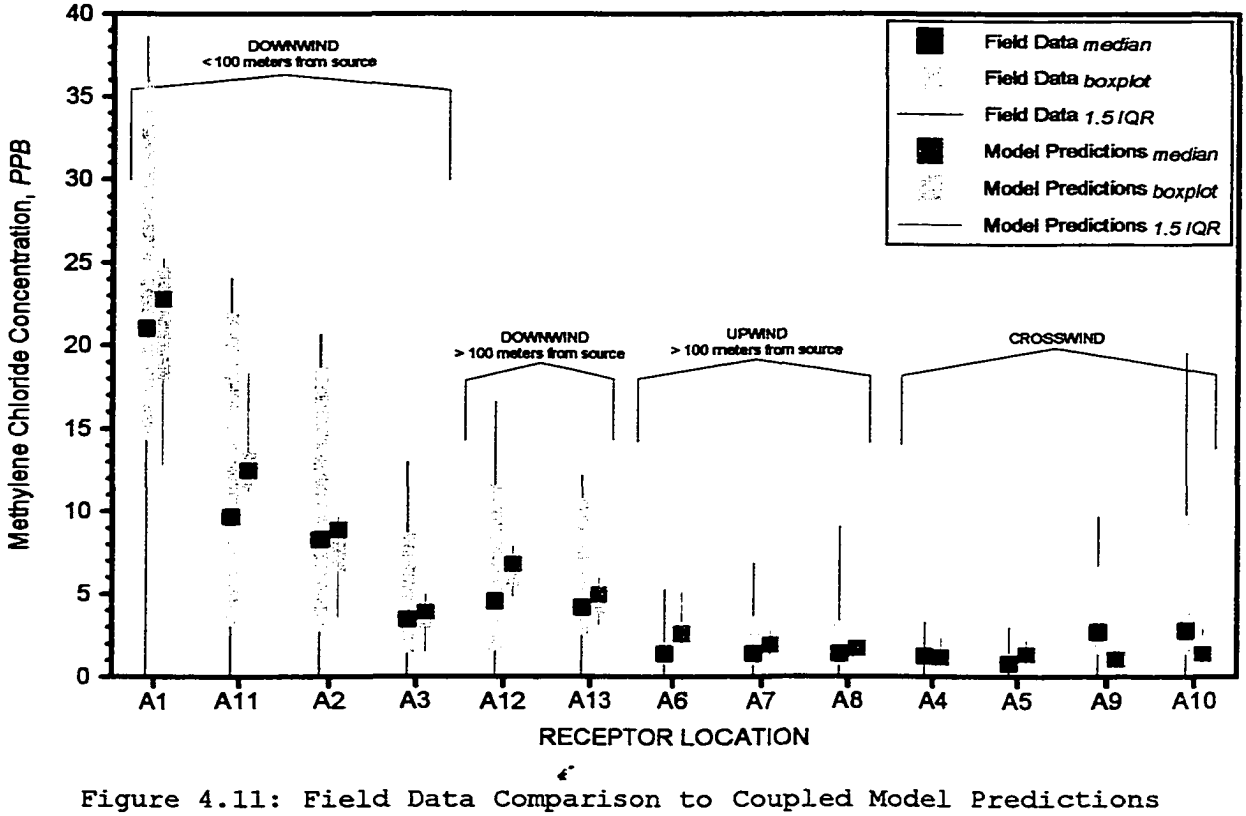

Figure 4.11: Field Data Comparison to Coupled Model Predictions for Methylene Chloride following Model Calibration

are just inside the 99.9 percent confidence limit. For sample sites downwind and less than 100 meters from the major emission sources [A1, A11, A2, A3], there is very good agreement [with a 99.9 percent confidence interval] between the coupled model predictions and field data for A2 and A3, while the model tends to slightly over-predict A1 and A11 [closer to the 99.9 percent confidence limit]. For sample sites downwind and greater than 100 meters from the major emission sources [A12 and A13], there is good agreement [99.9 percent confidence] between the coupled model predictions and field data. For sample sites upwind

and greater than 100 meters from the major emission sources [A6, A7, A8], there is relatively good agreement [99.9 percent confidence] between the coupled model predictions and field data for points A6, A7 and A8. For sample sites crosswind from the major emission sources [A4, A5, A9, A10], there is relatively good agreement [99.9 percent confidence] between the coupled model predictions and field data for all four points [slightly better for A4 and A5]. Quantitatively, all thirteen coupled model predictions are within the 99.9 percent confidence interval. In general, the coupled model does a better job of predicting downwind [both less and greater than 100 meters from the major sources], while slightly over-predicting for the upwind and crosswind concentrations [except for A9 and A10]. What makes the upwind and crosswind coupled model predictions slightly worse when compared to the other locations can be explained by two thoughts: the range of the field data [indicated by the width of the box and whisker plots] and the location of the receptors outside the major wind pathways. The range of upwind and crosswind concentrations measured in the field are slightly narrower when compared to the downwind receptors, thereby making the model predictions more difficult to correlate with the field canister data. In addition, the major winds are out of the south-southwest and north-northeast with little from the east or west direction, further hampering the coupled models ability to fit the field data.

Figure 4.12 illustrates the 1993 methylene chloride ambient air sample data [from Figure 4.11] after statistical manipulation of the data and calibration of the model parameters. The model appears to be within the 99.9 percent level of confidence for all the field data points. For sample sites downwind and less than 100 meters from the major emission sources [A1, A11, A2, A3], the coupled model predictions are within the 99.9 percent confidence interval with field data for A2 and A3, while slightly over-predicting with A1 and A11 [closer to the 99.9 percent confidence limit]. For sample sites downwind and greater than 100 meters from the major emission sources [A12 and A13], the model predictions are within the 99.9 percent confidence. For sample sites upwind and greater than 100 meters from the major emission sources [A6, A7, A8], there is good agreement [99.9 percent confidence] between the coupled model predictions and field data for points A7 and A8, while

slightly over-predicting for A6. For sample sites crosswind from the major emission sources [A4, A5, A9, A10], the model predictions are in within the 99.9 percent confidence limit for all four points [slightly better for A4 and A5]. Quantitatively, all thirteen coupled model predictions are within the 99.9 percent confidence interval.

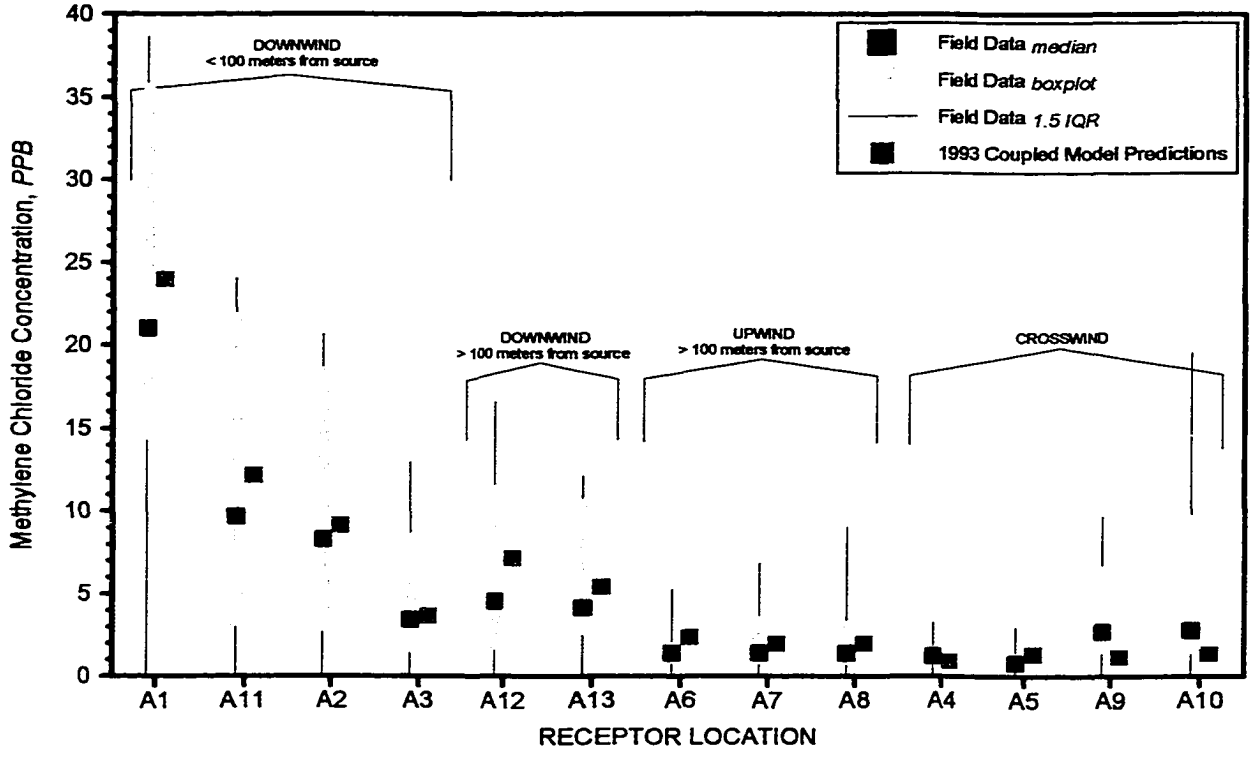

Figure 4.12: Field Data Comparison to 1993 Coupled Model Predictions for Methylene Chloride following Model Calibration

Figure 4.13 illustrates the phenol ambient air sample data [from Figure 4.5] after statistical manipulation of the data and calibration of the model. The black symbols represent the field canister data while the red squares represent the annual-average model predictions [following model calibration] for each of the ten years of meteorological data [1984-93]. For phenol, the model is in good agreement [with a 99.9 percent level of confidence] for all thirteen field data points. Sample sites downwind and less than 100 meters from the major emission sources [A1, A11, A2, A3] are within the 99 percent confidence interval between the coupled model predictions and field data for A2 and A3, while the model tends to slightly over-predict with A1

and A11 [closer to the 99.9 percent confidence limit]. For sample sites downwind and greater than 100 meters from the major emission sources [A12 and A13], there is good agreement [99.9 percent confidence] between the coupled model predictions and field data. Sample sites upwind and greater than 100 meters from the major emission sources [A6, A7, A8] are within the 99.9 percent level of confidence for points A7 and A8, while slightly over-predicting with A6. For sample sites crosswind from the major emission sources [A4, A5, A9, A10], there is relatively good

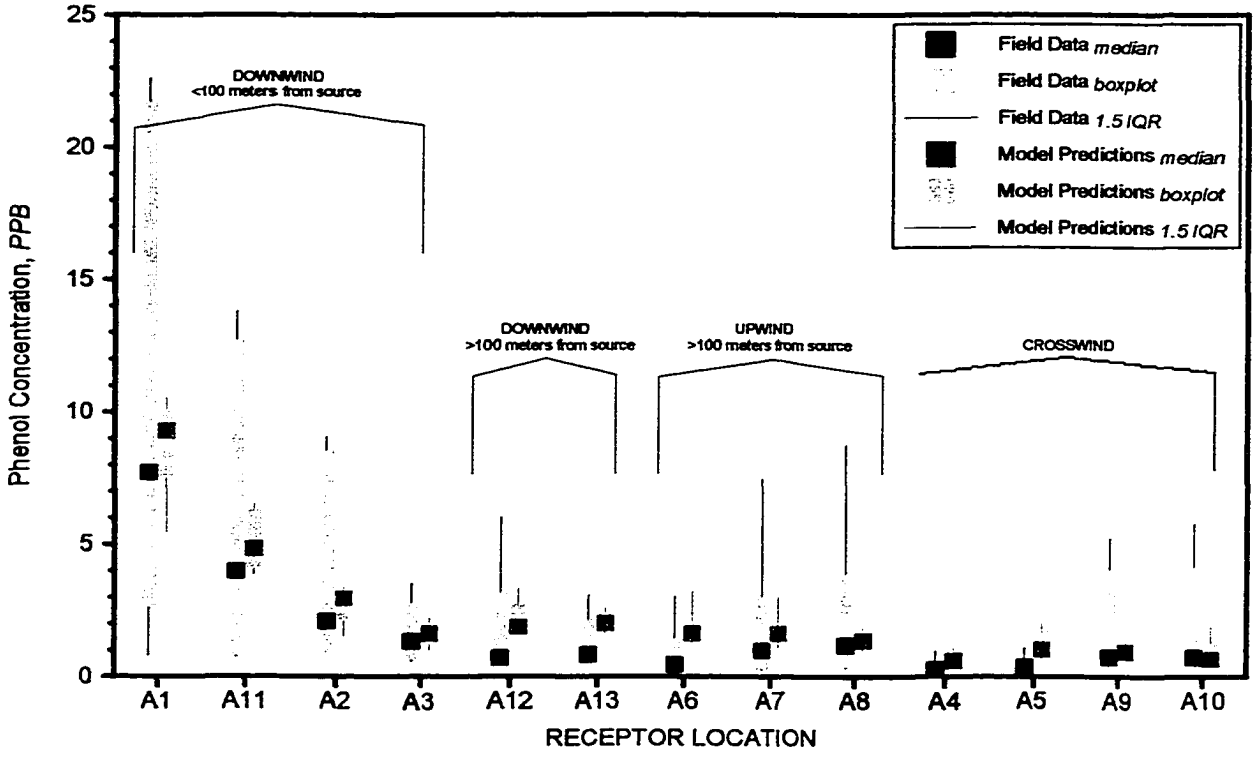

Figure 4.13: Field Data Comparison to Coupled Model Predictions for Phenol following Model Calibration

agreement [99.9 percent confidence] between the coupled model predictions and field data for all four points [slightly better for A4, A9, and A10]. Quantitatively, all thirteen coupled model predictions are within the 99.9 percent confidence interval. In general, the coupled model appears to do a better job of predicting downwind [both less and greater than 100 meters from the major sources], while slightly over-predicting for the upwind and crosswind concentrations. What makes the upwind and crosswind coupled model predictions slightly worse when

compared to the other locations can be explained by two thoughts: the range of the field data [indicated by the width of the box and whisker plots] and the location of the receptors outside the major wind pathways. The range of upwind and crosswind concentrations measured in the field are slightly narrower when compared to the downwind receptors, thereby making the model predictions more difficult to correlate with the field canister data. In addition, the major winds are out of the south-southwest and north-northeast with little from the east or west direction, further hampering the coupled models ability to fit the field data.

Figure 4.14 illustrates the 1993 phenol ambient air sample data [from Figure 4.13] after statistical manipulation of the data and calibration of the coupled model. The black symbols represent the field canister data while the red squares represent the 1993 annual-average model predictions [following model calibration]. For phenol, the model is in good agreement [with a 99.9 percent level of confidence] for all thirteen field data points. Sample sites downwind and less than 100

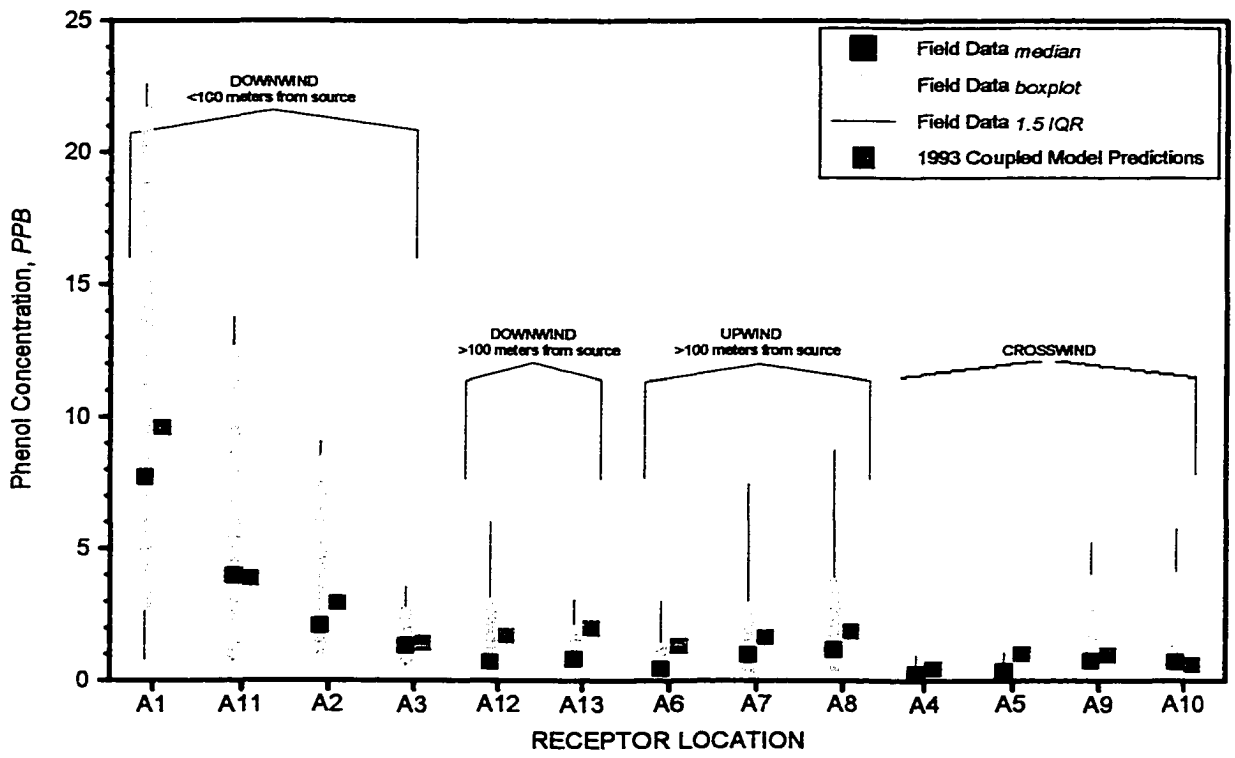

Figure 4.14: Field Data Comparison to 1993 Coupled Model Predictions for Phenol following the Model Calibration

meters from the major emission sources [A1, A11, A2, A3] are within the 99.9 percent confidence interval between the coupled model predictions and field data for A11 and A3, while the model tends to slightly over-predict with A1 and A2 [closer to the 99.9 percent confidence limit]. For sample sites downwind and greater than 100 meters from the major emission sources [A12 and A13], there is good agreement [99.9 percent confidence] between the coupled model predictions and field data. Sample sites upwind and greater than 100 meters from the major emission sources [A6, A7, A8] are within the 99.9 percent level of confidence for points A7 and A8, while slightly over-predicting with A6. For sample sites crosswind from the major emission sources [A4, A5, A9, A10], there is relatively good agreement [99.9 percent confidence] between the coupled model predictions and field data for all four points [slightly better for A4, A9, and A10]. Quantitatively, all thirteen coupled model predictions are within the 99.9 percent confidence interval.

SENSITIVITY ANALYSIS

Another distinctive element of this effort is the sensitivity analysis of the coupled model to determine which factors are most sensitive and to understand how the variation in input parameters will impact the predictive capability of the coupled model methodology. Sensitivity analysis is a means of identifying and evaluating the critical model parameters. There are a number of model parameters [*i.e.*, atmospheric stability categories, wind speed profile exponents, vertical potential temperature gradients, etc.] that control the downwind pollutant concentrations. The objective of this discussion is to quantify the impact of varying the chemical constituent concentration in the influent to the industrial wastewater treatment plant. In reviewing Figures 4.11 and 4.13, the range of the boxplots for the model predictions [shown in red] indicate the sensitivity of the model predictions to changes in the meteorological parameters [*i.e.*, wind speed, wind direction, atmospheric stability categories, wind speed profile exponents, vertical potential temperature gradients, etc.]. This necessitates the identification and quantification of impacts from the WATER8 model parameters. These parameters are identified in Equation 2.1 from Chapter 2. It is thought that there is little difference in

the overall mass transfer coefficient and surface area of the open impoundments. The coupled model parameter that has the greatest amount of fluctuation / instability is the influent chemical constituent concentrations [C_L].

This segment of the effort will quantify the sensitivity of the coupled model predictions while varying the industrial wastewater treatment facility influent constituent concentration. This effort will require the use of a Monte Carlo simulation to evaluate the uncertainty associated with the input parameter [IWTF influent chemical concentration] utilizing 100 randomly selected data points from the original chemical constituent data set illustrated in Figures 2.3 and 2.5. In stochastic modeling, uncertainty is addressed directly by assuming that the parameters are random variables [10]. Monte Carlo methods are statistical simulation methods that utilize sequences of random numbers [random sampling techniques] to perform a model simulation. The 100 data points were randomly selected using the Microsoft Excel analytical software tool package. For example, air quality modeling is assumed to be a stochastic process that can be described by a probability density function. The 100 random samples are shown plotted against the original methylene chloride and phenol influent concentration in Figures 4.15 and 4.17. Figures 4.16 and 4.18 are the frequency distributions of the original influent concentrations overlaying the random sample set in red. Note that the frequency distributions are relatively normally distributed, which will become important in later figures.

Figures 4.19 and 4.20 are shown to illustrate the sensitivity of the coupled model predictions to influent constituent concentrations. The green box and whisker plots are coupled model predictions [after model calibration] using the 100 randomly selected data points from the sensitivity analysis. Note that one receptor point was chosen in each of the four categories [A2, A13, A7, and A4]. It is interesting to note that they follow the similar trends observed in previous figures, in that, the range of the predicted concentrations vary with the range of the field data. For receptor A2, the range is wider than with receptor A4, which has a similar trend with the field data. What is important to realize is that the model predictions in red indicate the sensitivity to

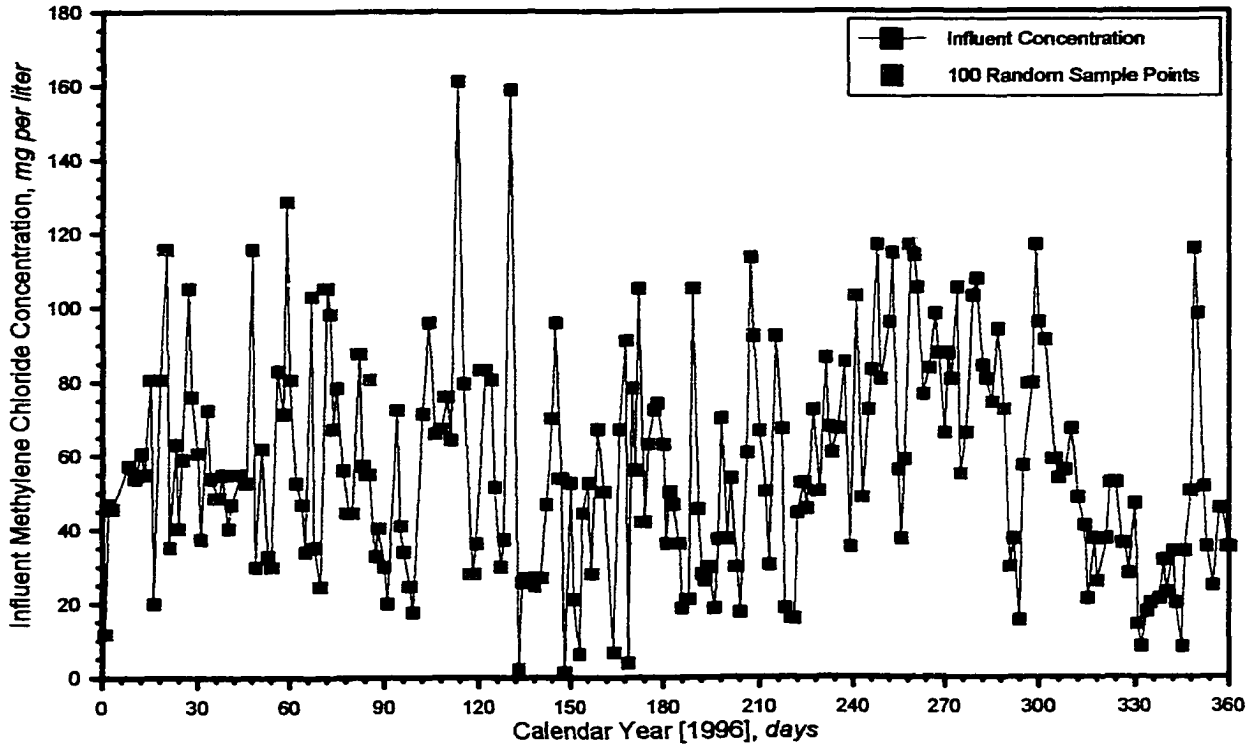

Figure 4.15: Methylene Chloride Influent Concentration and Random Numbers

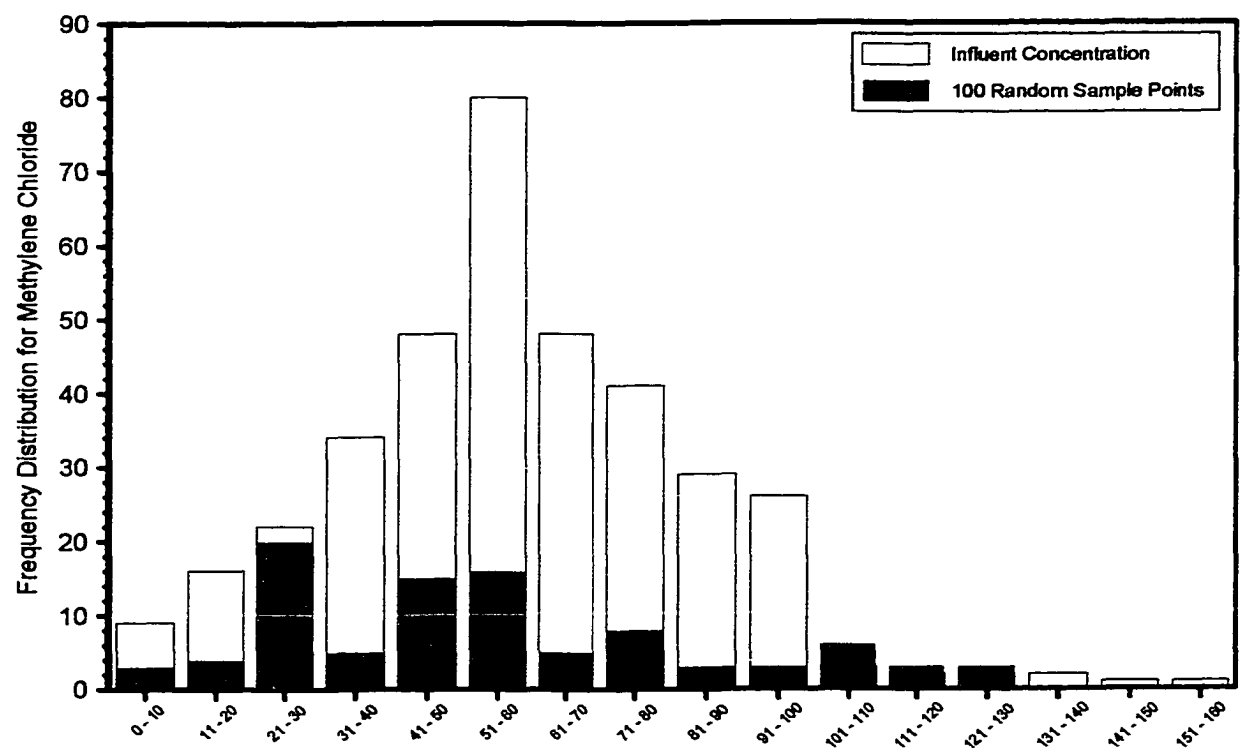

Figure 4.16: Methylene Chloride Frequency Distribution and Random Numbers Distribution

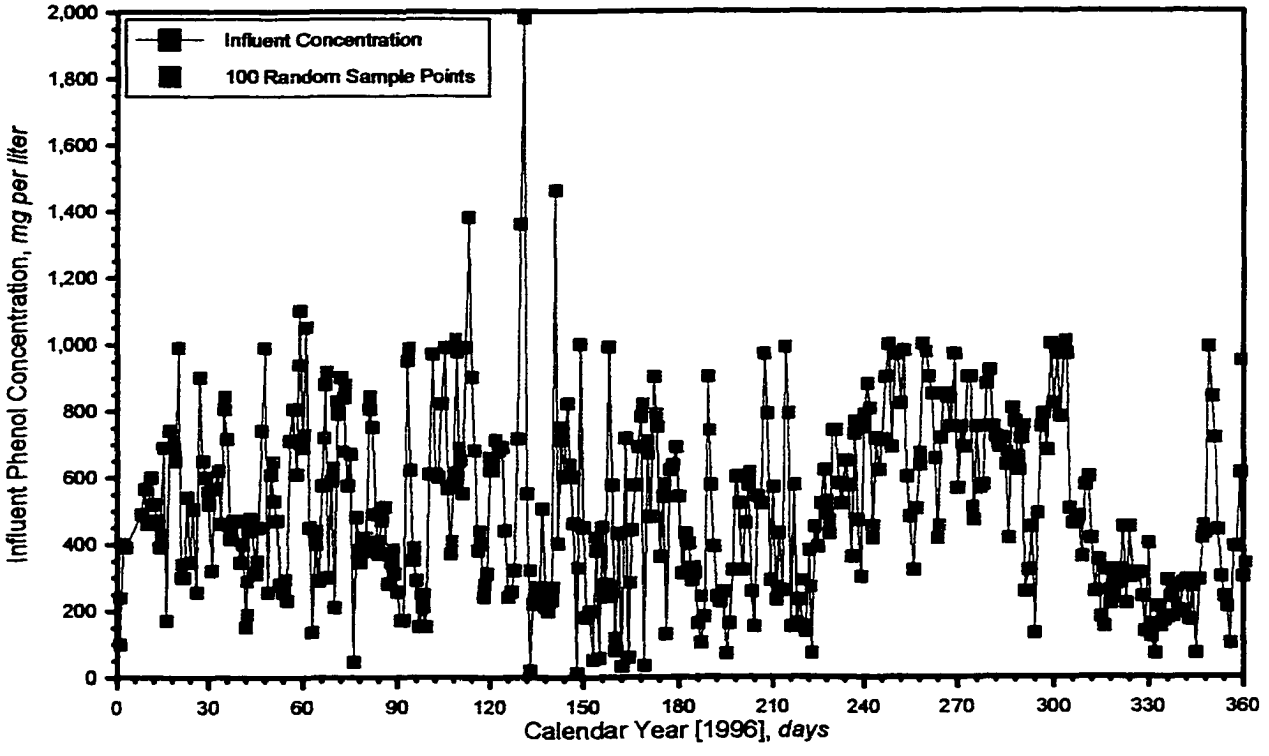

Figure 4.17: Phenol Influent Concentration and Random Numbers

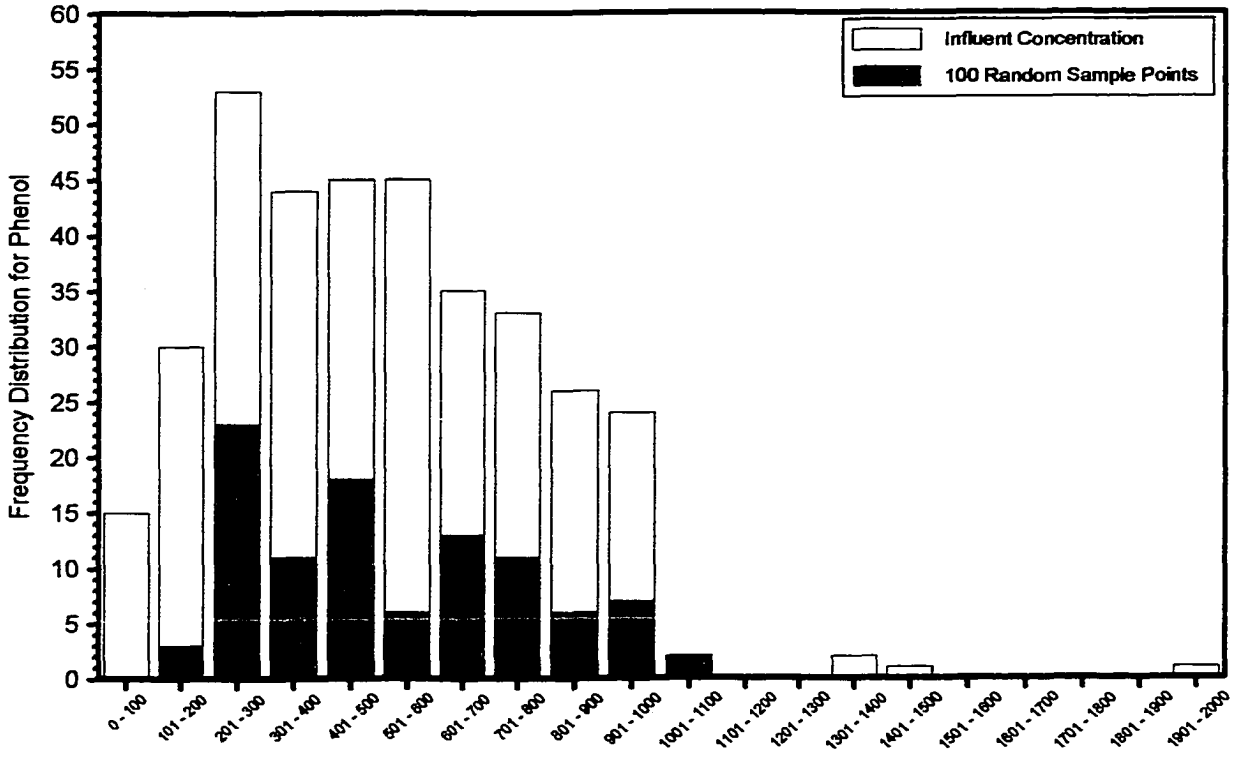

Figure 4.18: Phenol Frequency Distribution and Random Numbers Distribution

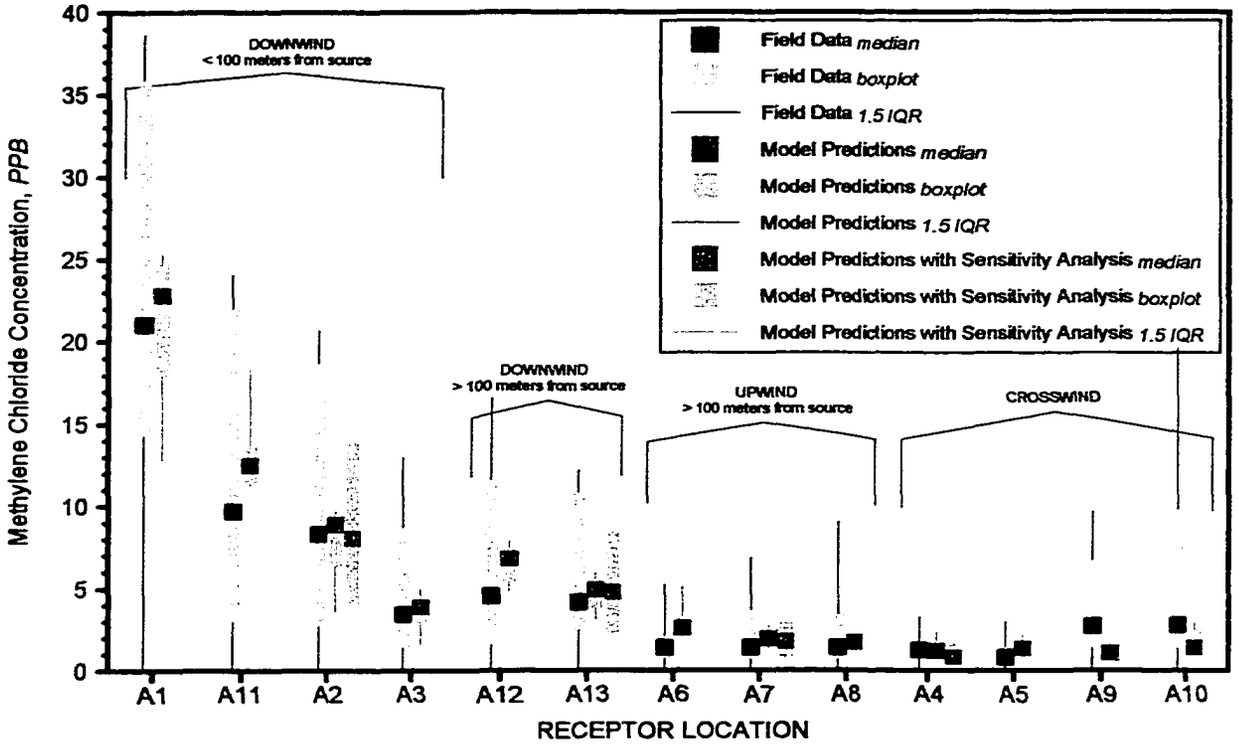

Figure 4.19: Methylene Chloride Sensitivity Analysis

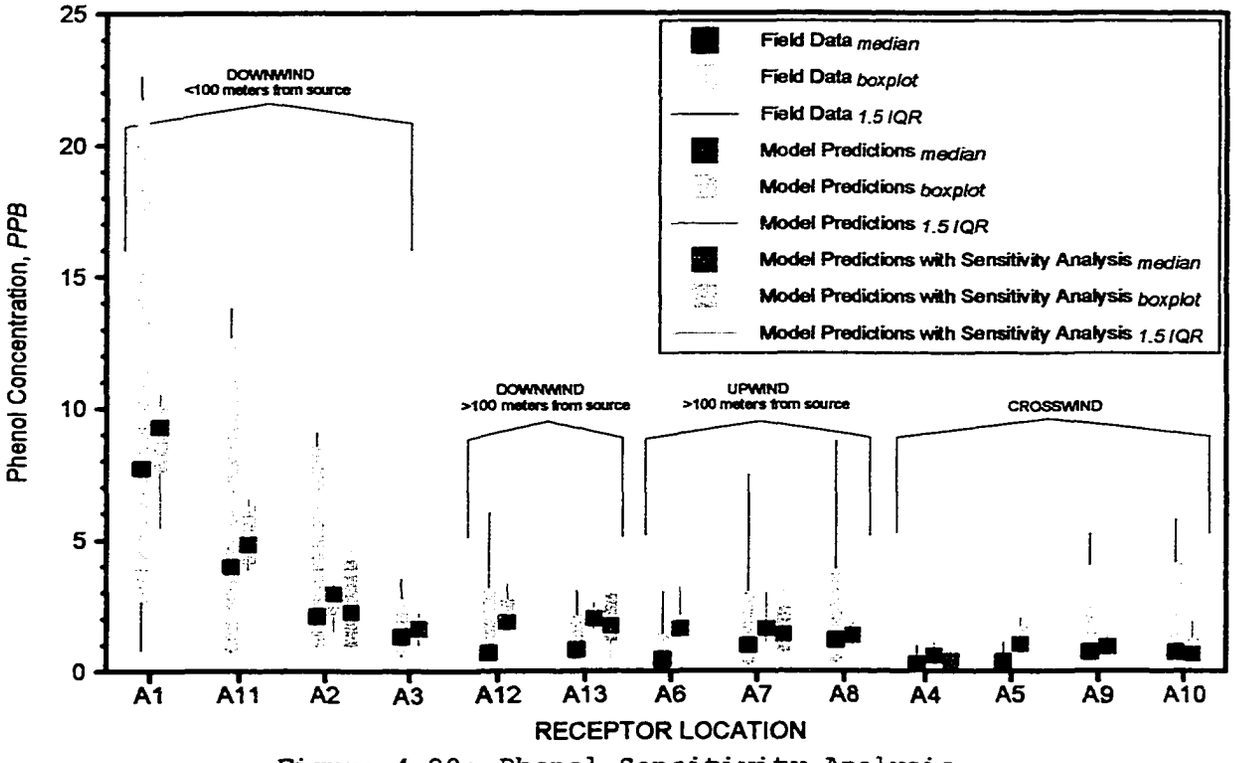

Figure 4.20: Phenol Sensitivity Analysis

meteorological changes [holding every other variable constant], while the model predictions in green indicate the sensitivity to influent constituent concentration changes [holding every other variable constant]. These figures illustrate that the coupled model input parameter with the greatest sensitivity is the influent constituent concentrations, as indicated by the width of the box and whisker plots [Figures 4.19 and 4.20].

The accuracy of the coupled model sensitivity analysis data will be compared to the coupled model predictions for receptor sites A2, A13, A7, and A4. The predictive accuracy of the coupled model sensitivity analysis will be evaluated using the z-test statistical method. The objective is to quantitatively determine the coupled model fit of the sensitivity analysis data to field canister data using the statistical z-test following the model calibration efforts. Assuming a significance level of $\alpha = 0.01$, determine the difference between the field data and the coupled model sensitivity analysis data using Equation 4.1. As with the previous statistical z-test example, H_o will be rejected if $z \geq 2.58$ or if $z \leq -2.58$. Methylene chloride and phenol results are illustrated in Figure 4.21. The coupled model z-test data for the four receptors from Figure 4.2 was included for comparison [as illustrated with the blue circle and green square]. The gray diamond [methylene chloride] and purple triangle [phenol] represent the coupled model predictions using the randomly selected data [100 points] from the sensitivity analysis. Note that only four points [A2, A13, A7, and A4] from each of the four categories were evaluated in the sensitivity analysis. For all four receptors and both chemicals, the coupled model predictions using the sensitivity analysis data are within a 99 percent level of confidence and are in very good agreement with the field canister data. There is an improvement in the coupled model performance using the data set from the sensitivity analysis [gray diamond and purple triangle] as compared to the complete data set [blue circle and green square].

For the assumption that the 100 randomly selected data points for the sensitivity analysis to be useful, the distribution must be a normally distributed probability density function. This normally distributed probability density function allows the use of the Monte Carlo simulation method [10]. The probability density function is

commonly assumed to be lognormal [10]. For the 100 random sample points to be normally distributed, the best-fit straight line through a probability plot [Figure 4.22] should be linear with an R-squared value of 1.0 [11]. Note that the curved shaped of the lines are similar to those found in the literature [11]. The literature recommends that the x-axis be plotted lognormal versus probability as shown in Figure 4.23. Again, the slight non-linearity of the best-fit straight lines are the result of the less than normal distribution of the 100 randomly selected sample points [Figures 4.16 and 4.18]. Figures 4.24 and 4.25 are the probability plot and lognormal-probability plot over similar normalized concentration ranges [C_i/C_{max}]. Both are similar in shape and slightly non-linear, as expected from the frequency distributions of the 100 randomly sampled data points. The assumption that the 100 randomly selected data points for the sensitivity analysis were normally distributed is valid as indicated by the R-squared value of 0.95 and greater. This supports the contention that the Monte Carlo simulation [random sampling] method can be employed for this application.

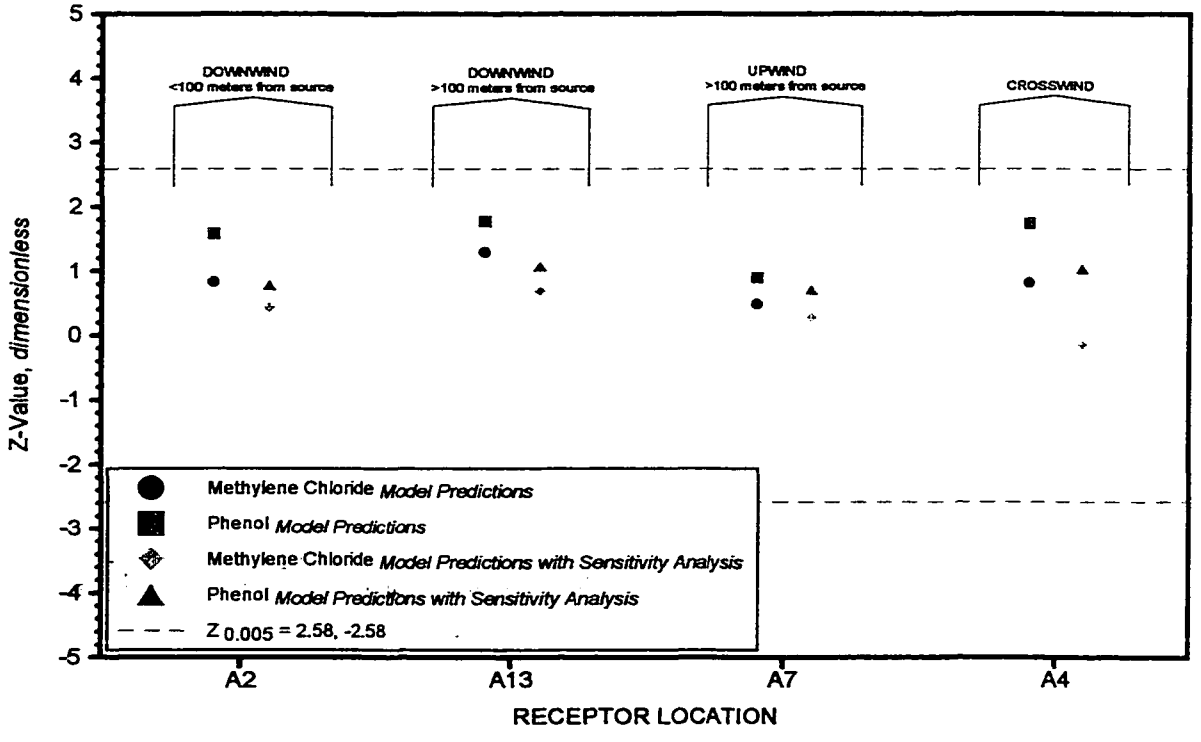

Figure 4.21: Z-values for Methylene Chloride and Phenol for the Randomly Selected Sensitivity Analysis Data

SELECTED REFERENCES

1. Compendium Method TO14A, *Determination of Volatile Organic Compounds [VOCs] in Ambient Air using Specially Prepared Canister with Subsequent Analysis by Gas Chromatography*, Office of Research and Development, U.S. EPA, January 1997.

2. Compendium Method TO15, *Determination of Volatile Organic Compounds [VOCs] in Ambient Air using Specially Prepared Canister with Subsequent Analysis by Gas Chromatography*, Office of Research and Development, U.S. EPA, January 1997.

3. Resource Conservation & Recovery Act [RCRA] Facility Investigation, U.S. Air Force Installation Restoration Program [IRP] prepared by Engineering-Science, Inc., April 1994.

4. Battelle Air Quality Study, prepared by Battelle Engineering Services, 1993.

5. Devore, J.L., *Probability and Statistics for Engineering and the Sciences*, Brooks-Cole Publishing Company, 1987.

6. Ostle, B., K.V. Turner, & G.W. McElrath, *Engineering Statistics—The Industrial Experience*, Wadsworth Publishing Company, 1994.

7. Schiff, D., & R.B. D'Agnostino, *Practical Engineering Statistics*, John Wiley & Sons, New York.

8. U.S. Environmental Protection Agency, *Users Guide for the Industrial Source Complex [ISC] Dispersion Models*, Office of Air Quality Planning and Standards, EPA-454/B-95-003a, Research Triangle Park, North Carolina, September, 1995.

9. Cooper, C.D., and F.C. Alley, *Air Pollution Control: A Design Approach*, Waveland Press, Inc., 1994.

10. Anderson, M.P., & W.W. Woessner, *Applied Groundwater Modeling*, Academic Press, New York, 1992.

11. Bedient, P.B., & W.C. Huber, *Hydrology and Floodplain Analysis*, Addison-Wesley Publishing, Reading, MA, 1992.

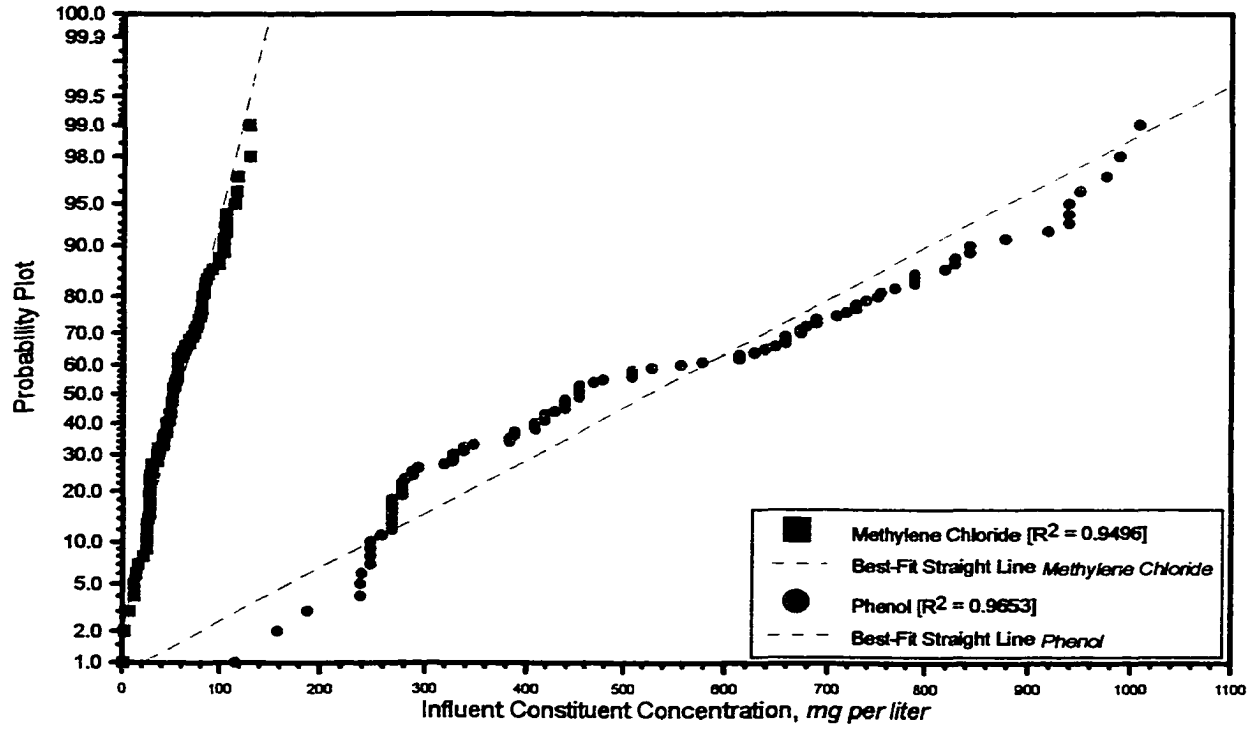

Figure 4.22: Probability Plot of Random Numbers

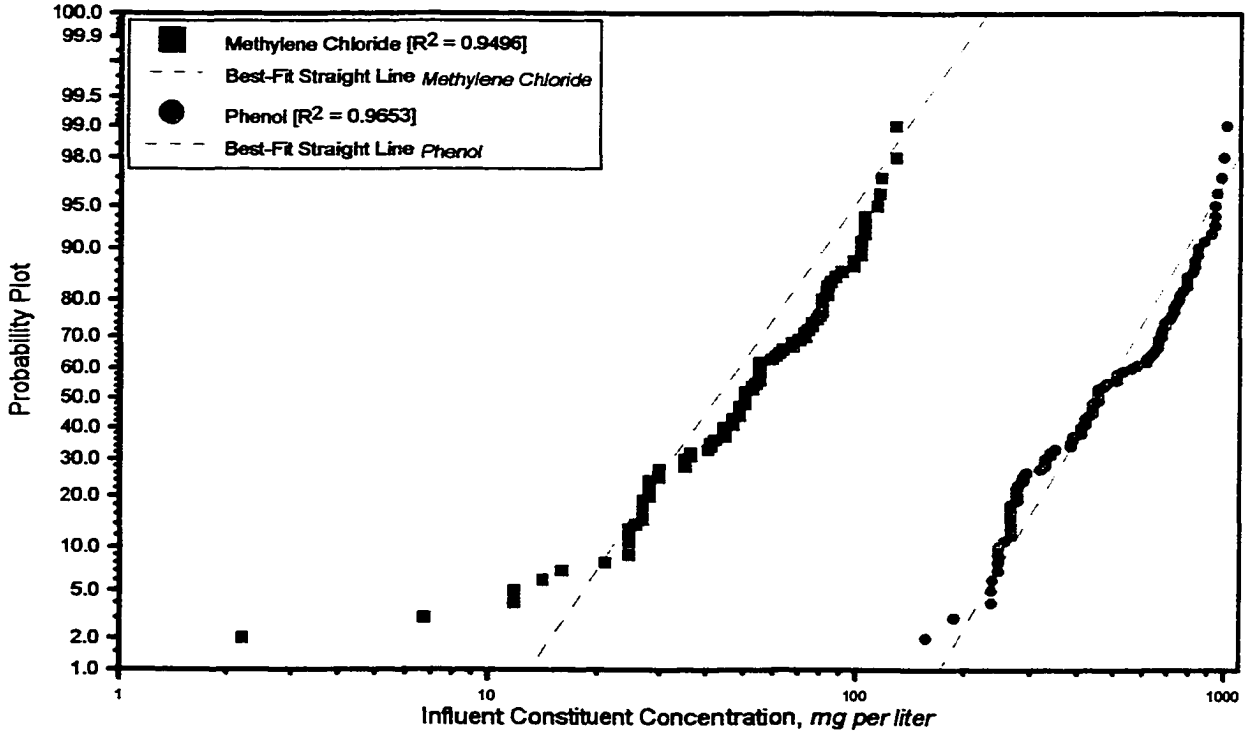

Figure 4.23: Lognormal-Probability Plot of Random Numbers

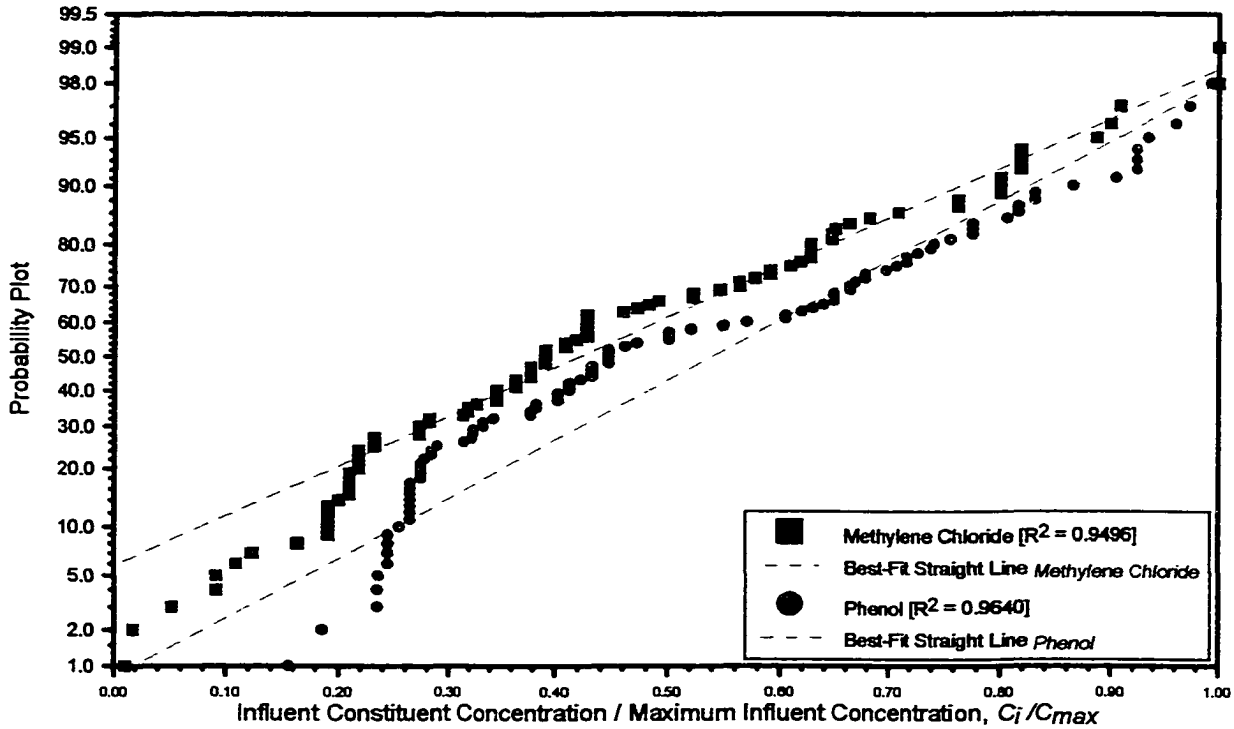

Figure 4.24: Probability Plot with Similar Axis [C_i/C_{max}]

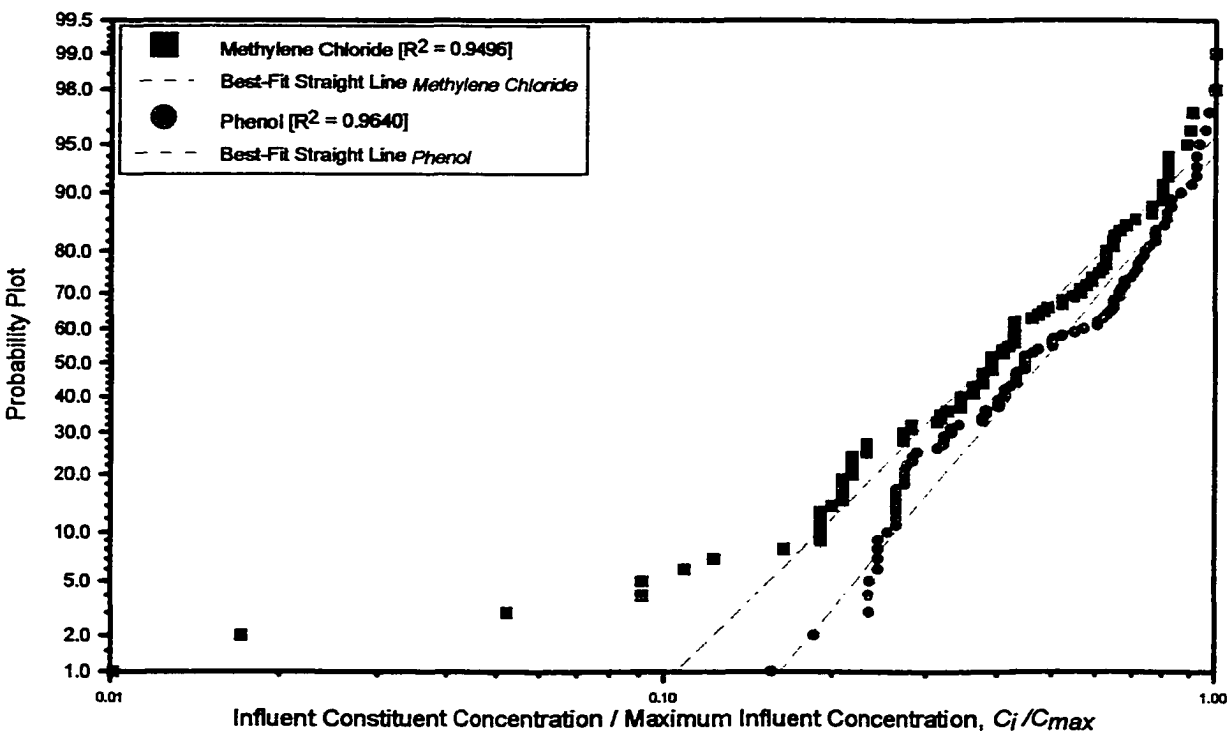

Figure 4.25: Lognormal-Probability Plot with Similar Axis [C_i/C_{max}]

CHAPTER 5
COMPARISON OF COUPLED MODEL PREDICTIONS TO OP-FTIR DATA

In Task 3 of this effort, computer-generated coupled model predictions will be compared to open-path monitoring data [Sub-task 3B]. Coupled model output [geographically based profiles of the ground level concentrations] will be compared to concentrations obtained by an open-path monitoring system using Fourier Transform InfraRed [OP-FTIR] spectroscopy. The open path FTIR monitoring system will measure atmospheric emissions by directing modulated infrared optical energy to retroreflectors [mirrors] along a physical path that crosses downwind of potential emission source plumes from the site. This chapter will discuss comparison of the coupled model predictions to the open-path monitoring FTIR data.

LITERATURE REVIEW

The open path monitoring system measures atmospheric emissions by directing modulated infrared optical energy to retroreflectors [mirrors] along a physical path that crosses downwind of potential emission source plumes from the site [1,2,3]. The OP-FTIR sensor receives the reflected signal, which has twice crossed the plume path. Pollutants in the plumes crossing this path modify the spectral signal in a quantitative way so that the quantities of different species in the path can be determined by analyzing the changes in this signal. The retroreflector returns the beam on the same path with the flat mirror. An important advantage of this system is that the instrumentation allows information to be gathered over a wide area without requiring multiple sensors. Many paths can be sequentially observed with the use of the multidirectional telescope scanner configured with the basic system. An automated approach will be used to measure the effect of the effluent plumes from the multiple open processes in the IWTF under different weather conditions. The FTIR measures a signal associated with the pollutant concentration over the pathlength [plume width]. The multi-directional scanner automatically changes the lines of sight in response to changes in wind direction to attempt to intersect with the plumes.

Initially, remote optical open-path monitoring systems were

developed for open-air use. These applications included battlefield detection of nerve agents by the military and environmental monitoring of ambient air by regulatory agencies [4]. Current uses include process monitoring, process control, and stationary source monitoring. Optical sensing is a valuable tool for determining the origin, identity, and amounts of fugitive emissions in an industrial environment. Optical sensing allows for real-time monitoring of gaseous emissions over a large region of space and therefore, is capable of providing a cost-effective means to meet certain ambient air monitoring objectives. Some of the key requirements for an advanced air monitoring system in an industrial facility is for the proposed technology to be cost-effective, reliable and simple, sensitive and accurate, operate continuously, large sensing volume, capable of detecting multiple analytes, and monitor a large dynamic range. Optical remote sensing offers promise as a cost-effective supplement to point monitoring systems [4]. Open-path Fourier Transform InfraRed systems offer versatility and commercial availability capable of monitoring long distances [typically greater than 100 meters]. The OP-FTIR has a larger dynamic range than the point monitor and does not require a recovery time before sensing is resumed. Automation is available which allows the determination of up to 40 compounds simultaneously on a continuous basis [4].

Optical monitoring systems are very powerful because of their ability to see many compounds simultaneously as well as their ability to report results in real time [5]. Optical remote sensing is rapidly being accepted as a viable means of performing industrial monitoring of all types. The U.S. EPA, as well as many state agencies, have now accepted FTIR for many monitoring applications [5]. OP-FTIR technology is going to clearly play a significant role in future environmental and industrial monitoring. FTIR systems are *spectral* meaning that they generate a full infrared spectrum of the sample. Any compound having infrared absorption will leave its characteristic signature [fingerprint] in this spectrum. The challenge is to detect the signature, to identify it, and to quantify it. The absorption signature arises from vibration / rotation transitions in the molecule [5,6]. Because these transitions are dependent on the molecular structure of the absorbing molecule, each compound will have a unique signature.

This uniqueness allows the spectral systems to differentiate between various compounds even in complex mixtures. In addition, the intensity of this signature is also proportional to the concentration of the compound so identification and quantification is possible. To detect a given compound in the infrared, the system must locate the absorption band of the molecule that is distinct and as free as possible of interferences from other compounds that will or could be present in the measurement environment. Typical spectral instruments [FTIR] store a library of references and use these to identify and quantitate unknown spectra. OP-FTIR systems are used for accurate, automated, and unmanned operation to monitor ambient air, detect accidental releases, and monitor industrial processes [4,5,6].

Most spectroscopic air-quality measurements are made either in the infrared or the ultraviolet regions of the spectrum [1]. The analytical techniques for these two regions are almost identical where interferometers [FTIR] are typically used in conjunction with IR systems. The FTIR system used for air quality measurements are configured either as extractive systems [with flow-through cells] or as open-path systems, which measure the pollutants in the atmosphere. The open-path system has additional advantages: measurements are performed in situ and therefore maintain the sample integrity, they can provide extensive spatial coverage at much less cost than point sampling methods, open-path systems are remote sensors that can probe inaccessible or difficult to sample regions, systems are well suited for continuous emission monitoring and detection of leaks, and can determine emission rates and downwind receptor concentrations [1,2]. The OP-FTIR is basically a spectrometer with special configurations. The system emits infrared radiation used to probe the sample. The system contains a dispersing element designed to convert broadband radiation into a spectrum where spectrum is defined as a plot of the light intensity versus the optical frequency. In open-path systems, the region where the chemical gases are measured is the open path of the light beam through the atmosphere [1,2]. In open-path systems, the interaction region is the open path through the atmosphere. The transfer optics to and from the atmosphere are referred to as the transmitter and receiver. In order to maintain a collimated beam with small divergence and to

increase the collection efficiency of the receiver, the transmitter and receivers are usually telescopes, most often of Cassegrain or Newtonian design [1,2].

Open-path FTIR sensors are configured as either bistatic or monostatic systems. In the bistatic configuration, the transmitter and receiver are placed on opposite ends of the atmospheric path of the light beam. In the monostatic configuration, the transmitter and receiver are essentially in the same location and a reflector is placed on the opposite side of the parcel of air to be measured. There are two types of monostatic systems, the coaxial single-telescope configuration and the two-telescope configuration [1,2]. In the single-telescope configuration, the light first passes through the interferometer and then through a second beam-splitter to the telescope. The telescope transmits the light as an enlarged collimated beam, which passes through the atmosphere to a corner-cube retroreflector array. The retroreflector returns the light beam to the receiver and the detector beam-splitter reflects the light to the IR detector. Combining the transmitter and receiver into a single telescope also lowers costs and improves the alignment stability of the system [1,3].

In 1990, Germany passed legislation to control emissions produced by waste incinerators [7]. This legislation required all existing waste incinerators to install a continuous emission monitor [CEM] to measure conventional gas pollutants [HCl, SO_2, NO_x, and CO]. They currently have more than 40 CEM units in operation. The German FTIR CEM units are positioned inside an incinerator stack. It is important to note that this application is somewhat different than the open-path FTIR system installed at OC-ALC IWTF. The OC-ALC OP-FTIR application is as an environmental monitor along a fenceline, whereas the German objective is directed more toward process control [and limited to four pollutants]. This paper does not report any numerical values, but concludes that with over 40 CEM units in place, the FTIR appears to be a cost-effective method of measuring, monitoring, and reporting process exhaust emissions [7].

The next article is directed at atmospheric monitoring of municipal wastewater treatment facilities [8]. The objective was to determine if VOCs are being emitted from wastewater treatment facilities and at what

concentration levels were the VOCs present in the atmosphere. The study sampled two wastewater treatment facilities in St. Louis and Springfield, Missouri. The sampling of these two wastewater treatment facilities allowed for a unique application of the mobile FTIR spectrometer system. The IR system is a Bomem DA02 Michelson interferometer with a broad band mercury cadmium telluride infrared detector with a 10-inch Cassegrain telescope operated in a single-pass configuration. The sampling began on 22 October and concluded on 27 October 1991 and covered a sampling distance of 64.5 meters. Target compounds for both facilities included toluene, methylene chloride, ammonia, trichloroethane, isopropanol, and methanol [8]. It was important to note that the methylene chloride spectrum was easily isolated from the other compounds. It is also important to note that the methylene chloride concentration surrounding the wastewater treatment facility ranged from zero to a high of 65 parts per billion with an average of 27.5 ppb. These methylene chloride concentrations are in agreement with what was determined from the air dispersion modeling predictions as part of this effort. The author concluded that VOC emissions can be detected at wastewater treatment facilities using the open-path FTIR method [8].

Another article in the literature discusses the use of an OP-FTIR at the Camacari Petrochemical Complex [largest petrochemical facility in Brazil] in Bahia, Brazil [9]. On the 16,000-acre site, there are 43 companies in operation manufacturing more than 150 different products including intermediary and transformed petrochemical products. The OP-FTIR was installed in 1993 and is used to measure toxic gases. The OP-FTIR is a MDA optical remote sensor configured as monostatic with a single transmitter / receiver Cassegrain telescope used in conjunction with a corner-cube retroreflector array. The OP-FTIR measurements were made at ten different locations within the complex in the period from August 1993 to September 1994. During this period, five monitoring campaigns were carried out with the FTIR at the complex. A total of 21 species were measured at the site. Although the paper presents the range of concentrations measured at the ten sites, the authors neglected to compare it to air quality samples or air dispersion model predictions. It is interesting to note that the range of concentrations

along the same path sometimes vary by several orders of magnitude [*i.e.*, 7-1059 ppb]. It is also interesting to note that the instrument is capable of measuring down to a few parts per billion on all 21 chemical species [of which none were phenol or methylene chloride]. The author concluded that the OP-FTIR technique allowed for a wide area coverage of a broad list of compounds at a low operating cost [9].

At OC-ALC [10], the air emission monitoring system utilized in this effort is an open-path Fourier Transform InfraRed spectrophotometer operated in a monostatic configuration with a single telescope, which functions both as a transmitter and a receiver. The infrared light from a silicon carbide glower is modulated by a Michelson interferometer and then transmitted by a single transmitter / receiver telescope, through the atmosphere being measured, to a retroreflector. The retroreflector returns the beam to the transmitter / receiver telescope and a beamsplitter directs the beam to a cryogenically-cooled, mercury cadmium telluride [MCT] detector. The FTIR Sensor system was designed to measure air emissions along five physical paths using a unistatic optical system coupled with a field-hardened MDA FTIR spectrometer system. The retroreflector placed at the end of each path is made up of an array of corner cubes that have sides aligned at 90 degrees. These three sides form a single corner-cube reflector. The optical properties of the corner cube are such that it always reflects back in the direction of the received beam, displaced only by some fraction of the cube width. The scanner output mirror is an elliptically shaped flat mirror. This optical component directs the modulated infrared beam toward a retroreflector or mirror along a path that traverses potential source plumes. The scanner output mirror also receives the reflected beam, which has returned across the plume path. The molecular species in the plume path absorbs infrared radiation at characteristic frequencies [wavelengths]. Three of the paths [P_1, P_2, and P_3] are directed along the northeast perimeter of the IWTF while two of the paths [P_4 and P_5] are directed within the perimeter. The five pathways are illustrated in Figure 5.1 and will be presented in the next section of this chapter. The installation cost of the single OP-FTIR was $300K and annual maintenance costs exceeded $100K [including the cost of two new cathode tubes]. The system was installed in 1995 and has operated

off and on for the last five years. During the five years, data have been collected over only three months [December 1995, January 1996, and February 1996] since installation [10]. It is interesting to note that of the data collected for the targeted chemicals [phenol and methylene chloride] during the three months of operation, only 64 percent of the gathered information was of value. The remaining 36 percent of the data were considered invalid because either the concentrations were negative or the position of the concentration maxima was at the FTIR instrument.

The literature describes an automated OP-FTIR system that has been installed at Tinker Air Force Base to continuously monitor volatile organic hydrocarbon emissions [methylene chloride, phenol, trichloroethane, tetrachloroethylene, etc.] from the industrial wastewater treatment plant [10]. The IWTF occupies an area 200 by 250 meters. Using mirrors and retroreflectors on elevated platforms near ground level, five optical paths were established for open monitoring over path lengths ranging from 60 to 200 meters. The scanner is programmed to automatically cycle through the different optical paths and record infrared absorption spectra. Spectral libraries and control software are available with the remote sensing system, so that spectra can be identified and quantified. The system is designed with 99 receptors or calculated point concentrations. To determine the concentration profiles along the optical paths, separate calculations are made with all 99 point receptors distributed along each optical path. A calculation routine is available to determine the maximum concentrations of a species and its coordinates at the fenceline. The comprehensive studies involved simultaneous open path measurements with tracer gas release and collection of gas samples. Smoke releases were also conducted to allow visualization of plumes. The author concluded that the OP-FTIR system was operational, but neglects to include how the FTIR concentration predictions compare to gas sample concentrations [10].

This next paper presents results from a field test of the OP-FTIR during trenching activities at the McColl Superfund Site in Fullerton, California [11]. The purpose of this particular study was to assess the appropriateness of FTIRs and related ancillary systems for use during McColl site remediation and in future long-term air monitoring projects.

The study was conducted at the 22-acre McColl Superfund Site between 4 May and 12 May 1994. OP-FTIR monitoring activities were conducted to measure near real-time, path-integrated concentrations of eight target compounds during trenching activities. The purpose of the trenching was to generate low levels of emissions from waste materials buried in the remediation site. The OP-FTIR system consisted of a Michelson interferometer, MCT detector, and Cassegrain telescope. The author concluded that the FTIR system could be configured to capture the contaminate plume with minimal difficulty. The FTIR was capable of monitoring typical fenceline configurations at the McColl site [11].

In late 1996, the American Petroleum Institute conducted optical remote sensing studies at an open field site in Duke Forest, North Carolina [12]. The field study featured several tracer gas releases from simulated point, area, and volume sources, with tracer gas samples and optical remote sensing measurements within 600 meters of the source. The study was named Project OPTEX [**O**perational **P**etrochemical **T**racer **EX**periment] and featured tracer releases from an active process unit at a petrochemical facility [12]. The study provided data to evaluate the feasibility of OP-FTIR spectroscopy to infer emissions of air contaminants from industrial sources, especially sources such as petroleum refineries. The major objective was to evaluate the ability of OP-FTIR to detect, locate, and quantify emission releases at one or more process areas. For this purpose, tracer gases were released at known rates from a series of points upwind and downwind of a heated process unit at an operational petrochemical facility. The facility was isolated from other external industrial sources and is located in a flat, rural setting. Two tracer gases were deployed during the study: sulfur hexafluoride [SF_6] and carbon tetrafluoride [CF_4]. These gases are non-toxic and non-flammable. The locations of the tracer gas release points were attached to structures at the process unit except for the near-surface releases. Bag samples [Tedlar] were placed along three rows for any given release experiment and were designed to collect two, one-hour samples. The project tested four OP-FTIR systems. OP-$FTIR_1$ was an ETG electro-optical system manufactured by MDA. The system was a monostatic system used in conjunction with a Cassegrain telescope. OP-$FTIR_2$ was an AIL system that uses a Newtonian telescope and Michelson

interferometer developed by the Midac Corporation. The system was a monostatic design and was used with one retroreflector. OP-$FTIR_3$ was a Midac Corporation system operated by Phillips Petroleum. The system uses a Newtonian telescope with Michelson interferometer and was bistatic [having a source at one end of the path]. OP-$FTIR_4$ was a monostatic, Midac Corporation system provided by Texaco. OP-FTIR and Tedlar bag monitoring were coordinated with the tracer releases so that the OP-FTIR monitoring started about five minutes before the start of the tracer release and continued until the tracer was dispersed below detection limits. Samples were collected on approximately 15 hours of tracer releases and bag sampling spread over five days in October. The author does not present any conclusions or recommendations, but plans to conduct dispersion modeling and OP-FTIR-derived emission calculations using the database to evaluate these analytical techniques as applied to a real-world operating facility [12].

The literature provides little costing information. One article reports a case where the ambient air is monitored along a 500 x 500 meter process perimeter [13]. Table 5.1 compares the estimated cost-to-own for three different systems used to monitor the perimeter averaged over an assumed 15-year life for the analyzer. The annual cost-to-own is derived from the installation cost plus the total operating costs [including maintenance, repair, parts, and labor] averaged over the working lifetime. The installation of a gas chromatographic system would require approximately four analyzer houses [$200K], four gas chromatographs [$120K], 240 sample lines [$3.6M] and associated operating costs [$80K]. A multi-point sensor system to monitor the same area would require 720 sensors, 240 mounting posts, 720 signal lines and power, and miscellaneous infrastructure. The total installation cost for such a situation is approximately $7.2M and obviously cost-prohibitive. The amount of maintenance associated with these types of sensors is expensive. The OP-FTIR system presents another alternative to monitor the process area. This example would require two scanning OP-FTIR systems [$170K each], analyzer structure [$100K], and utilities [$50K]. The total installation costs for this system is roughly $500K. The cost to operate the system is an estimate based on data collected from two commercial scanning systems [1].

Another potential option is to conduct canister studies throughout the year along the fenceline on the north perimeter. The cost of analyzing the canisters is roughly $46 per canister. If 100 samples are collected monthly, the cost would approach $55,000 per year. Computer modeling is another option that would cost pennies on the dollar when compared to the other alternatives. It would require an engineer only part-time and the initial start-up would require a semi-powerful desktop computer and software [$10K].

Table 5.1: Cost Comparison Between Systems [13]

SYSTEM	OPERATING COST	INSTALLATION COST	COST-TO-OWN
OP-FTIR [4]	$8,000	$500,000	$43,000
GC System [4]	$59,000	$4,080,000	$331,000
Multi-Sensor [4]	$1,650,000	$7,200,000	$2,130,000
OP-FTIR [OC-ALC]	$100,000	$300,000	$120,000
Canister Study	$46 per sample	N/A	$55,200
Computer Modeling	$10,000	$10,000	$10,700

There are other factors to consider when choosing an analyzer system, such as reliability. This reliability is defined as the amount of time the instrument is providing useful information to operations and not simply the total run-time of the instrument. A study reveals that high reliability for an instrument used for environmental / safety or process control applications is tantamount to a high return-on-investment. The reliability of the GC and sensor system is 99+ percent when properly maintained. However, current state-of-the-art for a scanning open-path FTIR appears to be about 95 percent. Typical applications require an OP-FTIR with 98+ percent reliability [13].

In northern Germany, two one-week measurement experiments were carried out in the fall of 1996 and spring 1997 on a municipal waste site [13]. The waste site under investigation had a total area of 208,000 m^2. The OP-FTIR was installed to establish the impact of waste site emissions on the population living 300 meters to the north. For the measurements, a monostatic OP-FTIR was used extending over a path distance of 85 meters. Monostatic means that the IR-light source and the FTIR-spectrometer were placed at one side of the measurement path

and the light beam was folded by a retroreflector at the other side of the measurement path. The measurements were recorded in the evening hours with under calm weather conditions. Remote optical sensing offers a big advantage, in that, the OP-FTIR is able to measure the concentration over a several hundred-meter path. This study does not report any numerical results, but concludes that the OP-FTIR is a powerful tool for characterizing waste site emissions [13].

Another article discusses an air quality study of the Yochon Industrial Estate in southern Korea [14]. The Korean Institute of Science and Technology [KIST] performed four major studies between October 1993 and April 1997. These studies were performed to measure VOCs surrounding an estate that encompasses more than 90 industrial facilities including petrochemical industries, machining and metal-working industries, a fertilizer industry, and power plants. The collected data will provide useful information for evaluating air quality impacts, planning future development, modeling and data analysis for health risk assessment. During a six-month period, air quality data were collected from one fixed continuous monitoring station located at the center of the estate, and ten temporary stations positioned around the estate perimeter. Analyses were conducted for more than 100 chemicals including organic compounds ranging from C2 to C9 chains and aromatics to halogenated VOCs, in addition to inorganic chemicals with offensive nuisance odors. Air sampling was performed with SUMMA canisters. During the study, more than several hundred canisters were collected for analysis. Each VOC canister was analyzed for about 100 different species. In general, the analysis error was determined to be about 5 to 30 percent depending on the different species, however the analysis error for the VOCs during the study is 14 percent on average [14]. This study presents an indication of the uncertainties associated with the SUMMA canister readings.

Open-Path FTIR measurements were made at the Fresh Kills Landfill in Staten Island, New York, over a six-day period in late August 1997 [15]. The U.S. EPA contracted SAIC to conduct a preliminary air quality study of landfill gas emissions. During the field study, real-time OP-FTIR measurements were made on 20 target compounds. At landfill sites, the major chemical emissions are methane, ammonia, and carbon monoxide. The

OP-FTIR system was the remote sensing MDA instrument operated with a monostatic sensor, which transmits the interferometrically modulated infrared beam to a corner-cube retroreflector array. The retroreflector array was placed at ranges from 20 to 120 meters from the sensor. Over 220 OP-FTIR measurements were made under a variety of wind speed and wind directions. The path determinations for methane ranged from 1.6 to 1044 parts per million [ppm]. The carbon monoxide values vary from 1.2 to 4.8 ppm. The determinations for ammonia varied from 10 to 15 ppb to high values of 68 ppb. The paper concluded that OP-FTIR is a valuable air quality measurement tool. The OP-FTIR data has shown utility for detecting and recording transient releases, which could easily be missed with other measurement technologies [15].

Another article utilizes an open-path FTIR spectrometer to make measurements of volatile organic compounds in an industrial complex in New Castle, Delaware as part of the Superfund Innovative Technology Evaluation [SITE] program [16]. The SITE program was developed by the U.S. EPA and supports the evaluation and testing of innovative measurement techniques in an attempt to identify the most effective tools for monitoring emissions from Superfund waste sites. The tests were conducted from 24 July to 3 August 1997. A Cassegrain telescope is used in combination with a retroreflector to determine the concentration of 41 VOCs along a single, downwind path at a distance of 250 meters. SUMMA canisters are used to obtain comparison data. The Delaware State Department of Natural Resources and Environmental Control selected the site because of anticipated high levels of *p*-dichlorobenzene. The terrain was part of the flood plain of the Delaware River and included a petrochemical refinery and several chemical manufacturing plants [16]. Of the 41 VOCs monitored, figures are presented in the article for four of the VOCs including methane, carbon monoxide, *p*-dichlorobenzene, and chlorobenzene. The OP-FTIR system was able to successfully measure methane concentrations down to 1.5 ppm, carbon monoxide to 125 ppb, *p*-dichlorobenzene to 25 ppb, and chlorobenzene down to 25 ppb. Figures not presented in the article include benzene, carbon tetrachloride, toluene, xylene, and a number of chlorofluorcarbons. Of the 41 VOCs reported, there were only two compounds for which canister and FTIR data were available for comparison [*p*-dichlorobenzene and chlorobenzene]

[16]. The article indicates that when the spectra are free from interferences, the FTIR can make very good measurements, even at concentrations that are close to the detection limits. Comparison of the chlorobenzene data from the canister and the OP-FTIR shows a fairly high variability, which does not seem to be concentration dependent. This variability may result from the low chlorobenzene levels, which were almost always very close to the detection limits of the FTIR. There were two conclusions drawn from this article: the FTIR can be used as a reliable monitoring instrument when the concentrations are greater than about 50 ppb [detection limit for time period], and the comparison procedure is a viable technique for comparing open-path and point-sampler measurements.

A technical report documented in the literature evaluates the feasibility of using a FTIR spectrometer from an airborne platform for remote sensing of air pollution [17]. The Air Force Phillips Laboratory mounted a FTIR spectrometer into a small twin-engine aircraft and obtained data used in this investigation. The aircraft was flown over sections of New York and New England. The spectrometry was operated where the spectrometer viewed the warm ground and atmosphere below the aircraft [approximately 1000-meter pathlength]. The spectral data were analyzed at AIL Systems for the presence of atmospheric pollutants including ozone, carbon monoxide, oxides of nitrogen [N_2O, NO_2], methanol, ammonia, aliphatic and aromatic hydrocarbons [17]. The article concluded that FTIR can be used to monitor several chemicals in the environment at levels appropriate for environmental monitoring, especially ozone. Although ozone can be problematic because of the contribution of sky reflection, ozone was detected at levels estimated to be 120 PPB. The detection limit is about half this, and could be reduced further with improved methods of water line removal. The airborne platform system would need to minimize the vibration of the system by developing a better isolation system before reductions in detection limits can be realized. It is important to note that the spectra were analyzed by a trained spectroscopist rather than pulling spectral data from a computerized spectral library. It is also interesting to note that the FTIR system had problems detecting aliphatic [ethylene, isobutane, etc.] and aromatic hydrocarbons

[benzene, toluene, etc.] because of the presence of water, which obscured the absorption spectra [17].

Enactment of the Clean Air Act Amendments of 1990 has resulted in increased ambient air monitoring needs for industry, some of which may be met efficiently using open-path optical remote sensing techniques [18]. Optical remote sensing technologies are expected to play a significant role in developing emission inventories for compliance with air quality regulations. Optical remote sensing technologies are expected to satisfy a more important and urgent application concerning requirements for detection of accidental releases. Expecting an expansion in the use of remote optical systems, the U.S. EPA has developed tables that list critical information [spectral range of each chemical, absorption coefficients, and minimum detectable concentrations]. The article concludes that remote optical measurement technologies are capable of making measurements down to as low as 10 ppbs over a 100-meter path length. It is important to note that this article reports the minimum detectable concentration for methylene chloride is a range from 48 to 80 ppb [average 65.6] at a distance of 200 meters [18]. The U.S. EPA is working to develop procedures to demonstrate equivalence with reference methods for use with some of the remote optical measurement technologies for toxic gases.

Another article estimates the uncertainty associated with open-path remote sensing of fugitive emissions [19]. Open-path remote sensing techniques such as FTIR spectrometry offer a powerful approach for measuring environmental pollution sources. The Air Pollution Prevention and Control Division [APPCD] conducted a greenhouse gas [GHG] measurement program during the summer of 1995. The purpose of the program was to develop a better estimate of GHGs being emitted from anaerobic lagoons commonly used for the treatment of human and industrial wastes. This measurement program was undertaken by the U.S. EPA because of the scarcity of field measurements to confirm estimated GHG emissions from these sources. The APPCD staff conducted an audit of a municipal wastewater treatment facility in Texas. The anaerobic lagoons were approximately 200 X 300 feet, aligned north to south. The FTIR beam was 570 feet in length and placed 175 feet downwind of four lagoons. Two tracer gases were used. One tracer gas was utilized to

determine location, wind speed, and direction of the wind, while the second tracer gas [SF_6] was used to estimate downwind concentrations. This article concluded that there is significantly less uncertainty associated with the upwind locations as compared to downwind locations. This is thought to be partially because of the distances. The upwind sides were farthest from the IR beam while the downwind points were nearest to the IR beam. This seems to imply that the uncertainties are less the farther away from the IR beam the measurement is recorded. Conversely, the uncertainties increase as the distance from the IR beam is decreased [19].

A distinctive element of this effort is the comparative studies where the computer-generated coupled model predictions are compared to open-path FTIR monitoring data along two perimeters [three optical paths]. Most of the literature evaluates a single, downwind optical path. Another distinctive element is that there are multiple retroreflectors that bend the optical path, whereas the literature is typically limited to one retroreflector designed to make a single pass along the downwind path [monostatic design]. Another feature unique to this effort is that chemical depainting agents [phenol and methylene chloride] are analyzed by the OP-FTIR, whereas much of the literature is limited to primary criteria pollutants or tracer gases [sulfur hexafluoride and carbon tetrafluoride]. Most of the FTIR literature is compared to limited, short-term tracer gas releases without comparisons to air dispersion model predictions. Much of the OP-FTIR literature pertains to the monitoring of other industrial sources [industrial complexes, incinerators, petrochemical facilities, landfills, municipal waste sites, etc.] and not directed toward environmental monitoring of IWTF fencelines [facility perimeter].

TINKER AFB APPLICATION OF THE OPEN-PATH MONITORING SYSTEM

The open-path monitoring system utilized in this effort is the open path Fourier Transform InfraRed [OP-FTIR] spectrophotometer operated in a monostatic configuration. The FTIR sensor system will measure air emissions along several distinct physical paths by using a unistatic optical system coupled with a field-hardened MDA FTIR spectrometer system. The molecular species in the plume path absorbs infrared

radiation at characteristic frequencies [wavelengths]. Figure 5.1 illustrates the series of paths over which this air monitoring system will be directed at the IWTF. The paths are labeled P_1 to P_5 and extend out from the IWTF control facility on which the FTIR is stationed [10]. The advantage of this location is that the system has direct optical access to most of the major pollution sources [see paths P_4 and P_5 in Figure 5.1] as well as having access to the paths along the fenceline [P_1, P_2, and P_3]. The paths over the sources will be coupled with the

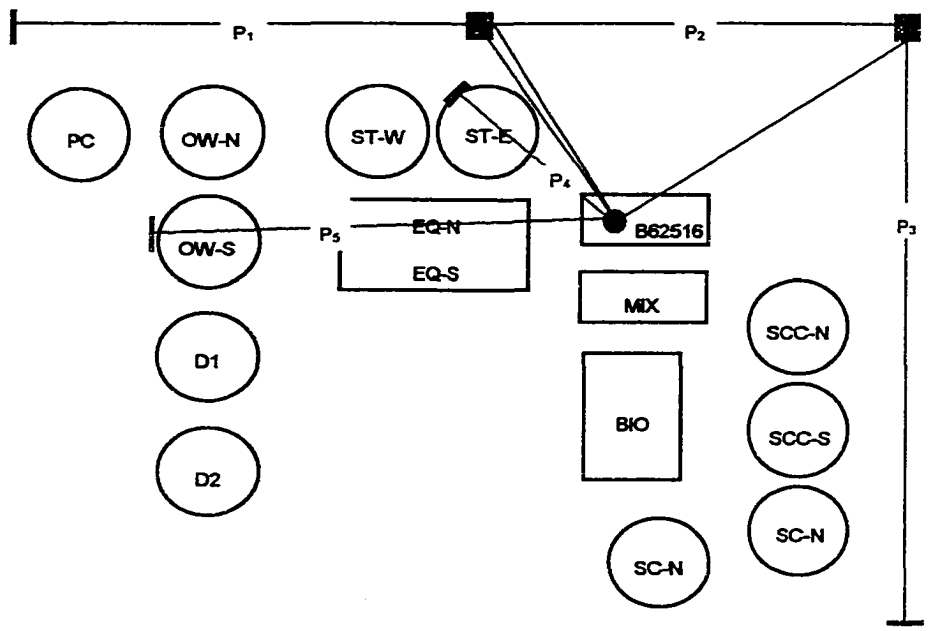

Figure 5.1: Top View of the IWTF Remote Optical Monitoring Paths

measurements made at the fenceline to validate the necessary pollution dispersion modeling. Usefulness of the paths for sample analysis along the fencelines is limited to the times when the wind is blowing plumes in the directions over those paths. Since the wind is from the south-southwest to south-southeast about 40 percent of the time, the northern paths will be used at least this much of the time. The eastern path [P_3] can be used as a background run during a southerly or northerly wind direction, and as a sample path during westerly winds. Optical paths P_4 and P_5 will not be considered because of the lack of comparison data [periodic canister monitoring data].

COMPARISON OF MODEL PREDICTIONS TO OPEN PATH MONITORING DATA

Sub-task 3B of the project involves comparing the computer-generated phenol and methylene chloride concentrations with open-path monitoring data. The Open Path Monitoring [OPM] system, a Fourier Transform InfraRed remote sensing system, is one such system designed to monitor species emission levels in real time, along paths where plumes are expected. The paths of the OPM, set for operation at the IWTF, allow concentration information to be determined along the fenceline of the facility. The FTIR measures the average concentration along the beam path on this fenceline directly, and with modeling can verify that the defined MAAC is not exceeded on a path average. Measurements of 5 to 11 compounds were made on each run. The FTIR sensor observes changes in the beams intensity in the specified wavelength regions, due to optical absorption by the pollutants present in the plume. The spectral wavelength patterns of the sets of spectral regions monitored are compound dependent. The size of the changes in these concentration patterns is directly related to the size of the observed spectral absorbance patterns. The calculated values are average values attained during a measurement, which usually lasts ten minutes. Assuming steady wind directions, this can be extrapolated directly for comparison to the annual-average chemical concentrations. Concentration data show maxima on the path where the concentration-pathlength has been measured. The coordinates give the positions of the maxima. These are obtained by modeling 99 receptor points equally spaced on the path. By knowing the location of the concentration maxima along the path, the chemical concentrations predicted by the OP-FTIR can be plotted as a function of distance along the optical path. These OP-FTIR concentration predictions can be compared to concentrations predicted by the coupled model and field canister sample data.

Figure 5.2 illustrates the methylene chloride concentration along optical Path P_1. This is a path running west-to-east along the fenceline north of the IWTF. The red squares indicate the coupled model predictions positioned every ten meters. The black circle, blue diamond, and gray triangles represent the field data [RCRA facility investigation, Battelle study, and OC-ALC Bioenvironmental data,

respectively]. The OP-FTIR predictions are represented with the green blocks. It is important to note that the concentrations predicted by the FTIR are clearly several orders of magnitude larger than both the coupled model predictions and field canister data. It is also important to notice that there are no obvious trends as observed with the coupled model predictions [higher concentrations in the middle and decreasing concentrations approaching the outer limits of the facility perimeter]. The OP-FTIR data appears to be a scattered clump of data orders of magnitude greater than what is predicted by the coupled model and periodic canister data.

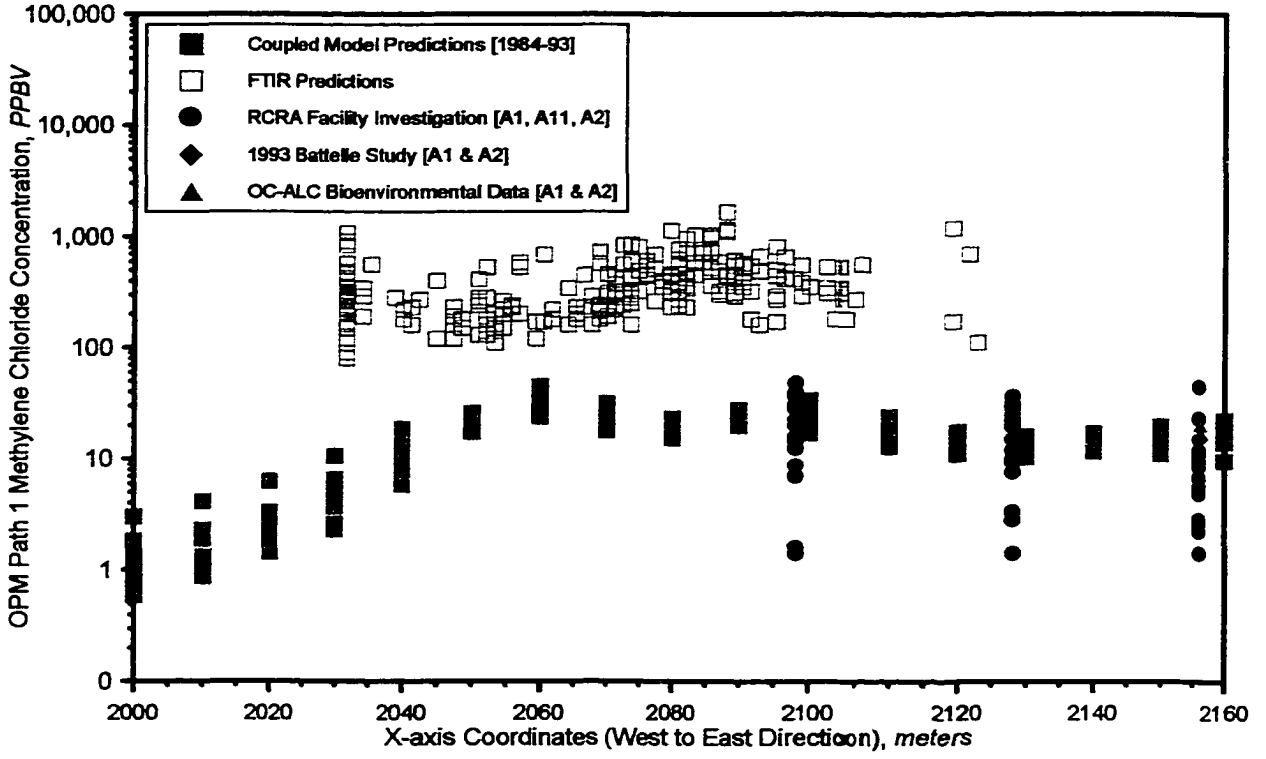

Figure 5.2: OPM Path P_1 Concentration Predictions for Methylene Chloride [*ppbv*]

Figure 5.3 illustrates the methylene chloride concentration along optical Path P_2. This is a path running west-to-east along the fenceline north of the IWTF. The red squares indicate the coupled model predictions positioned every ten meters while the black, blue, and gray symbols represent the field data. The OP—FTIR predictions are represented with the green blocks. It is important to note that the

concentrations predicted by the FTIR are clearly several orders of magnitude larger than both the coupled model predictions and field canister data. It is also important to notice that there are no obvious trends as observed with the coupled model predictions [higher concentrations in the middle and decreasing concentrations as you approach the outer limits of the facility perimeter]. The OP-FTIR data appears to be a scattered clump of data orders of magnitude greater than what is predicted by the coupled model and canister data. Another point that supports questioning the FTIR data is the fact that Path P_2 at x-axis coordinate 2152 in Figure 5.3 shows a large collection of FTIR data. This collection of data does not appear at x-axis coordinate 2152 in Figure 5.1 along Path P_1. The FTIR is able to detect the chemical concentration plume along one path [P_2], but miss it completely along an adjacent path [P_1] at the same coordinate location.

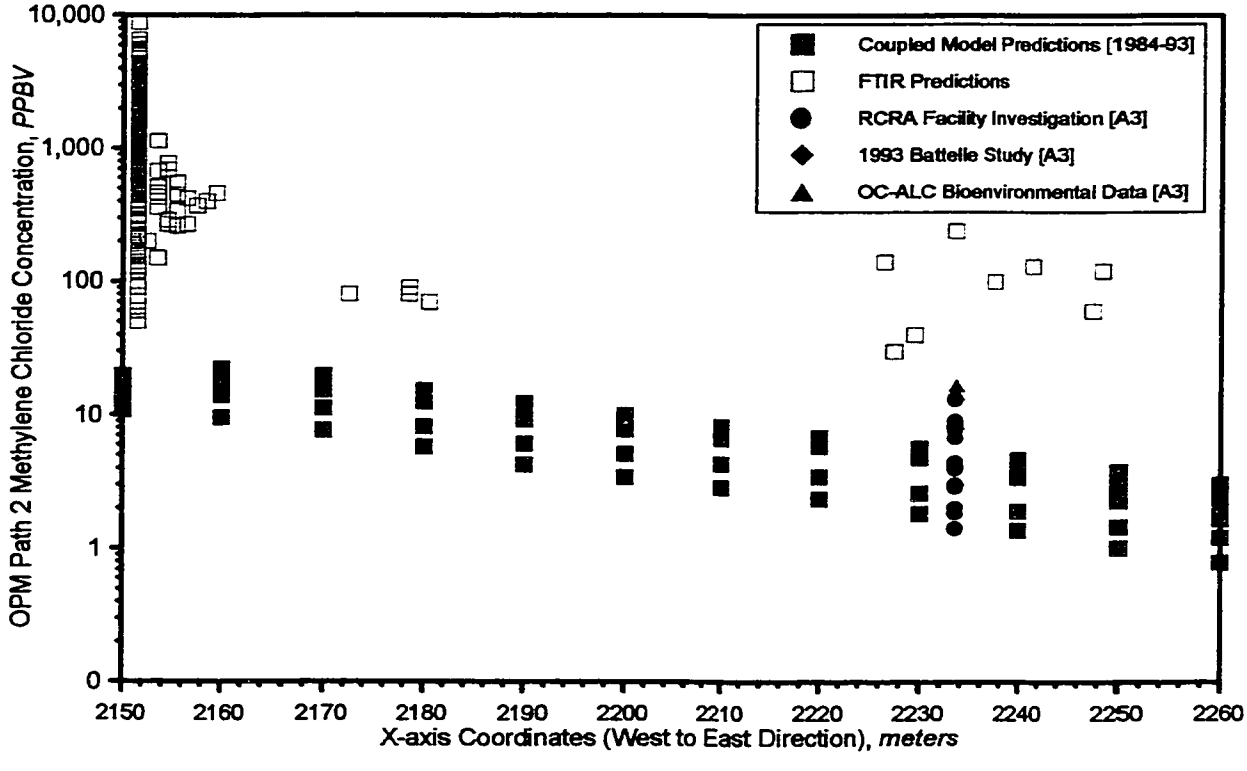

Figure 5.3: OPM Path P_2 Concentration Predictions for Methylene Chloride [*ppb*]

Figure 5.4 illustrates the methylene chloride concentration along optical Path P_3. Unlike P_1 and P_2, Optical Path P_3 extends south-to-

north along the east perimeter fenceline of the IWTF. The red squares indicate the coupled model predictions positioned every 10 meters while the black points represent the RCRA field data. Note that there are no Battelle or OC-ALC Bioenvironmental data for these sites [A4 and A5]. The OP-FTIR predictions are represented with the green blocks. As with the previous two optical paths, concentrations predicted by the FTIR are several orders of magnitude greater than both the coupled model predictions and RCRA field canister data. Figures 5.5, 5.6, and 5.7 illustrate the phenol concentrations along the same optical paths P_1, P_2, and P_3, respectively. These paths extend west-to-east along the fenceline north of the IWTF, and north-to-south along the eastern perimeter. The red squares indicate the coupled model predictions positioned every ten meters. The black, blue, and gray symbols represent the field canister data [RCRA investigation, Battelle study, and OC-ALC Bioenvironmental data, respectively]. The OP-FTIR predictions are represented with the green blocks. In each case, it is important to note that the phenol concentrations predicted by the FTIR are clearly several orders of magnitude larger than both the coupled model predictions and field canister monitoring data. It is also of interest to note that there are no obvious trends as observed with the coupled model predictions [as observed with the coupled model predictions and periodic field canister data]. The OP-FTIR data appears to be a scattered clump of data orders of magnitude greater than what is predicted by the coupled model and field canister data.

SUMMARY

The following discussion will objectively answer which of the methods are more accurate: the coupled model predictions or OP-FTIR data. In reviewing the figures, the coupled model predictions clearly appear to duplicate the field canister data for both the methylene chloride and phenol in every figure, whereas the OP-FTIR over-predicts the field canister data by one-to-three orders of magnitude for both constituents in every figure [along three different optical paths]. The coupled model predictions produced numerical values that were in very good agreement with the field canister data. For both chemicals, 100 percent of the coupled model predictions were within a 99.9 percent

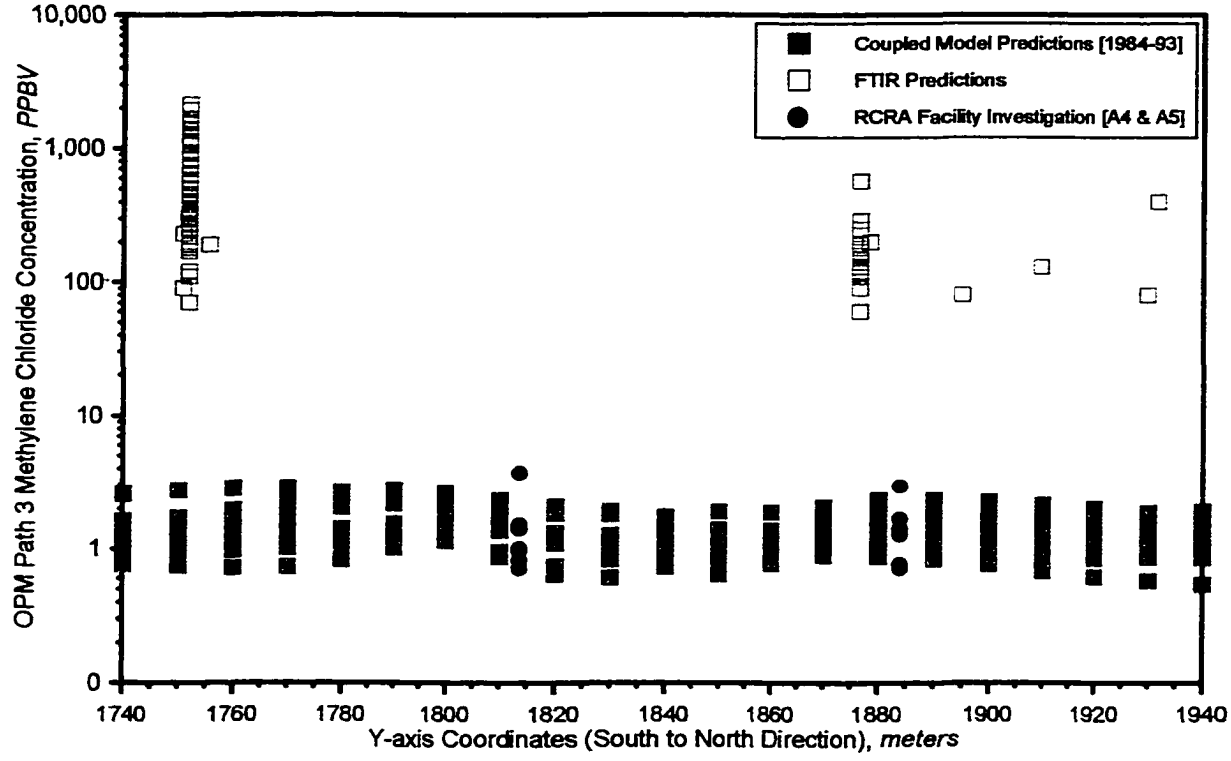

Figure 5.4: OPM Path P_3 Concentration Predictions for Methylene Chloride [*ppb*]

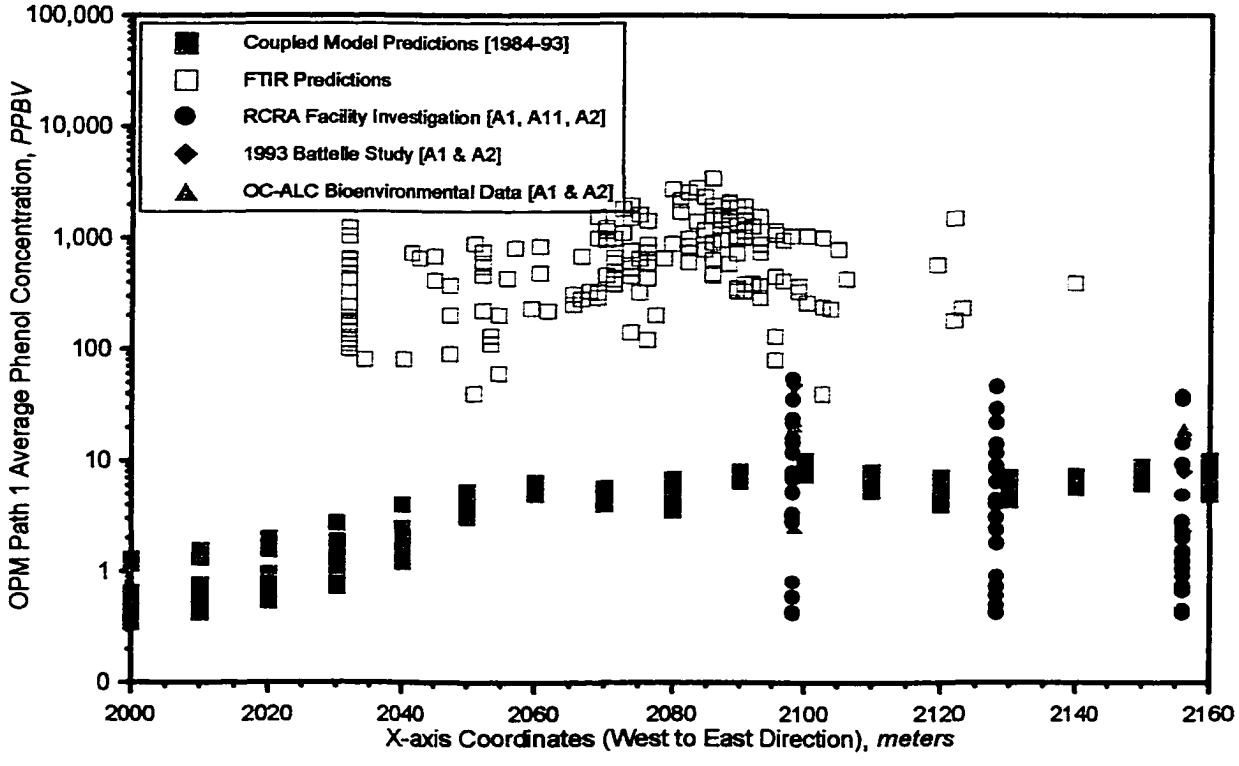

Figure 5.5: OPM Path P_1 Concentration Predictions for Phenol [*ppb*]

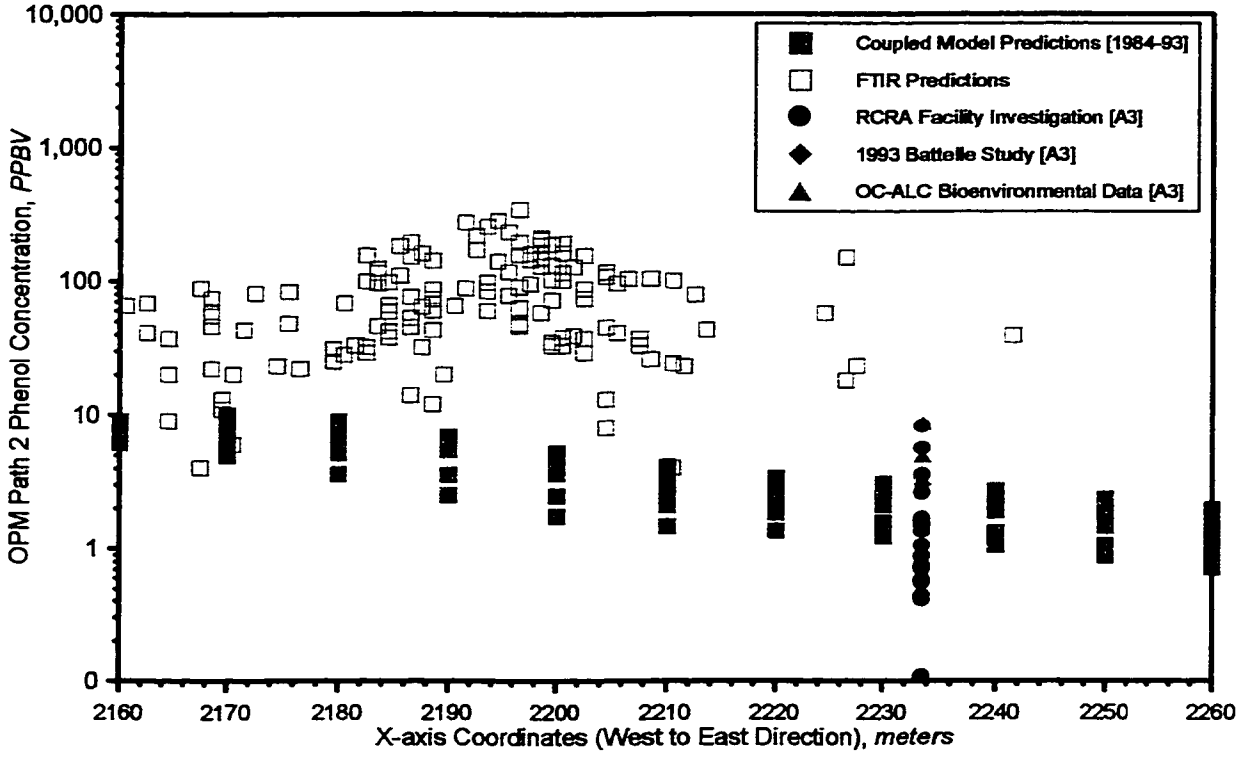

Figure 5.6: OPM Path P_2 Concentration Predictions for Phenol [*ppb*]

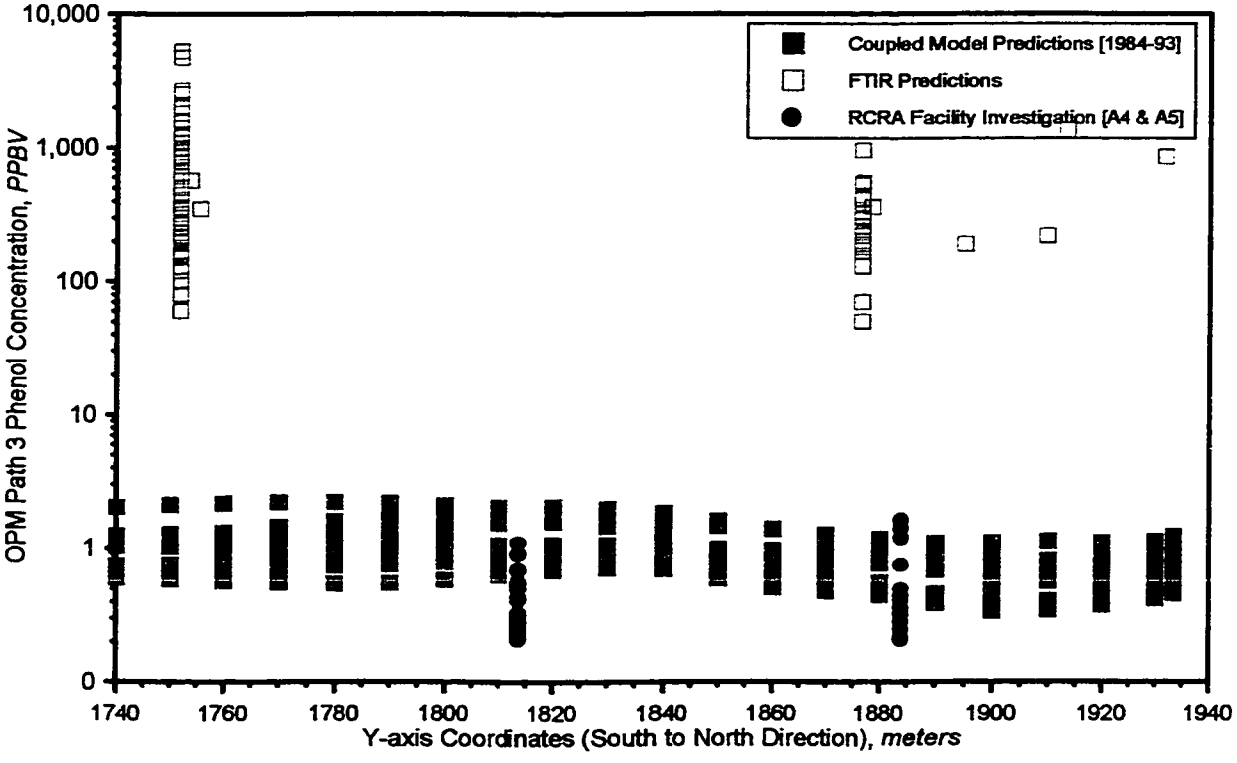

Figure 5.7: OPM Path P_3 Concentration Predictions for Phenol [*ppb*]

level of confidence. The field canister data consisted of over 270 data points from three independent sources [RCRA facility investigation, Battelle study, and OC-ALC Bioenvironmental study] collected over six weeks. There were 130 coupled model predictions made at 13 different receptor locations using ten years of meteorological data [1984 through 1993]. The coupled model predictions were compared using both a z-test and Student's-t test with both statistical tests indicating a high degree of correlation with the field canister data.

The FTIR was tested for a longer period of time [12 months], along multiple [three] optical paths, and down two facility perimeters [east-west and north-south] for both chemicals. The OP-FTIR was unable to predict the chemical concentrations for either chemical that was within one order of magnitude for either methylene chloride or phenol. Most OP-FTIR predictions were between two and three orders of magnitude difference with the field data.

Another indication that the OP-FTIR values are in question is the missing FTIR data along Optical Path P_1 at x-axis coordinate 2152 in Figure 5.2. This collection of data does not appear at x-axis coordinate 2152 in Figure 5.2 along Path P_1, but does detect the methylene chloride plume at the same location on the x-axis along Path P_2 in Figure 5.3. The FTIR is able to detect the chemical concentration plume along one path [P_2], but miss it completely along an adjacent path [P_1] at the same coordinate location. This fact not only brings into question the large collection of data in Figure 5.3 [x-axis coordinate 2152], but all of the methylene chloride concentrations along all three optical paths.

In reviewing the trends, there were no observed trends with the OP-FTIR predictions. Common sense dictates that the closer [shorter distance] that the measurement or predictive tool is to the emission source, the greater will be the dispersion plume concentration. For the coupled model predictions and field canister data, the receptors closest [within 100 meters] to the major emission sources [A1, A11, A2, and A3] showed a greater chemical concentration while the receptors farther away [over 100 meters] from the major emissions sources [A6, A7, A8, etc.] had lower chemical concentrations. The OP-FTIR data appears to be a scattered cluster of data without any similar trend and orders of

magnitude greater than what was measured by the periodic canister monitoring data.

Critical to the investigation is the reliability and reproducibility of the existing data. The OP-FTIR installed at Tinker AFB provided a reliability-of-operation of less than three months over five years of operation [10]. Of that three-months of data, more than 36 percent of the collected information is considered unusable because of technically unsound data [negative concentrations, etc.].

Independent of this effort, the OP-FTIR has been shown to misidentify and produce predictions for chemical concentrations that are orders of magnitude greater than measured at the IWTF [20]. In a 1998 odor investigation of the industrial wastewater treatment facility, the OP-FTIR misidentified and misrepresented the chemical concentration of several pollutant plumes discharged from the IWTF. This study supports the information and conclusions provided in this effort [20].

There are a number of reasons for the OP-FTIR to over-predict the field canister data. Some of the potential reasons include interferences from stray light spectra, water vapor concentration, background or reference spectra, inappropriate location of the remote optical paths, routine noise interferences, calibration standards outside the range of interest, to name a few. Stray light inside the instrument can be caused by strong sources of IR energy that are in the field of view of the instrument [21]. For example, it is possible to have the sun in the instruments field of view during sunrise and sunset. This will probably give rise to an unwanted signal that actually comes from reflections inside the instrument. The stray light actually causes an error in the determination of the gas concentration and must be subtracted from the data spectra before processing [21]. Thus, the stray light component must be recorded at every monitoring session.

Another potential concern is the impact the water vapor concentration has on the performance of the instrument. The return-beam intensity is a function of not only the path length, but also of the water vapor concentration in the atmosphere [21]. It is critical that the water vapor spectra be measured along each path at every monitoring session. The change in water vapor concentration must be considered the biggest potential source of error in the background measurement [21].

An accurate record of the partial pressure of water vapor should be maintained. These data should be taken continuously, or at least every two hours during quiet days or every half hour during times when weather fronts are passing [21].

Reference or background spectra can have a significant impact on the performance of the instrument. Ideally, the background spectrum is collected under the same experimental conditions as those for the sample spectrum, but without the target gas or gases present [21]. Errors are introduced into the measurements if background spectra are not obtained with every monitoring session. Acquisition of the reference spectrum represents one of the more difficult tasks in open-path FTIR monitoring [21]. Currently, there is not a universal method for obtaining a satisfactory background spectrum. The method chosen to obtain the reference spectrum must be determined on a site-by-site basis. General advice about the background spectra are that the spectra cannot contain any absorption features due to the target gases and the spectrum are only valid for the time period over which it was used [21].

Location of the remote optical paths is another consideration that can impact the accuracy of the instrument. According to the literature guidelines, 90 percent of the path must be at least 20 meters from the drip lines of trees [21]. This recommendation is violated along the north perimeter where 75 percent of Optical Paths P_1 and P_2 are well within the drip lines of the trees along the north perimeter.

Another consideration critical to the performance is the use of calibration standards for defining the concentration range for specific chemical constituents. The calibration standards should include the expected concentration within the range of standards to ensure correct identification and quantification of the target gases.

In addition, routine noise measurements [instrument electronic noise and random baseline noise] should be taken during every monitoring session. The noise measurements should be taken daily and recorded on a control chart to alert the operator of any gross changes or trends in the deterioration of the baseline noises [21].

SELECTED REFERENCES

1. Beer, R., *Remote Sensing by Fourier Transform Spectrometry*, Wiley-

Interscience Publishing, New York, 1992.

2. Camagni, P., & S. Sandroni, *Optical Remote Sensing of Air Pollution*, Elsevier Publishing, New York, 1984.

3. Tate, J.D., & P. Chauvel, *Industrial Applications of Optical Sensing*, Air & Waste Management Association, 90th Annual Meeting & Exhibition, Toronto, Ontario, 8-13 June 1997.

4. Spellicy, R.L., & S.E. Hall, *Early Test Results on a FTIR Industrial Process Monitoring System*, Air & Waste Management Association, 90th Annual Meeting & Exhibition, Toronto, Ontario, 8-13 June 1997.

5. Spellicy, R.L., *Analytical Methods for Optical Remote Sensing*, Air & Waste Management Association, 90th Annual Meeting & Exhibition, Toronto, Ontario, 8-13 June 1997.

6. Perry, R.H., & C.H. Chilton, *Chemical Engineers' Handbook*, Fifth Edition, New York, McGraw-Hill, 1973.

7. Lamp, T., M. Radmacher, & K. Weber, *Calibration of an Open-Path FTIR Spectrometer for Methane, Ethylene, and Carbon Monoxide*, Air & Waste Management Association, 90th Annual Meeting & Exhibition, Toronto, Ontario, 8-13 June 1997.

8. Fateley, W.G., M.R. Witkowski, C.T. Chaffin, & T.L. Marshall, *Art of Atmospheric Monitoring*, Proceedings from SPIE, International Society of Optical Engineering, Vol. 1637, pp. 50-61, 1992.

9. Neves, N., E.D. Couto, R.H. Kagann, *Use of an Open-Path FTIR Sensor at Camacari Petrochemical Brazil*, Proceedings from SPIE, International Society of Optical Engineering, Vol. 2365, Society of Photo-Optical Instrumentation Engineers, pp. 426-435, 1995.

10. Ivancic, W.A., P.R. Sticksel, M.W. Holdren, J.R. Satola, R. Mukund, & C. Barker, *Infrared Open-Path Monitoring for Studies of Atmospheric Gaseous Pollutants*, Proceedings from SPIE, International Society of Optical Engineering, Vol. 2365, Society of Photo-Optical Instrumentation Engineers, pp. 262-272, 1995.

11. Leo, M.R., R.J. Klicks, & S.H. Perry, *Evaluation of Open-Path FTIR and UV Air Monitoring for use at the McColl Superfund Site*, Air & Waste Management Association Proceedings, 88th Annual Meeting & Exhibition, San Antonio, TX, 18-23 June 1995.

12. Paine, R.J., *Project OPTEX: Field Study at a Petrochemical Facility to Assess Optical Remote Sensing and Dispersion Modeling Techniques*, Air & Waste Management Association, 90th Annual Meeting & Exhibition, Toronto, Ontario, 8-13 June 1997.

13. Lamp, T., *Measurement of Municipal Waste Site Emissions with the Open-Path FTIR Measurement Technique*, Air & Waste Management

Association, 91st Annual Meeting & Exhibition, San Diego, California, 14-18 June 1998.

14. Moon, K.C., Y.P. Kim, Y.S. Ghim, & J.Y. Kim, *Air Quality Study for the Yochon Industrial Estate*, Air & Waste Management Association, 91st Annual Meeting & Exhibition, San Diego, California, 14-18 June 1998.

15. Kagann, R.H., & W.T. Walter, *Open-Path FTIR Measurements at the Fresh Kills Municipal Landfill*, Air & Waste Management Association Proceedings, 88th Annual Meeting & Exhibition, San Antonio, TX, 18-23 June 1995.

16. Russwurm, G.M., R.H. Kagann, A.O. Simpson, & W.F. Herget, *Long-Path FTIR Measurements of Volatile Organic Compounds in an Industrial Setting*, EPA-68-D0-0106, EPA/600/J92/262, NTIS PB92-206424.

17. Malik, H., *Advanced FTIR Signal Processing for Airborne and Spaceborne Remote Sensing of Chemical Clouds*, 22 July 1997, ADA330590, NTIS PL-TR-97-2053.

18. Grant, W.B., R.H. Kagann, & W.A. McClenny, *Optical Remote Measurement of Toxic Gases*, EPA/600/J93/319, NTIS PB93-229409.

19. Flanagan, J., R. Shores, & S. Thorneloe, *Uncertainty Estimate for Open-Path Remote Sensing of Fugitive Emissions*, EPA-68-D3-0045, EPA/600/A96/067, NTIS PB96-184288.

20. Keough, E., *Odor Investigation at the OC-ALC Industrial Wastewater Treatment Facility*, prepared by Parsons Engineering, September 1998.

21. Russworm, G.M., J.W. Childers, & W.A. McClenny, *FTIR Open-Path Monitoring Guidance Document*, EPA/600/R96/040, April 1996.

CHAPTER 6
RISK ASSESSMENT

The final task of this effort is to demonstrate the potential uses of this methodology by conducting a site-specific health risk assessment. There are benefits to using a coupled model approach besides generating information for emissions reporting and regulatory compliance determinations relative to maximum ambient air concentrations for phenol and methylene chloride. Additional advantages include the evaluation of on-base process change scenarios and pollution prevention activities regarding the use of phenol and methylene chloride, in addition to evaluating changes in the design or operation of the IWTF for purposes of minimizing atmospheric emissions of phenol and methylene chloride. This coupled model approach has applicability for air quality management purposes at other similar U.S. Air Force Bases or industrial [private sector] chemical depainting operations.

Task 4 of this effort involves performing a risk assessment of the IWTF impact region to quantify risks associated with phenol and methylene chloride emissions on the general population in the housing community north of the treatment facility and impact of exposures on industrial wastewater treatment plant personnel. The industrial wastewater treatment facility is located on the northeast quadrant of the installation. The treatment facility is situated with a small housing addition to the north, open field and creek system [Soldier Creek] to the south, four-lane highway [Douglas Blvd] on the east, and motor-vehicle parking structure on the west perimeter. Historically, there has been concern about chemical exposures on the housing community to the north. The following tasking will attempt to quantify some of the risks to both the surrounding general population and treatment plant workforce. The risk assessment will include calculation of an equivalent human dose [based on animal mortality studies], the maximum risk for individuals in the general population and IWTF personnel, excess number of cases of cancer in the general population and IWTF personnel, the average excess number of cases of cancer generated per year for the general population and IWTF personnel, and loss of life expectancy for the general population and IWTF worker subgroup.

Population characteristics of the housing edition north of the IWTF show that approximately 133 [2.66 persons per household in 50 households] people living in the surrounding area will be exposed to annual average air concentrations of a potential carcinogen [*i.e.*, methylene chloride and phenol] as shown in Table 6.1. The majority of the housing community residents are white [85.7 percent], above the age of 18 [72.2 percent], and male [51 percent]. The OC-ALC treatment facility worker subgroup consists of approximately 50 workers of which the population characteristics are white [84 percent] and male [92 percent].

Table 6.1: Results from the Coupled Model

CHEMICAL	NUMBER EXPOSED	POPULATION GROUP	MAXIMUM AIR CONCENTRATIONS, *PPBV*
Methylene Chloride	133	General population	70
Methylene Chloride	50	Adult workers	180
Phenol	133	General population	40
Phenol	50	Adult workers	130

LITERATURE REVIEW

The literature reports a health statistics review of the community adjacent to Tinker Air Force Base that was completed in early 1998 [1]. The housing community is exposed to airborne volatile organic compounds from the on-site industrial wastewater treatment plant from the time it was built in 1956 to current. The study was performed by the Agency for Toxic Substances and Disease Registry [ATSDR] with the U.S. Department of Health and Human Service. The study was conducted to evaluate cancer mortality using vital records [mortality] data [1]. The results of the death certificates indicated that the crude cancer mortality rates in both sexes were lower in the housing addition than in Oklahoma state, or city and county rates for that period. The study concluded that there were no overall excessive cancer cases for the period from 1965 to 1994. There were a documented total of 14 cases of cancer observed versus the 15.5 expected with Oklahoma state cancer rate, or 19.7 expected with Oklahoma city / county cancer rate. There were no known cases of liver, colon, pancreatic, or childhood cancers [1]. It is important to note

that the ATSDR study did not evaluate other factors [*i.e.*, socio-economic, cultural, etc.] that could impact the outcome of the study.

Some of the literature focuses on the Risk Management Program [RMP] rule under the Clean Air Act Amendments that requires industry to reduce the risk of a facilities accidental release of toxic substances to the community [2,3]. For example, the U.S. EPA estimates that over 30,000 public drinking water and wastewater treatment systems will be impacted by this rule, and that compliance costs will vary from $1.7K to $153K per system. Most of the literature involves the review of processes that include chlorine, sulfur dioxide, and digester gas systems. CH2M-Hill developed a RMP for Dallas Water Utilities at two large municipal wastewater treatment plants. The RMP included a hazard assessment as part of an initial screening procedure to determine into which program level the wastewater treatment facilities fall. From the initial screening, the RMP included an estimate of the toxic worst case, which predicts the worst case release rate from each of the containers. Air dispersion modeling is performed to determine the concentration of the chemical cloud under the worst conditions. The article highlights the need to develop current hazard review procedures. The foundation of any RMP is development and/or updating the operating and maintenance procedures for each regulated system [2]. The last recommendation [and most forgotten] is to communicate the risk management plan to the public and in particular the surrounding community.

The next article highlights the U.S. EPAs requirements related to the prevention of accidental chemical releases via the Risk Management Program, Section 112 [r] of the Clean Air Act Amendments [CAAA] [4]. As a result of the CAAA requirements, the U.S. EPA promulgated the Risk Management Program rule in June 1996. The rule affects facilities that handle greater than threshold quantities of any regulated substances. The U.S. EPAs list of regulate substances include [but not limited to] chlorine, propane, ammonia, acrolein, and butane. Activities at DOD and certain federal facilities that could be subject to the RMP are ammonia storage and refrigeration, water and wastewater treatment [that use chlorine], and propane storage. These activities will be required to identify and analyze worst-case scenarios and evaluate their impacts off-site. Further, these facilities will be required to implement a full

accident prevention program and an emergency response program [4]. The article concludes that Risk Management Program requirements are here to stay and facility managers must get ready to meet these additional requirements.

Another article discusses the U.S. EPA RMP requirements for an off-site analysis for a worst case accidental release scenario [5]. This analysis includes residential population estimates and the presence of critical receptors. Critical receptors include schools, hospitals, prisons, public recreation areas, arenas, and major commercial and industrial developments. Air dispersion modeling is used to determine the downwind extent of the worst-case release scenario for each pollutant. The facility must provide the following information within the endpoint distance: residential population, public receptors, and environmental receptors. The article highlights a relatively new method for displaying the area surrounding a facility called the Desktop Geographic Information System [GIS]. The Desktop GIS MapInfo Professional is a commercially available software system that allows the personnel who are performing the modeling to analyze and control the display of the information. The GIS MapInfo system typically works in a layer approach for managing maps and data. A map will be made up of many layers of information such as streets, political boundaries, base boundaries, critical receptors, water bodies and streams, and data points. A layer containing the facility boundary and worst-case area of influence is typically included in the analysis. Once the base maps are developed and the accidental release modeling is performed, GIS gives the user the ability to visualize the results. Additional data sources can be added to better communicate the accidental release modeling results. The article concludes that the use of a map to communicate understanding of a facility surrounding area is a powerful communication tool. Using a GIS software package, such as MapInfo, allows the user to better evaluate the population surrounding a facility and provide population estimates for a RMP. Using maps and data to better understand the area surrounding a facility can improve a risk communication program [5].

A feature unique to this effort is the use of the coupled model to perform a risk assessment of the impact region to include the housing

community population and IWTF workforce. The literature does not reference a risk assessment for chemical depainting agents at an industrial wastewater treatment facility. The literature does not report the calculation of an equivalent human dose [based on animal mortality studies], the maximum risk for individuals in the general population and IWTF personnel, excess number of cases of cancer in the general population and IWTF personnel, the average excess number of cases of cancer generated per year for the general population and IWTF personnel, and loss of life expectancy for the general population and IWTF worker subgroup. The closest mention in the literature concerns a health survey conducted by the ATSDR on the housing community adjacent to Tinker AFB [1]. The risk assessment tasking is considered unique to this effort.

RISK ASSESSMENT

Risk assessment is defined as a body of knowledge [methodology] that evaluates and derives a probability of an adverse effect of an agent [chemical, physical, or other], industrial process, technology, or natural process [6]. Traditionally, most risk assessments deal with health effects. The elements of a risk assessment includes the characterization of the types of health effects expected, characterization of the exposure, evaluation of experimental studies [animal and/or epidemiological], characterization of the relationship between dose and response, estimation of the risk of occurrence of health effects, estimation of the number of cases expected, characterization of the uncertainty of the analysis, and recommendation of an acceptable concentration in air, food, or water [7]. The risk assessment demonstration of this effort will attempt to satisfy some of these elements. Risk assessments are necessary for informed regulatory decisions regarding worker exposures, industrial emissions and effluents, ambient air and water contaminants, chemical residues in foods, cleanup of hazardous waste sites, and naturally occurring contaminants [7]. This portion of the effort will calculate the following for both phenol and methylene chloride: equivalent human dose [based on animal mortality studies], the maximum risk for individuals in the general population and IWTF personnel, excess number of cases of

cancer in the general population and IWTF personnel, the average excess number of cases of cancer generated per year for the general population and IWTF personnel, and loss of life expectancy for the general population and IWTF worker subgroup [7].

The risk assessments will be conducted with information from the Integrated Risk Information System [IRIS] prepared and maintained by the U.S. EPA [8]. IRIS is an electronic database containing information on human health effects that may result from exposure to various chemicals in the environment. IRIS was initially developed for EPA staff in response to a growing demand for consistent information on chemical substances for use in risk assessments, decision-making and regulatory activities. The heart of the IRIS system is its collection of computer files covering individual chemicals. These chemical files contain descriptive and quantitative information in the following categories: oral reference doses and inhalation reference concentrations, hazard identification, slope factors, and oral and inhalation risks for carcinogenic effects [8]. It is important to note that although the IRIS system is a tool that provides hazard identification and dose-response assessment information, it does not provide situational information on individual instances of exposure. Combined with specific exposure information [via coupled modeling], the data in IRIS can be used for characterization of the public health risks of a given chemical in a given situation that can ultimately lead to a risk management decision designed to protect the public health.

METHYLENE CHLORIDE

Methylene chloride is widely used as a multi-purpose solvent and paint remover that is not known to occur naturally in the environment [9,10,11]. High concentrations have been measured in industrial indoor environments and during the use of methylene chloride as a paint remover. The general population is exposed to much lower levels of the solvent in the ambient air, drinking water, and food. About 80 percent of the world production of methylene chloride is estimated to be released into the atmosphere, but photodegradation takes place at a rate that make accumulation in the atmosphere unlikely [9,10,11]. In surface water, volatilization is the major process of removal, hydrolysis and

photodegradation being insignificant. The solvent is readily aerobically biodegradable. The major route of human exposure is through inhalation, while absorption of liquid methylene chloride via the skin is slow [9,10,11].

Methylene Chloride is dichloromethane [CH_2Cl_2], molecular weight of 84.93, vapor pressure of 349 mm Hg, and odor threshold of 743 mg per m^3 [208 PPM]. Tinker AFB utilizes methylene chloride in depot maintenance operations as a chemical depainting agent used to chemically remove coatings from aircraft surfaces and components. In 1993, methylene chloride purchases accounted for almost 33.2 percent of all hazardous materials brought on the installation.

RISK ASSESSMENT COMPUTATIONS FOR METHYLENE CHLORIDE EXPOSURES

Given the following assumptions, calculate the equivalent human dose, maximum risk for individuals in the general population and IWTF personnel, excess cases in the general population and IWTF personnel, average excess cases generated per year for the general population and IWTF personnel. Existing air emission sources are assumed to operate continuously. Air dispersion modeling data show that approximately 133 people living in the surrounding area [housing area to the north of the facility] and 50 white male workers will be exposed to an annual average pollutant concentration of potential carcinogens as shown in Table 6.1. The following assumptions will be made: the source of emission [IWTF process units] will operate for 45 years, the general population will be continuously exposed for 45 years, the number of people in the general population exposure subgroup [IWTF personnel] will remain constant for 45 years, the exposure concentration for the general population subgroup [IWTF staff] will remain constant for 45 years, workers will be exposed for eight hours per day, five days per week, 50 weeks per year for 45 years [45 years maximum for an individual worker], the size of the worker risk group will remain constant for 45 years, all workers will be exposed to one concentration over 45 years.

Human and animal dose rates are frequently reported in terms of the lowest observed adverse effect level [LOAEL]. The LOAEL is the lowest experimentally determined dose rate which produces a statistically or biologically significant adverse effect [7]. From documented animal

mortality studies, the methylene chloride LOAEL of inhalation exposure of non-smoking healthy individual is 694 mg per m^3 [200 PPM] for 24 months, 6 hours per day, and 5 days per week. There were 11 of the 95 that reported a dose-related increase in the total number of benign tumors with an associated 8 of 95 in the control group [7]. The intake [I] in units of mass or volume of contaminated media per day is determined from tables of standard values of intake as illustrated in Table 6.2 [volumetric flow rate], and converted to units of volume of contaminated air per day, as given. Note that the average air intake for a male rat is 0.10 liter per minute [7]. The T is the median time [exposure frequency] of exposure in days and the average male rat body weight [W] in kilograms is tabulated in Table 6.2 [7].

Table 6.2: Standard Values for Adults [7]

SPECIES	SEX	LIFESPAN, *years*	BODY WEIGHT, *kg*	AIR INTAKE, *liter/min*
Human	Male	72	75	7.5
Human	Female	79	60	6
Mouse	Male	2.5	0.03	0.03
Mouse	Female	2.5	0.025	0.03
Rat	Male	2.5	0.5	0.1
Rat	Female	2.5	0.35	0.1
Hamster	Male	2	0.125	0.06
Hamster	Female	2	0.11	0.06

$$I = \left[\frac{0.10\,l}{min}\right]\left[\frac{m^3}{1000\,l}\right]\left[\frac{60\,min}{hour}\right]\left[\frac{6\,hours}{day}\right] = 0.0360\,m^3\ of\ contaminated\ air\ per\ day \qquad 6.1$$

$$T = \left[5\,days/week\right]\left[52\,weeks/year\right]2\,years = 520\,days \qquad 6.2$$

$$W = 0.50\,kg \qquad 6.3$$

To account for interspecies and intraspecies variability, the literature recommends use of a safety factor, F. This safety factor is the product of three components F_1, F_2, and F_3. The potential for interspecies variation in response sensitivity is represented by F_1. Values for F_1 may range from one to ten for animal data depending on the match of biokinetics [absorption, distribution, storage, biotransformation, and elimination as a function of time] and mechanism of the toxicity. If the biokinetics and mechanism of the toxicity match, F_1 is equal to one for an animal study. For human data, F_1 is

typically unity. For methylene chloride, there appears to be a wide range of response sensitivity between species [rats to mice, hamsters, etc.], therefore, F_1 is assumed to be a value of ten [7]. The potential for intraspecies variation in human sensitivity is represented by F_2. Values may range from one to ten. If there is no human data regarding human variation in sensitivity, the suggested value for F_2 is one. The third safety factor component [F_3] is derived from the length of the study. A F_3 safety factor element of ten can be applied if the LOAEL is derived from a short-term study [as in this case]. Thus, the safety factor [F] is 100. Note that this safety factor is recommended by the IRIS database [8].

The lifespan [L] is the lifetime of the experimental species [male rat] expressed in days. The equivalent human dose [D] can be calculated from the animal study as follows. As shown, the equivalent human dose is a function of the LOAEL, contaminated air intake, exposure duration, weight of the animal species, lifespan of the experimental species, human lifetime [75 years], human body weight [70 kilograms], and a safety factor.

$$L = 2.5\,years\left[365\,days/year\right] = 912.5\,days \tag{6.4}$$

$$D = 75 \cdot 365 \cdot 70\left[\frac{C \cdot I \cdot T}{W \cdot F \cdot L}\right] \tag{6.5}$$

$$D = 75\,years \cdot \left[\frac{365\,days}{year}\right] \cdot 70\,kg \cdot \left[\frac{\left(694\ mg/m^3\right)\left(0.0360\,m^3/day\right)520\,days}{\left(0.50\,kg\right)100\ \left(912.5\,days\right)}\right] = 545{,}651\,mg \tag{6.6}$$

The risk factor [R] in inverse milligrams is defined as the excess risk per unit of dose [derived from the lowest available experimental equivalent human dose-response point]. IRIS tabulates the risk factor for specific chemicals and exposure routes [oral, inhalation, etc.]. For methylene chloride, IRIS documents a risk factor of 4.7E-7, which will be used the following risk assessment calculations.

For determining the maximum dose to an individual in the general population, the maximum methylene chloride concentration is used. From Table 6.1, the maximum methylene chloride exposure to the general population is 70 PPB [0.250 mg/m^3]. This maximum exposure is illustrated in Figure 3.9. For the maximum methylene chloride exposure to the

general population, focus on the area surrounding the housing edition [in the upper right quadrant of Figure 3.9]. In Figure 3.9, the maximum methylene chloride dose occurs along the fenceline north of the facility at x-y coordinates 2170-1936.

$$C = 70\ PPB\left[\frac{PPM}{1000\ PPB}\right]\left[\frac{mg/m^3}{0.28\ PPM}\right] = 0.25\ mg\ per\ m^3 \qquad 6.7$$

$$I = \left[\frac{7.5\,l}{min}\right]\left[\frac{m^3}{1000\,l}\right]\left[\frac{60\,min}{hour}\right]\left[\frac{24\,hour}{day}\right] = 10.8\,m^3\ of\ contaminated\ air\ per\ day \qquad 6.8$$

$$T = 75\ years\left[365\ days/year\right] = 27{,}375\ days \qquad 6.9$$

$$L = 75\ years\left[365\ days/year\right] = 27{,}375\ days \qquad 6.10$$

$$D = C \cdot I \cdot T = 0.25 \cdot 10.8 \cdot 27{,}375 = 73{,}913\ mg \qquad 6.11$$

The general population risk group dose of 73,913 mg is well below the equivalent human dose of 545,651 mg from the animal study. The maximum dose calculation for an individual in the general population is repeated for each of the receptor locations and illustrated in Figure 6.1. Note that the interest is the maximum dose to an individual in the general population as exists in the housing community located north of the treatment facility.

In calculating the maximum individual worker dose, refer to the maximum methylene chloride dose as illustrated in Figure 3.9. The maximum methylene chloride dose is approximately 180 PPB and occurs at three x-y Cartesian coordinate locations [2160-1900, 2100-1925, and 2060-1925].

$$C = 180\ PPB\left[\frac{PPM}{1000\ PPB}\right]\left[\frac{mg/m^3}{0.28\ PPM}\right] = 0.643\ mg\ per\ m^3 \qquad 6.12$$

$$I = \left[\frac{29\,l}{min}\right]\left[\frac{m^3}{1000\,l}\right]\left[\frac{60\,min}{hour}\right]\left[\frac{8\,hours}{day}\right] = 13.9\,m^3\ of\ contaminated\ air\ per\ day \qquad 6.13$$

$$T = \left[5days/week\right]\left[50weeks/year\right] \cdot 45years = 11{,}250\ days \qquad 6.14$$

$$L = 75years \cdot \left[365days/year\right] = 27{,}375\ days \qquad 6.15$$

$$D = C \cdot I \cdot T = 0.643 \cdot 13.9 \cdot 11{,}250 = 100{,}527\ mg \qquad 6.16$$

The worker risk group dose of 100,527 mg is well below the lowest

effective dose of 545,651 mg from the animal study. The maximum dose calculation for an individual worker is repeated for each of the receptor locations and illustrated in Figure 6.2.

Maximum individual excess risk for the general population and workers are determined as follows. The maximum individual excess risk for the general population and worker subgroup calculations are repeated for each of the receptor locations and illustrated in Figures 6.3 and 6.4.

$$P_{e,\,general\,population} = R \cdot D = 4.7E-7 \cdot [73{,}913] = 0.035\ general\ population \qquad 6.17$$

$$P_{e,\,worker} = R \cdot D = 4.7E-7 \cdot [100{,}527] = 0.047\ workers \qquad 6.18$$

An important part of risk analysis is the estimation of the number of cases, which may be generated by a certain scenario of exposure [7]. Risk groups of primary concern are the general population and subsets of the general population such as worker groups. The following expressions are used to quantify the excess cases [EC] and average number of excess cases generated per year for the general population. The computation determining the number of excess cases for the general population is repeated for each of the receptor locations and illustrated in Figure 6.5.

$$EC = R \cdot I \cdot T \sum_{i=1}^{n} [C \cdot N]_i \qquad 6.19$$

$$EC = 4.7E-7 \cdot (10.8) \cdot (365 \cdot 75) \cdot [(0.25)133] = 4.6 \qquad 6.20$$

The average number of excess cases generated per year of exposure can be calculated from the following expression. The computation determining the number of excess cases for the general population for a given year is repeated for each of the receptor locations and illustrated in Figure 6.6.

$$\overline{EC} = \left[\frac{excess\ cases}{year}\right] = \left[\frac{excess\ cases}{years\ of\ risk\ group\ exposure}\right] \qquad 6.21$$

$$\overline{EC}_{general\,population} = \left[\frac{4.6}{75}\right] = 0.062\ average\ excess\ cases\ generated\ per\ year \qquad 6.22$$

Use the following expressions to quantify the excess cases [EC] and average number of excess cases generated per year for the worker subgroup, where N is defined as the number within the affected

population subgroup. The computation determining the number of excess cases for the worker group is repeated for each of the receptor locations and illustrated in Figures 6.7 and 6.8 [7].

$$EC = R \cdot C \cdot I \cdot T \cdot N \qquad 6.23$$

$$EC = 4.7E-7 \cdot (0.643) \cdot 13.9 \cdot (250\ days/year)\ 45\ years \cdot 50 = 2.36 \qquad 6.24$$

$$\overline{EC}_{worker} = \left[\frac{2.36}{45}\right] = 0.053\ average\ excess\ cases\ generated\ per\ year \qquad 6.25$$

The loss of life expectancy [*LLE*] is the life [days or years] lost due to a particular exposure or activity [7]. For example, smoking will shorten the average male smoker's life by 6.2 years. Any risk factor to which a person is exposed can affect that person's life expectancy, the decrease or increase in life expectancy can be calculated using the following.

$$LLE = individual\ lifetime\ risk \cdot average\ remaining\ lifetime \qquad 6.26$$

$$LLE = 0.00000047 \cdot (37.5) = 0.000018\ years \qquad 6.27$$

PHENOL

Phenol is a colorless or white solid when it is pure, but usually used as a liquid [12,13,14]. It has a characteristically strong odor that is sickeningly sweet and irritating. It evaporates more slowly than water and dissolves fairly well in water. Phenol is a primarily man-made chemical, although it is found in nature in animal wastes and organic material [formed during the natural decomposition process of organic materials]. The largest single use is in the manufacturing of plastics, but it is used to synthesize phenolic resins. It is also used as a slimicide [which kills bacteria and fungi found in watery slimes] and as a disinfectant in medical products. The main emissions of phenol occur to air with an estimated half-life of four to five hours [because of photochemical reactivity] [12,13,14]. Phenol is usually found in the environment [background levels] below 100 parts per billion, although much higher levels have been reported. Occupational exposure to phenol may occur during the production of phenol and phenolic derivatives, during the application of phenolic resins [wood and iron / steel

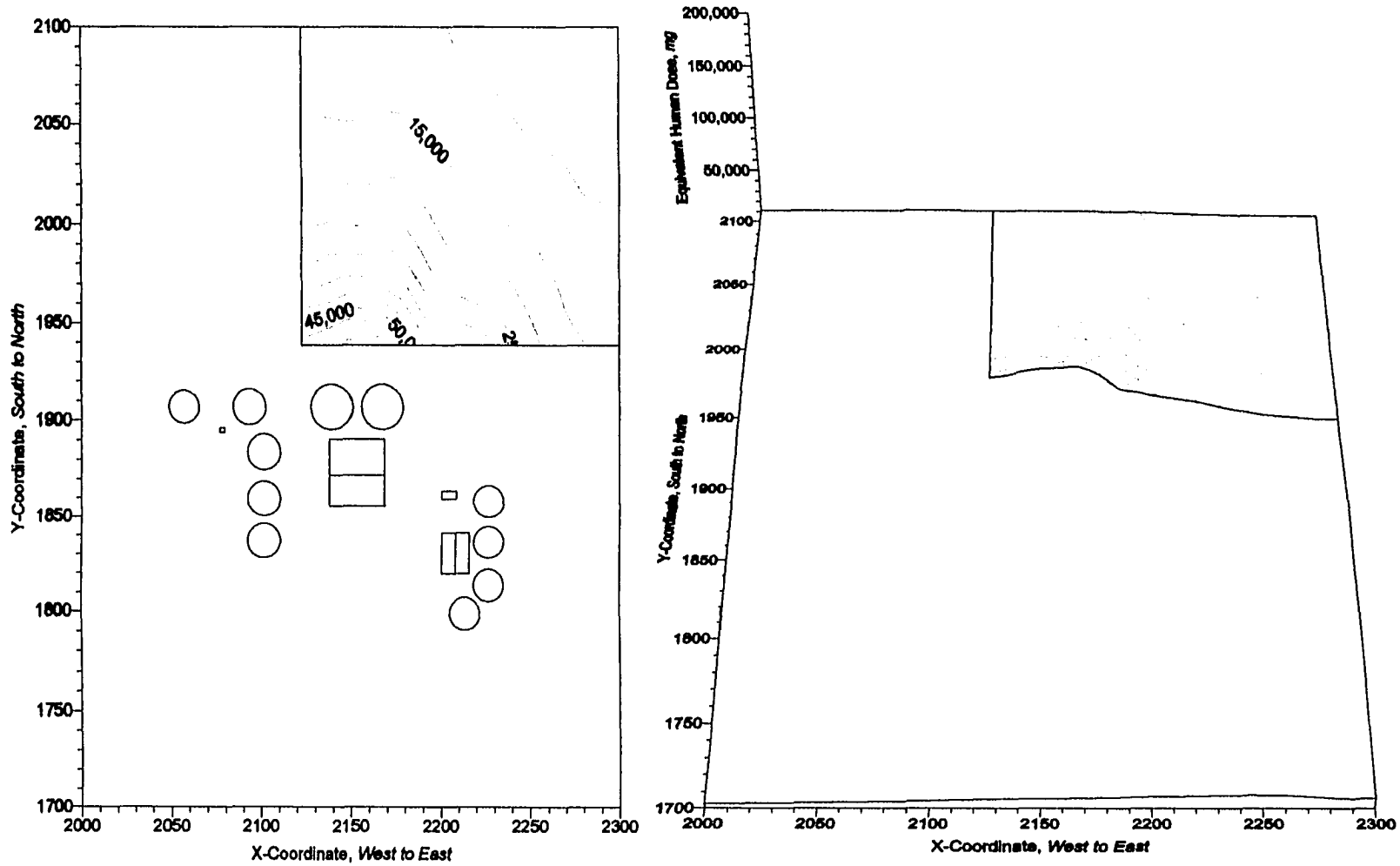

Figure 6.1: Equivalent Methylene Chloride Human Dose for Individuals in the General Population, *mg*

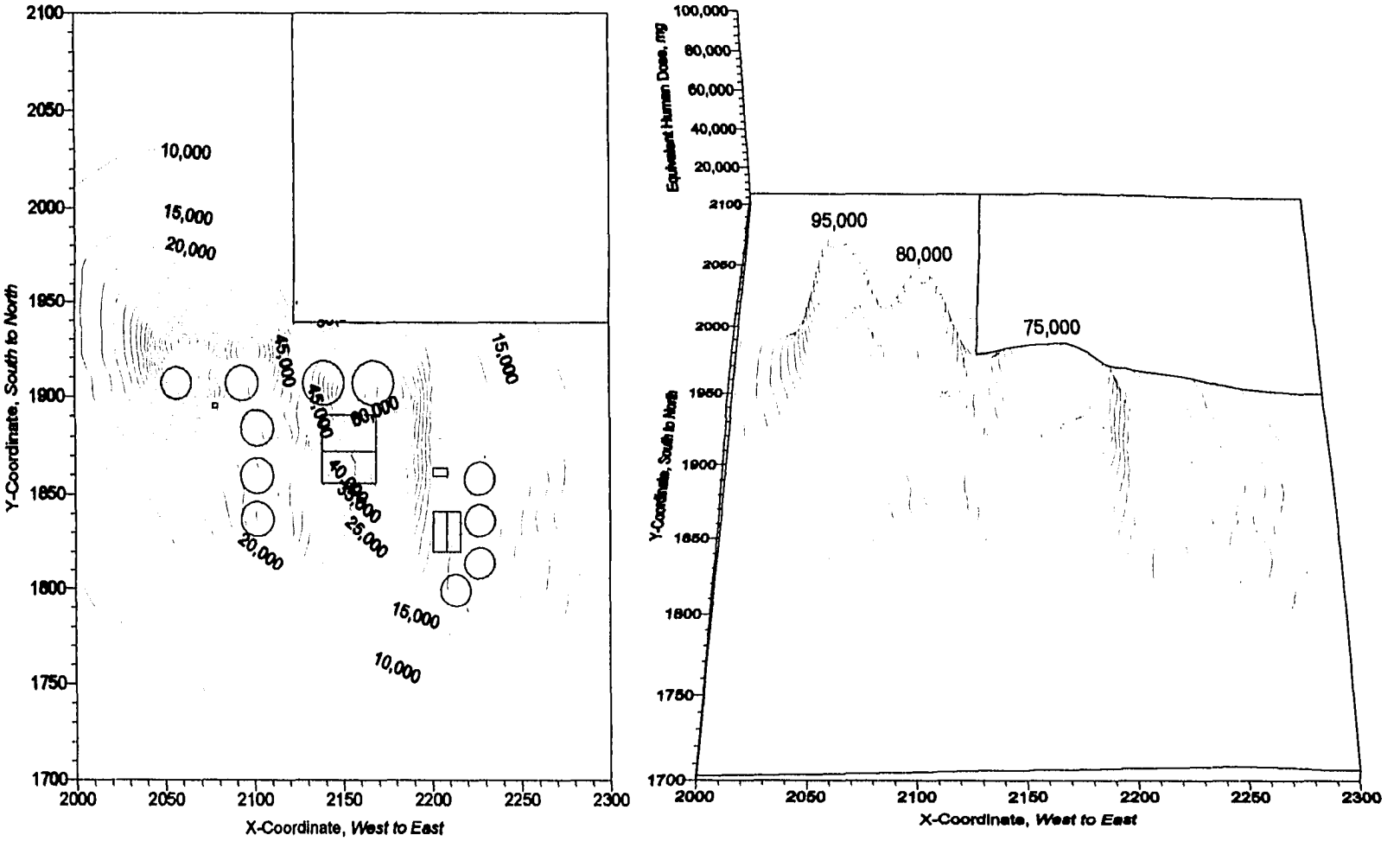

Figure 6.2: Equivalent Methylene Chloride Human Dose for the Individual Worker, *mg*

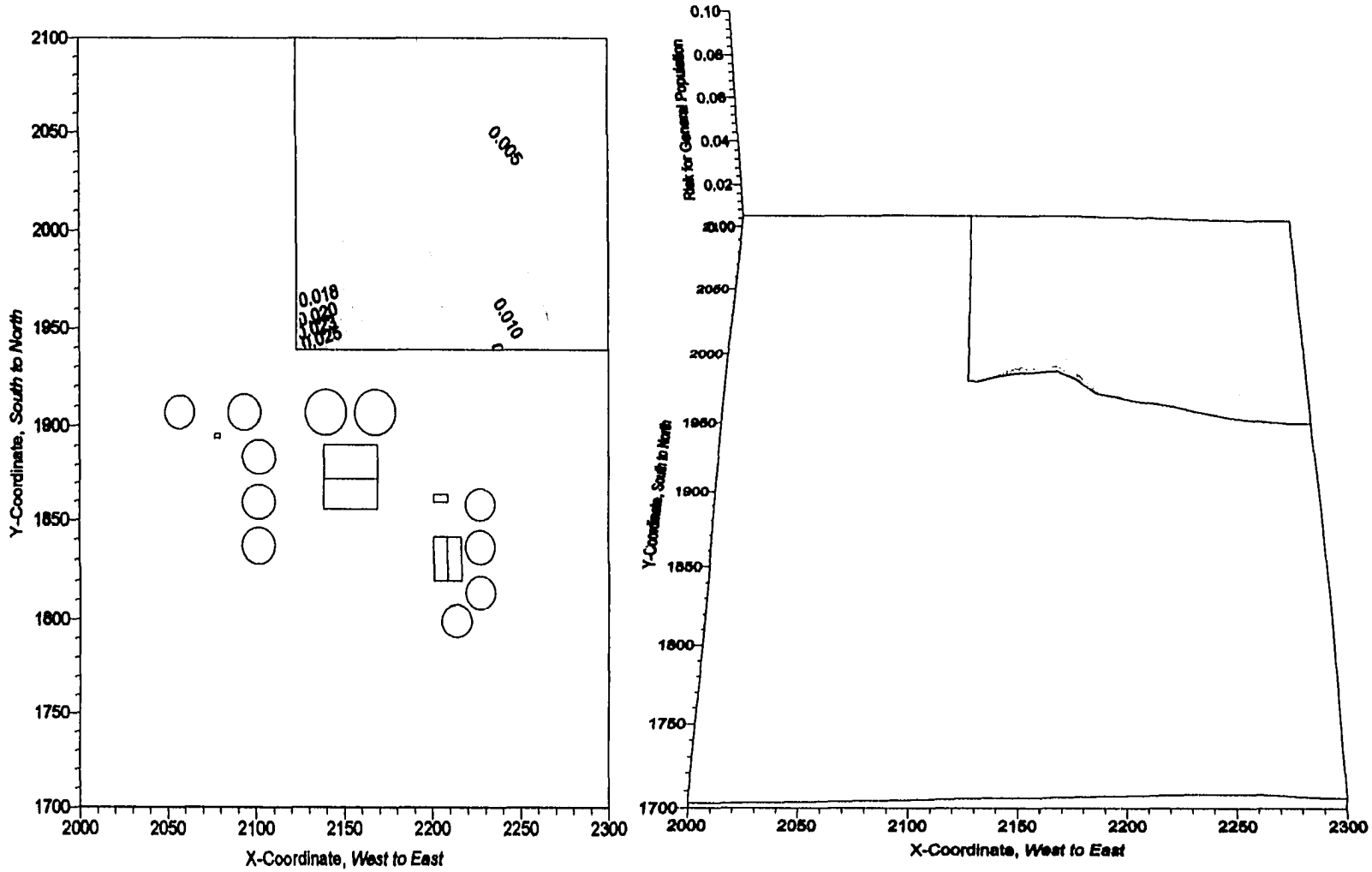

Figure 6.3: Maximum Individual Risk for Methylene Chloride in the General Population

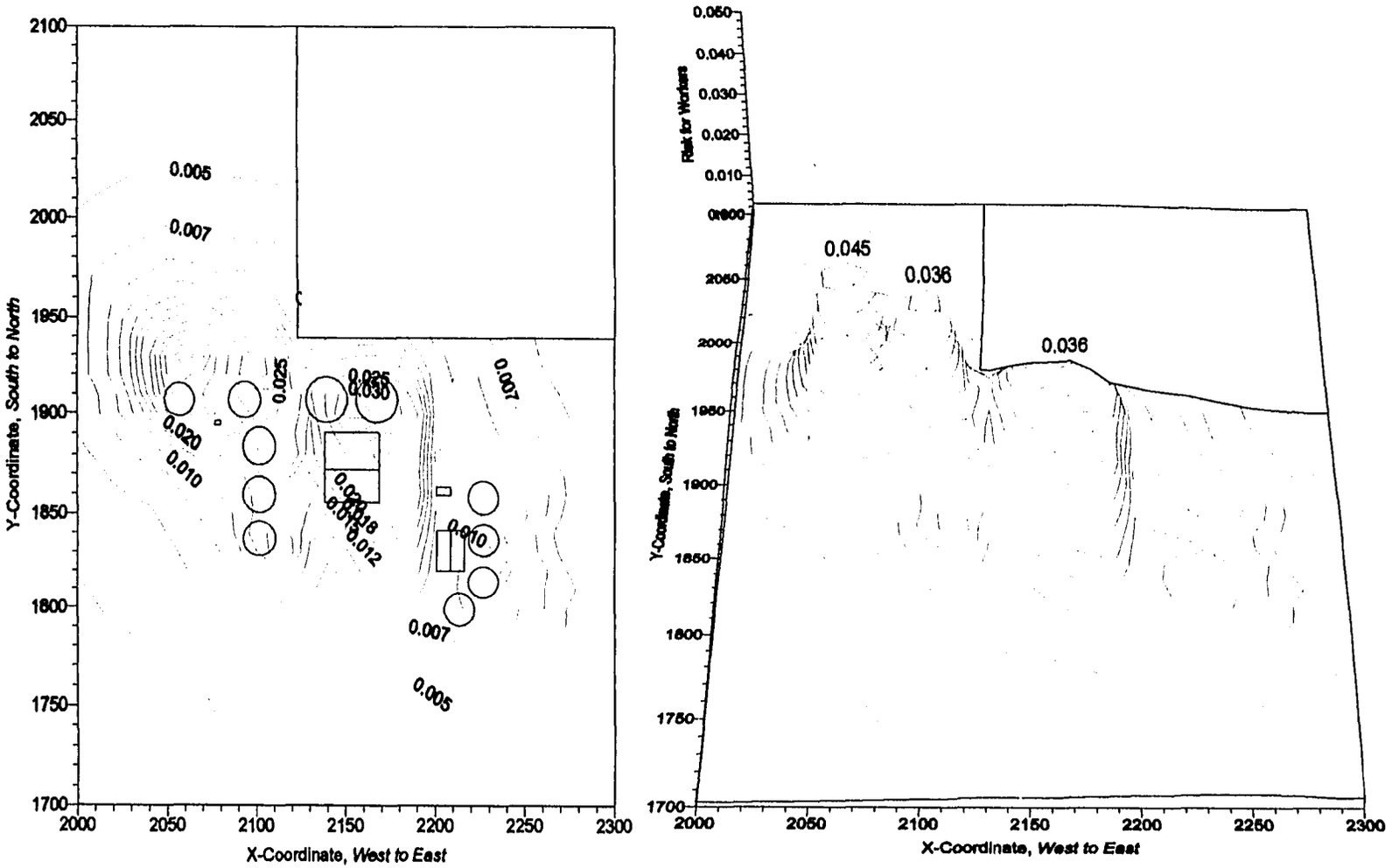

Figure 6.4: Maximum Individual Risk for Methylene Chloride in Workers

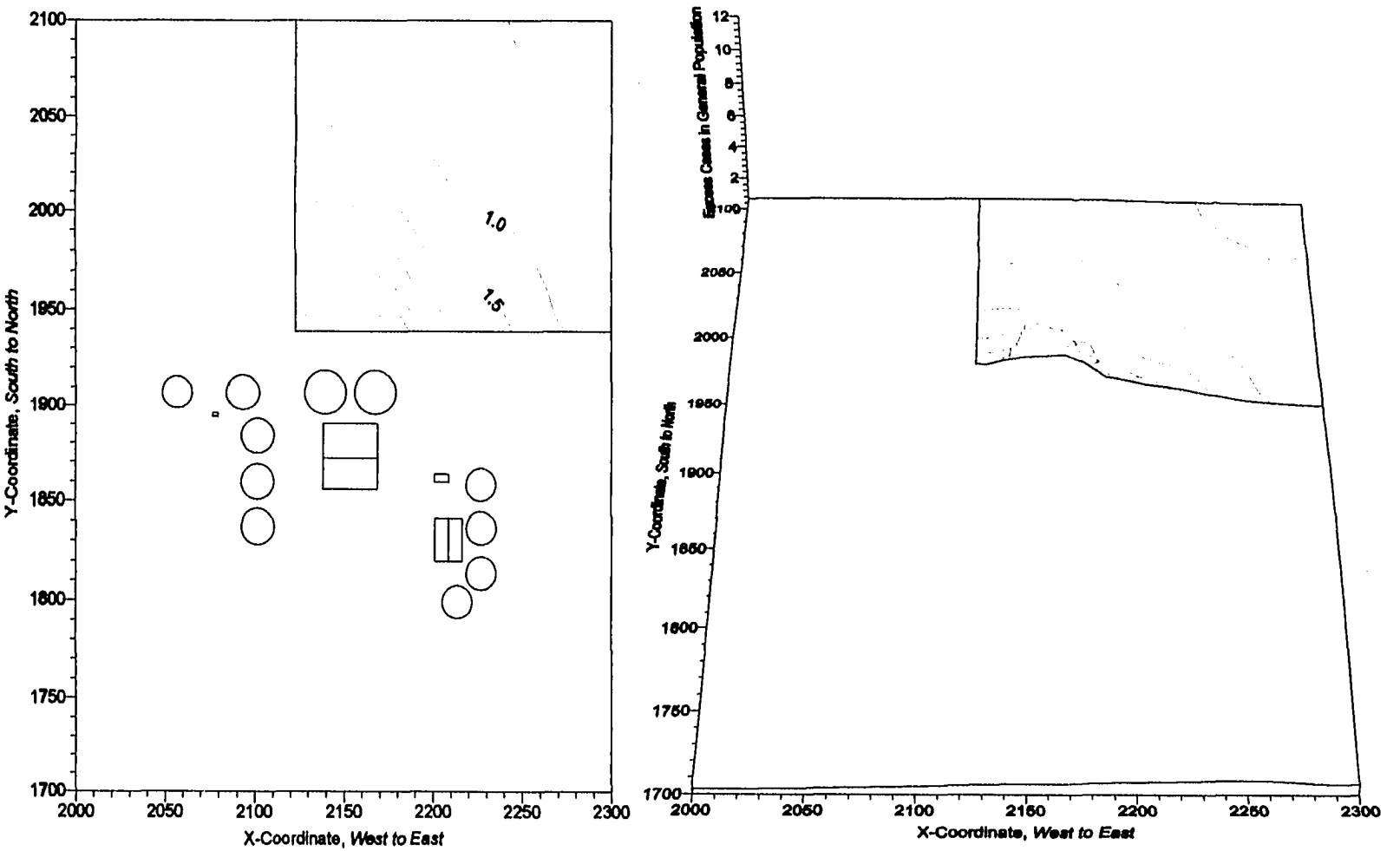

Figure 6.5: Maximum Number of Excess Cases for Methylene Chloride in the General Population

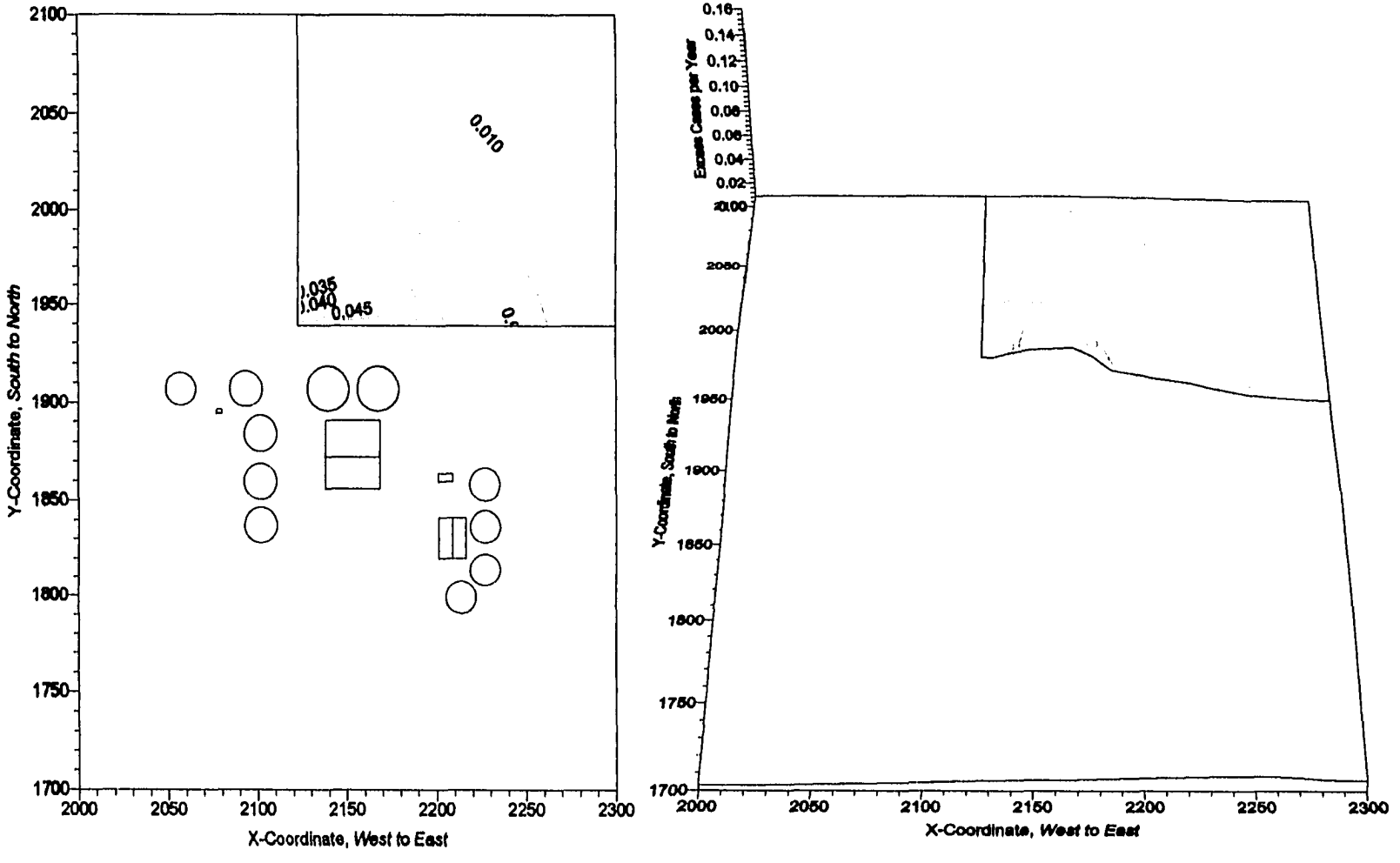

Figure 6.6: Maximum Number of Excess Cases per Year for Methylene Chloride in the General Population

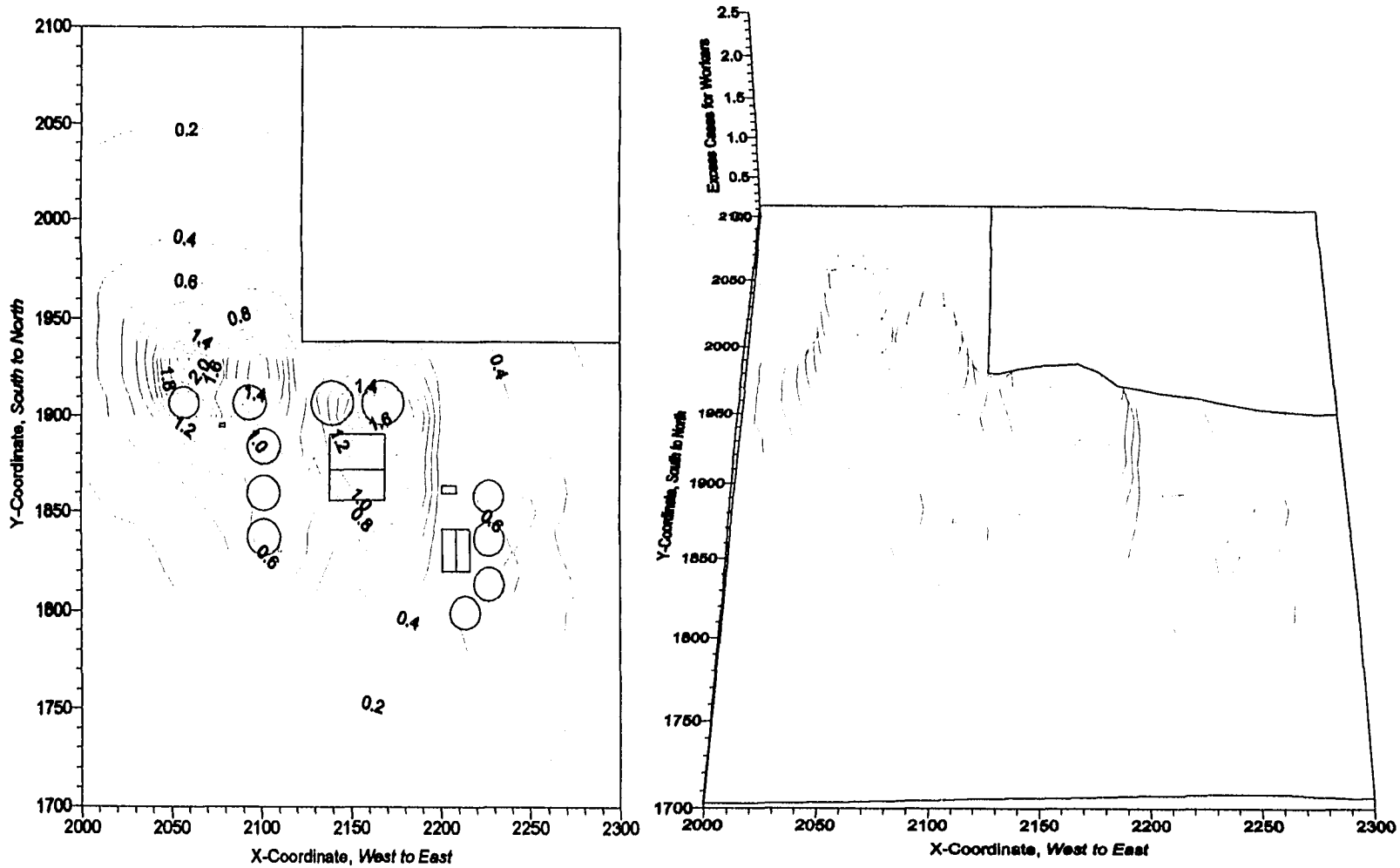

Figure 6.7: Maximum Number of Excess Cases for Methylene Chloride for Workers

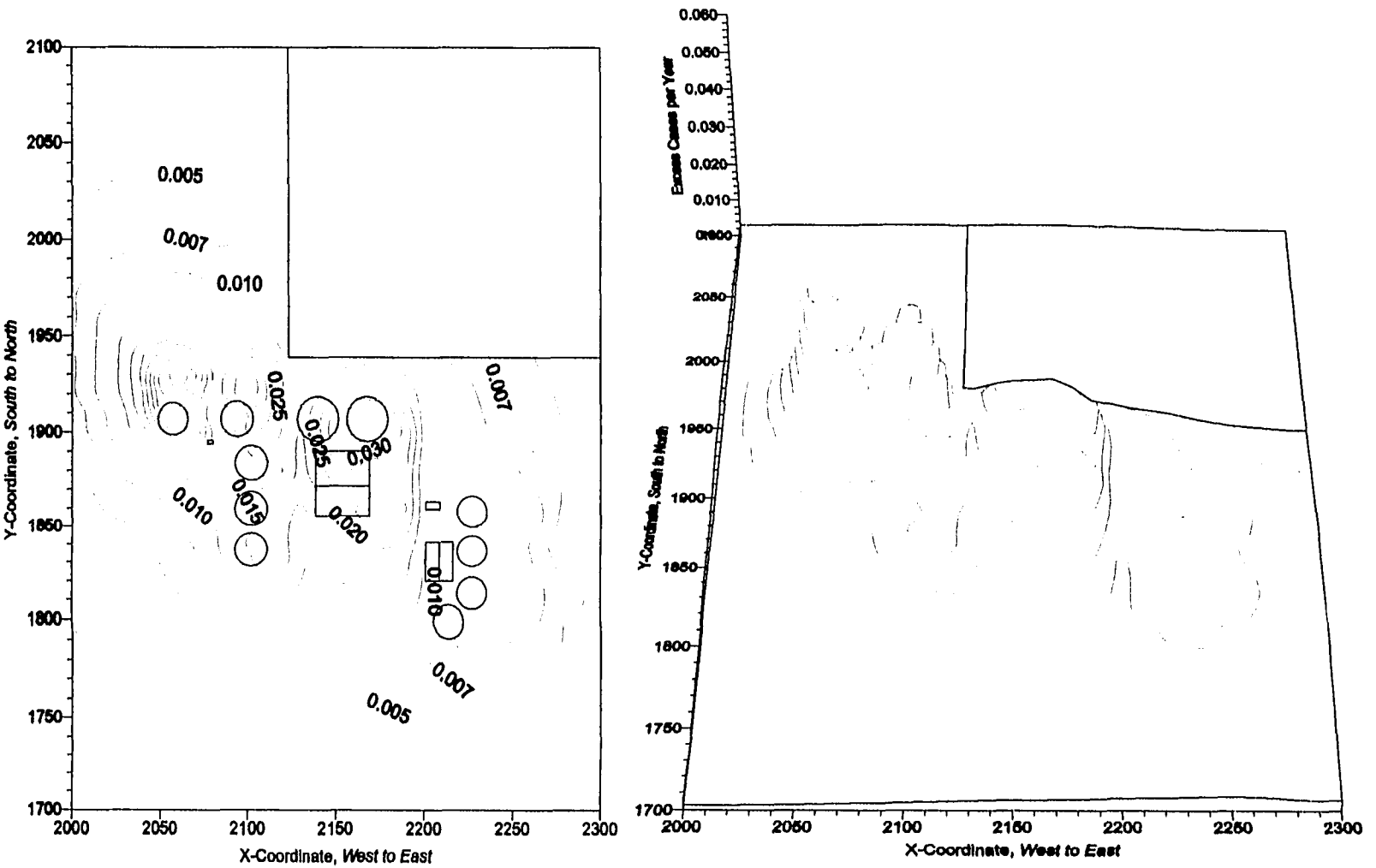

Figure 6.8: Maximum Number of Excess Cases per Year for Methylene Chloride for Workers

industry] and during other industrial activities. For the general population, cigarette smoke and smoked food products [liquid smoke derivatives] are the most important sources of phenol exposure, apart from the industrial exposure via air. Exposure by way of drinking water and inadvertently contaminated food products is assumed to be low, primarily because of the objectable phenolic smell and taste.

Phenol is monohydroxybenzene [C_6H_5OH], molecular weight of 94.11, vapor pressure of 0.357 mm Hg [20°C], and odor threshold of 1.0 part per million. Tinker AFB utilizes phenol in depot maintenance operations as a chemical-depainting agent used to chemically remove coatings from aircraft surfaces and components. In 1993, phenol purchases accounted for almost 16.5 percent of all hazardous materials brought on installation.

RISK ASSESSMENT COMPUTATIONS FOR THE PHENOL EXPOSURES

From documented animal mortality studies, the phenol LOAEL for inhalation exposure conditions is as follows: 100-200 mg per m^3, 5 days per week, 7 hours per day for a median of 5.8 weeks [29 days]. The intake [I] in units of mass or volume of contaminated media per day is determined from tables of standard values of intake as illustrated in Table 6.2 [volumetric flow rate], and converted to units of volume of contaminated air per day, as given. Note that the average air intake for a male guinea pig [hamster] is 0.06 liter per minute [7]. The T is the median time [exposure frequency] of exposure in days. The average male guinea pig body weight [W] in kilograms is tabulated in Table 6.2 [7].

$$I = \left[\frac{0.06\,l}{min}\right]\left[\frac{m^3}{1000\,l}\right]\left[\frac{60\,min}{hour}\right]\left[\frac{7\,hours}{day}\right] = 0.0252\,m^3\ of\ contaminated\ air\ per\ day \qquad 6.28$$

$$T = \left[5\ days/week\right] 5.8\ weeks = 29\ days \qquad 6.29$$

$$W = 0.125\ kg \qquad 6.30$$

Similar to methylene chloride, to account for interspecies and intraspecies variability, the literature recommends use of a safety factor, F. This safety factor is the product of three components F_1, F_2, and F_3. For phenol, there appears to be a wide range of response

sensitivity between species [guinea pigs to rats, monkeys, rabbits, etc.], therefore, F_1 is assumed to be a value of ten [7]. The potential for intraspecies variation in human sensitivity is represented by F_2 with a recommended value of one [since there is no human data regarding human variation in sensitivity. A F_3 safety factor element of ten can be applied if the LOAEL is derived from a short-term study [as in this case]. Thus, the safety factor [F] is 100.

The lifespan [L] is the lifetime of the experimental species [guinea pig] expressed in days. The equivalent human dose [D] can be calculated from the animal study as follows. As shown, the equivalent human dose is a function of the LOAEL, contaminated air intake, exposure duration, weight of the animal species, lifespan of the experimental species, human lifetime [75 years], human body weight [70 kilograms], and a safety factor.

$$L = 2.0\ years\left[365\ days/year\right] = 730\ days \tag{6.30}$$

$$D = 75 \cdot 365 \cdot 70\left[\frac{C \cdot I \cdot T}{W \cdot F \cdot L}\right] \tag{6.31}$$

$$D = 75 years \cdot \left[\frac{365 days}{year}\right] \cdot 70 kg \cdot \left[\frac{\left(100 mg/m^3\right)\left(0.0252 m^3/day\right) 520 days}{\left(0.125 kg\right) 100 \left(730 days\right)}\right] = 275{,}184\ mg \tag{6.32}$$

The risk factor [R] is defined as the excess risk per unit of dose [derived from the lowest available experimental equivalent human dose-response point]. IRIS tabulates the risk factor for specific chemicals and exposure routes [oral, inhalation, etc.]. IRIS documents a risk factor of 1.50E-5, which will be used the following risk assessment calculations.

For determining the maximum dose to an individual in the general population, the maximum phenol concentration is used. From Table 6.1, the maximum phenol exposure to the general population is 40 PPB [0.154 mg per m^3]. This maximum exposure is illustrated in the upper right quadrant of Figure 3.11. For the maximum phenol exposure to the general population, focus on the area surrounding the housing edition. In Figure 3.11 [upper right quadrant], the maximum phenol dose occurs along the fenceline north of the facility at x-y coordinates 2170-1936.

$$C = 40\,PPB\left[\frac{PPM}{1000\,PPB}\right]\left[\frac{mg/m^3}{0.26\,PPM}\right] = 0.154\ mg\ per\ m^3 \quad 6.33$$

$$I = \left[\frac{7.5\,l}{min}\right]\left[\frac{m^3}{1000\,l}\right]\left[\frac{60\,min}{hour}\right]\left[\frac{24\,hour}{day}\right] = 10.8\ m^3\ of\ contaminated\ air\ per\ day \quad 6.34$$

$$T = 75\ years\left[365\ days/year\right] = 27{,}375\ days \quad 6.35$$

$$L = 75\ years\left[365\ days/year\right] = 27{,}375\ days \quad 6.36$$

$$D = C \cdot I \cdot T = 0.154 \cdot 10.8 \cdot 27{,}375 = 45{,}530\ mg \quad 6.37$$

The general population risk group dose of 45,530 mg is well under the equivalent human dose of 275,184 mg from the animal study. The maximum dose calculation for an individual in the general population is repeated for each of the receptor locations and illustrated in Figure 6.9. Note that the interest is the maximum dose to an individual in the general population as exists in the housing community located north of the treatment facility.

In calculating the maximum individual worker dose, refer to the maximum phenol dose as illustrated in Figure 3.11. The maximum phenol dose is approximately 130 PPB and occurs at three x-y Cartesian coordinate locations [2160-1900, 2100-1925, and 2060-1925].

$$C = 130\,PPB\left[\frac{PPM}{1000\,PPB}\right]\left[\frac{mg/m^3}{0.26\,PPM}\right] = 0.50\ mg\ per\ m^3 \quad 6.38$$

$$I = \left[\frac{29\,l}{min}\right]\left[\frac{m^3}{1000\,l}\right]\left[\frac{60\,min}{hour}\right]\left[\frac{8\,hours}{day}\right] = 13.9\ m^3\ of\ contaminated\ air\ per\ day \quad 6.39$$

$$T = \left[5days/week\right]\left[50weeks/year\right] \cdot 45years = 11{,}250days \quad 6.40$$

$$L = 75\ years \cdot \left[365\ days/year\right] = 27{,}375\ days \quad 6.41$$

$$f = \left[T/L\right] = \left[11{,}250/27{,}375\right] = 0.40 \quad 6.42$$

$$D = C \cdot I \cdot T = 0.50 \cdot 13.9 \cdot 11{,}250 = 78{,}188\ mg \quad 6.43$$

The worker risk group dose of 78,188 mg is well under the value of the lowest effective dose of 275,184 mg from the animal study. The maximum dose calculation for an individual worker is repeated for each of the receptor locations and illustrated in Figure 6.10.

Maximum individual excess risk for the general population and

workers are determined as follows. The calculation for the maximum individual excess risk for the general population and worker subgroup is repeated for each of the receptor locations and illustrated in Figures 6.11 and 6.12.

$$P_{e,\,general\,population} = R \cdot D = 1.50E-5 \cdot [45{,}530] = 0.68\ general\ population \qquad 6.44$$

$$P_{e,\,worker} = R \cdot D = 1.50E-5 \cdot [78{,}188] = 1.17\ workers \qquad 6.45$$

An important part of risk analysis is the estimation of the number of cases, which may be generated by a certain scenario of exposure [7]. Risk groups of primary concern are the general population and subsets of the general population such as worker groups. The following expressions are used to quantify the excess cases [EC] and average number of excess cases generated per year for the general population. The computation determining the number of excess cases for the general population is repeated for each of the receptor locations and illustrated in Figure 6.13.

$$EC = R \cdot I \cdot T \sum_{i=1}^{n} [C \cdot N]_i \qquad 6.46$$

$$EC = 1.50E-5 \cdot (10.8) \cdot (365 \cdot 75) \cdot [(0.154)133] = 90.8 \qquad 6.47$$

The average number of excess cases generated per year of exposure can be calculated from the following expression. The computation determining the number of excess cases [phenol] for the general population for a given year is repeated for each of the receptor locations and illustrated in Figure 6.14.

$$\overline{EC} = \left[\frac{excess\ cases}{year}\right] = \left[\frac{excess\ cases}{years\ of\ risk\ group\ exposure}\right] \qquad 6.48$$

$$\overline{EC}_{general\,population} = \left[\frac{90.8}{75}\right] = 1.2\ average\ excess\ cases\ generated\ per\ year \qquad 6.49$$

Use the following expressions to quantify the excess cases [EC] and average number of excess cases generated per year for the worker subgroup, where N is defined as the number within the affected population subgroup. The computation determining the number of excess cases for the worker group is repeated for each of the receptor

locations and illustrated in Figure 6.15 and on a per year basis, Figure 6.16.

$$EC = R \cdot C \cdot I \cdot T \cdot N \qquad 6.50$$

$$EC = 1.50E-5 \cdot (0.50) \cdot 13.9 \cdot (250 days/year) 45 years \cdot 50 = 58.6 \qquad 6.51$$

$$\overline{EC}_{worker} = \left[\frac{58.6}{45}\right] = 1.3 \ average\ excess\ cases\ generated\ per\ year \qquad 6.52$$

The loss of life expectancy [*LLE*] is the life [days or years] lost due to a particular exposure or activity. For example, smoking will shorten the average male smoker's life by 6.2 years. Any risk factor to which a person is exposed can affect that person's life expectancy, the decrease or increase in life expectancy can be calculated using the following [7].

$$LLE = individual\ lifetime\ risk \cdot average\ remaining\ lifetime \qquad 6.53$$

$$LLE = 0.0000150 \cdot (37.5) = 0.00056\ years \qquad 6.54$$

SELECTED REFERENCES

1. Agency for Toxic Substances and Disease Registry, *Health Statistics Review of the Community Adjacent to Tinker Air Force Base, Oklahoma*, U.S. Department of Health and Human Service, January 1998.

2. Phillips, B.A., J. Witherspoon, & J. Taylor, *Risk Management Planning for the Water and Wastewater Treatment Industry: Case Study with Lessons Learned*, Air & Waste Management Association, 8-13 June 1997, Toronto, Canada.

3. Chettri, R., *Risk Management Planning for a Military Industrial Complex*, Air & Waste Management Association, 8-13 June 1997, Toronto, Canada.

4. Narayanan, R., U.S. *EPAs Risk Management Program: Strategies to Comply at DoD Facilities*, Air & Waste Management Association, 8-13 June 1997, Toronto, Canada.

5. Karpovich, R.A., *Data Sources and Software for Performing Off-Site Risk Management Plan Analysis*, Air & Waste Management Association, 14-18 June 1998, San Diego, CA.

6. Molak, V., *Fundamentals of Risk Analysis and Risk Management*, Lewis Publishers, New York, 1996.

7. Hallenbeck, W.H., *Quantitative Risk Assessment for Environmental*

and Occupational Health, Lewis Publishers, Chicago, IL, 1993.

8. U.S. Environmental Protection Agency, Integrated Risk Information System [IRIS], 1996.

9. U.S. Department of Health, Education, and Welfare, National Institute for Occupational Safety and Heath [NIOSH], Current Intelligence Bulletin 46—Methylene Chloride, July 1976.

10. International Programme on Chemical Safety, Environmental Health Criteria 164—Methylene Chloride, 1996.

11. U.S. Department of Health and Human Services, Agency for Toxic Substances and Disease Registry [ATSDR], Methylene Chloride, 1976.

12. International Programme on Chemical Safety, Environmental Health Criteria 161—Phenol, 1994.

13. U.S. Department of Health and Human Services, Agency for Toxic Substances and Disease Registry [ATSDR], Phenol, 1976.

14. U.S. Department of Health, Education, and Welfare, National Institute for Occupational Safety and Heath [NIOSH], Phenol, July 1976.

15. LaPoint, T.W., F.T. Price & E.E. Little, *Environmental Toxicology and Risk Assessment*, ASTM Publication, STP 1262, 1996.

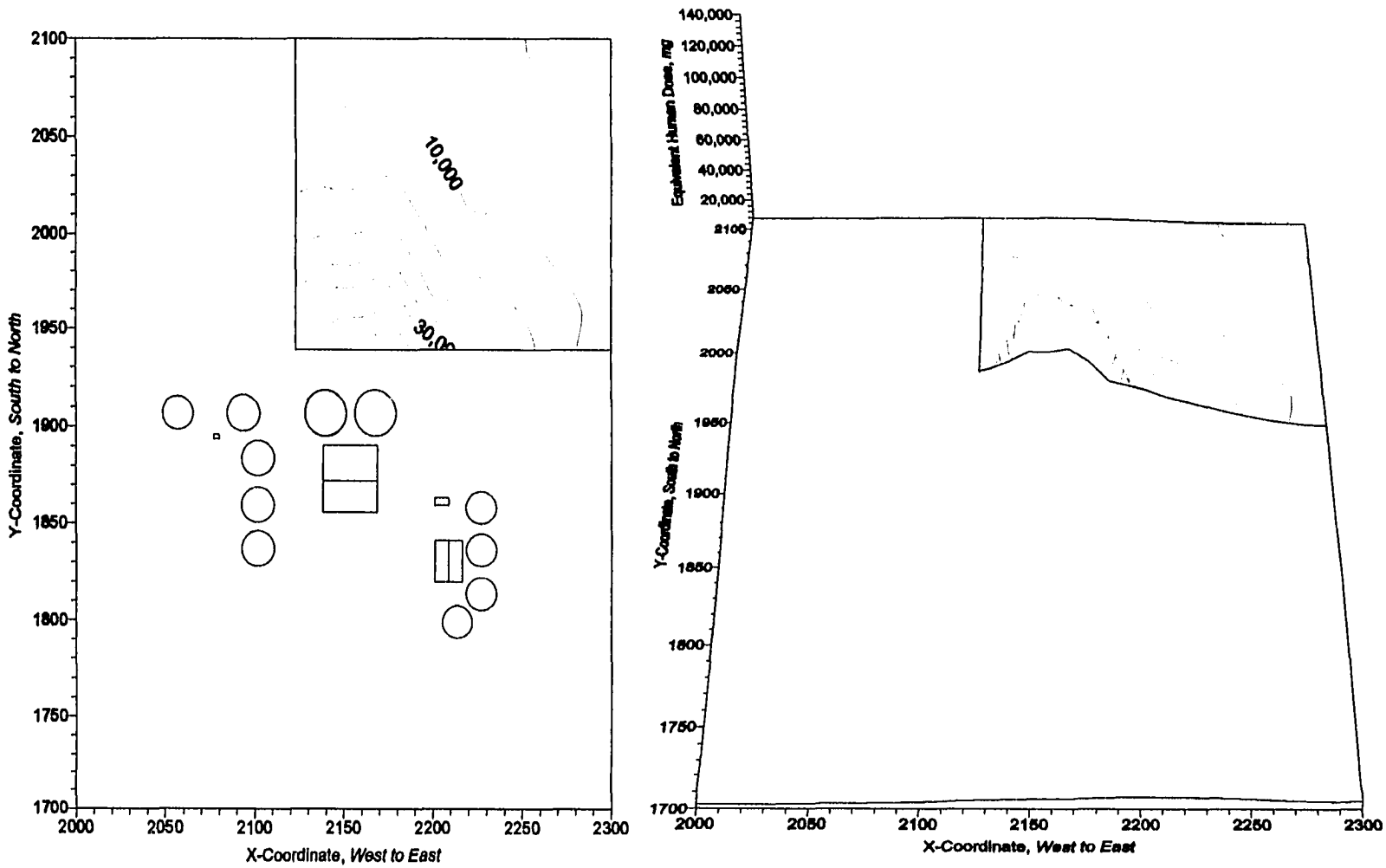

Figure 6.9: Equivalent Phenol Human Dose for Individuals in the General Population, *mg*

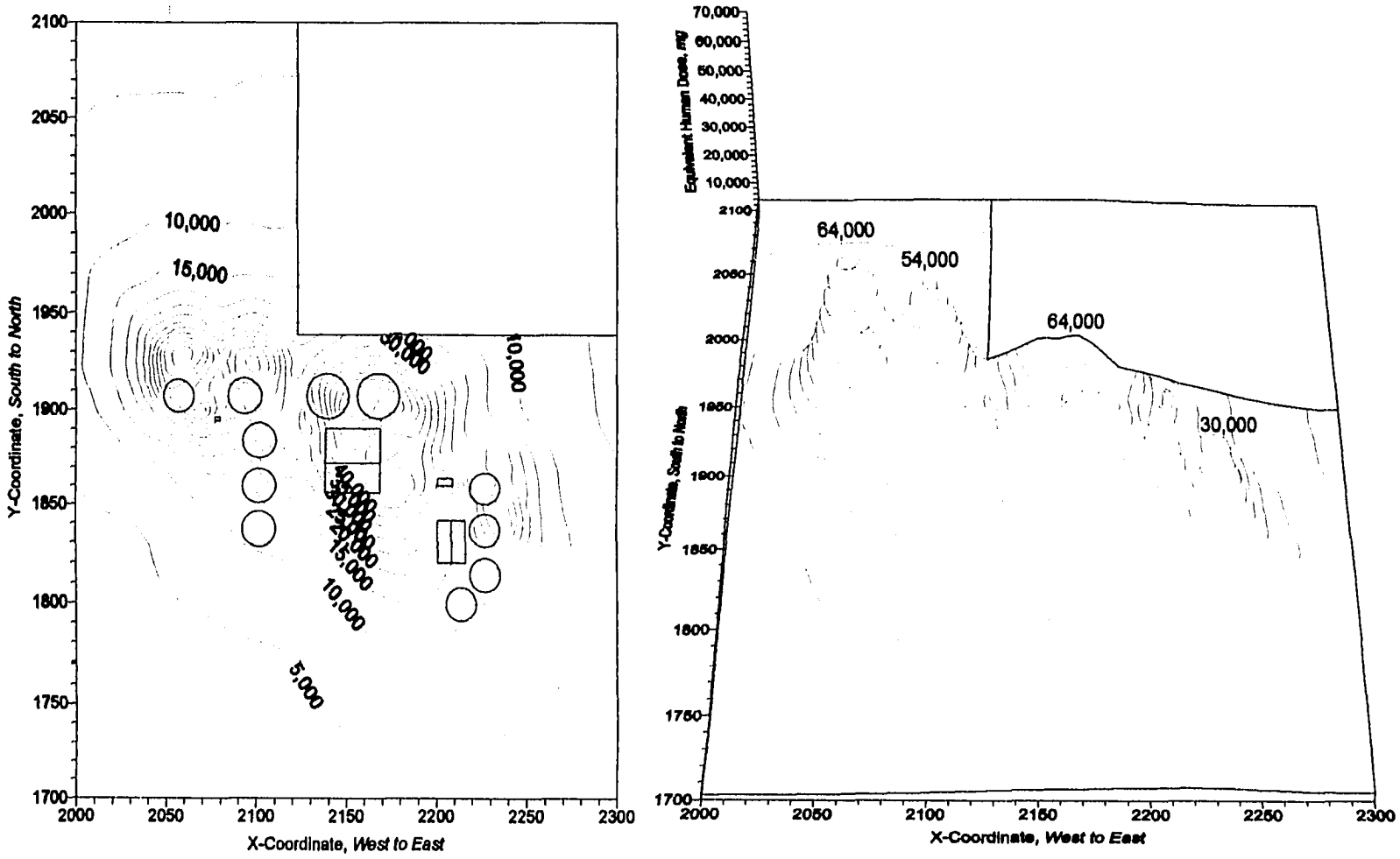

Figure 6.10: Equivalent Phenol Human Dose for the Individual Worker, *mg*

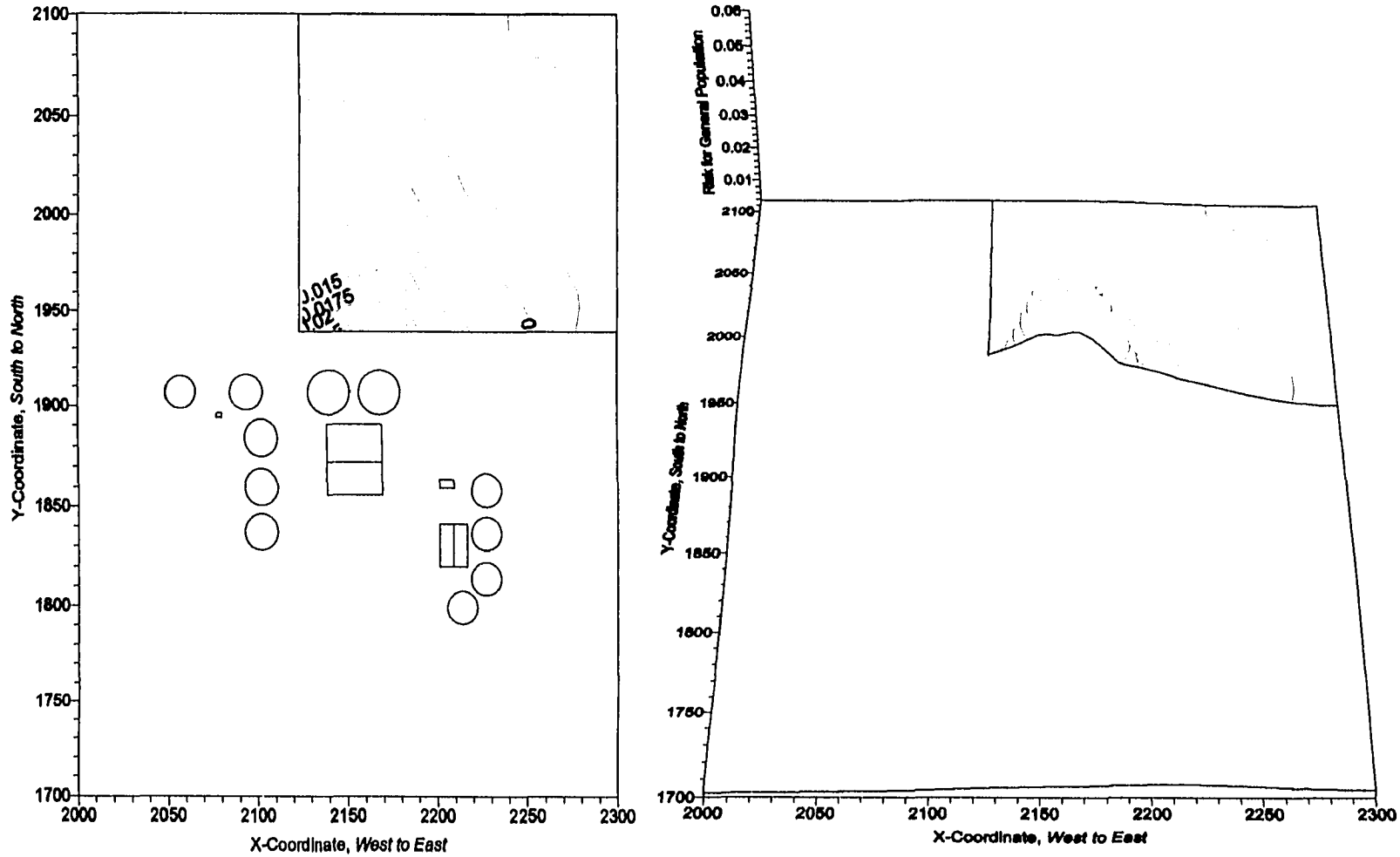

Figure 6.11: Maximum Individual Risk for Phenol in the General Population

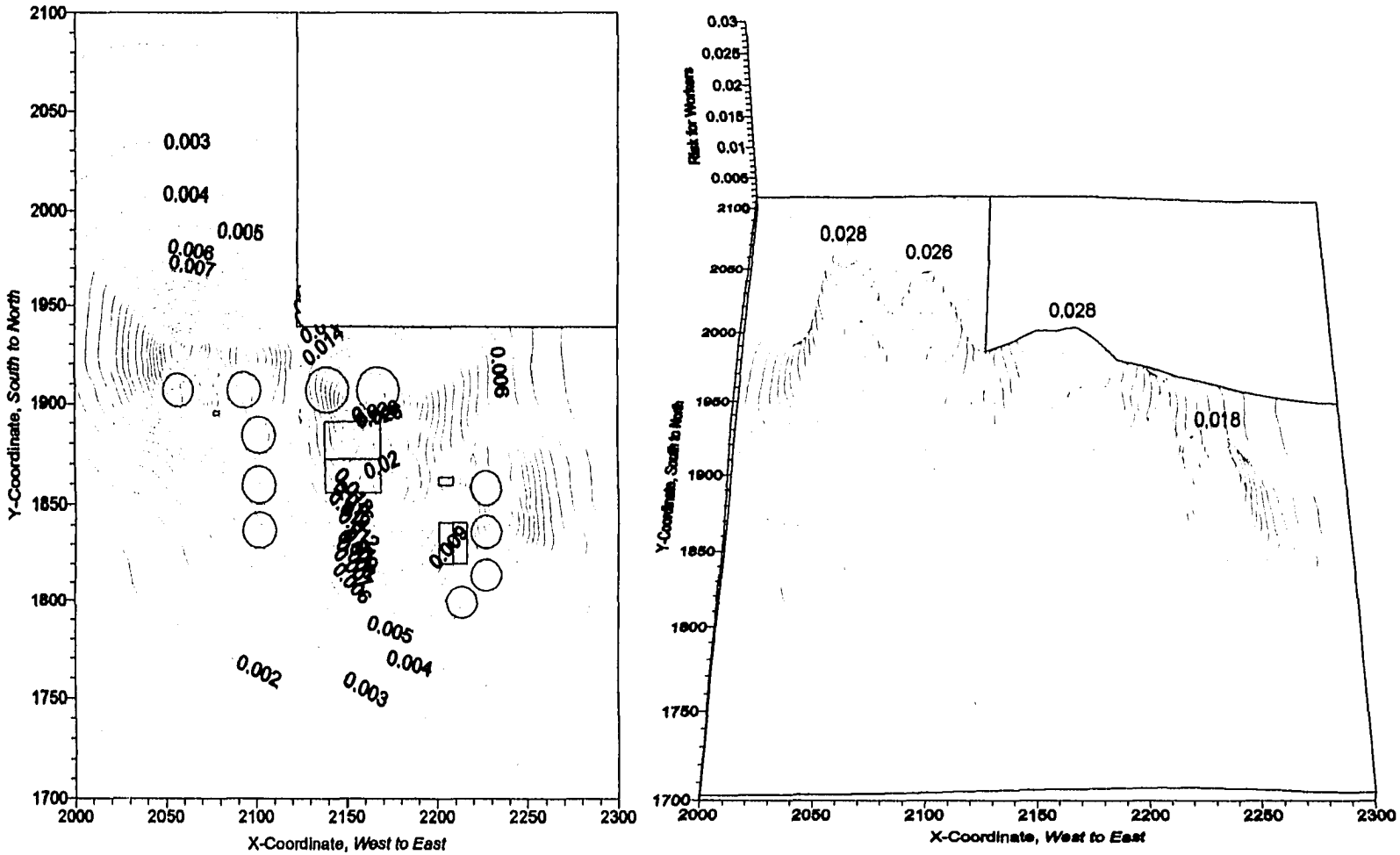

Figure 6.12: Maximum Individual Risk for Phenol In Workers

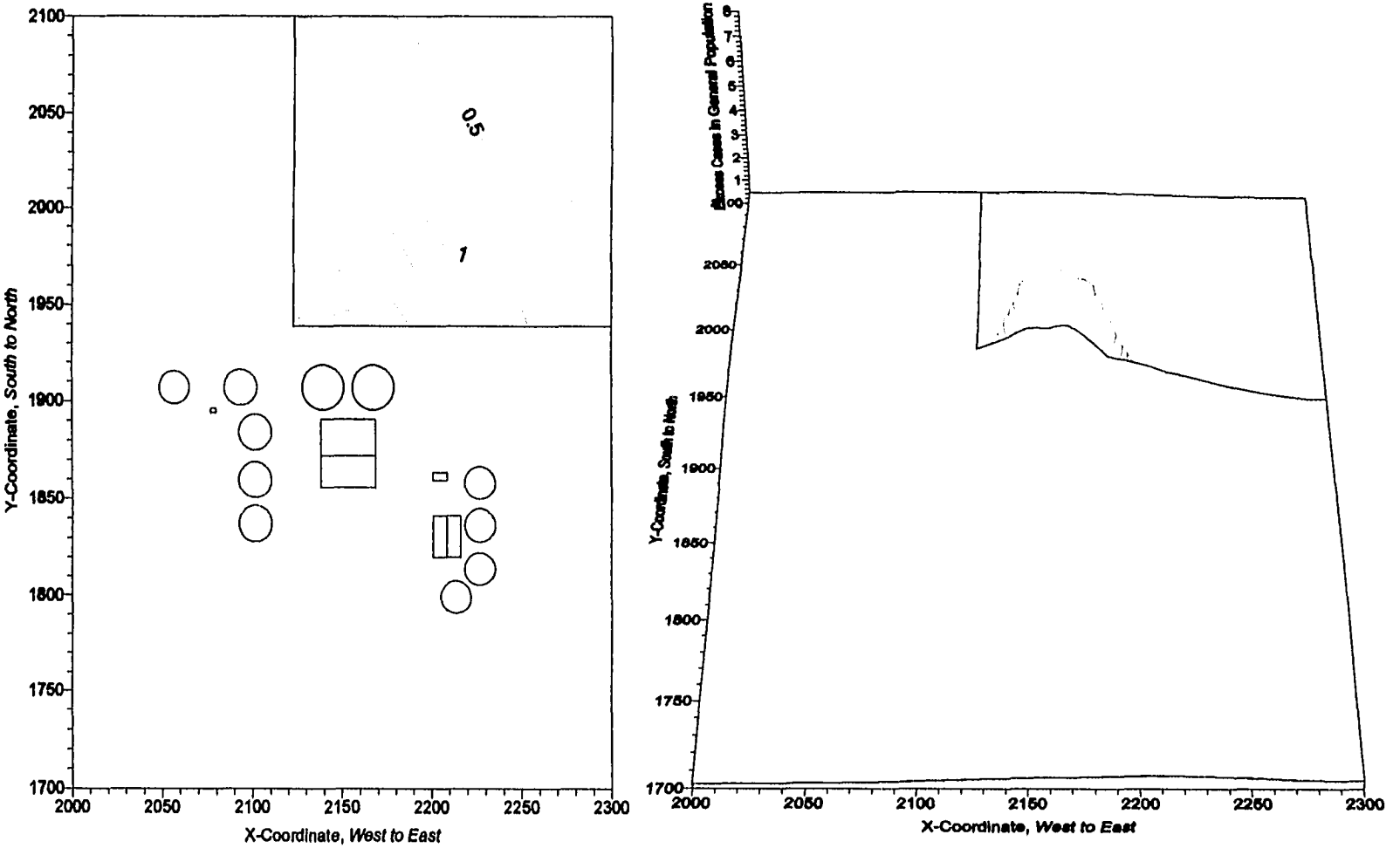

Figure 6.13: Maximum Number of Excess Cases for Phenol in the General Population

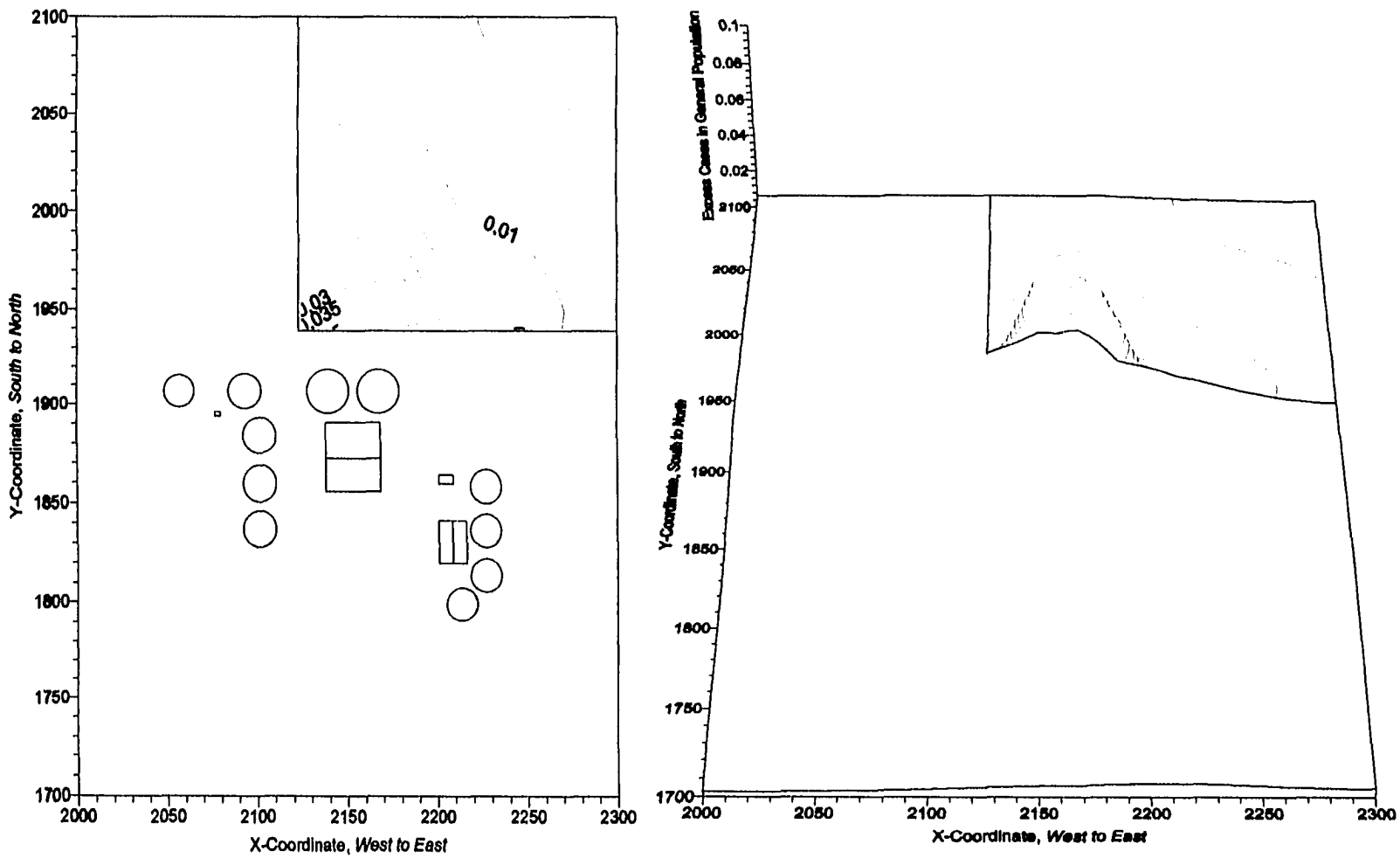

Figure 6.14: Maximum Number of Excess Cases per Year for Phenol in the General Population

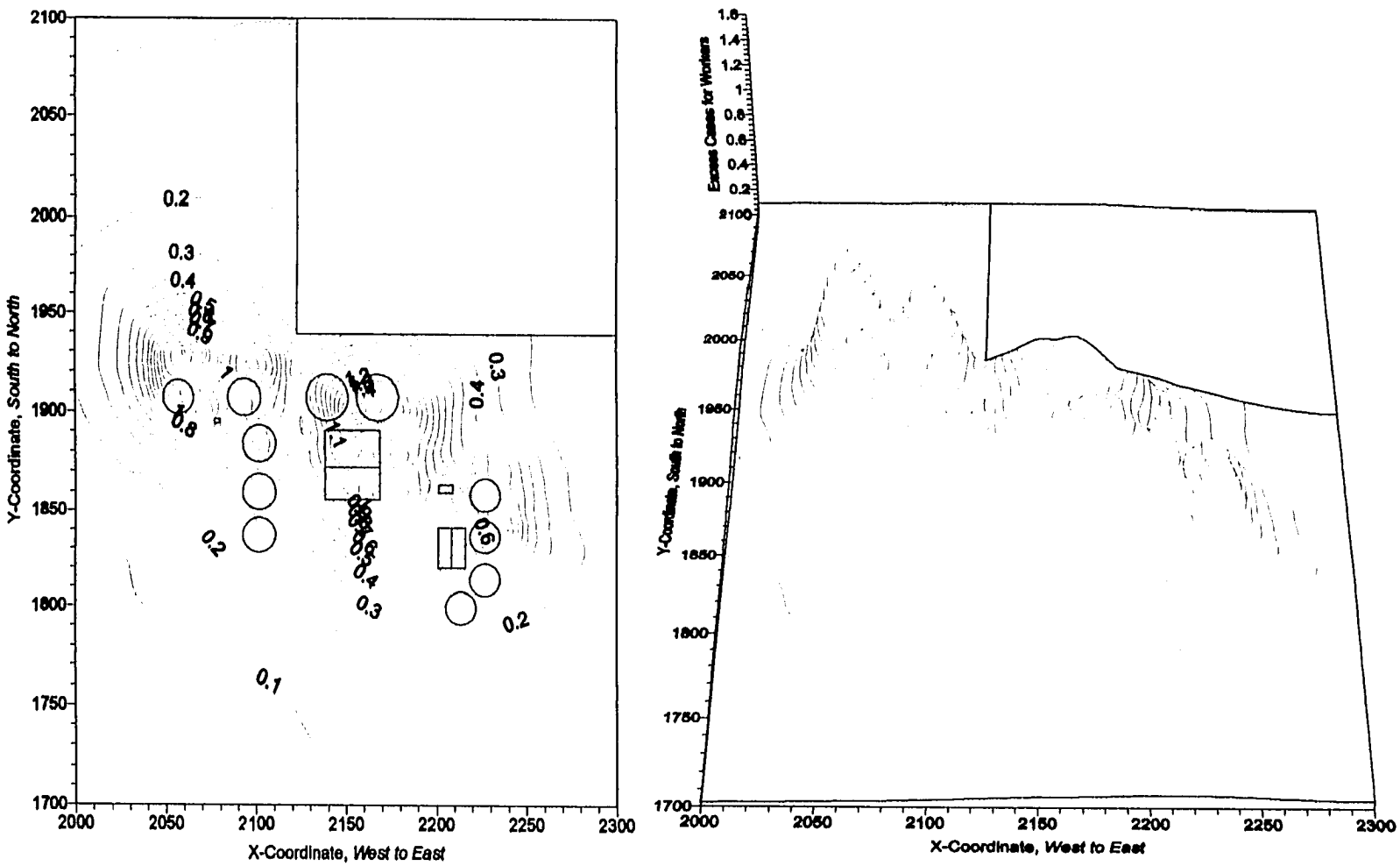

Figure 6.15: Maximum Number of Excess Cases for Phenol for Workers

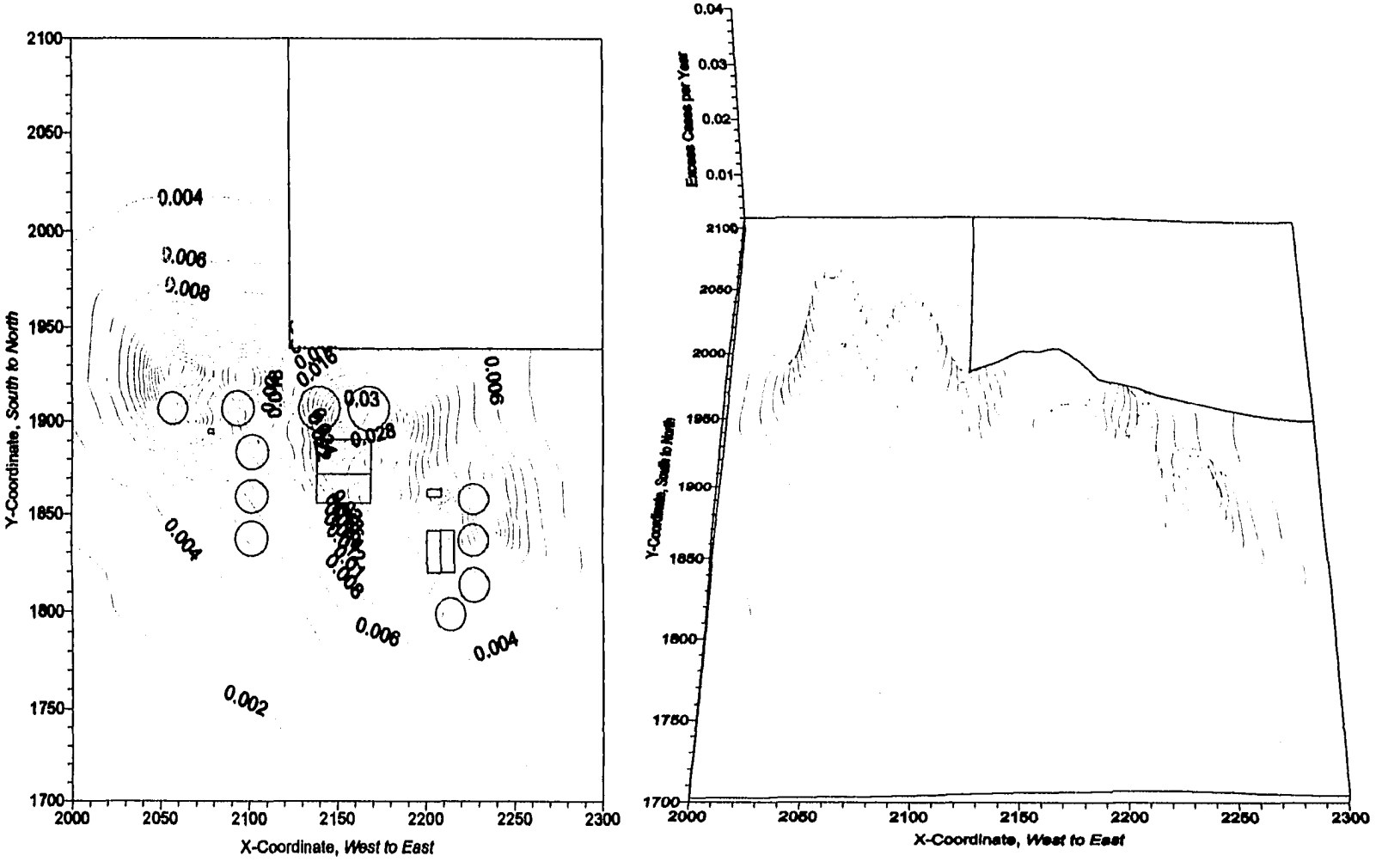

Figure 6.16: Maximum Number of Excess Cases per Year for Phenol for Workers

CHAPTER 7
ADDITIONAL COUPLED MODEL APPLICATIONS

An additional part of this research effort is to demonstrate other potential uses of this coupled model methodology. There are benefits to using a coupled model approach besides generating information for emissions reporting and regulatory compliance determinations relative to maximum ambient air concentrations for phenol and methylene chloride. Additional advantages include the evaluation of on-base process change scenarios and pollution prevention activities regarding the use of phenol and methylene chloride, in addition to evaluating changes in the design or operation of the IWTF for purposes of minimizing atmospheric emissions of phenol and methylene chloride. The literature mentions several references that have used air dispersion models to quantify odors and their impact on the surrounding air quality. This coupled model approach has applicability for air quality management purposes at other similar U.S. Air Force Bases or industrial [private sector] chemical depainting operations.

The Pollution Prevention Act of 1990 required the U.S. EPA Administrator to develop and implement a strategy to promote source reduction. To comply with the requirements established by the U.S. EPA, the Air Force released Air Force Policy Directive 19-4, Policy for the Pollution Prevention Program, Air Force Instruction 19-40, and the Instruction for the Pollution Prevention Program. These documents supply general policy and directive requirements for the Pollution Prevention Program. The Secretary of the Air Force policy memoranda, Air Force Pollution Prevention Program and Air Force Ban on Purchases of ozone depleting compounds [ODCs], give specific objectives for the U.S. Air Force program. The Air Force Instruction [AFI] 19-40 requires each installation to develop a Pollution Prevention Management Program [PPMP] to outline the overall program strategy. The coupled model methodology can help quantify [and track] targeted emissions from industrial wastewater treatment facility sources.

This PPMP fulfills the requirements under the Resource Conservation and Recovery Act [RCRA] for Hazardous Waste Minimization; the DOD Directive 4210.15 for a Hazardous Material Pollution Prevention Plan;

and AFI 19-40 for a Pollution Prevention Management Plan. This program addresses the following areas: the Tinker AFB pollution prevention objectives, goals and strategies; the program structure, organization and responsibilities; program elements and goals; and program reporting and tracking [metrics]. The coupled model can be used to report and track the progress of the program [metrics].

Economics are important but not the only factor that will be considered when selecting a pollution prevention project. Other factors considered are benefits, completion time, technology availability, experience with technology, mission impact, degree of liability, compliance with laws and regulations, and environmental impact. The discussion in Chapter 5 indicated that the coupled model is a cost-effective method of maintaining, recording, and reporting compliance with environmental regulatory constraints.

The coupled model methodology can be used to achieve the goals and objectives of the Pollution Prevention Program strategy. The Pollution Prevention Program strategy is based on the following: preliminary assessment of projects to reduce or eliminate the amount or toxicity of waste disposed; define pollution prevention options [propose, screen and prioritize pollution prevention project options]; perform feasibility study [technical, environmental and economical feasibility studies]; write assessment report; implement pollution prevention projects; and measure progress. The coupled model approach can be used in each of the program elements.

The coupled model approach can be used to satisfy the Comprehensive Environmental Response, Compensation and Liability Act [CERCLA], which requires hazardous waste generators to evaluate and document their procedures for controlling the environmental impact of their operations. However, the Pollution Prevention Act goes beyond wastes designated as hazardous. It encourages the maximum possible elimination of wastes of all types. It emphasizes that the preferred method of preventing pollution is to reduce at the source the volume of waste generated and that reuse [closed loop recycling] should be performed whenever possible. In this way, it is fundamentally different from off-site recycling, treatment, and disposal and is meant to reduce the need for these measures.

The coupled model approach may be of value in meeting additional environmental requirements, *i.e.*, EPCRA is composed of five basic parts: emergency notification and planning [Sections 301 to 303], emergency release notification [Section 304], Community Right-to-Know or list of material safety data sheets [Section 311], annual chemical inventory [Section 312] and annual toxic chemical release [Section 313]. Sections 301 through 312 are intended to provide neighboring communities with all the information they need about hazardous chemicals on the federal facility for proper emergency response and planning. Section 313 requires the only report that is submitted to the U.S. EPA. The intent is to notify surrounding communities of any potential hazards.

Another application for the coupled model methodology includes the EPCRA Section 313 report, which provides a nationwide view of total annual releases to the environment, and off-site transfers, of certain toxic chemicals. The toxic release inventory [TRI] report or Form R was initially intended to inform the public and government officials of routine releases to the environment of toxic chemicals. With passage of the Pollution Prevention Act of 1990, the Form R was expanded to include pollution prevention and waste minimization progress as well. Completion of a Form R requires detailed transaction records, utilization and release data [all which involve the coupled model].

The chemical monitoring required under Executive Order [EO] 12856 tracks substance use throughout all operations [including industrial wastewater treatment plants] at a facility [including what is vented, evaporated, and spilled]. All DOD facilities are required to provide documentation satisfying this Executive Order. The coupled model could be used in this activity to track compliance with goals via metrics.

The latest application for the coupled model methodology is to satisfy the U.S. EPA NESHAP for publicly owned treatment works [40 CFR Part 63, National Emission Standards for Hazardous Air Pollutants: Publicly Owned Treatment Works]. The POTW NESHAP took affect 30 October 1999, and requires all POTWs [including IWTF] to quantify the emissions from each of the process units and report annually to the federal, state, and local regulating agencies. This action promulgates national emission standards for hazardous air pollutants [NESHAP] for new and existing publicly owned treatment works [POTW]. The primary hazardous

air pollutants [HAPs] emitted by these sources include xylenes, methylene chloride, phenol, toluene, ethyl benzene, chloroform, tetrachloroethylene, benzene, and naphthalene. Each of these HAPs can cause adverse health effects provided sufficient exposure. With this final rule, the U.S. EPA is requiring air pollution controls on a new or reconstructed treatment plant at a POTW that is a major source of HAP. The standards also require that new and existing POTW treating regulated waste streams [*i.e.*, wastewaters produced by industrial, commercial, and domestic sources] from an industrial user, for the purpose of allowing that industrial user to comply with another NESHAP, meet the treatment and control requirements of the other relevant NESHAP.

A potential future use for the couple model approach is in achieving International Standards Organization [ISO] 14000 certification. The ISO 14000 concept was developed out of a concern to achieve and demonstrate sound environmental performance by controlling the impact of their activities, products and services on the environment, taking into account their environmental policy and objectives. Many organizations have undertaken environmental *reviews* or *audits* to assess their environmental performance. For these audits to be effective, they need to be conducted within a structured management system and integrated with overall management activity. International Standards covering environmental management are intended to provide organizations with the elements of an effective environmental management system, which can be integrated with other management requirements, to assist organizations to achieve environmental and economic goals. This International Standard specifies the requirements of such an environmental management system. It has been written to be applicable to all types and sizes of organizations and to accommodate diverse geographical, cultural, and social conditions. A system of this kind enables an organization to establish, and assess the effectiveness of, procedures to set an environmental policy and objectives, achieve conformance with them, and demonstrate such conformance to others. The overall aim of the International Standard is to support environmental protection and prevention of pollution in balance with socio-economic needs. The coupled model can be used to track performance and conformance with ISO 14000 standards for industrial wastewater treatment facilities. The

model could also be used as part of the auditing process to measure and forecast current and future environmental compliance.

The coupled model approach can be used in the development of environmental impact assessments [EIAs]. An environmental impact assessment is defined as the systematic identification and evaluation of potential impacts of proposed projects, plans, programs, or legislative actions relative to the physical-chemical, biological, cultural, and socio-economic components of the total environment. The primary objective of the EIA process is to encourage the consideration of the environment in planning and decision making and to ultimately arrive at actions which are more environmentally compatible. The coupled model approach could improve the environmental inventory [*i.e.*, description of the environment in an area where a particular action is being considered]. The coupled model could be incorporated to improve the decision making process.

In summary, the coupled model could be used as a tool to develop realistic goals for pollution prevention, waste reduction, and hazardous waste minimization programs. The model could be used to assist in prioritizing projects [*i.e.*, pollution prevention, waste reduction, hazardous waste minimization, etc.]. The model could be used to develop, evaluate, and investigate pollution prevention techniques, technologies, and methodologies. Engineers could identify and minimize future threats to human health and environment. It could be used to develop, evaluate, investigate, and prioritize control technologies. There have been numerous examples of how the coupled model has been used to demonstrate and measure environmental compliance with current and future environmental laws. The model has been used to predict compliance with future environmental regulatory constraints [*i.e.*, POTW NESHAP]. The model could be used to identify, rank, and prioritize better business practices and opportunities [*i.e.*, determine mission impact, degree of liability, and environmental impacts]. The model has been used to identify and prioritize process improvements; develop short, intermediate, and long-term pollution prevention alternatives. The regulating agencies could potentially use the coupled model approach to identify and prioritize lists of chemicals targeted for future environmental regulatory compliance and develop regulatory policy mandates.

CHAPTER 8
SUMMARY AND CONCLUSIONS

This research effort illustrated that the coupling of an appropriate source emission model and an atmospheric dispersion model represents a cost-effective and environmentally responsible approach for meeting prediction and regulatory reporting requirements, as well as problem analysis and pollution prevention needs, associated with emissions of two chemical depainting agents [phenol and methylene chloride] from a liquid industrial wastewater treatment facility. This effort was completed at the industrial wastewater treatment facility at Tinker Air Force Base in Oklahoma City, Oklahoma. The research was based upon the comparison of three strategies for meeting air quality management requirements: (1) use of the coupled model; (2) use of air quality monitoring data collected via air sampling and analysis [referred to herein as *periodic canister monitoring*]; and (3) use of air quality data generated by open-path monitoring via the use of Fourier Transform InfraRed Spectroscopy [FTIR]. The following activities were satisfied with respect to this research effort:

(1) Development of the coupled model via review of source emissions models for liquid holding tanks and surface impoundments and selection of an appropriate model for phenol and methylene chloride emissions from a liquid IWTP; and via review of atmospheric dispersion models and selection of an appropriate model for phenol and methylene chloride dispersion from a liquid IWTF. The coupled model involved using the source emission model to generate emissions data for use in the dispersion model.

(2) Use of the coupled model in the predictive mode; that is, to develop geographically-based profiles of the ground-level concentration of phenol and methylene chloride in the nearby environment [at specific receptor locations within the impact region] of the IWTF under differing meteorological conditions [1984-1993], on-base chemical usage practices, and IWTF operating scenarios.

(3) Validation of the predictive accuracy of the coupled model via (a)

comparisons and statistical testing of receptor location predictions with actual air quality data from *periodic canister monitoring*, (b) comparisons and statistical testing of predictions along the remote optical open path monitoring line with measured concentrations with FTIR; and (c) comparisons and statistical testing of pertinent canister monitoring data with FTIR monitoring results.

(4) Demonstration of the potential uses, advantages, and limitations of the three strategies relative to: (a) the conduction of site specific health risk assessments; (b) generation of information for emissions reporting and regulatory compliance determinations relative to maximum ambient air concentrations [MAAC] for phenol and methylene chloride; (c) evaluation of on-base process change scenarios and pollution prevention activities regarding the use of phenol and methylene chloride; (d) evaluation of changes in the design or operation of the IWTF for purposes of minimizing atmospheric emissions of phenol and methylene chloride; and (e) their applicability for air quality management purposes at other similar U.S. Air Force bases or industrial [private sector] chemical depainting operations.

CONCLUSIONS

1. Coupling of the WATER8 source emission model and ISC-ST3 atmospheric air dispersion model represents a cost-effective and environmentally responsible approach for meeting prediction and regulatory reporting requirements.

2. Coupling of the WATER8 source emission model and ISC-ST3 atmospheric air dispersion model represents a cost-effective and environmentally responsible approach for problem analysis and pollution prevention needs associated with phenol and methylene chloride emissions from a liquid industrial wastewater treatment facility.

3. The coupled model can be used to develop geographically-based profiles of the ground-level concentration of phenol and methylene chloride at specific receptor locations within the impact region of the industrial wastewater treatment facility under differing meteorological conditions, on-base chemical usage practices, and IWTF operating

scenarios.

4. The coupled model can be used to evaluate changes in the design or operation of the industrial wastewater treatment facility for purposes of minimizing atmospheric emissions of phenol and methylene chloride [*i.e.*, source reduction].

5. The coupled model approach can have direct applicability for air quality management purposes at other similar U.S. Air Force Bases, DOD installations, and industrial [private sector] chemical depainting operations.

6. The coupled model can be used to provide situational information on individual chemical exposures to conduct a site-specific health risk assessment for chemical depainting agents [phenol and methylene chloride] at an industrial wastewater treatment facility.

7. The coupled model methodology is effective for generating information for emissions reporting and environmental regulatory compliance determination relative to maximum ambient air concentrations [MAAC] for both volatile and semi-volatile organic compounds [phenol and methylene chloride].

8. The coupled model approach is an effective methodology for quantifying the maximum ambient air concentrations [MAAC] at any impact region boundary line [facility perimeter] and determining environmental regulatory compliance.

9. The coupled model approach is an adequate methodology for modeling both volatile and semi-volatile organic compounds from an industrial wastewater treatment facility.

10. The WATER8 flexible building block approach satisfactorily simulates common industrial wastewater collection / treatment processes.

11. The major removal mechanism for the Tinker AFB industrial wastewater treatment facility processes appears to be driven by volatilization losses. As illustrated, the biological degradation mechanism is primarily limited to the biological reactor.

12. Other potential wastewater treatment mechanisms [*i.e.*, adsorption, migration, runoff, chemical degradation, hydrolysis, oxidation, and hydroxyl radical reaction] contribute little to the treatment of Tinker AFB industrial wastewater.

13. The WATER8 air emission model represents a cost-effective and environmentally responsible method of generating emissions data from an industrial wastewater treatment facility for use in an EPA-approved atmospheric dispersion model.

14. For the more-volatile methylene chloride, the volatilization mechanism is the primary removal pathway with the majority of the releases discharged in the primary treatment phase [*i.e.*, primary clarifier, oil-water separators, equalization basins, and storage tanks]. As observed, little biological digestion of methylene chloride occurs in the bioreactor.

15. For the less-volatile phenol, the driving mechanism is biological digestion occurring late in the treatment process [bioreactor] with very little volatilized to the ambient air environment.

16. The more volatile the component, the more critical the Henrys Law constant is to the coupled model methodology.

17. For methylene chloride, the coupled model was able to predict the field canister data within a 99.9 percent level of confidence at all thirteen receptors.

18. For phenol, the coupled model was able to predict the field canister data within a 99.9 percent level of confidence at all thirteen receptors.

19. For this application, the OP-FTIR system was shown to be an ineffective and cost-prohibitive method of remote optical open path monitoring of phenol and methylene chloride emissions [environmental monitoring] along the facility perimeter of an industrial wastewater treatment facility.

20. The OP-FTIR installed at Tinker AFB provided a reliability-of-

operation of less than three months over five years of operation. Of that three-months of data, more than 36 percent of the collected information is considered unusable.

21. Phenol and methylene chloride concentrations predicted by the OP-FTIR [along three optical paths] are one-to-three orders of magnitude greater than periodic field canister monitoring data [three data sources—RCRA facility investigation, Battelle Study, OC-ALC Bioenvironmental data].

22. There are no observed trends with the OP-FTIR predictions [as illustrated with the field canister data]. The OP-FTIR data appears to be a scattered cluster of data orders of magnitude greater than what was measured by the periodic canister monitoring data.

23. An Agency for Toxic Substances and Disease Registry Study concluded that exposure to current ambient air emission from the industrial wastewater treatment plant does not pose a public health concern. This is in agreement with the conclusion from the risk assessment portion of this research effort. The risk assessment results concluded that current phenol and methylene chloride exposure concentrations are not of public health concern.

24. Additional advantages of the coupled model approach includes the evaluation of on-base process change scenarios and pollution prevention activities regarding the use of phenol and methylene chloride, in addition to evaluating changes in the design or operation of the IWTF for purposes of minimizing atmospheric emissions of phenol and methylene chloride.

25. The coupled model methodology can be used to satisfy current and future regulatory requirements [*i.e.*, Pollution Prevention Act of 1990, Air Force Policy Directive 19-4, Policy for the Pollution Prevention Program, Air Force Instruction 19-40, and the Instruction for the Pollution Prevention Program].

26. The coupled model can be used to addresses the following areas: pollution prevention objectives, goals and strategies; the program

structure, organization and responsibilities; program elements and goals; program reporting and tracking [metrics], and progress of the program [metrics].

27. The coupled model approach can be used to satisfy the Pollution Prevention Program strategy based on the following: preliminary assessment of projects to reduce or eliminate the amount or toxicity of waste disposed; define pollution prevention options [propose, screen and prioritize pollution prevention project options]; perform feasibility study [technical, environmental and economical feasibility studies]; write assessment report; implement pollution prevention projects; and measure progress. The coupled model approach can be used in each of the program elements.

28. The coupled model methodology can be used to satisfy the U.S. EPA NESHAP for publicly owned treatment works [40 CFR Part 63, National Emission Standards for Hazardous Air Pollutants: Publicly Owned Treatment Works]. The POTW NESHAP took affect 30 October 1999, and requires all POTWs [including IWTF] to quantify the emissions from each of the process units and report annually to the federal, state, and local regulating agencies. This action promulgates national emission standards for hazardous air pollutants [NESHAP] for new and existing publicly owned treatment works [POTW].

29. A potential future use for the couple model approach is in achieving International Standards Organization [ISO] 14000 certification. The ISO 14000 concept was developed out of a concern to achieve and demonstrate sound environmental performance by controlling the impact of their activities, products and services on the environment, taking into account their environmental policy and objectives. Many organizations have undertaken environmental *reviews* or *audits* to assess their environmental performance. International Standards covering environmental management are intended to provide organizations with the elements of an effective environmental management system, which can be integrated with other management requirements, to assist organizations to achieve environmental and economic goals. The coupled model can be used to track performance and conformance with ISO

14000 standards for industrial wastewater treatment facilities. The model could also be used as part of the auditing process to measure and forecast current and future environmental compliance.

30. The coupled model approach can be used in the development of environmental impact assessments [EIAs]. An environmental impact assessment is defined as the systematic identification and evaluation of potential impacts of proposed projects, plans, programs, or legislative actions relative to the physical-chemical, biological, cultural, and socio-economic components of the total environment. The coupled model approach could improve the environmental inventory [*i.e.*, description of the environment in an area where a particular action is being considered]. The coupled model could be incorporated to improve the decision making process.

31. In conclusion, the coupled model could be used as a tool to develop realistic goals for pollution prevention, waste reduction, and hazardous waste minimization programs. The model could be used to assist in prioritizing projects [*i.e.*, pollution prevention, waste reduction, hazardous waste minimization, etc.]. The model could be used to develop, evaluate, and investigate pollution prevention techniques, technologies, and methodologies. Engineers could identify and minimize future threats to human health and environment. It could be used to develop, evaluate, investigate, and prioritize control technologies. The model has been used to predict compliance with future environmental regulatory constraints [*i.e.*, POTW NESHAP]. The model could be used to identify, rank, and prioritize better business practices and opportunities [*i.e.*, determine mission impact, degree of liability, and environmental impacts]. The model has been used to identify and prioritize process improvements; develop short, intermediate, and long-term pollution prevention alternatives. The regulating agencies could potentially use the coupled model approach to identify and prioritize lists of chemicals targeted for future environmental regulatory compliance and develop regulatory policy mandates.